

# **Deciphering the mechanism of cytotoxicity and cancer-selective activity of the delocalized lipophilic cation D112**

by

Ning Yang

A thesis submitted in partial fulfillment of the requirements for the degree of  
Doctor of Philosophy

Department of Biochemistry  
University of Alberta

© Ning Yang, 2016

## ABSTRACT

Chemotherapeutic drugs that are used in anti-cancer treatments often cause death of both cancerous and noncancerous cells. This non-selective toxicity is the root cause of untoward side effects that limits the effectiveness of therapy. To improve the therapeutic options for cancer patients, there is a pressing need to identify novel compounds with a greater discrimination for cancer cells. Delocalized lipophilic compounds (DLCs) are a class of molecules that have long been investigated for therapeutic potential in oncology. These compounds enter mitochondria in response to the electrochemical potential gradient across the inner membrane. In particular, the high negative inside properties of cancer mitochondria are proposed to facilitate selective accumulation into cancer mitochondria. Following uptake, DLCs induce cell death through various mechanisms. While the inhibitory effects to cancer mitochondria are well-demonstrated *in vitro*, toxicities identified from *in vivo* studies have precluded clinical development. Identifying novel DLCs with enhanced efficiency and selectivity are thus critical next steps for this class of molecules.

D112 is a cyanine-based dye that was identified by the Eastman Kodak Company as a photosensitizer for use in photographic emulsions. Initial observations that cyanine dyes with certain reduction potentials inhibited mitosis of sea urchin eggs triggered the company to initiate a drug-screening program to test these compounds for cytotoxicity against cancer cells. Approximately 2000 dyes were evaluated in this program, and D112 emerged as a lead compound based on its selectivity against a human colon cancer cell line relative to a normal monkey

kidney epithelial cell line. Despite these intriguing results, investigations into D112 were not pursued due to changes in industry priorities. We decided to revive investigations on D112 to evaluate its potential as a novel anticancer agent.

In this thesis, I first characterized D112-induced cell death in cancer cells and identified that D112 induced apoptosis through a mitochondrial-centered pathway. Its selective cytotoxicity against cancer cells was demonstrated in a panel of cell lines derived from solid tumors. In addition, insights into the molecular mechanisms of D112-induced toxicity indicated that D112 preferentially accumulated in cancer mitochondria, where it interacted with mitochondrial DNA, induced ROS production and caused mitochondrial DNA damage. D112-induced ROS was a critical upstream mediator, as ROS inhibition prevented Bax activation and subsequent apoptosis. Anti-cancer cell cytotoxicity of D112 was thus likely a function of both selective cancer cell uptake and cancer cell sensitivity to oxidative stress. Finally, encouraged by the observation that D112 induced ROS-mediated apoptosis, we investigated methodologies with which to increase the apoptotic index between cancer and non-transformed cells. In consideration of the inherent fluorescent properties of D112, we therefore tested the effect of photo-activation on D112 toxicity, and found D112's cancer-selective toxicity was greatly potentiated by photo-activation. Thus, results from this thesis identify D112 as a potential new prototype for drug development, and in conjunction with photodynamic therapy might lead to an appropriate therapeutic window for D112-based cancer treatment in the future.

## PREFACE

This thesis is an original work by Ning Yang.

Chapter 3 of this thesis has been published as Yang, N., Gilman, P., Mirzayans, R., Sun, X., Touret, N., Weinfeld, M., and Goping, I.S. (2015). Characterization of the apoptotic response induced by the cyanine dye D112: a potentially selective anti-cancer compound. *PLoS One* 10, e0125381. Chapter 4 of this thesis is in the process of submission. I performed all experiments and data analysis, and also prepared and edited the manuscripts. Dr. Ing Swie Goping was the supervisory author and was involved in both manuscript preparations.

The literature review presented in chapter 1 is my original work, as is the concluding analysis presented in chapter 5.

**I dedicate this work to my father, Yuxing, who offers unconditional love and support, and has always been there for me.**

謹以此论文献给我的父亲杨玉星

## ACKNOWLEDGEMENTS

This research thesis would not have been possible without the assistance of numerous people and organizations. Here, I would like to thank a few of them by name.

First and foremost, I would like to express sincere appreciation to my PhD supervisor, Professor Ing Swie Goping, who welcomed me into her lab and let me fulfill my dream of being a research scientist in Canada. Over the past four years, she has continuously encouraged me to pursue this project, and has generously guided me through numerous difficulties. This dissertation would not have been completed without all of her supports. As an international student, I especially appreciate her understanding and patience.

I am grateful to my supervisory committee members, Professor Michael Weinfeld and Professor Chris Bleackley, for their invaluable advice and constructive criticism. Their criticisms and critiques greatly contributed to the improvement of my critical thinking skills.

Special thanks go to Dr. Paul Gilman from Eastman Kodak Company, Dr. Jack Williams (now deceased), and Dr. Gregory Taylor from University of Alberta for bringing compound D112 to our attention. This project would not have been possible without their commitments to drug discovery.

I would like to express my thanks to Dr. Ben Montpetit, whose expertise and skills helped me to develop the yeast system for D112 study. Additional thanks are in order to Dr. Xuejun Sun for his assistance with confocal microscope, to Dr. Gary Eitzen for his help with D112 spectra scan, to Dr. Lynne Postovit for sharing hypoxia

chamber, and to Dr. Razmik Mirzayans for providing his valuable opinions on data interpretation.

I am also indebted to our former lab manager Rachael Montpetit and my colleagues in the Goping Lab: Diane Marganski, Jasdeep Mann, Vrajesh Pandya, Dr. Namita Tripathi, Namrata Patel and Dr. John Githaka, for their assistance to my project and also their contributions to a friendly and stimulating work environment.

This project was made possible in part by the Graduate Studentship from the Women and Children's Health Research Institute. I also want to thank the University of Alberta for the Recruitment Scholarship and Faculty of Medicine and Dentistry for the 75<sup>th</sup> Anniversary Graduate Student Award.

I would like to further express my thanks to Dr. Richard Fahlman and Dr. Charles Holmes for serving on my candidacy exam and Dr. Carrie Simone Shemanko and Dr. Gary Eitzen for participating in my thesis defense.

Finally, and most importantly, I want to acknowledge all my family and friends who helped me survive the stress involved in completing this research thesis and convey my gratitude for their efforts in not allowing me to give up.

# TABLE OF CONTENTS

<b>CHAPTER 1 INTRODUCTION .....</b>	<b>1</b>
1.1 Anticancer drug development–history and trends .....	2
1.2 Mitochondria as drug targets.....	12
1.2.1 Rationales for targeting cancer mitochondria.....	12
1.2.1.1 Evasion of mitochondrial-centered apoptosis.....	12
1.2.1.2 Reprogramming of cancer mitochondrial metabolism pathway .....	16
1.2.1.3 ROS elevation in cancer cells.....	18
1.2.2 Mitochondrial-targeting drugs.....	24
1.2.2.1 Drugs targeting Bcl-2.....	24
1.2.2.2 Drugs targeting metabolism.....	25
1.2.2.3 Drugs targeting mitochondrial ROS.....	27
1.2.3 Mitochondrial-targeted drug: DLCs .....	29
1.2.4 Determination of apoptosis.....	34
1.3 Photodynamic therapy (PDT).....	37
1.4 D112.....	43
1.5 Research Objective.....	48
Reference.....	49
<b>CHAPTER 2 METHODS AND MATERIALS .....</b>	<b>78</b>
2.1 Reagents.....	79
2.2 Cell culture and treatments .....	79
2.2.1 Mammalian cell culture.....	79

2.2.2 Yeast cell culture .....	80
2.2.3 D112 treatment.....	81
2.3 Cell viability assays in mammalian cells .....	81
2.3.1 Determination of apoptosis.....	81
2.3.1.1 Measurement of phosphatidylserine exposure .....	81
2.3.1.2 Measurement of mitochondrial membrane potential .....	81
2.3.1.3 Caspase enzymatic activation assay.....	82
2.3.1.4 DNA fragmentation assay.....	83
2.3.1.5 Subcellular fractionation to enrich for mitochondrial fractions .....	83
2.3.2 Detection of cellular plasma membrane damage (necrosis).....	84
2.3.3 Cell proliferation.....	84
2.3.4 Single colony formation .....	84
2.4 Protein assays.....	85
2.4.1 Western blotting.....	85
2.4.2 Immunoprecipitation for identification of activated Bax .....	86
2.5 Analysis of D112 fluorescence .....	87
2.5.1 D112 spectra .....	87
2.5.2 D112 spectra with nucleic acids .....	88
2.5.3 Measurement of D112 fluorescence in tissue culture medium.....	88

2.6 Examination of D112 Localization .....	88
2.6.1 Plasmids .....	88
2.6.2 Transient transfections .....	88
2.6.3 Confocal microscopy .....	89
2.7 Localization and viability assays in yeast .....	89
2.7.1 D112 localization in yeast.....	89
2.7.2 Yeast growth curves .....	90
2.7.3 Yeast recovery assay .....	90
2.8 Assays for ROS detection .....	91
2.8.1 Measurement of ROS levels .....	91
2.8.2 NAC treatment.....	92
2.8.3 Hypoxia treatment .....	92
2.9 Assays examining D112 interaction with DNA .....	93
2.9.1 D112 electrophoretic gel-shift assay .....	93
2.9.2 mtDNA damage assay .....	93
2.9.3 Assay to test for the induction of the petite phenotype.....	94
2.10 Photodynamic therapy treatment .....	95
2.11 Statistical analysis.....	95
Reference.....	96

**CHAPTER 3 D112 INDUCES THE MITOCHONDRIAL-APOPTOTIC PATHWAY  
AND SHOWS HIGHER SELECTIVITY FOR TRANSFORMED CELLS .....**

3.1 Introduction.....	98
3.2 D112 induces apoptosis in Jurkat cells .....	99

3.2.1 D112 causes phosphatidylserine exposure.....	99
3.2.2 D112 causes mitochondrial dysfunction and caspases activation .....	103
3.2.3 D112 causes caspases activation .....	105
3.2.4 D112 induced DNA fragmentation.....	105
3.3 Mitochondria play a critical role in D112-induced cell death .....	108
3.3.1 Anti-apoptotic Bcl-2 blocks D112-induced cell death .....	108
3.3.2 Bax/Bak deficient cells are resistant to D112-induced cell death.....	110
3.3.3 Extrinsic pathway does not contribute to D112-induced cell death.....	113
3.3.4 D112 inhibits long-term cell viability .....	113
3.3.5 Lysosomes do not appear to be involved in D112 toxicity	116
3.4 D112 co-localizes with mitochondria .....	116
3.4.1 D112 spectra scan.....	118
3.4.2 D112 co-localized with mitochondria .....	118
3.4.3 Mitochondrial electrochemical potential is responsible for D112 accumulation in the mitochondria .....	120
3.5 D112 shows increased toxicity to breast cancer cells and metastatic melanoma cells .....	127
3.6 Discussion .....	133
Reference.....	138

<b>CHAPTER 4 D112-INDUCED ROS PRODUCTION IS SELECTIVELY POTENTIATED IN CANCER CELLS BY PHOTO-ACTIVATION .....</b>	<b>143</b>
4.1 Introduction.....	144
4.2 D112-induced cell death is enhanced by mitochondrial respiration	145
4.3 D112 binds to DNA.....	151
4.4 ROS induction is required for D112-mediated cell death .....	157
4.5 ROS contributes to D112 selective cytotoxicity.....	163
4.6 D112 is preferentially taken up by cancer cells .....	166
4.7 Photo-activation of D112 increases its cytotoxic potential .....	168
4.8 Discussion .....	177
Reference.....	182
<b>CHAPTER 5 DISCUSSION .....</b>	<b>186</b>
5.1 Introduction.....	187
5.2 D112 properties.....	187
5.3 The mechanisms of D112-induced cytotoxicity .....	188
5.4 D112 in chemotherapy .....	192
5.4.1 Application of DLCs .....	192
5.4.2. D112 as a chemotherapeutic compound.....	197
5.5 D112 potential in photodynamic therapy .....	203
5.5.1 Photodynamic therapy in oncology .....	203
5.5.2 The consideration of D112 in PDT .....	207
5.6 Concluding remarks .....	211
Reference.....	213

**BIBLIOGRAPHY..... 220**

## LIST OF TABLES

<b>Table 4.1</b> Yeast mutant strains .....	152
---	-----

## LIST OF FIGURES

<b>Figure 1.1</b> The development of anticancer drugs.....	3
<b>Figure 1.2</b> Model of apoptotic pathways .....	14
<b>Figure 1.3</b> The multiple effects of ROS .....	20
<b>Figure 1.4</b> Structures of DLCs.....	30
<b>Figure 1.5</b> Photodynamic therapy .....	38
<b>Figure 1.6</b> Summary of first report of D112 cytotoxicity <i>in vitro</i> .....	45
<b>Figure 1.7</b> <i>In silico</i> comparison of “drug-like” properties of D112 relative to currently used chemotherapeutic agents .....	47
<b>Figure 3.1</b> D112 causes phosphatidylserine exposure in Jurkat cells .....	101
<b>Figure 3.2</b> D112 induces apoptosis and secondary necrosis.....	102
<b>Figure 3.3</b> D112 induces mitochondrial dysfunction in Jurkat cells.....	104
<b>Figure 3.4</b> D112 induces caspase activation and DNA fragmentation in Jurkat cells .....	106
<b>Figure 3.5</b> D112-induced apoptosis is blocked by Bcl-2 .....	109
<b>Figure 3.6</b> Bax/Bak expression is required for D112-induced cell death .....	111
<b>Figure 3.7</b> The extrinsic pathway does not contribute to D112-induced apoptosis .....	114
<b>Figure 3.8</b> Lysosomes do not contribute to D112-induced cell death .....	117
<b>Figure 3.9</b> D112 spectra.....	119
<b>Figure 3.10</b> D112 co-localizes with mitochondria. ....	121
<b>Figure 3.11</b> Early endosomes are not associated with D112 intracellular uptake. ....	122

<b>Figure 3.12</b> Late endosomes are not associated with D112 intracellular uptake.....	124
<b>Figure 3.13</b> Mitochondrial membrane potential is required for D112 accumulation.....	126
<b>Figure 3.14</b> D112 shows selective cytotoxicity against transformed cells.....	128
<b>Figure 3.15</b> D112 selectively inhibits clonogenic survival of transformed Cells.....	131
<b>Figure 4.1</b> D112 enters yeast cells and inhibits cell growth.....	147
<b>Figure 4.2</b> Mitochondrial respiration renders yeast more sensitive to D112 toxicity.....	149
<b>Figure 4.3</b> Mitochondrial DNA-deleted mutants are resistant to D112 Toxicity.....	153
<b>Figure 4.4</b> D112 binds to nucleic acid <i>in vitro</i> and induces a petite phenotype in yeast.....	155
<b>Figure 4.5</b> D112 induces ROS production.....	159
<b>Figure 4.6</b> ROS contributes to D112 toxicity.....	161
<b>Figure 4.7</b> ROS generation contribute to D112 selectivity.....	164
<b>Figure 4.8</b> D112 preferentially accumulates in cancer cells.....	167
<b>Figure 4.9</b> Photo-activation of D112 causes various cell death morphologies in cancer cells.....	170
<b>Figure 4.10</b> D112 toxicity is enhanced after photo-activation.....	172
<b>Figure 4.11</b> D112 photo-activation is selectively toxic to cancer cells.....	175
<b>Figure 4.12</b> Photo-activation increases ROS production in cancer cells.....	176

<b>Figure 5.1</b> Physical properties of D112 .....	189
<b>Figure 5.2</b> Proposed model of D112-induced mitochondrial dysfunction .....	191
<b>Figure 5.3</b> Structures of MKT-077 and JG98 .....	199
<b>Figure 5.4</b> Structures of MKT-077 and D112.....	201
<b>Figure 5.5</b> Summary of FDA-approved photosensitizers. ....	205

## LIST OF ABBREVIATIONS

AD	Alzheimer's disease
AIF	Apoptosis-Inducing-Factor
AML	Acute myelogenous leukemia
ANOVA	Analysis of Variance
Ask-1	Apoptosis signal-regulating kinase-1
ATP	Adenosine triphosphate
Bad	BCL-2 antagonist of cell death
BAG3	Bcl2-associated athanogene 3
Bak	BCL-2-associated X protein
Bax	BCL-2 antagonist/killer protein
Bcl-2	B-cell lymphoma 2
Bcl-w	BCL-2 like protein 2
Bcl-X <sub>L</sub>	BCL-2 like protein extra large
Bid	BH3-interacting domain death agonist
Bik	BCL-2-interacting killer
Bim	BCL-2-interacting mediator of cell death
CaCl <sub>2</sub>	Calcium chloride
CAD/DFF-40	Caspase-activated DNase
CCCP	Carbonyl cyanide <i>m</i> -chlorophenyl hydrazine
CHAPS	3-[(3-cholamidopropyl)dimethylammonio]-1-propanesulfonate
CHOP	c/EBP homologous protein
CLL	Chronic lymphocytic leukemia

CML	Chronic myeloid leukemia
cypD	Cyclophilin D
CX-1	Human colon adenocarcinoma cell line
DCs	Dendritic cells
DCA	Dichloroacetate
DECA	Dequalinium chloride
DiOC <sub>6</sub>	3,3'-Dihexyloxacarbocyanine Iodide
DMSO	Dimethyl sulfoxide
DNA	Deoxyribonucleic acid
Dox	Doxorubicin
DLC	Delocalized lipophilic cation
DTT	Dithiothreitol
EB	Ethidium bromide
ECL	Enhanced chemiluminescence
EDTA	Ethylenediaminetetraacetic acid
EGF	Epidermal growth factor
ER	Endoplasmic reticulum
Ex/Em	Excitation/Emission
FCS	Fetal calf serum
GFP	Green fluorescent protein
GSH	Glutathione
HCl	Hydrochloric acid
HEPES	4-(2-hydroxyethyl)-1-piperazineethanesulfonic acid

HER2	Human epidermal growth factor receptor 2
HIF-1	Hypoxia-inducible factor-1
HRP	Horseradish peroxidase
HSPs	Heat shock proteins
IC50	Inhibitory concentration of 50%
ICAD/DFP-45	Inhibitor of caspase-activated DNase
IMM	Inner mitochondrial membrane
JNKs	c-Jun N-terminal kinases
KCl	Potassium chloride
KH <sub>2</sub> PO <sub>4</sub>	Potassium phosphate monobasic
MAPKs	Mitogen-activated protein kinases
MgCl <sub>2</sub>	Magnesium chloride
MRPs	Multidrug resistance proteins
mtDNA	Mitochondrial DNA
MTT	Methylthiazole tetrazolium assay
NAC	N-Acetyl-Cysteine
NaCl	Sodium chloride
NADH	Nicotinamide adenine dinucleotide, reduced form
NaH <sub>2</sub> PO <sub>4</sub>	Sodium phosphate monobasic monohydrate
Na <sub>2</sub> HPO <sub>4</sub> ·7H <sub>2</sub> O	Sodium phosphate dibasic heptahydrate
NaOH	Sodium hydroxide
NP-40	IGEPAL® CA-630
OD	Optical density

PBS	Phosphate-buffered saline
PCR	Polymerase chain reaction
PDK1	Pyruvate dehydrogenase kinase 1
PDT	Photodynamic therapy
PEITCs	Phenylethyl isothiocyanates
PS	Phosphatidylserine
PSA	Prostate-specific antigen
PTP	Permeability Transition Pore
Puma	p53-upregulated modulator of apoptosis
PVDF	polyvinylidene fluoride
Rh123	Rhodamine 123
ROCK	Rho-associated kinase
ROS	Reactive oxygen species
RTK	Receptor tyrosine kinase
SD	Standard deviation
SDS-PAGE	Sodium dodecyl sulfate-Polyacrylamide gel electrophoresis
SLL	Small lymphocytic lymphoma
SOD2	Superoxide dismutases 2
STS	Staurosporine
TBE	Tris/Borate/EDTA
TBHP	<i>tert</i> -Butyl hydroperoxide
TBS-T	Tris-buffered saline Tween 20
TCA	Tricarboxylic acid cycle

TNFRs	Tumor Necrosis Factor Receptors
Tom20	Translocase of outer mitochondrial membranes 20 kDa
TPP	Triphenylphosphonium
VDAC	Voltage-dependent anion channel
YPD	Yeast Peptone Dextrose
YPG	Yeast Peptone Glycerol
2-DG	2-deoxyglucose
2-ME	2-mercaptoethanol
5-FU	5-fluorouracil
17-AAG	17-allylamino, 17-demethoxygeladanamycin
$\Delta\psi$	Mitochondrial membrane potential

**CHAPTER 1**  
**INTRODUCTION**

## 1.1 Anticancer drug development—history and trends

Cancer is caused by the uncontrolled proliferation of aberrant cells that harbor multiple oncogenic mutations. These mutations not only enable cells to divide abnormally, but also contribute to resistance to apoptosis, immune evasion, tumor-promoting inflammation, tumor angiogenesis, activation of invasion and metastasis and metabolic reprogramming (Hanahan and Weinberg, 2011; Liu et al., 2015; Michor et al., 2004). Despite considerable advances in our understanding of the molecular and cellular biology of cancer, it remains a leading cause of death, accounting for nearly 1 in every 4 deaths in North America (American Cancer Society, 2014). Moreover, bringing a new drug to market is estimated to cost approximately US \$1 billion (Hait, 2010), with a disappointingly low overall success rate (5~10%) of anticancer drug approval for clinical use (Hait, 2010; Kamb et al., 2007). Therefore, evaluating past successes and failures of anticancer drug development can provide rationale for areas of future exploration.

In general, the history of anticancer drug development can be divided into three stages (Fig. 1.1). The first-generation of anticancer drugs plays a dominant role in clinical applications for a few decades after the first successful case of human cancer remission was achieved in the 1940s (Goodman et al., 1946). Drugs in this generation are sometimes called “dirty” drugs due to their low selectivity and they are initially identified through empirical observations (Mukherjee, 2010). Later, insights into their mechanisms reveal that they act mainly by impairing DNA integrity and replication, or by blocking mitosis through interference with the mitotic apparatus. For instance, the widely used doxorubicin and cisplatin kill tumor cells by

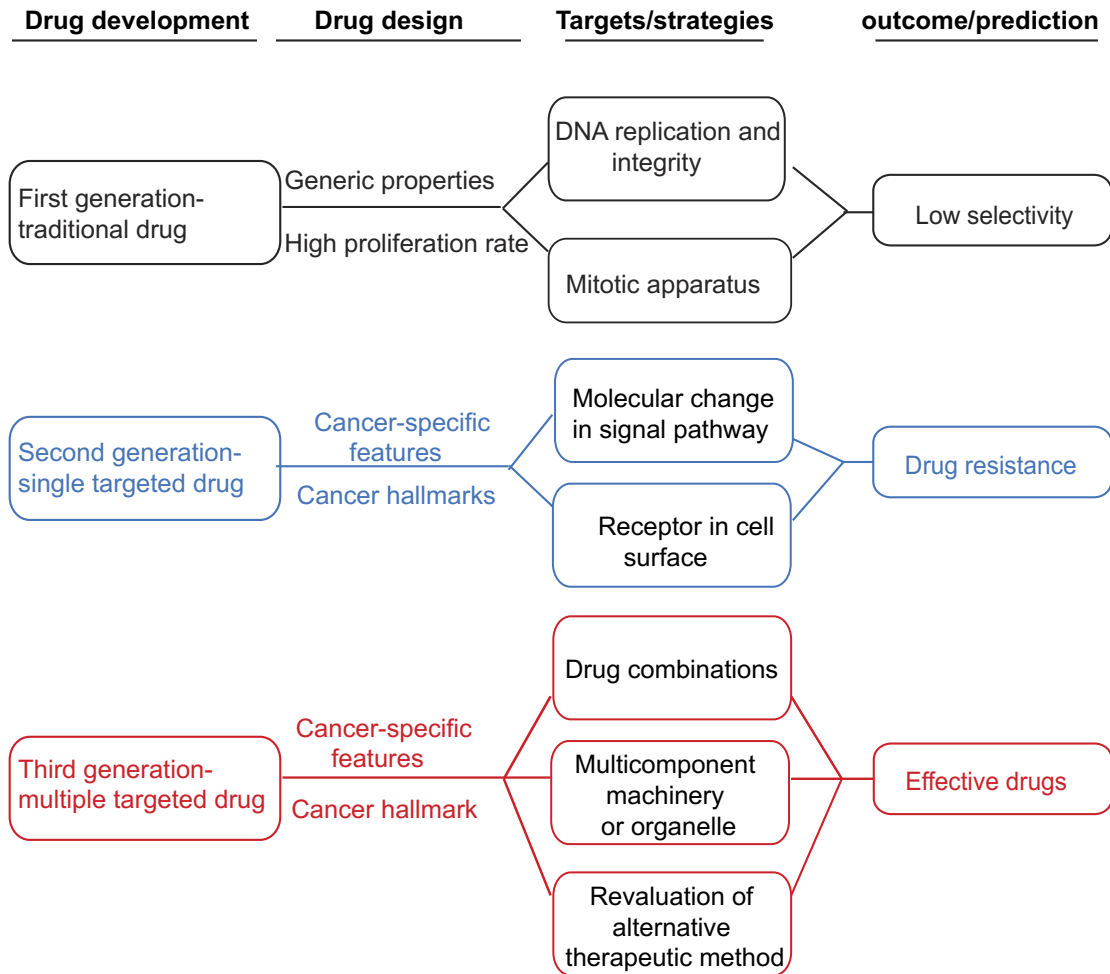


**Figure 1.1 The development of anti-cancer drugs.** The history of anti-cancer drug development is generally divided into three generations. First-generation drugs target DNA integrity and the mitotic apparatus. They are effective but toxic. Second-generation molecular-targeted drugs are selective but are prone to drug resistance. Third-generation drugs target multicomponent machineries or organelles and also encompass the re-evaluation of already existing but underestimated approaches.

damaging their DNA (Siddik, 2003), whereas paclitaxel and vincristine affect tumor microtubules (Jackson et al., 2007). First-generation drugs have been highly successful in treating some cancer types, such as childhood leukemia and testicular carcinoma (Dobbelstein and Moll, 2014). They still represent the majority of clinically used drugs at present. However, owing to their inability to discriminate cancer cells from normal cells, first-generation drugs cause severe side effects, such as substantial toxicity to normal rapidly dividing cells (exemplified by gut and hair follicles) (Botchkarev et al., 2000; Umeki et al., 1989) and post-mitotic tissues (exemplified by heart muscle) (Octavia et al., 2012). Consequently, patients suffer from nausea, loss of appetite, hair loss, or even severe effects, such as doxorubicin-induced cardiotoxicity (Octavia et al., 2012). Further, this non-specific toxicity to normal cells can induce DNA damage that can consequently give rise to secondary malignancies in patients (Armstrong et al., 2011; Travis et al., 2005). For instance, secondary acute myelogenous leukemia (AML) occurred in non-Hodgkin lymphoma patients following cisplatin therapy (Andre et al., 2004), and also breast cancer patients following doxorubicin treatment (Smith et al., 2003). Moreover, chemotherapy-induced AML is relatively resistant to subsequent therapy and the cure rate is only 10% to 20% (Leone et al., 2001; Neugut et al., 1990). These limitations lead to the development of the second generation of anticancer drugs that focus on the susceptibilities, or “Achille’s heel” of cancer cells.

Advances in the understanding of the molecular determinants of cancer have facilitated the development of these second-generation of anticancer drugs. It is well established that in order to initiate and progress, tumor cells must display several

characteristics that are crucial for their survival. These characteristics are summarized by Hanahan and Weinberg as hallmarks of cancer: “sustaining proliferative signaling, evading growth suppressors, resisting cell death, enabling replicative immortality, inducing angiogenesis, activating invasion and metastasis, deregulating cellular energetics, genome instability and mutation, avoiding immune destruction and tumor-promoting inflammation” (Hanahan and Weinberg, 2011). The molecules that drive these alterations have attracted great interest as new drug targets. Thus this second generation of anticancer drugs, either in the form of small-molecules or monoclonal antibodies, are designed to target cellular oncoproteins or gain-of-function mutations involved in various signaling pathways (Blume-Jensen and Hunter, 2001; Lemmon and Schlessinger, 2010). For instance, the receptor tyrosine kinase (RTK)-stimulated pathway, which is involved in several cellular processes, such as cell proliferation, survival, metabolism and cell migration (Blume-Jensen and Hunter, 2001; Lemmon and Schlessinger, 2010; Roberts and Der, 2007), is aberrantly stimulated in cancer cells and is correlated with the progression of numerous cancers (Takeuchi and Ito, 2011). This finding drives the development of drugs that block the RTK pathway. One such drug is the BCR-ABL inhibitor Imatinib/Gleevec, which is the first selective tyrosine kinase inhibitor approved by the FDA for the treatment of chronic myeloid leukemia (CML) (Capdeville et al., 2002). The development of Imatinib was primarily driven by the observation that 90% of chronic myeloid leukemia (CML) patients harbor a chromosomal translocation that encodes a constitutively active tyrosine kinase, BCR-ABL (Nowell and Hungerford, 1960; Salesse and Verfaillie, 2002). Since this fusion protein is not expressed in the

patient's normal cells, BCR-ABL is a prime druggable target, which would conceivably have minimal impact on normal cells. Imatinib was discovered in a high throughput chemical screen aiming to identify molecules that bound and specifically inhibited BCR-ABL (Capdeville et al., 2002). Imatinib is an optimized compound from a series of BCR-ABL selective inhibitors that was selected for satisfactory oral bioavailability and lack of mutagenic potential. Insights into the mechanism of action demonstrate that Imatinib binds to the inactive conformation of the BCR-ABL tyrosine kinase and competitively blocks the ATP binding site (Grebien et al., 2011). It thus prevents the BCR-ABL conformational switch to the active form, resulting in the inhibition of tumor proliferation (Capdeville et al., 2002). Imatinib was approved for the treatment of CML in 2001, and since then it has been a successful therapeutic drug, contributing to 80% progression-free survival over 5 years (Druker et al., 2006).

In addition to small molecule inhibitors of oncogenic tyrosine kinases, monoclonal antibodies targeting cell-surface receptors that are highly expressed in cancer cells have also been successfully developed. A pioneering example is Trastuzumab (Vogel et al., 2002), a monoclonal antibody that specifically binds to the receptor tyrosine kinase HER2. HER2, also known as ERBB2 or Neu, belongs to the EGF receptor family. It is activated by forming homodimers or heterodimers with other EGF family members, which then triggers downstream signaling cascades to promote tumor proliferation and survival (Vu and Claret, 2012; Yarden and Sliwkowski, 2001). The amplification of HER2 has been observed in up to 20~25% breast cancer patients, and its overexpression is linked to constitutive activation of

growth signaling pathways, an aggressive phenotype and subsequent poor prognosis (Slamon et al., 1987; Yan et al., 2015). Based on these associations, Trastuzumab, a humanized recombinant monoclonal antibody against HER2, was developed by Genentech Inc. This antibody shows anticancer activity through several mechanisms, including down-regulating HER2 expression by binding to its extracellular domain (Harries and Smith, 2002), inhibiting angiogenesis by modulating the effects of pro-angiogenic and anti-angiogenic factors (Izumi et al., 2002) and stimulating immune response as seen in *in situ* infiltration of leukocytes in patients achieving remission (Gennari et al., 2004). In 1998, Trastuzumab received FDA approval for use in women with metastatic breast cancer. It has proven to be successful in the treatment of HER2-positive breast cancer patients (Vogel et al., 2002) as evidenced by extended time to disease progression and overall survival rate (Vogel et al., 2002; Zhu et al., 2013).

Given that this second-generation of drugs inhibits cancer-cell specific targets, these compounds show milder side effects in comparison to the first generation of anticancer drugs. Clinical experience, however, demonstrates that the application of such molecular-targeted drugs also eventually fails to meet therapeutic needs (Gottesman, 2002; Hait, 2010; Nahta et al., 2006; Zahreddine and Borden, 2013). The primary challenge facing the second-generation drugs is acquired resistance in cancer patients after a period of treatment (Gottesman, 2002; Zahreddine and Borden, 2013). Various resistance mechanisms have been identified that highlight the adaptiveness and heterogeneity of tumor cells (Nahta et al., 2006; Quintas-Cardama et al., 2009; Villamor et al., 2003; Zahreddine and

Borden, 2013). These adaptations include the emergence of mutations and amplifications in the targeted gene, the overexpression of multidrug-resistance protein, as well as the activation of alternative signaling pathways for tumor survival (Berns et al., 2007; Kunjachan et al., 2013; Nahta et al., 2006; Quintas-Cardama et al., 2009; Zahreddine and Borden, 2013). Drug resistance results in treatment failure, suggesting that targeting single molecules is not effective for most cancer treatments.

To address the limitations encountered in the first two generations, three strategies have been proposed to improve therapeutic outcomes: (i) drug combination, (ii) the identification of novel drugs targeting multicomponent cellular machineries or organelles, and (iii) the re-evaluation of already existing but underestimated therapeutic approaches.

Drug combination is a therapeutic approach combining already validated drugs in order to target various signaling pathways. The likelihood of developing drug resistance due to the activation of alternative signaling pathways in cancer cells is therefore reduced. One successful example is the combination of the HER2 antibody trastuzumab with doxorubicin or paclitaxel. In comparison to chemotherapy alone, combination treatment increased the overall response rate from 32% to 50% and extended median progression-free survival time from 3 months to 6.9 months (Slamon et al., 2001). Currently, trastuzumab is being evaluated in combination with many other therapeutics (Bang et al.; European Cancer Organisation; Ko et al., 2015; Mukai et al., 2015). Furthermore, owing to the variety of drug resistance mechanisms (Zahreddine and Borden, 2013), attention has been drawn to optimize

and personalize drug combination for cancer treatment. For example, a pharmacogenomics platform was developed by Engelman and colleagues (Crystal et al., 2014). In this platform, cell culture models derived from biopsy samples of lung cancer patients, who showed progressive disease while on treatment with tyrosine kinase inhibitor, were firstly established. Then these cells were subjected to a pharmacological screen that combined the tyrosine kinase inhibitor with a panel of 76 drugs targeting key regulators of cell proliferation and survival. The screen successfully identified multiple effective drug combinations that halted the growth of resistant tumor cells both in cell culture and mouse models (Crystal et al., 2014), thus providing a promising and rational therapeutic option for individual cancer patients.

In addition to drug combinations, significant efforts have been made to develop drugs that target cellular multicomponent machineries that facilitate the growth needs of cancer cells. Similar to targeting the DNA replication machinery and cell division machinery, this new generation of drugs target cellular processes that are required for tumor cell proliferation and survival. Such machineries direct protein folding, chromatin modification, or proteasome-mediated protein degradation (Dobbelstein and Moll, 2014). The development of the heat shock proteins (HSPs) inhibitor is an example of machinery-targeted drugs (Sidera and Patsavoudi, 2014). Heat shock proteins are evolutionarily conserved molecular chaperones that participate in protein activation and stabilization, multiprotein complex assembly, and protein degradation (Nahleh et al., 2012). Owing to genetic mutations, high ROS production, as well as unfavorable acidic and/or hypoxic environments, cancer cells

experience chronic proteotoxic stress (Dai et al., 2012). This condition consequently creates a high demand for the HSP chaperone machinery, which consists of HSP90, HSP70 and other co-chaperones proteins, to protect protein, especially oncoproteins, from misfolding and degradation (Nahleh et al., 2012). Indeed, HSPs overexpression has been seen in many types of cancers (Miyata et al., 2013b; Trepel et al., 2010; Xu et al., 2009). In addition, HSPs are anti-apoptotic proteins (Bruey et al., 2000; Garrido et al., 2006), and high HSP expression is associated with a poor clinical outcome (Gehrmann et al., 2014; Nonaka et al., 2004; Romani et al., 2007). Thus, the inhibition of HSPs is emerging as a novel strategy for cancer therapy. The first HSP90 inhibitor evaluated in clinical trial is 17-AAG (17-allylamino, 17-demethoxygeldanamycin, tanespimycin). 17-AAG disrupted HSP90 activity by binding to its ATP-binding pocket, which in turn led to degradation of client proteins (Usmani et al., 2009). Preclinical studies verified that 17-AAG prevented cell proliferation, survival and metastasis in tumor cells (Kim et al., 2012; Kim et al., 2013; Powers et al., 2013). The results of several clinical trials of 17-AAG have been published (Modi et al., 2008; Richardson et al., 2009). The preliminary data from a phase II trial in patients with advanced HER-2 positive breast cancer demonstrated reduced breast lesion and metastases in patients receiving the combination therapy of 17-AAG and trastuzumab. The response rate was 24% and clinical benefit rate was 57% (Modi et al., 2008). Currently, more than ten HSP90 inhibitors are undergoing clinical evaluation in cancer patients (Trepel et al., 2010).

The chaperone HSP70 is another target (Assimon et al., 2013) and substantial efforts have been made to identify HSP70 inhibitors, with limited success

in bringing such inhibitors to the clinic (Evans et al., 2010). The primary reason is its unpredictable off-target effects. For example, the first approach to inhibit HSP70 targeted inhibition of its transcriptional factor HSF1. However this affected multiple stress-inducible heat shock proteins, thus affecting their housekeeping functions in normal cells (Goloudina et al., 2012). Recently, it is proposed that targeting the interactions between HSP70 and its co-chaperones might be an alternative strategy, as co-chaperones diversify HSP70's functions (Assimon et al., 2013). In particular, compound MKT-077 and its analogs modulated the interaction between HSP70 and BAG3 (Li et al., 2015; Miyata et al., 2013a; Rousaki et al., 2011; Wadhwa et al., 2000). MKT-077 was initially discovered in a drug-screening program aiming to identify suitable agents for clinical trial in the 1970s (described in the section 1.2.3) and it showed cancer-selective toxicity in preclinical studies (Koya et al., 1996; Modica-Napolitano et al., 1996). The molecular targets of MKT-077 remained unknown until the year 2000 when HSP70 was identified as a MKT-077-binding protein. MKT-077 and HSP70 interactions interfered with binding of the co-chaperone BAG3 (Wadhwa et al., 2000). BAG3 forms a complex with HSP70 and inhibits apoptosis by interfering with cytochrome c release, apoptosome assembly and other events in the apoptosis process (Colvin et al., 2014; Rosati et al., 2007). Indeed recent studies have demonstrated that MKT-077 and its analog JG98 inhibited cancer growth in both tissue culture and mouse models (Li et al., 2015). Thus by modulating the interaction between HSP70 and its specific co-chaperone, targeting HSP70 machinery might become a feasible approach in cancer therapy.

## **1.2 Mitochondria as drug targets**

### 1.2.1 Rationales for targeting cancer mitochondria

It is well established that mitochondria exert dual functions as energy producing organelles and regulators of cell death. Given that both functions are often altered in neoplasia mitochondria, comparable to multicomponent cellular machineries, mitochondria are being considered as therapeutic targets in the development of new anticancer drugs (Wenner, 2012). Altered cancer cell mitochondria favor tumorigenesis by contributing to the evasion of cell death, metabolism reprogram and ROS production (Wenner, 2012).

#### 1.2.1.1 Evasion of mitochondrial-centered apoptosis

Apoptosis, also called “programmed cell death”, is critical for the proper development of multicellular organisms (Yang and Goping, 2013). In addition to its vital involvement in sculpting tissue structures and maintaining homeostasis, apoptosis also contributes to the elimination of aged or damaged cells, functioning as a quality control mechanism for the organism. Consequently, organisms with defective apoptosis show severe phenotypes, and in fact, dysfunctional apoptosis is the root cause of many human diseases, including cancer (Sankari et al., 2012; Wong, 2011). Cancer cells are generally insensitive to apoptotic signals due to imbalanced apoptotic regulators (Alam, 2003; Boland et al., 2013). Moreover, as many anticancer therapies rely on apoptosis to eliminate cancer cells, impaired apoptotic pathways create a major barrier to effective treatment. This challenge

makes it imperative to decipher the molecular mechanism of action of specific cancer drugs in the apoptotic network.

Two well-studied signaling processes termed the intrinsic and extrinsic pathways represent the major mechanisms of apoptosis (Portt et al., 2011) (Fig 1.2). Extrinsic apoptosis involves the extracellular ligand-mediated activation of plasma membrane-localized death receptors, while intrinsic apoptosis is initiated by intracellular stresses, such as hypoxia, DNA damage, oxidative stress, and anti-cancer therapies (Wong, 2011). These apoptotic stimuli lead to mitochondrial membrane permeabilization (Estaquier et al., 2012) and the release of apoptotic factors, such as cytochrome c (Liu et al., 1996), from the mitochondrial inter-membrane space. The intrinsic pathway is tightly regulated by the Bcl-2 family of proteins (Gross et al., 1999; Martinou and Youle, 2011), which comprises anti-apoptotic (such as Bcl-2, Bcl-XL, Bcl-w) and pro-apoptotic proteins (such as Bax, Bak, Bid, Bad, Bim) (Susin et al., 1999). Pro-apoptotic proteins stimulate formation of the Bax/Bak pore (Wei et al., 2001) or regulate the existing mitochondrial permeability transition pore (De Giorgi et al., 2002) to release mitochondrial apoptosis-inducing proteins. Anti-apoptotic proteins, such as Bcl-2 and Bcl-XL (Noriko Yasuhara, 1997; Tsujimoto, 1998), inhibit mitochondrial dysfunction, thus blocking apoptosis. When pro-apoptotic Bcl-2 proteins prevail, the released cytochrome c stimulates the formation of an oligomeric structure called the 'apoptosome', which includes apoptotic protease activating factor-1 and initiator caspase, caspase-9. This structure triggers the caspase cascade by activating downstream effector caspases such as caspase 3. The extrinsic pathway is

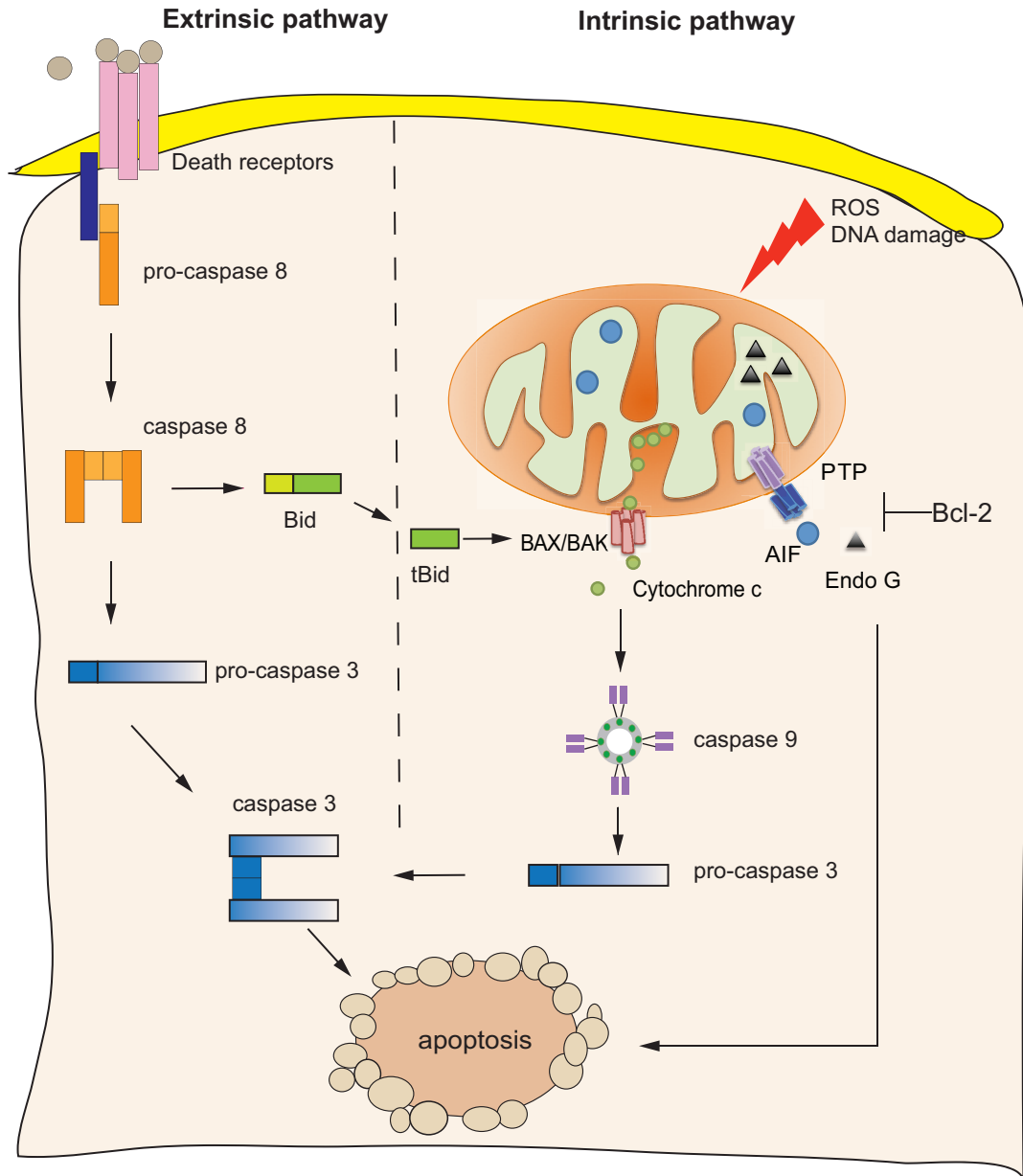


**Figure 1.2 Model of apoptotic pathways.** Intrinsic apoptosis is initiated by intracellular stresses, such as DNA damage and oxidative stress. These apoptotic stimuli lead to mitochondrial membrane permeabilization and the release of apoptotic factors. This pathway is tightly regulated by the Bcl-2 family of proteins that comprise anti-apoptotic and pro-apoptotic proteins. When pro-apoptotic proteins prevail, the released apoptotic factors, such as cytochrome c, stimulate formation of the 'apoptosome' that triggers the caspase cascade by activating downstream effector caspases such as caspase 3. Extrinsic apoptosis involves extracellular ligand-mediated activation of plasma membrane-localized death receptors, such as Tumor Necrosis Factor Receptors (TNFR). Activation of TNFR leads to the recruitment and activation of initiator caspase 8. Once caspase 8 is activated, it will in turn cleave and activate caspase 3, inducing apoptosis. The extrinsic and intrinsic apoptosis pathways are linked by the pro-apoptotic protein Bid.

mediated by Tumor Necrosis Factor Receptors (TNFRs) residing on the plasma membrane (Wang et al., 2008). Activation of TNFR by extracellular ligand stimulation leads to the recruitment and activation of initiator caspase 8. Once caspase 8 is activated, it will in turn cleave and activate caspase 3, inducing apoptosis. The extrinsic and intrinsic apoptosis pathways are linked by the pro-apoptotic protein Bid (Luo et al., 1998). Bid is a substrate of caspase 8. Full-length Bid resides in the cytosol, whereas caspase-8-truncated Bid translocates to mitochondria, where it binds to the pro-apoptotic protein Bax and thus transduces apoptotic signals from the death receptor to the mitochondria.

Evasion of cell death is a hallmark of human cancers (Hanahan and Weinberg, 2011). Insights into the mechanism of apoptotic signaling pathways shed light on potential apoptosis-targeted therapies. Drugs designed to activate the cell death machinery therefore represent promising therapeutic options. As describe above, mitochondria are central to the intrinsic apoptosis pathway (Wang and Youle, 2009). By releasing cell death factors that are normally sequestered inside the mitochondrial intermembrane space, mitochondria trigger caspase-dependent and independent forms of apoptosis (Estaquier et al., 2012). Ample studies illustrate that mitochondrial-centered apoptosis is blocked by oncogenic mutants in many cancer types (Bean et al., 2013; Fernald and Kurokawa; Modica-Napolitano et al., 2007). These oncogenic mutants may violate cell cycle checkpoints, as exemplified by tumor suppressor gene p53 that is frequently mutated in cancer cells (Muller and Vousden, 2013), or keep pro-apoptotic proteins in check by increasing anti-apoptotic protein expression (Bellance et al., 2009; Fulda, 2010; Gogvadze et al., 2008). For

instance, pro-apoptotic proteins Bax mutants are seen in ~50% of colorectal cancers (Miquel et al., 2005), while Bcl-2 overexpression is found in a majority of follicular lymphomas (Tsujiimoto et al., 1985). Such mitochondrial deficiencies are therefore supportive for tumor survival, and also account for a major cause of treatment failure (Fulda, 2009; Fulda and Debatin, 2006).

#### 1.2.1.2 Reprogramming of cancer mitochondrial metabolism pathway

One characteristic of cancer cells is their rapid growth (Hanahan and Weinberg, 2011). Fast growing tumors become hypoxic owing to the inability of the local vasculature to supply sufficient amounts of oxygen (Kroemer and Pouyssegur, 2008). Under those conditions, mitochondrial oxidative phosphorylation therefore might not be able to provide ATP for cell survival. To overcome energy limitations under hypoxic conditions, tumor cells reprogram their metabolism by increasing glucose uptake and stimulating aerobic glycolysis—a phenomenon termed the “Warburg effect” (Warburg et al., 1924). During mitochondrial respiration, pyruvate generated from glucose enters the citric acid cycle in the mitochondria where it is completely oxidized to carbon dioxide. In contrast, in glycolysis, pyruvate is converted to lactate in the cytoplasm (Kroemer and Pouyssegur, 2008). Metabolic reprogramming has been seen in most cancer cells and the molecular mechanisms underlying are complex. Activation of hypoxia-inducible factor-1 (HIF-1) by hypoxia stress (Brahimi-Horn et al., 2007; Semenza, 2013) is considered as a principal factor in tumor metabolic reprogramming. HIF-1 is a transcription factor that stimulates glycolysis by up-regulating its key factors (Semenza, 2003), such as glucose transporter (Hayashi et al., 2004) and hexokinase (Riddle et al., 2000). It also

compromises mitochondrial oxidative phosphorylation by activating pyruvate dehydrogenase kinase 1 (PDK1) (Kim et al., 2006). PDK1 inhibits pyruvate dehydrogenase and subsequently decreases the conversion of pyruvate to acetyl-CoA. Interestingly, cancer cells metabolize most of their glucose through glycolysis regardless of whether oxygen is present, suggesting that other mechanisms contribute to altered metabolism (Bellance et al., 2009; Chatterjee et al., 2006; Modica-Napolitano et al., 2007). One possible mechanism is that mtDNA mutants may cause mitochondria dysfunction. It has been seen that the  $\beta$ -F1 subunit of the ATPase is down-regulated in tumor mitochondria (Lopez-Rios et al., 2007), and a mutant mtDNA-encoded NADH dehydrogenase subunit 2 is expressed in head and neck squamous carcinoma (Zhou et al., 2007). Both mutants compromise mitochondrial oxidative phosphorylation, leading to the dependence on alternative energy-producing pathways. Of note, in addition to providing energy, glycolysis facilitates tumor growth by incorporating nutrients into biomass (DeBerardinis et al., 2007; Lunt and Vander Heiden, 2011), favors tumor invasion and metastasis by creating an acidic environment, and blocks apoptosis by stabilizing mitochondrial membranes (Mathupala et al., 2009).

Glucose addiction and glycolysis dependence renders cancer cells more vulnerable to specific metabolic perturbations than normal cells. Although there is a small subset of cancers displaying compromised mitochondrial metabolism due to mutations in the electron transport chain ETC complex (Lopez-Rios et al., 2007; Zhou et al., 2007), the majority of cancer cells retain functional mitochondria or even enhance mitochondrial metabolism (Wenner, 2012). Recent evidence indicate that

tumor mitochondria not only provide the majority of ATP for cell survival (Fan et al., 2013; Zu and Guppy, 2004), but also supply intermediates for biosynthesis, such as citrate for lipid synthesis (Metallo et al., 2012; Mullen et al., 2012), and ROS for tumorigenesis (Guzy et al., 2008; Woo et al., 2012) and metastasis (Ishikawa et al., 2008; Porporato et al., 2014). Thus, tumor-enhanced mitochondrial metabolism offers a rationale for therapeutic strategies.

#### 1.2.1.3 ROS elevation in cancer cells

Reactive oxygen species (ROS) are products of normal cellular metabolism and play vital roles in regulating cellular signaling pathways (Schieber and Chandel, 2014). The major site of ROS generation inside the cell is the mitochondria (Liu et al., 2002). In mitochondria, the electrons derived from the TCA cycle are passed down the electron transport chain (ETC) and transferred to oxygen at complex IV. This process is coupled with proton pumping across the inner mitochondrial membrane and the resultant electrochemical gradient provides free energy to drive ATP synthesis. During respiration, a leak of electrons to oxygen from complex I, II and complex III generates superoxide (Sabharwal and Schumacker, 2014). Complex IV is not implicated in ROS generation because of the increased binding affinity for oxygen upon receiving the first electron (Murphy, 2009). Complex V does not participate in electron transport directly, however, changes in complex V activity will effect mitochondrial membrane potential, which in turn favors ROS generation in other sites (Formentini et al., 2012; Martinez-Reyes and Cuezva, 2014; Sgarbi et al., 2006). The majority of superoxide is transferred to the mitochondrial matrix where it is dismutated to  $H_2O_2$  by the superoxide dismutases 2 (SOD2). Some of it is

transferred to the cytosol where it is dismutated to  $H_2O_2$  by the cytosolic superoxide dismutases 1 (SOD1) (Andreyev et al., 2005).  $H_2O_2$  is then decomposed to water and oxygen by catalase. Additionally, ROS is produced by NADPH oxidase in cytoplasm (Kimura et al., 2005). The generated ROS can be beneficial or harmful to cells, depending on the concentration. Specifically, a moderate level of ROS can promote cell proliferation and differentiation (Behrend et al., 2003; Wu, 2006), whereas excessive amounts of ROS cause oxidative damage to lipids, proteins and DNA, leading to cell death (Fig. 1.3) (Kimura et al., 2005; Perry et al., 2000). To defend against possible deleterious effects of ROS, cells have a sophisticated antioxidant system to scavenge excessive ROS. This system consists of enzymatic components, such as the dismutases and catalase mentioned above, the glutathione (GSH) system (Townsend and Tew, 2003), the thioredoxin system (Arner and Holmgren, 2000), and vitamin E (Traber and Atkinson, 2007) and C (Padayatty et al., 2003). GSH is the major component of antioxidant defenses, playing a central role in maintaining redox balance. Despite the presence of antioxidant systems, when the cellular redox balance is irreversibly disturbed, cell death occurs.

The mechanisms of ROS-mediated apoptosis have been addressed in many studies. First, ROS may damage mitochondrial DNA (mtDNA). mtDNA is a circular double-stranded DNA that is prone to oxidative damage due to its proximity to the ETC and lack of protein protection. ROS results in the rapid formation of DNA lesions, such as oxidized DNA bases, and single strand and double strand breaks (de Grey, 2005; Ishikawa et al., 2008; Maynard et al., 2009). Since mtDNA encodes 13 polypeptides of the respiratory chain, damaged mtDNA therefore reduces the

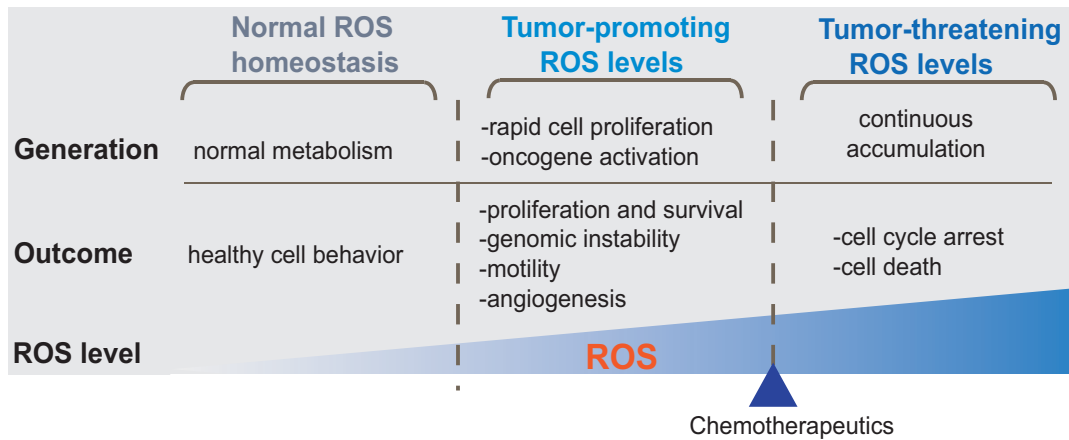


**Figure 1.3 The multiple effects of ROS.** The concentration of ROS determines cell fate. Low levels of ROS contribute to signal transduction and cell proliferation, whereas high levels of ROS threaten cell survival. Tumor cells harbor elevated levels of ROS in comparison to normal cells, providing a window for oxidative stress manipulations to kill tumor cells while sparing normal cells.

level of respiration components and compromises mitochondrial respiratory function. The resultant respiration deficiency further enhances ROS generation. This vicious cycle of ROS-mtDNA damage ultimately induces apoptosis by triggering mitochondrial permeability transition (Ricci et al., 2008).

Moreover, ROS-mediated apoptosis could be achieved by modifying apoptotic proteins (Boonstra and Post, 2004; Quinlan et al., 2013). For example, in response to H<sub>2</sub>O<sub>2</sub>-induced apoptosis, ROS reacts with Bax on cysteine residue 62, causing Bax conformational change, mitochondrial translocation, subsequent pore formation, and eventually impairment of mitochondrial membrane integrity (Nie et al., 2008). ROS could also directly trigger mitochondrial permeability transition by modifying mitochondrial permeability pore components, such as voltage-dependent anion channel (VDAC) (Madesh and Hajnoczky, 2001), adenine nucleotide translocator (ANT) (Giron-Calle et al., 1994) and cyclophilin D (cypD) (Baines et al., 2005). In addition to direct damage on mitochondrial components, ROS can induce apoptosis through several cytoplasmic signal transduction pathways, such as the MAPK pathway. Studies show MAPK family member c-Jun N-terminal kinases (JNKs) and p38 are implicated in the ROS-induced apoptotic pathway (Cherukuri and Nelson, 2008; Kang and Lee, 2008; Park et al., 2014). Both p38 and JNK are activated through Ask-1 (apoptosis signal-regulating kinase-1), whose activity is regulated by its interaction with the redox-regulated protein thioredoxin. While reduced thioredoxin binds and inhibits Ask-1, oxidation of thioredoxin by ROS releases ASK-1 and leads to JNK/p38 activation (Cherukuri and Nelson, 2008; Kang and Lee, 2008; Park et al., 2014). JNK/p38 in turn catalyze the phosphorylation of

anti-apoptotic proteins such as Bcl-2. Reduced anti-apoptotic activity of Bcl-2 causes the release of pro-apoptotic proteins, thus inducing cell death (Yamamoto et al., 1999). In addition, JNK alters the composition of the Bax/Bcl-2 complex by increasing the expression of Bax (Zhang et al., 2008) and Bak (Fan et al., 2001).

Additionally, ROS can induce apoptosis by targeting mitochondrial lipids. One such example is the oxidation of cardiolipin. Cardiolipin is an anionic phospholipid that is predominantly localized in the inner mitochondrial membrane (IMM) (Krebs et al., 1979). It binds cytochrome c to the outer leaflet of the IMM, where cytochrome c transfers electrons from complex III to complex IV (Ow et al., 2008). Cardiolipin is regarded as especially vulnerable to oxidative attack due to its unsaturated carbon chains and its proximity to ROS producing sites (Paradies et al., 2002; Petrosillo et al., 2003; Polyak et al., 1997). Oxidized cardiolipin distributes to the outer mitochondrial membrane where it functions as a docking platform for pro-apoptotic protein tBid, and also leads to a decreased interaction with cytochrome c (Liu et al., 2004; Lutter et al., 2000). tBid subsequently enhances the translocation and activation of Bax and Bak, leading to mitochondrial membrane permeabilization and cytochrome c release (Gonzalvez et al., 2005). Significant loss of cytochrome c subsequently disrupts the ETC, leading to secondary ROS production (Akopova et al., 2012; Huttemann et al., 2011; Petrosillo et al., 2003). Thus through modifications of nucleic acid, proteins or lipid, ROS impinges on multiple signaling cascades to regulate apoptosis.

Elevated cellular ROS levels—a condition known as oxidative stress—has been found in many cancer types. Oxidative stress results from increased

mitochondrial metabolism, mitochondrial dysfunction and/or oncogene activity (Kawanishi et al., 2006; Szatrowski and Nathan, 1991; Toyokuni et al., 1995). As discussed before, mitochondrial metabolism is boosted in cancer cells in order to provide sufficient ATP for cell survival (Ward and Thompson, 2012), with an estimation of 1~2% oxygen consumed by mitochondria contributing to ROS production (Chance et al., 1979). In addition, mtDNA mutants have also been linked to increased ROS level in some cancer types (Stratton, 2011). For example, mtDNA mutations of the ETC complex V, increase ROS generation (Mattiuzzi et al., 2004). Oncogenic transformation also increases ROS levels (DeNicola et al., 2011; Ogrunc et al., 2014). For instance, Ras- (Irani et al., 1997; Weinberg et al., 2010) or c-Myc- (Vafa et al., 2002) transformed human fibroblast cells produced elevated ROS. Elevated oxidative stress is often viewed as an adverse event, because ROS facilitates cancer initiation and progression by modifying signal pathways (Ray et al., 2012; Wu, 2006) and generating mtDNA mutants (Ishikawa et al., 2008). Therefore, ROS production correlates with the aggressiveness of tumor and poor prognosis (Hirsch et al., 2009; Shaw et al., 2005). To survive under higher oxidative stress and evade ROS-induced apoptosis, cancer cells increase the antioxidant response through increased expression of dismutases (Hu et al., 2005) and glutathione-related enzymes (Saydam et al., 1997). It is believed that the adaption to oxidative stress makes cancer cells more dependent on antioxidants for survival, and moreover, the ROS scavenging capacity of cancer cells to buffer further ROS insults by exogenous agents is reduced in comparison to normal cells (Pelicano et al., 2004; Trachootham et al., 2009) (Fig.1.3). Hence, ROS-based therapies are

currently exploited for clinical benefit. Based on these differences, drugs that target pathophysiological mitochondrial features are being evaluated as options to selectively kill cancer cells (Wenner, 2012).

### 1.2.2 Mitochondrial-targeting drugs

To date, several mitochondrial-targeted drugs have been investigated. These drugs are designed to trigger mitochondrial-centered cell death by releasing or activating proteins that mediate apoptosis; disrupting electron transport (Modica-Napolitano et al., 1996) and energy metabolism; or altering cellular redox potential, in particular ROS production (Pelicano et al., 2004; Trachootham et al., 2009; Wu, 2006).

#### 1.2.2.1 Drugs targeting Bcl-2

Taking advantage of the function of BH3-only proteins in promoting apoptosis, multiple BH3 mimetics have been developed as cancer therapeutics. BH3 mimetics ABT-737 and ABT-263 (navitoclax) are small molecule inhibitors of BCL-2, BCL-X<sub>L</sub>, and BCL-w (Lock et al., 2008; Oltersdorf et al., 2005). In preclinical studies, both ABT-737 and ABT-263 showed activity against multiple myeloma (Chauhan et al., 2007), acute lymphoblastic leukemia and lymphoma (High et al., 2010; Ishitsuka et al., 2012; Suryani et al., 2014). ABT-737 displayed low solubility and oral bioavailability, and thus the orally bioavailable ABT-263 was evaluated in phase I and II clinical trials of chronic lymphocytic leukemia (Kipps et al., 2015; Roberts et al., 2012; Suryani et al., 2014). Antitumor activity of ABT-263 was observed, along with hematologic toxicities. Insights into its toxic side effect revealed that inhibition of

BCL-X<sub>L</sub> by ABT-263 induced a rapid decrease in the number of circulating platelets (Kipps et al., 2015). The dose-limiting hematologic toxicities from ABT-263 highlighted the importance of BCL-X<sub>L</sub> in platelet survival. Understanding the molecular mechanism of toxicity led to the development of the BCL-2-specific inhibitor, ABT-199 (venetoclax), that retained antitumor activity while sparing platelets (Souers et al., 2013; Vandenberg and Cory, 2013). Data from a phase I trial of ABT-199 confirmed its anticancer activity in patients with relapsed/refractory chronic lymphocytic leukemia (CLL) and small lymphocytic lymphoma (SLL) achieving a response rate of 84% (Davids et al., 2013). Since then, ABT-199 has been widely evaluated in treating patients with non-Hodgkin lymphoma, follicular lymphoma (Davids et al., 2012), acute myelogenous leukemia, multiple myeloma (Touzeau et al., 2014) or chronic lymphocytic leukemia (CLL) (Seymour et al., 2013) as monotherapy or combination therapy (Cang et al., 2015). In 2016, the U.S. Food and Drug Administration approved ABT-199 for the treatment of patients with chronic lymphocytic leukemia.

#### 1.2.2.2 Drugs targeting metabolism

The concept of altered metabolism in tumor mitochondria was first introduced by Warburg about 70 years ago. This perception has since become the rationale that drives the discovery of metabolism targeting drugs. Interestingly, most anticancer drugs on the market or even drugs in treating other diseases, have metabolic targets (Rodriguez-Enriquez et al., 2014). For a large portion of them, the metabolic target is recognized long after the drugs were developed. For example, the widely used chemotherapy drug 5-fluorouracil (5-FU) inhibited tumor growth by interfering with

DNA synthesis, however, later studies demonstrated that the 5-FU active metabolite fluorodeoxyuridine monophosphate, bound to thymidylate synthase, thus inhibiting nucleic acid synthesis (Longley et al., 2003). Metformin, a drug for diabetic patients, also showed antitumor activity (Evans et al., 2005). The primary target of metformin was mitochondrial complex I, and the interaction between metformin and complex I impaired mitochondrial ETC in tumor cells (Viollet et al., 2012). As a consequence, metformin decreased blood glucose and consequently diminished circulating insulin levels. Insulin is known as a mitogen favoring tumor growth by stimulating the PI3K signaling pathway (Pollak, 2012), thus decreased insulin may further potentiate its antitumor activity.

At present, a multitude of drugs that are specifically designed to target different aspects of cancer cell metabolism are undergoing clinical trials. Two well-studied metabolism-targeting drugs are 2-deoxyglucose (2-DG) and Dichloroacetate (DCA). 2-DG is a glucose analog that acts as a competitive inhibitor of G6P isomerase. It is phosphorylated by HK to 2-DG-phosphate (2-DG-P), which cannot be further metabolized by G6P isomerase. Subsequently it inhibits the high rate of glucose metabolism in cancer cells (Aft et al., 2002). The anticancer activity of 2-DG was tested in patients with prostate cancer (Stein et al., 2010), glioblastoma and other advanced solid tumors (Landau et al., 1958), unacceptable toxicity was observed when it was administered to patients at doses that were sufficient to limit glucose metabolism in cancer cells. However, low doses of 2-DG was evaluated in combination with other chemotherapeutic agents, such as docetaxel (Raez et al., 2013), ABT-263 (Yamaguchi et al., 2011) or radiation therapy (Dwarakanath et al.,

2009), and the preliminary data suggested a clinical benefit from these combination therapies. DCA is a PDK inhibitor. In cancer cells, PDK is up-regulated by HIF (Michelakis et al., 2010). As described before, activated PDK favors glycolysis by negatively regulating the pyruvate dehydrogenase complex, thus DCA-mediated PDK inhibition leads to increased mitochondrial metabolism at the expense of glycolysis. *In vitro*, studies demonstrated that DCA depolarized mitochondria, increased mitochondrial reactive oxygen species, and induced apoptosis in glioblastomas derived from patients (Michelakis et al., 2010). Preliminary clinical results indicated that DCA was well tolerated by patients with glioblastoma (Michelakis et al., 2010). In addition, a complete remission was achieved with DCA in a patient with non-Hodgkin's lymphoma who was documented with relapse after conventional chemotherapy (Strum et al., 2013). DCA is currently being evaluated in several clinical trials in patients with head and neck cancer, glioblastoma and other solid tumors (Sborov et al., 2015). It is reported that DCA also showed potential in combination therapy. It increased cancer cell sensitivity to chemotherapeutic agents such as 5-FU (Xuan et al., 2014) and platinum-based chemotherapy (Garon et al., 2014). Insights into the mechanisms underlying the altered tumor metabolism will reveal more rational strategies in drug development.

#### 1.2.2.3 Drugs targeting mitochondrial ROS

The idea of inducing preferential cell death by manipulating ROS levels within tumor cells was firstly proposed in 1990s (Kong and Lillehei, 1998). To date, numerous ROS-targeted drugs have been investigated with an aim to either increase ROS generation or decrease ROS-scavenging capability (Trachootham et

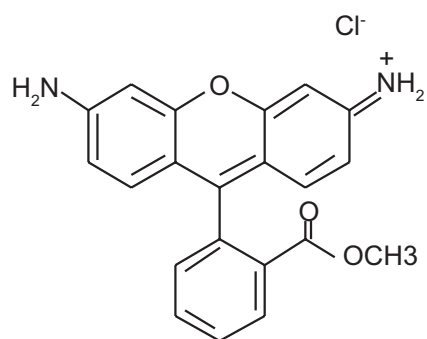
al., 2009). For instance, Motexafin gadolinium, a compound that preferentially accumulates in cancer cells, displayed an elevated oxidizing potential that triggered excess generation of ROS (Evens, 2004). Unfortunately, the results from a phase II trial in refractory chronic lymphocytic leukemia showed that intracellular generation of ROS was not optimal (Lin et al., 2009). However, Motexafin gadolinium successfully enhanced the *in vivo* response to radiation and chemotherapy of xenografted tumors, and recently, data from phase III clinical trials suggested it as a radiation sensitizer in brain metastasis (Mehta et al., 2009; Thomas and Khuntia, 2011). Another example of a ROS-inducing agent that was evaluated in clinical trials is arsenic trioxide. Arsenic trioxide exerted its effect mainly through impairing the function of the respiratory chain (Cha et al., 2006; Pelicano et al., 2003), and/or inhibiting thioredoxin and GSH systems, both of which led to ROS elevation and subsequent apoptosis (Lu et al., 2007). Arsenic trioxide was approved for the treatment of acute promyelocytic leukemia as an effective cancer therapeutic drug (Zhang et al., 2001). It also showed efficacy against a wide range of solid tumors (Murgo, 2001; Subbarayan and Ardalan, 2014). Of note, other ROS-targeting compounds show potential anticancer activities, such as thiol modifiers  $\beta$ -phenylethyl isothiocyanates (PEITCs) (Chen et al., 2011; Jiao et al., 1997) and Diamide (diazenedicarboxylic acid bis 5N,N-dimethylamide). Both of these compounds not only deplete the GSH pool by binding to thiols, but also oxidize the thiol of ANT (Costantini et al., 2000; Edelhauser et al., 1976). Decreased ANT disrupts mitochondrial membrane permeability, thereby inducing apoptosis (Vieira et al., 2000). In light of these finding, the elevated ROS generation in cancer cells

makes it an interesting target for anticancer drug discovery programs.

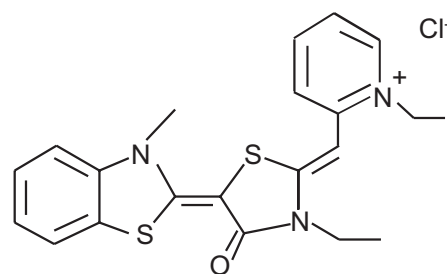
### 1.2.3 Mitochondrial-targeted drug: DLCs

Delocalized lipophilic cations (DLCs) are a class of compounds preferentially accumulating in mitochondria due to their lipophilic property and delocalized positive charge (Modica-Napolitano and Aprile, 2001). The discovery of DLCs dates back to the 1970s when an unexpected similarity was observed between fast dividing cancer cells and non-dividing cardiac muscle cells in their sensitivity to doxorubicin (Dox, Adriamycin). The non-specific toxicity was the main cause of serious and even fatal cardiomyopathy in patients (Bonadonna and Monfardini, 1969). To address the underlying mechanism, the accumulation and retention of Dox and its analogs in cardiac muscle cells *versus* non-muscle cells were measured *in vitro* (Lampidis et al., 1981). The study found positively charged compounds showed increased accumulation and nucleoli fragmentation in cardiac-muscle cells while neutral analogs accumulated poorly. The connection between the positive charge and drug accumulation was confirmed by a later finding that Rhodamine 123 (Rh123), a DLC compound, also preferential accumulated in cardiac muscle cells (Lampidis et al., 1984; Summerhayes et al., 1982) (Fig. 1.4). Moreover, Rh123 specifically accumulated in mitochondria and thus was utilized as a probe for mitochondria in living cells (Chen et al., 1982; Johnson et al., 1980). The association between positive charge and drug accumulation in turn led to a study which demonstrated that positively charged drugs preferentially accumulated in carcinoma cells as compared to normal epithelial cells (Lampidis et al., 1983). This selectivity was attributed to the higher plasma and/or mitochondrial membrane potentials of

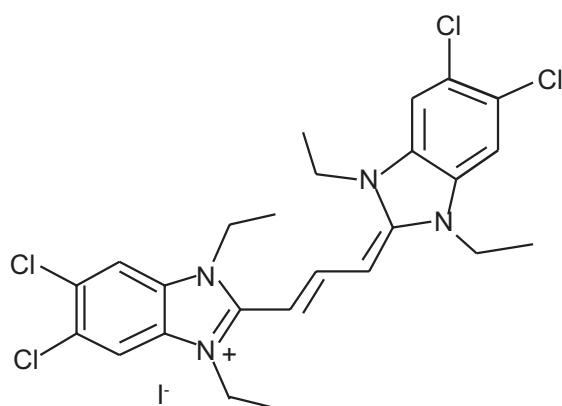
**Rh123**



**MKT-077**



**JC-1**



**TPP**

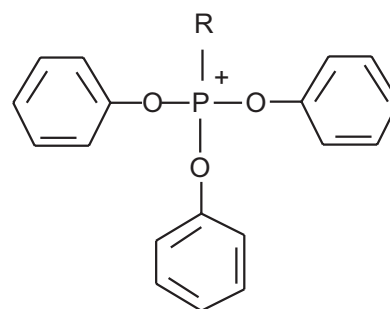


**Figure 1.4 Structures of DLCs**

carcinoma cells (Madak and Neamati, 2015; Modica-Napolitano and Aprille, 2001). Although the mechanisms underlying the higher membrane potentials in carcinoma cells remained unclear, it has been suggested that ATP synthase deficiency (Cuezva et al., 1997) and altered mitochondrial metabolism in cancer cells (Sukumar et al., 2016) may be contributing factors. Once inside the cell, DLCs accumulated in mitochondria, induced mitochondrial dysfunction and triggered cell death (Davis et al., 1985; Modica-Napolitano and Aprille, 2001). These early studies on DLCs have stimulated interest in their development as anti-cancer compounds (Bernal et al., 1983; Bleday et al., 1986; Lampidis et al., 1983; Lampidis et al., 1985; Sun et al., 1994). To date, a number of DLCs have been identified with selective toxicity to carcinoma cells over normal cells.

Rh123 was the first DLC to demonstrate anticancer toxicity. Early studies showed that *in vitro* continuous exposure of Rh123 selectively killed carcinoma cells while normal epithelial cells were relatively unaffected (Lampidis et al., 1983; Modica-Napolitano and Aprille, 1987). Rh123 mitochondrial-accumulation suggested that Rh123 might affect electron transport activity. Indeed, using freeze-thawed preparations of isolated mitochondria Rh123 was shown to impair  $F_0F_1$ -ATPase (Baracca et al., 2003; Castro et al., 1989; Modica-Napolitano and Aprille, 1987). Rh123 anticancer activity was then evaluated in animal models. Rh123 treatment prolonged the survival of tumor-bearing mice implanted with Ehrlich ascites tumor or mouse bladder carcinoma (Bernal et al., 1983; Modica-Napolitano and Aprille, 1987). Finally, a phase I clinical trial of Rh123 was carried out in hormone refractory prostate cancer patients, and the preliminary data indicated that this compound

could be safely administered to cancer patients, and therapeutic efficacy was also achieved as assessed by increased prostate-specific antigen (PSA) doubling time. However, the data did not reach statistical significance (Jones et al., 2005). As far as I know, further clinical examinations of Rh123 were not conducted due to a lack of sufficient positive data (Lawrence Jones, personal communication).

Another DLC that was evaluated in clinical trials is Rhodacyanine MKT-077 (Britten et al., 2000) (Fig. 1.4). MKT-077 and other rhodacyanine dyes were known as sensitizers for silver halides (James, 1977). They were discovered in a screening program performed by Fuji Photo Film Co., Ltd to identify suitable DLCs for clinical trials. 1000 rhodacyanine dye candidates exhibited anticancer activity, and MKT-077 was chosen for further characterization due to its favorable properties, such as high solubility and low toxicity to normal cells (Koya et al., 1996). MKT-077 preferentially accumulated in cancer cell mitochondria (Koya et al., 1996), whereby it inhibited the growth of multiple human cancer cell lines, including colon carcinoma CX-1, breast carcinoma MCF-7, pancreatic carcinoma CRL 1420 and melanoma LOX, while normal epithelial cells were spared (Chiba et al., 1998b). MKT-077 also inhibited the proliferation of cells obtained from fresh surgical specimens. The efficacy rates (sensitive cases/total evaluated cases) were 52.6% for gastric cancer, 77.8% for colon cancer, and 35.7% for hepatocellular carcinoma, resulting in an overall efficacy rate of 52.4% (Chiba et al., 1998b). MKT-077 efficacy was then tested and confirmed in several animal models. For example, MKT-077 inhibited the growth of implanted human renal and prostate carcinoma in nude mice and prolonged the survival of mice bearing human melanoma xenografts (Koya et al., 1996). Safety

assessment studies in animal models indicated that the respiratory rate of rat liver mitochondria was decreased, however, this effect was reversed following drug withdrawal (Chiba et al., 1998a). Insights into its mechanism of action indicate that MKT-077 selectively inhibited cancer cells through two proposed mechanisms: perturbation of mitochondrial membranes and concomitant non-specific inhibition of mitochondrial respiratory chain components; and/or MKT-077-binding to HSP70 causing p53 translocation and cell growth inhibition (Chunta et al., 2012; Wadhwa et al., 2000). These findings lead to subsequent evaluation of MKT-077 in clinical trials. One phase I trial of MKT-077 was performed with patients of various advanced cancers. Results indicated that the drug efficiency was not satisfactory; only one renal cancer patient attained stable disease while the remainder had progressive disease. Further recruitment was halted as the renal toxicity was found to be eventually irreversible in animal models (Propper et al., 1999). Of note, in another independent clinical trial, it was reported that this adverse effect could be well controlled in patients treated with magnesium supplementation. Unfortunately, drug efficiency was not fully demonstrated in this report (Britten et al., 2000). To enhance the effectiveness, MKT-077 analogs with improved selective activity, such as JG98, have been synthesized and evaluated both *in vitro* and *in vivo* (Abdul and Hoosein, 2003; Li et al., 2013; Rousaki et al., 2011). JG98 inhibited cancer cell growth by modulating the interaction between HSP70 and its co-chaperone BAG3 (as described in 1.1) (Li et al., 2015). Owing to its HSP70 binding activity, MKT-077 and its analogs have also been investigated in the treatment of misfolding disorders, particularly tauopathies such as Alzheimer's disease (AD) (Umesh et al., 2014).

Thus, although the therapeutic benefits of MKT-077 have yet to be ascertained, it currently serves as a prototype for the development of novel DLCs that might seek their applications in both cancer and other diseases.

It is interesting to note that based on their mitochondria-sensing ability, DLCs have been developed for various applications. Fluorescent DLCs, such as Rh123 and JC-1 (Fig. 1.4), have become important tools for directly measuring mitochondrial membrane potential (Kodiha et al., 2015; Smiley et al., 1991). In addition, the mitochondria-targeting aspects of these compounds make them potential vehicles for targeted drug delivery (Madak and Neamati, 2015; Murphy and Smith, 2000). It is well established that drug efflux caused by multidrug resistance proteins (MRPs) overexpression lowers the intracellular concentration of anticancer agents, resulting in a protective effect for cancer cells (Higgins, 2007). It is speculated that mitochondrial membrane potential can provide sufficient driving force for DLC conjugated compounds to overcome drug efflux mechanisms. For example, the most commonly used DLC to transport anticancer drugs to mitochondria is triphenylphosphonium (TPP) (Madak and Neamati, 2015) (Fig. 1.4). TPP-conjugated doxorubicin was able to enter doxorubicin-resistant MDA-MB-435 cells, and correspondingly, enhanced its cytotoxicity (Han et al., 2014). Clearly, the structural variety of DLCs contributes to their broad applications, and further investigation into DLCs will expand their uses in biological research.

#### 1.2.4 Determination of apoptosis

Several biochemical features are routinely used to identify cells undergoing apoptosis. These markers include phosphatidylserine exposure, loss of

mitochondrial membrane potential, caspase activation and DNA fragmentation (Borden et al., 2008; Yang and Goping, 2013). Phosphatidylserine (PS) exposure is recognized as a universal phenomenon during apoptosis (Borisenko et al., 2003). In normal conditions, PS is restricted to the inner leaflet of the lipid bilayer, and this lipid asymmetry is maintained by a combined action of flippases, scramblases and transfer proteins (Hankins et al., 2015). After induction of apoptosis, the scramblase Xkr8 is activated by caspase cleavage, and the active Xkr8 promotes the exposure of PS on the cell surface (Marino and Kroemer, 2013). Also, flippase ATP11A and ATP11C are cleaved by caspases during apoptosis (Nagata et al., 2016), consequently, PS is flipped from the inner to the outer bilayer of cell membrane (Bever and Williamson, 2010). Of note, other non-caspase-dependent factors, for example Apoptosis-Inducing-Factor (AIF) may contribute to PS exposure (Susin et al., 1999). Annexin V, a blood-clotting factor that exhibits a high specificity for PS (van Engeland et al., 1998), is widely used to detect exposed PS in apoptotic cells.

Loss of mitochondrial membrane potential ( $\Delta\psi$ ) is another important indicator of apoptosis.  $\Delta\psi$  is created during mitochondrial respiration, whereby the reductive transfer of electrons through electron transport Chains (Complex I-IV) provides the energy to pump protons out of the mitochondria inner membrane.  $\Delta\psi$  is a charged gradient. The forces from  $\Delta\psi$ , along with the mitochondrial pH gradient, are used by F1/F0 ATP-synthase (complex V) to generate ATP (Perry et al., 2011). In response to apoptotic stimuli, this membrane potential is disturbed (Dussmann et al., 2003; Gottlieb et al., 2003). The collapse of mitochondrial membrane potential coincides with the opening of the Bax/Bak pore (Feldmann et al., 2000) or/and mitochondrial

permeability transition pores (Tsujiimoto and Shimizu, 2007), resulting in the release of mitochondrial resident death factors. Mitochondrial potential can be detected using fluorescent cationic dyes such as DiOC6 (3,3'-dihexyloxacarbocyanine iodide), that accumulate in healthy mitochondria and do not stain apoptotic cells that have undergone electrochemical potential loss.

Active caspases are responsible for the morphological features of apoptotic cells, such as membrane blebbing, cell rounding and detachment from neighbors (Johnson et al., 2000; Shi, 2002; Thornberry, 1999). The caspase family is composed of highly conserved cysteine proteases that are synthesized as inactive pro-caspases. They are generally grouped into initiator caspases (caspase 2, 8, 9 and 10) and executioner caspases (caspase 3, 6 and 7). In response to apoptosis, initiator pro-caspases undergo an autocatalytic intrachain cleavage that results in the activation and stabilization of active initiator caspases. Executioner caspases, on the other hand, are activated by proteolytic cleavage, which is carried out by upstream initiator caspases and/or other proteases. Active caspases, mostly caspase 3, in turn induce the morphological changes of apoptotic cells by acting on a variety of downstream factors (Johnson et al., 2000). For example, by activating the downstream target ROCK (Rho-associated kinase 1) (Chang et al., 2006; Coleman et al., 2001), caspases trigger cell blebbing; by inactivating cytoskeletal constituents, such as actin, tubulin and vimentins, caspases cause cell rounding (Ndozangue-Touriguine et al., 2008; Taylor et al., 2008); by cleaving cell-matrix focal adhesion sites, caspase detach apoptotic cells from neighboring cells or the extracellular matrix (Levkau et al., 1998; Sasaki et al., 2002). Therefore, caspase activation is a

hallmark feature of apoptosis and plays an essential role in the ordered dismantling of cell components.

DNA fragmentation occurs as one of the final stages of apoptosis (Nagata, 2000). Active caspases cleave the inhibitor/chaperone ICAD/DFF-45 (inhibitor of caspase-activated DNase), which forms a complex with the nuclease CAD/DFF-40 (caspase-activated DNase) in the cytoplasm. This cleavage results in release and migration of CAD/DFF-40 to the nucleus. In the nucleus, CAD/DFF-40 cleaves spacer DNA that is not associated with histones, resulting in the characteristic DNA ladder pattern (Enari et al., 1998; Sakahira et al., 2001). The DNA ladder in apoptotic cells is usually observed by agarose gel electrophoresis.

### **1.3 Photodynamic therapy (PDT)**

The therapeutic properties of light have been known for thousands of years. According to historical records, ancient Egyptian, Indian and Chinese civilizations used light to treat various diseases, including psoriasis and skin cancer (Dolmans et al., 2003). However, it was not until the early 1900s that light therapy, in combination with certain chemicals, was experimentally tested in cancer treatment. This work led to the beginning of modern photodynamic therapy.

Rather than single targeted therapy, PDT is a combination therapeutic approach. It consists of three essential components: a photosensitizer, oxygen and light (Fig 1.5A). A photosensitizer is a light-absorbing compound that becomes activated from a ground state to a relatively long-lived electronically excited state when exposed to specific wavelengths of light (Dolmans et al., 2003). As it returns to

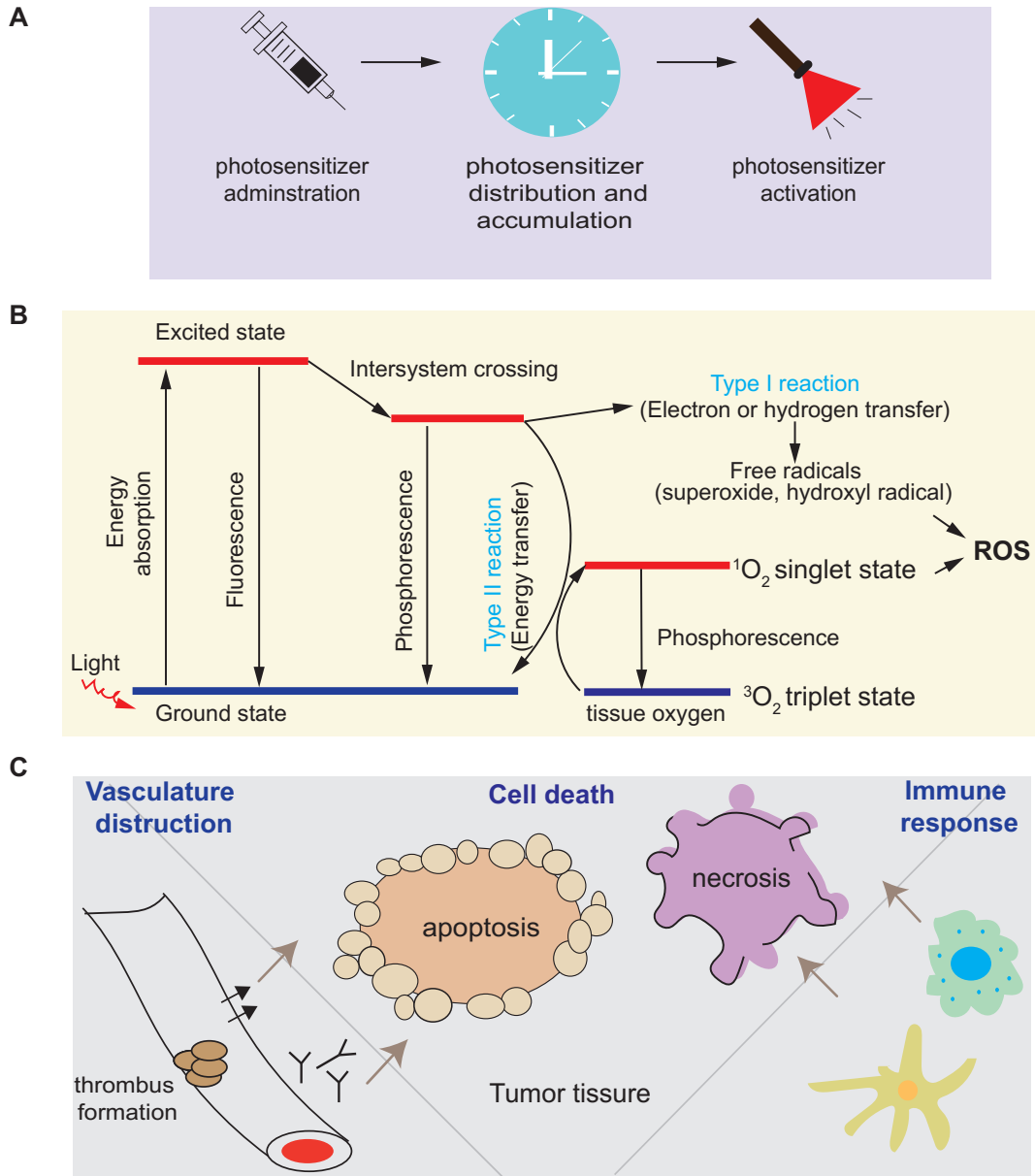


**Figure 1.5 Photodynamic therapy.** **A.** The procedure of photodynamic therapy includes three steps: photosensitizer administration, distribution and activation. **B.** Photosensitization processes. In response to light exposure, the photosensitizer absorbs energy and reaches an excited state. The excited photosensitizer returns to ground state emitting fluorescence, or undergoes intersystem crossing to an excited triplet state and then either forms radicals via a type I reaction or transfers its energy to molecular oxygen and forms singlet oxygen. Both free radicals and singlet  $^1\text{O}_2$  cause damage to cells. **C.** Three mechanisms contribute to PDT-induced tumor destruction: directly killing cancer cells, destroying vasculature and evoking immune response.

the ground state, the photosensitizer releases energy. This energy either reacts with a cellular substrate, such as the cell membrane or molecule, to form radicals, or is directly transferred to oxygen to generate singlet oxygen—a higher reactive oxygen species (Vrouenraets et al., 2003) (Fig. 1.5B). The principle therapeutic value of PDT lies in targeting cancer by the site-specific generation of ROS. Studies have demonstrated that photosensitizers preferentially accumulate in neoplastic lesions (Hahn et al., 2006; Sibani et al., 2008; Svensson et al., 2007). Given that the biological responses to photosensitizers are activated only in the areas of tissue that have been exposed to light, the selective cytotoxicity of PDT to cancer cells would be enhanced by the precise administration of light exposure to targeted areas.

Numerous studies have elucidated the underlying mechanisms of PDT-mediated toxicity. To date, it is believed that there are three main mechanisms involved in PDT-induced tumor destruction (Agostinis et al., 2011) (Fig 1.5C). First, PDT kills tumor cells directly by eliciting either apoptosis (He et al., 1996; Oleinick et al., 2002) or necrosis (Buytaert et al., 2007; Vanlangenakker et al., 2008). Due to the short half-life and spatially limited diffusion of the effector species, ROS, intracellular targets of PDT and induced cell death pathways depend on the intracellular localization of the photosensitizer (Moan et al., 1989). While in theory, the photosensitizer can accumulate almost anywhere within the cell, mitochondria and ER are the preferential targets (Vrouenraets et al., 2003). Photosensitizers that localize within mitochondria or the endoplasmic reticulum (ER) promote apoptosis (Kessel, 2002; Moserova and Kralova, 2012; Oleinick et al., 2002), while activation of photosensitizers targeting either the plasma membrane or lysosomes instead

induces necrosis (Allison and Sibata, 2010). Light intensity is another factor determining cellular fate in response to PDT. Specifically, necrosis appears to be the predominant mode of cell death when cells are strongly photosensitized, while apoptosis becomes the principal cell death pathway when photosensitization is not extensive (Henderson et al., 1985). Given that apoptosis is the preferred pathway for therapeutic intervention, the precise administration of photosensitizer and light intensity are critical parameters in the PDT procedure. How PDT causes apoptosis is yet to be defined. It has been showed that early in mitochondrial-mediated cell death, cytochrome c was released. Cytochrome c then participated in the formation of the apoptosome complex that ultimately activated caspase 3 (He et al., 1996; Xue et al., 2001). Some studies also showed that intracellular  $Ca^{2+}$  was responsible for the increase in mitochondrial membrane permeabilization, and therefore contributed to PDT-induced apoptosis. Notably, high ROS generated by PDT could activate caspases 8 and 3 through the induction of the FAS/TNF receptor multimerization; thus, an extrinsic apoptotic pathway was involved in PDT-induced killing (Liu et al., 2010). Interestingly, Bcl-2 is an antagonistic factor that prevents apoptosis by inhibiting the cleavage of pro-caspase 3 and 9 (He et al., 1996). Additionally, Bcl-2 may undergo direct oxidative damage from PDT-generated ROS, which down-regulates its anti-apoptotic activity (Usuda et al., 2003; Xue et al., 2001). ER is another organelle widely studied as a PDT subcellular target. Recent data indicated that PDT caused the induction of c/EBP homologous protein (CHOP), activation of the ER stress-mediated caspase-12 and eventually apoptosis (Moserova and Kralova, 2012).

Vasculature is aberrantly activated during tumorigenesis, and tumor-associated vasculature facilitates cancer proliferation and metastasis by providing an adequate supply of nutrients and oxygen (Chung et al., 2010; Nishida et al., 2006). PDT, in addition to effects on cancer cells, has also been shown to damage the tumor-associated vasculature, leading to tumor infarction. ROS production after drug and light administration caused the shutdown of vessels, which consequently deprived the tumor cells of nutrients and oxygen (Chen et al., 2006; Tseng et al., 1988). PDT also increased tumor vessel permeability, which in turn facilitated the accumulation of other anticancer drugs, such as Doxil (a liposome-encapsulated formulation of doxorubicin). Administration of doxil after PDT potentiated its tumor selectivity (Snyder et al., 2003). Indeed, vascular-targeted PDT represents an important research direction in PDT development (Azzouzi et al., 2013).

Finally, PDT can activate an inflammatory and immune response against tumor cells (Kabingu et al., 2007; Kousis et al., 2007; Sur et al., 2008). In contrast to most cancer therapies that are generally immunosuppressive, PDT may induce a pro-inflammatory response. Evidence has been found of leukocytes infiltrating tumor areas, increased presentation of tumor-derived antigen T-cells as well as recruitment of host leukocytes, lymphocytes, neutrophils and macrophages into tumor tissues (Krosl et al., 1995). In contrast, in some tumor-bearing mice models, depletion of neutrophils decreased the PDT mediated growth inhibition. Research into this mechanism suggested that stimulation of dendritic cells (DCs) by dead and dying tumor cells played an important role in the PDT-mediated enhancement of anti-tumor immunity (Kousis et al., 2007; Sur et al., 2008). Interestingly, tumor lysates

isolated following PDT could be used to vaccinate mice against the development of further tumors, indicating the potential use of PDT in systemic immune therapy (Gollnick et al., 2002; Korbek et al., 2007). Direct cell damage, anti-vascular effect and immune response can also enhance each other. As described above, tumor destruction is maximized in photodynamic therapy.

Although the potential of PDT has been recognized for more than 25 years, it is only now starting to be used in the clinic. The first photosensitizer, Porfimer sodium, received approval for PDT in the 1990s; it is widely used and remains the most common photosensitizer for the treatment of cancers, including early-stage lung cancers, superficial gastric cancer, oesophageal adenocarcinoma, cervical cancer, and bladder cancer (Brown et al., 2004; Dolmans et al., 2003). PDT has also been used for other indications in which a cure is not feasible. For instance, in advanced lung cancer, studies showed PDT might achieve tumor necrosis and reopening of the airway, thereby improving the quality of patients' life (Moghissi et al., 1999). At present, more than 5 photodynamic therapy drugs have been approved for oncological indications and over 200 clinical trials are being tested (O'Connor et al., 2009). However, several unfavorable properties of PDT slow its application in oncology. These include skin sensitivity, low efficiency caused by oxygen shortage in tumor cells, and lack of a proper light source for photo-activation. Chemical and biological research has sought to overcome these limitations. Work has been done to identify new photosensitizers with a higher selectivity for tumor cells and stronger absorption at longer generation lengths, and also to improve the PDT administration protocol, for instance by fractionating PDT light delivery to allow re-oxygenation of

the tissue. With continuing efforts, PDT may potentially be integrated into the mainstream of cancer treatment.

#### **1.4 D112**

Cyanine dye D112 was identified by the Eastman Kodak Company through a cancer drug screening program initiated at the Dana Farber Institute in the 1970s (Gilman et al., 2006). Cyanine dyes with certain reduction potentials could shut off the photoelectronic activity of silver halide substrates, and therefore they were used to control silver halide responses in emulsions. This property suggested that cyanine dyes had a potential to modify electronic events in living cells. To test the biological activity of cyanine dyes, 22 cyanine dyes were added to fertilized sea urchins eggs, and the effects on division and mitotic apparatus formation were observed using microscopy (Zigman and Gilman, 1980). Cyanine dyes with reduction potential more negative than -1.0 volt penetrated the cells, entered all subcellular compartments and inhibited mitosis and cell growth. Dyes with more negative electrochemical potential caused the greatest inhibition of mitosis. It was postulated that the inhibitory activity of cyanine dyes was due to interrupted electrochemical interactions between macromolecules and electrons, and one of the possible sites were mitochondria. The authors suggested that dyes with electrochemical potential more negative than that of respiratory chain components could occupy electron acceptor sites, disrupting the transport of electrons and cellular respiration that eventually slowed the synthesis of macromolecules and delayed mitosis (Zigman and Gilman, 1980).

Building on this discovery, the Kodak Laboratory selected drugs for screening of anti-cancer properties based on their electrochemical reduction potential (Gilman et al., 2006). Briefly, a variety of cancer cells and normal cells were seeded in 48-well plates, and serial dilutions of each compound were added to the cell culture. After a 7-day incubation period, cell survival/growth was tested using an MTT assay. It was observed that the electrochemical potential of each compound was associated with selective toxicity to cancer cells. Specifically, compounds with an electrochemical potential around -1 V had higher selective toxicity towards cancer cells. Approximately 2000 dye structural variants were tested and D112 (2-((E)-((2Z,5E)-3,3'-diethyl-5-(3-ethylbenzo[d]thiazol-2(3H)-ylidene)-4,4'-dioxo-3',4,4',5-tetrahydro-2'H,3H-[2,5'-bithiazolylidene]-2'-ylidene)methyl)-3-ethylbenzo[d]thiazol-3-ium iodide) (Fig. 1.6A), with an electrochemical potential of -1.1V, emerged as a lead compound with higher cytotoxic activity against a cancer cell line versus a non-transformed cell line. Specifically, the IC<sub>50</sub> of D112 to the normal monkey kidney epithelial cell line CV-1 was 9 µg/ml (1 µg/ml = 1.4 µM), compared to 0.01 µg/ml to the human colon cancer cell line CX-1. The compound thus achieved a killing ratio (IC<sub>50</sub> CV-1/ IC<sub>50</sub> CX-1) of 900 (Fig. 1.6B). Furthermore, D112 showed enhanced selectivity compared to the widely used clinical chemotherapeutic agent, Adriamycin (Fig. 1.6C). Due to changes in industry priorities, investigations into D112 were not further pursued despite these promising results.

Dr. Paul Gilman, the scientist who formerly worked on cyanine sensitizing dyes at the Eastman Kodak Company, brought D112 to our attention. We became particularly interested in D112 due to its apparent preferential killing of cancer cells.

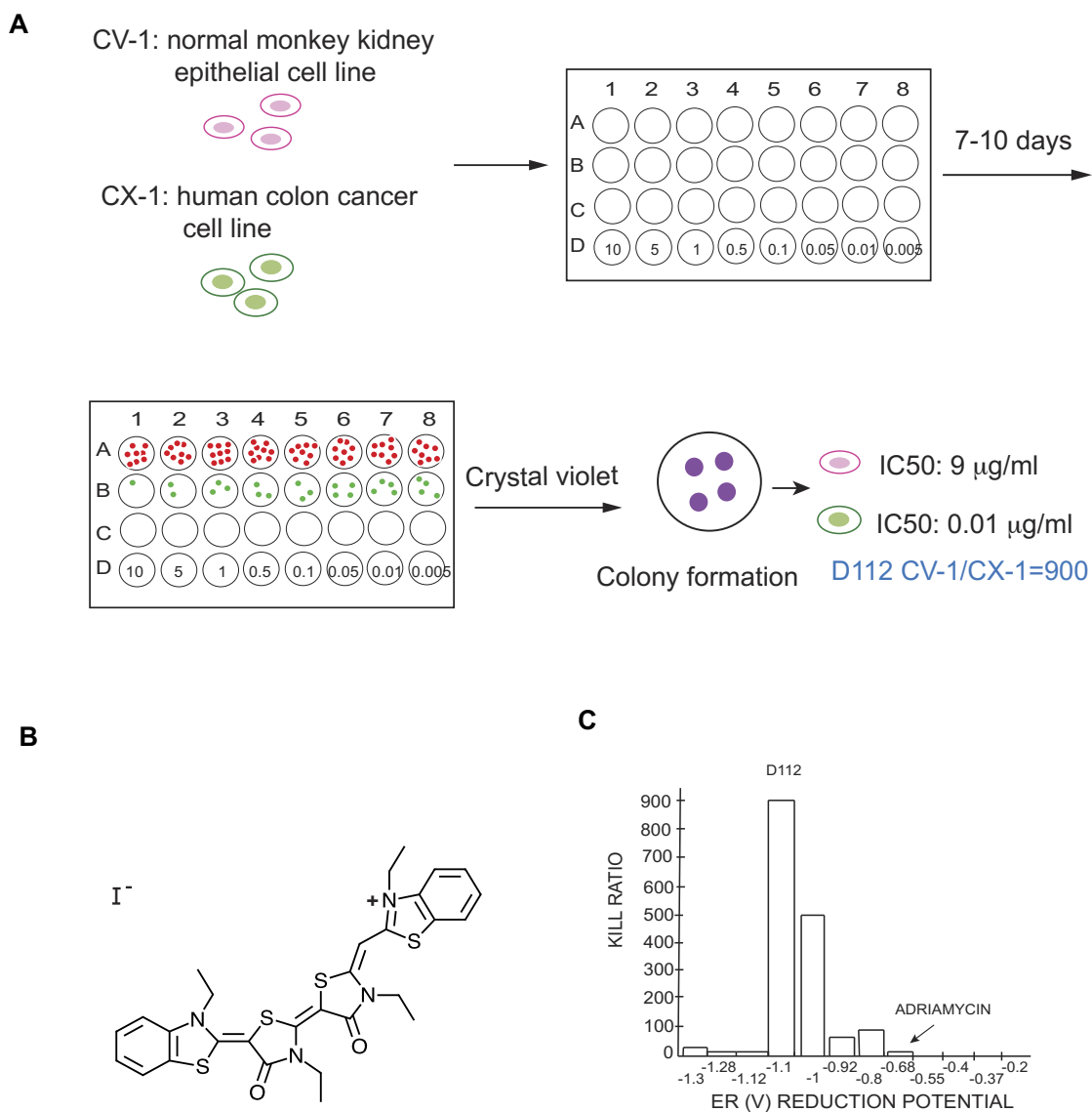


**Figure 1.6 Summary of first report of D112 cytotoxicity *in vitro*.** **A.** Cytotoxicity assay. A non-transformed (CV-1) and cancer (CX-1) cell lines were incubated with D112 at indicated concentrations ( $\mu\text{g/ml}$ ). Cell survival was assessed by crystal violet staining (Gilman et al., 2006). **B.** D112 structure. **C.** Killing ratio of tested cyanine dyes relative to reduction potentials. D112 (with a reduction potential of -1.1 V) is indicated. Adriamycin is also shown.

We first did a general assessment on the “druggable” properties of D112 using Osiris Property Predictor (a computer program available through the Organic Chemistry Portal: [www.organic-chemistry.org/prog/peo](http://www.organic-chemistry.org/prog/peo)). In this program, a “drug score” was applied to judge the compound’s overall potential as a qualified drug. This score was calculated by evaluating as toxicity risks, molecular weight, solubility and hydrophilicity (or absorption). We also compared D112 with several other chemotherapeutic drugs already in use (Fig. 1.7). We found that D112 had several unattractive properties: it carried a risk of producing deleterious reproductive side effects and had a low solubility caused by a poor total surface area. Despite this, D112 showed no risk of tumorigenicity, mutagenicity and irritating effects. It scored 0.21 overall, which was higher than some of the other drugs assessed, such as docetaxel and fluorouracil. Thus we decided to investigate the properties of D112 with respect to cellular cytotoxicity.

## Drug Evaluation

	Mutagenic	Tumorigenic	Irritant	Reproductive effect	cLogP	Solubility	Molweight	Drug-Score	Druglikeness
D112	Green	Green	Green	Red	1.4	-6.88	593	0.21	4.75
Docetaxel	Green	Green	Green	Green	2.61	-5.81	807	0.16	-60.4
Cyclophosphamide	Red	Red	Green	Red	0.73	-1.9	260	0.1	-10.3
paclitaxel	Green	Green	Green	Green	3.19	-6.29	853	0.22	0.19
Doxorubicin	Green	Green	Red	Green	0.17	-4.51	543	0.33	7.19
Epirubicin	Green	Green	Red	Green	0.17	-4.51	543	0.33	7.19
Methotrexate	Green	Red	Green	Green	-1.23	-3.77	454	0.22	-7.09
fluorouracil	Red	Red	Red	Red	-0.04	-1.76	130	0.06	-4.5
Carboplatin	Red	Green	Green	Green	-0.08	-0.69	353	0.28	-11.4

**Figure 1.7 In silico comparison of “drug-like” properties of D112 relative to currently used chemotherapeutic agents.** Drug properties were assessed by Osiris Property Predictor. Green: low risk; Red: high risk; cLog p: measure of the compound's hydrophilicity. High logP values indicate poor absorption or permeation; Solubility: the aqueous solubility of a compound. Low values indicate low solubility. Low solubility indicates poor absorption; Druglikeness: evaluation of a compound's druglikeness based on properties such as cLogP and molecular weights. Low values indicate poor drug properties. Drug-score: combination of druglikeness, cLogP, solubility, molecular weight and toxicity risks that is used to judge the compound's overall potential as a drug.

## 1.5 Research Objective

Owing to a high failure rate in the development of anticancer drugs, there is a pressing need to identify novel compounds with a greater discrimination for cancer cells. Given the cancer cell selectivity for DLCs in general, and D112 specifically, we decided to investigate whether D112 had potential as an anti-cancer agent. Thus we initially explored the mechanism of cellular cytotoxicity for D112. I first characterized D112-induced cell death in cancer cells and extended its selective cytotoxicity against a panel of cell lines derived from solid tumors (Chapter 3). Next, I sought to identify the molecular mechanism of D112-induced toxicity. Encouraged by the observation that D112 induced apoptosis, I investigated methodologies with which to increase the apoptotic index between cancer and non-transformed cells. In consideration of the inherent fluorescent properties of D112, I identified a strong response to photo-activation (Chapter 4). Thus, the discoveries from this thesis re-introduce an “old” molecule as a potential prototype for novel photodynamic therapy applications in the future.

## Reference

- Abdul, M., and Hoosein, N. (2003). Potentiation of the antiproliferative activity of MKT-077 by loperamide, diltiazem and tamoxifen. *Oncol Rep* 10, 2023-2026.
- Aft, R.L., Zhang, F.W., and Gius, D. (2002). Evaluation of 2-deoxy-D-glucose as a chemotherapeutic agent: mechanism of cell death. *Br J Cancer* 87, 805-812.
- Agostinis, P., Berg, K., Cengel, K.A., Foster, T.H., Girotti, A.W., Gollnick, S.O., Hahn, S.M., Hamblin, M.R., Juzeniene, A., Kessel, D., *et al.* (2011). Photodynamic therapy of cancer: an update. *CA Cancer J Clin* 61, 250-281.
- Akopova, O.V., Kolchinskaya, L.I., Nosar, V.I., Bouryi, V.A., Mankovska, I.N., and Sagach, V.F. (2012). Cytochrome C as an amplifier of ROS release in mitochondria. *Fiziol Zh* 58, 3-12.
- Alam, J.J. (2003). Apoptosis: target for novel drugs. *Trends Biotechnol* 21, 479-483.
- Allison, R.R., and Sibata, C.H. (2010). Oncologic photodynamic therapy photosensitizers: a clinical review. *Photodiagnosis Photodyn Ther* 7, 61-75.
- American Cancer Society (2014). *Cancer Facts & Figures 2014*.
- Andre, M., Mounier, N., Leleu, X., Sonet, A., Brice, P., Henry-Amar, M., Tilly, H., Coiffier, B., Bosly, A., Morel, P., *et al.* (2004). Second cancers and late toxicities after treatment of aggressive non-Hodgkin lymphoma with the ACVBP regimen: a GELA cohort study on 2837 patients. *Blood* 103, 1222-1228.
- Andreyev, A.Y., Kushnareva, Y.E., and Starkov, A.A. (2005). Mitochondrial metabolism of reactive oxygen species. *Biochemistry (Mosc)* 70, 200-214.
- Armstrong, G.T., Liu, W., Leisenring, W., Yasui, Y., Hammond, S., Bhatia, S., Neglia, J.P., Stovall, M., Srivastava, D., and Robison, L.L. (2011). Occurrence of multiple subsequent neoplasms in long-term survivors of childhood cancer: a report from the childhood cancer survivor study. *J Clin Oncol* 29, 3056-3064.
- Arner, E.S., and Holmgren, A. (2000). Physiological functions of thioredoxin and thioredoxin reductase. *Eur J Biochem* 267, 6102-6109.
- Assimon, V.A., Gillies, A.T., Rauch, J.N., and Gestwicki, J.E. (2013). Hsp70 protein complexes as drug targets. *Curr Pharm Des* 19, 404-417.
- Azzouzi, A.R., Barret, E., Moore, C.M., Villers, A., Allen, C., Scherz, A., Muir, G., de Wildt, M., Barber, N.J., Lebda, S., *et al.* (2013). TOOKAD((R)) Soluble vascular-targeted photodynamic (VTP) therapy: determination of optimal treatment conditions

and assessment of effects in patients with localised prostate cancer. *BJU Int* 112, 766-774.

Baines, C.P., Kaiser, R.A., Purcell, N.H., Blair, N.S., Osinska, H., Hambleton, M.A., Brunskill, E.W., Sayen, M.R., Gottlieb, R.A., Dorn, G.W., *et al.* (2005). Loss of cyclophilin D reveals a critical role for mitochondrial permeability transition in cell death. *Nature* 434, 658-662.

Bang, Y.-J., Van Cutsem, E., Feyereislova, A., Chung, H.C., Shen, L., Sawaki, A., Lordick, F., Ohtsu, A., Omuro, Y., Satoh, T., *et al.* Trastuzumab in combination with chemotherapy versus chemotherapy alone for treatment of HER2-positive advanced gastric or gastro-oesophageal junction cancer (ToGA): a phase 3, open-label, randomised controlled trial. *The Lancet* 376, 687-697.

Baracca, A., Sgarbi, G., Solaini, G., and Lenaz, G. (2003). Rhodamine 123 as a probe of mitochondrial membrane potential: evaluation of proton flux through F<sub>0</sub> during ATP synthesis. *Biochim Biophys Acta* 1606, 137-146.

Bean, G.R., Ganesan, Y.T., Dong, Y., Takeda, S., Liu, H., Chan, P.M., Huang, Y., Chodosh, L.A., Zambetti, G.P., Hsieh, J.J., *et al.* (2013). PUMA and BIM are required for oncogene inactivation-induced apoptosis. *Sci Signal* 6, ra20.

Behrend, L., Henderson, G., and Zwacka, R.M. (2003). Reactive oxygen species in oncogenic transformation. *Biochem Soc Trans* 31, 1441-1444.

Bellance, N., Lestienne, P., and Rossignol, R. (2009). Mitochondria: from bioenergetics to the metabolic regulation of carcinogenesis. *Front Biosci (Landmark Ed)* 14, 4015-4034.

Bernal, S.D., Lampidis, T.J., McIsaac, R.M., and Chen, L.B. (1983). Anticarcinoma activity in vivo of rhodamine 123, a mitochondrial-specific dye. *Science* 222, 169-172.

Berns, K., Horlings, H.M., Hennessy, B.T., Madiredjo, M., Hijmans, E.M., Beelen, K., Linn, S.C., Gonzalez-Angulo, A.M., Stemke-Hale, K., Hauptmann, M., *et al.* (2007). A functional genetic approach identifies the PI3K pathway as a major determinant of trastuzumab resistance in breast cancer. *Cancer Cell* 12, 395-402.

Bervers, E.M., and Williamson, P.L. (2010). Phospholipid scramblase: an update. *FEBS Lett* 584, 2724-2730.

Bleday, R., Weiss, M.J., Salem, R.R., Wilson, R.E., Chen, L.B., and Steele, G., Jr. (1986). Inhibition of rat colon tumor isograft growth with dequalinium chloride. *Arch Surg* 121, 1272-1275.

- Blume-Jensen, P., and Hunter, T. (2001). Oncogenic kinase signalling. *Nature* 411, 355-365.
- Boland, M.L., Chourasia, A.H., and Macleod, K.F. (2013). Mitochondrial dysfunction in cancer. *Front Oncol* 3, 292.
- Bonadonna, G., and Monfardini, S. (1969). Cardiac toxicity of daunorubicin. *Lancet* 1, 837.
- Boonstra, J., and Post, J.A. (2004). Molecular events associated with reactive oxygen species and cell cycle progression in mammalian cells. *Gene* 337, 1-13.
- Borden, E.C., Kluger, H., and Crowley, J. (2008). Apoptosis: a clinical perspective. *Nat Rev Drug Discov* 7, 959-959.
- Borisenko, G.G., Matsura, T., Liu, S.X., Tyurin, V.A., Jianfei, J., Serinkan, F.B., and Kagan, V.E. (2003). Macrophage recognition of externalized phosphatidylserine and phagocytosis of apoptotic Jurkat cells--existence of a threshold. *Arch Biochem Biophys* 413, 41-52.
- Botchkarev, V.A., Komarova, E.A., Siebenhaar, F., Botchkareva, N.V., Komarov, P.G., Maurer, M., Gilchrist, B.A., and Gudkov, A.V. (2000). p53 is essential for chemotherapy-induced hair loss. *Cancer Res* 60, 5002-5006.
- Brahimi-Horn, M.C., Chiche, J., and Pouyssegur, J. (2007). Hypoxia signalling controls metabolic demand. *Curr Opin Cell Biol* 19, 223-229.
- Britten, C.D., Rowinsky, E.K., Baker, S.D., Weiss, G.R., Smith, L., Stephenson, J., Rothenberg, M., Smetzer, L., Cramer, J., Collins, W., *et al.* (2000). A phase I and pharmacokinetic study of the mitochondrial-specific rhodocyanine dye analog MKT 077. *Clin Cancer Res* 6, 42-49.
- Brown, S.B., Brown, E.A., and Walker, I. (2004). The present and future role of photodynamic therapy in cancer treatment. *Lancet Oncol* 5, 497-508.
- Bruey, J.M., Ducasse, C., Bonniaud, P., Ravagnan, L., Susin, S.A., Diaz-Latoud, C., Gurbuxani, S., Arrigo, A.P., Kroemer, G., Solary, E., *et al.* (2000). Hsp27 negatively regulates cell death by interacting with cytochrome c. *Nat Cell Biol* 2, 645-652.
- Buytaert, E., Dewaele, M., and Agostinis, P. (2007). Molecular effectors of multiple cell death pathways initiated by photodynamic therapy. *Biochim Biophys Acta* 1776, 86-107.
- Cang, S., Iragavarapu, C., Savooji, J., Song, Y., and Liu, D. (2015). ABT-199 (venetoclax) and BCL-2 inhibitors in clinical development. *J Hematol Oncol* 8, 129.

Capdeville, R., Buchdunger, E., Zimmermann, J., and Matter, A. (2002). Glivec (STI571, imatinib), a rationally developed, targeted anticancer drug. *Nat Rev Drug Discov* 1, 493-502.

Castro, D.J., Saxton, R.E., Rodgerson, D.O., Fu, Y.S., Bhuta, S.M., Fetterman, H.R., Castro, D.J., Tartell, P.B., and Ward, P.H. (1989). Rhodamine-123 as a new laser dye: in vivo study of dye effects on murine metabolism, histology and ultrastructure. *Laryngoscope* 99, 1057-1062.

Cha, Y., Park, D.W., Lee, C.H., Baek, S.H., Kim, S.Y., Kim, J.R., and Kim, J.H. (2006). Arsenic trioxide induces apoptosis in human colorectal adenocarcinoma HT-29 cells through ROS. *Cancer Res Treat* 38, 54-60.

Chance, B., Sies, H., and Boveris, A. (1979). Hydroperoxide metabolism in mammalian organs. *Physiol Rev* 59, 527-605.

Chang, J., Xie, M., Shah, V.R., Schneider, M.D., Entman, M.L., Wei, L., and Schwartz, R.J. (2006). Activation of Rho-associated coiled-coil protein kinase 1 (ROCK-1) by caspase-3 cleavage plays an essential role in cardiac myocyte apoptosis. *Proc Natl Acad Sci U S A* 103, 14495-14500.

Chatterjee, A., Mambo, E., and Sidransky, D. (2006). Mitochondrial DNA mutations in human cancer. *Oncogene* 25, 4663-4674.

Chauhan, D., Velankar, M., Brahmandam, M., Hideshima, T., Podar, K., Richardson, P., Schlossman, R., Ghobrial, I., Raje, N., Munshi, N., *et al.* (2007). A novel Bcl-2/Bcl-X(L)/Bcl-w inhibitor ABT-737 as therapy in multiple myeloma. *Oncogene* 26, 2374-2380.

Chen, B., Pogue, B.W., Luna, J.M., Hardman, R.L., Hoopes, P.J., and Hasan, T. (2006). Tumor vascular permeabilization by vascular-targeting photosensitization: effects, mechanism, and therapeutic implications. *Clin Cancer Res* 12, 917-923.

Chen, G., Chen, Z., Hu, Y., and Huang, P. (2011). Inhibition of mitochondrial respiration and rapid depletion of mitochondrial glutathione by beta-phenethyl isothiocyanate: mechanisms for anti-leukemia activity. *Antioxid Redox Signal* 15, 2911-2921.

Chen, L.B., Summerhayes, I.C., Johnson, L.V., Walsh, M.L., Bernal, S.D., and Lampidis, T.J. (1982). Probing mitochondria in living cells with rhodamine 123. *Cold Spring Harb Symp Quant Biol* 46 Pt 1, 141-155.

Cherukuri, D.P., and Nelson, M.A. (2008). Role of reactive oxygen species (ROS) and JNKs in selenite-induced apoptosis in HepG2 cells. *Cancer Biol Ther* 7, 697-698.

Chiba, Y., Kubota, T., Watanabe, M., Matsuzaki, S.W., Otani, Y., Teramoto, T., Matsumoto, Y., Koya, K., and Kitajima, M. (1998a). MKT-077, localized lipophilic cation: antitumor activity against human tumor xenografts serially transplanted into nude mice. *Anticancer Res* 18, 1047-1052.

Chiba, Y., Kubota, T., Watanabe, M., Otani, Y., Teramoto, T., Matsumoto, Y., Koya, K., and Kitajima, M. (1998b). Selective antitumor activity of MKT-077, a delocalized lipophilic cation, on normal cells and cancer cells in vitro. *J Surg Oncol* 69, 105-110.

Chung, A.S., Lee, J., and Ferrara, N. (2010). Targeting the tumour vasculature: insights from physiological angiogenesis. *Nat Rev Cancer* 10, 505-514.

Chunta, J.L., Vistisen, K.S., Yazdi, Z., and Braun, R.D. (2012). Uptake rate of cationic mitochondrial inhibitor MKT-077 determines cellular oxygen consumption change in carcinoma cells. *PLoS One* 7, e37471.

Coleman, M.L., Sahai, E.A., Yeo, M., Bosch, M., Dewar, A., and Olson, M.F. (2001). Membrane blebbing during apoptosis results from caspase-mediated activation of ROCK I. *Nat Cell Biol* 3, 339-345.

Colvin, T.A., Gabai, V.L., Gong, J., Calderwood, S.K., Li, H., Gummuluru, S., Matchuk, O.N., Smirnova, S.G., Orlova, N.V., Zamulaeva, I.A., *et al.* (2014). Hsp70-Bag3 interactions regulate cancer-related signaling networks. *Cancer Res* 74, 4731-4740.

Costantini, P., Belzacq, A.S., Vieira, H.L., Larochette, N., de Pablo, M.A., Zamzami, N., Susin, S.A., Brenner, C., and Kroemer, G. (2000). Oxidation of a critical thiol residue of the adenine nucleotide translocator enforces Bcl-2-independent permeability transition pore opening and apoptosis. *Oncogene* 19, 307-314.

Crystal, A.S., Shaw, A.T., Sequist, L.V., Friboulet, L., Niederst, M.J., Lockerman, E.L., Frias, R.L., Gainor, J.F., Amzallag, A., Greninger, P., *et al.* (2014). Patient-derived models of acquired resistance can identify effective drug combinations for cancer. *Science* 346, 1480-1486.

Cuezva, J.M., Ostronoff, L.K., Ricart, J., Lopez de Heredia, M., Di Liegro, C.M., and Izquierdo, J.M. (1997). Mitochondrial biogenesis in the liver during development and oncogenesis. *J Bioenerg Biomembr* 29, 365-377.

Dai, C., Dai, S., and Cao, J. (2012). Proteotoxic stress of cancer: implication of the heat-shock response in oncogenesis. *J Cell Physiol* 227, 2982-2987.

Davids, M.S., Pagel, J.M., Kahl, B.S., Wierda, W.G., Miller, T.P., Gerecitano, J.F., Kipps, T.J., Anderson, M.-A., Huang, D.C.S., Rudersdorf, N.K., *et al.* (2013). Bcl-2 Inhibitor ABT-199 (GDC-0199) Monotherapy Shows Anti-Tumor Activity Including

Complete Remissions In High-Risk Relapsed/Refractory (R/R) Chronic Lymphocytic Leukemia (CLL) and Small Lymphocytic Lymphoma (SLL). *Blood* 122, 872-872.

Davids, M.S., Roberts, A.W., Anderson, M.A., Pagel, J.M., Kahl, B.S., Gerecitano, J.F., Darden, D.E., Nolan, C.E., Gressick, L.A., Yang, J., *et al.* (2012). The BCL-2-Specific BH3-Mimetic ABT-199 (GDC-0199) Is Active and Well-Tolerated in Patients with Relapsed Non-Hodgkin Lymphoma: Interim Results of a Phase I Study. *Blood* 120, 304-304.

Davis, S., Weiss, M.J., Wong, J.R., Lampidis, T.J., and Chen, L.B. (1985). Mitochondrial and plasma membrane potentials cause unusual accumulation and retention of rhodamine 123 by human breast adenocarcinoma-derived MCF-7 cells. *J Biol Chem* 260, 13844-13850.

De Giorgi, F., Lartigue, L., Bauer, M.K., Schubert, A., Grimm, S., Hanson, G.T., Remington, S.J., Youle, R.J., and Ichas, F. (2002). The permeability transition pore signals apoptosis by directing Bax translocation and multimerization. *Faseb j* 16, 607-609.

de Grey, A.D. (2005). Reactive oxygen species production in the mitochondrial matrix: implications for the mechanism of mitochondrial mutation accumulation. *Rejuvenation Res* 8, 13-17.

DeBerardinis, R.J., Mancuso, A., Daikhin, E., Nissim, I., Yudkoff, M., Wehrli, S., and Thompson, C.B. (2007). Beyond aerobic glycolysis: transformed cells can engage in glutamine metabolism that exceeds the requirement for protein and nucleotide synthesis. *Proc Natl Acad Sci U S A* 104, 19345-19350.

DeNicola, G.M., Karreth, F.A., Humpton, T.J., Gopinathan, A., Wei, C., Frese, K., Mangal, D., Yu, K.H., Yeo, C.J., Calhoun, E.S., *et al.* (2011). Oncogene-induced Nrf2 transcription promotes ROS detoxification and tumorigenesis. *Nature* 475, 106-109.

Dobbelstein, M., and Moll, U. (2014). Targeting tumour-supportive cellular machineries in anticancer drug development. *Nat Rev Drug Discov* 13, 179-196.

Dolmans, D.E., Fukumura, D., and Jain, R.K. (2003). Photodynamic therapy for cancer. *Nat Rev Cancer* 3, 380-387.

Druker, B.J., Guilhot, F., O'Brien, S.G., Gathmann, I., Kantarjian, H., Gattermann, N., Deininger, M.W., Silver, R.T., Goldman, J.M., Stone, R.M., *et al.* (2006). Five-year follow-up of patients receiving imatinib for chronic myeloid leukemia. *N Engl J Med* 355, 2408-2417.

Dussmann, H., Rehm, M., Kogel, D., and Prehn, J.H. (2003). Outer mitochondrial membrane permeabilization during apoptosis triggers caspase-independent

mitochondrial and caspase-dependent plasma membrane potential depolarization: a single-cell analysis. *J Cell Sci* 116, 525-536.

Dwarakanath, B.S., Singh, D., Banerji, A.K., Sarin, R., Venkataramana, N.K., Jalali, R., Vishwanath, P.N., Mohanti, B.K., Tripathi, R.P., Kalia, V.K., *et al.* (2009). Clinical studies for improving radiotherapy with 2-deoxy-D-glucose: present status and future prospects. *J Cancer Res Ther* 5 *Suppl* 1, S21-26.

Edelhauser, H.F., Van Horn, D.L., Miller, P., and Pederson, H.J. (1976). Effect of thiol-oxidation of glutathione with diamide on corneal endothelial function, junctional complexes, and microfilaments. *J Cell Biol* 68, 567-578.

Enari, M., Sakahira, H., Yokoyama, H., Okawa, K., Iwamatsu, A., and Nagata, S. (1998). A caspase-activated DNase that degrades DNA during apoptosis, and its inhibitor ICAD. *Nature* 391, 43-50.

Estaquier, J., Vallette, F., Vayssiere, J.L., and Mignotte, B. (2012). The mitochondrial pathways of apoptosis. *Adv Exp Med Biol* 942, 157-183.

European Cancer Organisation. EBCC-10 NEWS: Combination of lapatinib and trastuzumab shrinks HER2 positive breast cancer significantly in 11 days after diagnosis (ECCO).

Evans, C.G., Chang, L., and Gestwicki, J.E. (2010). Heat shock protein 70 (hsp70) as an emerging drug target. *J Med Chem* 53, 4585-4602.

Evans, J.M., Donnelly, L.A., Emslie-Smith, A.M., Alessi, D.R., and Morris, A.D. (2005). Metformin and reduced risk of cancer in diabetic patients. *BMJ* 330, 1304-1305.

Evens, A.M. (2004). Motexafin gadolinium: a redox-active tumor selective agent for the treatment of cancer. *Curr Opin Oncol* 16, 576-580.

Fan, J., Kamphorst, J.J., Mathew, R., Chung, M.K., White, E., Shlomi, T., and Rabinowitz, J.D. (2013). Glutamine-driven oxidative phosphorylation is a major ATP source in transformed mammalian cells in both normoxia and hypoxia. *Mol Syst Biol* 9, 712.

Fan, M., Goodwin, M.E., Birrer, M.J., and Chambers, T.C. (2001). The c-Jun NH(2)-terminal protein kinase/AP-1 pathway is required for efficient apoptosis induced by vinblastine. *Cancer Res* 61, 4450-4458.

Feldmann, G., Haouzi, D., Moreau, A., Durand-Schneider, A.M., Bringuier, A., Berson, A., Mansouri, A., Fau, D., and Pessayre, D. (2000). Opening of the mitochondrial permeability transition pore causes matrix expansion and outer

membrane rupture in Fas-mediated hepatic apoptosis in mice. *Hepatology* 31, 674-683.

Fernald, K., and Kurokawa, M. Evading apoptosis in cancer. *Trends in Cell Biology* 23, 620-633.

Formentini, L., Sanchez-Arago, M., Sanchez-Cenizo, L., and Cuezva, J.M. (2012). The mitochondrial ATPase inhibitory factor 1 triggers a ROS-mediated retrograde prosurvival and proliferative response. *Mol Cell* 45, 731-742.

Fulda, S. (2009). Tumor resistance to apoptosis. *Int J Cancer* 124, 511-515.

Fulda, S. (2010). Exploiting mitochondrial apoptosis for the treatment of cancer. *Mitochondrion* 10, 598-603.

Fulda, S., and Debatin, K.M. (2006). Extrinsic versus intrinsic apoptosis pathways in anticancer chemotherapy. *Oncogene* 25, 4798-4811.

Garon, E.B., Christofk, H.R., Hosmer, W., Britten, C.D., Bahng, A., Crabtree, M.J., Hong, C.S., Kamranpour, N., Pitts, S., Kabbinar, F., *et al.* (2014). Dichloroacetate should be considered with platinum-based chemotherapy in hypoxic tumors rather than as a single agent in advanced non-small cell lung cancer. *J Cancer Res Clin Oncol* 140, 443-452.

Garrido, C., Brunet, M., Didelot, C., Zermati, Y., Schmitt, E., and Kroemer, G. (2006). Heat shock proteins 27 and 70: anti-apoptotic proteins with tumorigenic properties. *Cell Cycle* 5, 2592-2601.

Gehrmann, M., Specht, H.M., Bayer, C., Brandstetter, M., Chizzali, B., Duma, M., Breuninger, S., Hube, K., Lehnerer, S., van Phi, V., *et al.* (2014). Hsp70--a biomarker for tumor detection and monitoring of outcome of radiation therapy in patients with squamous cell carcinoma of the head and neck. *Radiat Oncol* 9, 131.

Gennari, R., Menard, S., Fagnoni, F., Ponchio, L., Scelsi, M., Tagliabue, E., Castiglioni, F., Villani, L., Magalotti, C., Gibelli, N., *et al.* (2004). Pilot study of the mechanism of action of preoperative trastuzumab in patients with primary operable breast tumors overexpressing HER2. *Clin Cancer Res* 10, 5650-5655.

Gilman, P., Parton, R.L., and Lenhard, J.R. (2006). Correlation of anti-cancer activity of dyes with redox potential In Patent Application Publication (US: Eastman Kodak Company).

Giron-Calle, J., Zwizinski, C.W., and Schmid, H.H. (1994). Peroxidative damage to cardiac mitochondria. II. Immunological analysis of modified adenine nucleotide translocase. *Arch Biochem Biophys* 315, 1-7.

- Gogvadze, V., Orrenius, S., and Zhivotovsky, B. (2008). Mitochondria in cancer cells: what is so special about them? *Trends Cell Biol* 18, 165-173.
- Gollnick, S.O., Vaughan, L., and Henderson, B.W. (2002). Generation of effective antitumor vaccines using photodynamic therapy. *Cancer Res* 62, 1604-1608.
- Goloudina, A.R., Demidov, O.N., and Garrido, C. (2012). Inhibition of HSP70: A challenging anti-cancer strategy. *Cancer Letters* 325, 117-124.
- Gonzalvez, F., Pariselli, F., Dupaigne, P., Budihardjo, I., Lutter, M., Antonsson, B., Diolez, P., Manon, S., Martinou, J.C., Gubern, M., *et al.* (2005). tBid interaction with cardiolipin primarily orchestrates mitochondrial dysfunctions and subsequently activates Bax and Bak. *Cell Death Differ* 12, 614-626.
- Goodman, L.S., Wintrobe, M.M., and *et al.* (1946). Nitrogen mustard therapy; use of methyl-bis (beta-chloroethyl) amine hydrochloride and tris (beta-chloroethyl) amine hydrochloride for Hodgkin's disease, lymphosarcoma, leukemia and certain allied and miscellaneous disorders. *J Am Med Assoc* 132, 126-132.
- Gottesman, M.M. (2002). Mechanisms of cancer drug resistance. *Annu Rev Med* 53, 615-627.
- Gottlieb, E., Armour, S.M., Harris, M.H., and Thompson, C.B. (2003). Mitochondrial membrane potential regulates matrix configuration and cytochrome c release during apoptosis. *Cell Death Differ* 10, 709-717.
- Grebien, F., Hantschel, O., Wojcik, J., Kaupe, I., Kovacic, B., Wyrzucki, A.M., Gish, G.D., Cerny-Reiterer, S., Koide, A., Beug, H., *et al.* (2011). Targeting the SH2-kinase interface in Bcr-Abl inhibits leukemogenesis. *Cell* 147, 306-319.
- Gross, A., McDonnell, J.M., and Korsmeyer, S.J. (1999). BCL-2 family members and the mitochondria in apoptosis. *Genes Dev* 13, 1899-1911.
- Guzy, R.D., Sharma, B., Bell, E., Chandel, N.S., and Schumacker, P.T. (2008). Loss of the SdhB, but Not the SdhA, subunit of complex II triggers reactive oxygen species-dependent hypoxia-inducible factor activation and tumorigenesis. *Mol Cell Biol* 28, 718-731.
- Hahn, S.M., Putt, M.E., Metz, J., Shin, D.B., Rickter, E., Menon, C., Smith, D., Glatstein, E., Fraker, D.L., and Busch, T.M. (2006). Photofrin uptake in the tumor and normal tissues of patients receiving intraperitoneal photodynamic therapy. *Clin Cancer Res* 12, 5464-5470.
- Hait, W.N. (2010). Anticancer drug development: the grand challenges. *Nat Rev Drug Discov* 9, 253-254.

Han, M., Vakili, M.R., Soleymani Abyaneh, H., Molavi, O., Lai, R., and Lavasanifar, A. (2014). Mitochondrial delivery of doxorubicin via triphenylphosphine modification for overcoming drug resistance in MDA-MB-435/DOX cells. *Mol Pharm* 11, 2640-2649.

Hanahan, D., and Weinberg, R.A. (2011). Hallmarks of cancer: the next generation. *Cell* 144, 646-674.

Hankins, H.M., Baldrige, R.D., Xu, P., and Graham, T.R. (2015). Role of flippases, scramblases and transfer proteins in phosphatidylserine subcellular distribution. *Traffic* 16, 35-47.

Harries, M., and Smith, I. (2002). The development and clinical use of trastuzumab (Herceptin). *Endocr Relat Cancer* 9, 75-85.

Hayashi, M., Sakata, M., Takeda, T., Yamamoto, T., Okamoto, Y., Sawada, K., Kimura, A., Minekawa, R., Tahara, M., Tasaka, K., *et al.* (2004). Induction of glucose transporter 1 expression through hypoxia-inducible factor 1alpha under hypoxic conditions in trophoblast-derived cells. *J Endocrinol* 183, 145-154.

He, J., Agarwal, M.L., Larkin, H.E., Friedman, L.R., Xue, L.Y., and Oleinick, N.L. (1996). The induction of partial resistance to photodynamic therapy by the protooncogene BCL-2. *Photochem Photobiol* 64, 845-852.

Henderson, B.W., Waldow, S.M., Mang, T.S., Potter, W.R., Malone, P.B., and Dougherty, T.J. (1985). Tumor destruction and kinetics of tumor cell death in two experimental mouse tumors following photodynamic therapy. *Cancer Res* 45, 572-576.

Higgins, C.F. (2007). Multiple molecular mechanisms for multidrug resistance transporters. *Nature* 446, 749-757.

High, L.M., Szymanska, B., Wilczynska-Kalak, U., Barber, N., O'Brien, R., Khaw, S.L., Vikstrom, I.B., Roberts, A.W., and Lock, R.B. (2010). The Bcl-2 homology domain 3 mimetic ABT-737 targets the apoptotic machinery in acute lymphoblastic leukemia resulting in synergistic in vitro and in vivo interactions with established drugs. *Mol Pharmacol* 77, 483-494.

Hirsch, H.A., Iliopoulos, D., Tsiachlis, P.N., and Struhl, K. (2009). Metformin selectively targets cancer stem cells, and acts together with chemotherapy to block tumor growth and prolong remission. *Cancer Res* 69, 7507-7511.

Hu, Y., Rosen, D.G., Zhou, Y., Feng, L., Yang, G., Liu, J., and Huang, P. (2005). Mitochondrial manganese-superoxide dismutase expression in ovarian cancer: role in cell proliferation and response to oxidative stress. *J Biol Chem* 280, 39485-39492.

- Huttemann, M., Pecina, P., Rainbolt, M., Sanderson, T.H., Kagan, V.E., Samavati, L., Doan, J.W., and Lee, I. (2011). The multiple functions of cytochrome c and their regulation in life and death decisions of the mammalian cell: From respiration to apoptosis. *Mitochondrion* 11, 369-381.
- Irani, K., Xia, Y., Zweier, J.L., Sollott, S.J., Der, C.J., Fearon, E.R., Sundaresan, M., Finkel, T., and Goldschmidt-Clermont, P.J. (1997). Mitogenic signaling mediated by oxidants in Ras-transformed fibroblasts. *Science* 275, 1649-1652.
- Ishikawa, K., Takenaga, K., Akimoto, M., Koshikawa, N., Yamaguchi, A., Imanishi, H., Nakada, K., Honma, Y., and Hayashi, J. (2008). ROS-generating mitochondrial DNA mutations can regulate tumor cell metastasis. *Science* 320, 661-664.
- Ishitsuka, K., Kunami, N., Katsuya, H., Nogami, R., Ishikawa, C., Yotsumoto, F., Tanji, H., Mori, N., Takeshita, M., Miyamoto, S., *et al.* (2012). Targeting Bcl-2 family proteins in adult T-cell leukemia/lymphoma: in vitro and in vivo effects of the novel Bcl-2 family inhibitor ABT-737. *Cancer Lett* 317, 218-225.
- Izumi, Y., Xu, L., di Tomaso, E., Fukumura, D., and Jain, R.K. (2002). Tumour biology: herceptin acts as an anti-angiogenic cocktail. *Nature* 416, 279-280.
- Jackson, J.R., Patrick, D.R., Dar, M.M., and Huang, P.S. (2007). Targeted anti-mitotic therapies: can we improve on tubulin agents? *Nat Rev Cancer* 7, 107-117.
- James, T.H. (1977). *The Theory of the Photographic Process* (New York: The Macmillan Company).
- Jiao, D., Smith, T.J., Yang, C.S., Pittman, B., Desai, D., Amin, S., and Chung, F.L. (1997). Chemopreventive activity of thiol conjugates of isothiocyanates for lung tumorigenesis. *Carcinogenesis* 18, 2143-2147.
- Johnson, L.V., Walsh, M.L., and Chen, L.B. (1980). Localization of mitochondria in living cells with rhodamine 123. *Proc Natl Acad Sci U S A* 77, 990-994.
- Johnson, V.L., Ko, S.C., Holmstrom, T.H., Eriksson, J.E., and Chow, S.C. (2000). Effector caspases are dispensable for the early nuclear morphological changes during chemical-induced apoptosis. *J Cell Sci* 113 ( Pt 17), 2941-2953.
- Jones, L.W., Narayan, K.S., Shapiro, C.E., and Sweatman, T.W. (2005). Rhodamine-123: therapy for hormone refractory prostate cancer, a phase I clinical trial. *J Chemother* 17, 435-440.
- Kabingu, E., Vaughan, L., Owczarczak, B., Ramsey, K.D., and Gollnick, S.O. (2007). CD8+ T cell-mediated control of distant tumours following local photodynamic therapy is independent of CD4+ T cells and dependent on natural killer cells. *Br J Cancer* 96, 1839-1848.

Kamb, A., Wee, S., and Lengauer, C. (2007). Why is cancer drug discovery so difficult? *Nat Rev Drug Discov* 6, 115-120.

Kang, Y.H., and Lee, S.J. (2008). The role of p38 MAPK and JNK in Arsenic trioxide-induced mitochondrial cell death in human cervical cancer cells. *J Cell Physiol* 217, 23-33.

Kawanishi, S., Hiraku, Y., Pinlaor, S., and Ma, N. (2006). Oxidative and nitrative DNA damage in animals and patients with inflammatory diseases in relation to inflammation-related carcinogenesis. *Biol Chem* 387, 365-372.

Kessel, D. (2002). Relocalization of cationic porphyrins during photodynamic therapy. *Photochem Photobiol Sci* 1, 837-840.

Kim, J.W., Tchernyshyov, I., Semenza, G.L., and Dang, C.V. (2006). HIF-1-mediated expression of pyruvate dehydrogenase kinase: a metabolic switch required for cellular adaptation to hypoxia. *Cell Metab* 3, 177-185.

Kim, S.H., Bajji, A., Tangallapally, R., Markovitz, B., Trovato, R., Shenderovich, M., Baichwal, V., Bartel, P., Cimbor, D., McKinnon, R., *et al.* (2012). Discovery of (2S)-1-[4-(2-{6-amino-8-[(6-bromo-1,3-benzodioxol-5-yl)sulfanyl]-9H-purin-9-yl]ethyl)piperidin-1-yl]-2-hydroxypropan-1-one (MPC-3100), a purine-based Hsp90 inhibitor. *J Med Chem* 55, 7480-7501.

Kim, T., Keum, G., and Pae, A.N. (2013). Discovery and development of heat shock protein 90 inhibitors as anticancer agents: a review of patented potent geldanamycin derivatives. *Expert Opin Ther Pat* 23, 919-943.

Kimura, H., Sawada, T., Oshima, S., Kozawa, K., Ishioka, T., and Kato, M. (2005). Toxicity and roles of reactive oxygen species. *Curr Drug Targets Inflamm Allergy* 4, 489-495.

Kipps, T.J., Eradat, H., Grosicki, S., Catalano, J., Cosolo, W., Dyagil, I.S., Yalamanchili, S., Chai, A., Sahasranaman, S., Punnoose, E., *et al.* (2015). A phase 2 study of the BH3 mimetic BCL2 inhibitor navitoclax (ABT-263) with or without rituximab, in previously untreated B-cell chronic lymphocytic leukemia. *Leuk Lymphoma* 56, 2826-2833.

Ko, B.-K., Lee, S.-Y., Lee, Y.-H., Hwang, I.-S., Persson, H., Rockberg, J., Borrebaeck, C., Park, D., Kim, K.-T., Uhlen, M., *et al.* (2015). Combination of novel HER2-targeting antibody 1E11 with trastuzumab shows synergistic antitumor activity in HER2-positive gastric cancer. *Molecular Oncology* 9, 398-408.

Kodiha, M., Pié, B., Wang, Y.M., Flamant, E., Boppana, N.B., Young, J.C., Separovic, D., Cooper, E., and Stochaj, U. (2015). Detecting changes in the mitochondrial membrane potential by quantitative fluorescence microscopy.

Kong, Q., and Lillehei, K.O. (1998). Antioxidant inhibitors for cancer therapy. *Med Hypotheses* 51, 405-409.

Korbelik, M., Stott, B., and Sun, J. (2007). Photodynamic therapy-generated vaccines: relevance of tumour cell death expression. *Br J Cancer* 97, 1381-1387.

Kousis, P.C., Henderson, B.W., Maier, P.G., and Gollnick, S.O. (2007). Photodynamic therapy enhancement of antitumor immunity is regulated by neutrophils. *Cancer Res* 67, 10501-10510.

Koya, K., Li, Y., Wang, H., Ukai, T., Tatsuta, N., Kawakami, M., Shishido, and Chen, L.B. (1996). MKT-077, a novel rhodacyanine dye in clinical trials, exhibits anticarcinoma activity in preclinical studies based on selective mitochondrial accumulation. *Cancer Res* 56, 538-543.

Krebs, J.J., Hauser, H., and Carafoli, E. (1979). Asymmetric distribution of phospholipids in the inner membrane of beef heart mitochondria. *J Biol Chem* 254, 5308-5316.

Kroemer, G., and Pouyssegur, J. (2008). Tumor cell metabolism: cancer's Achilles' heel. *Cancer Cell* 13, 472-482.

Krosi, G., Korbelik, M., and Dougherty, G.J. (1995). Induction of immune cell infiltration into murine SCCVII tumour by photofrin-based photodynamic therapy. *Br J Cancer* 71, 549-555.

Kunjachan, S., Rychlik, B., Storm, G., Kiessling, F., and Lammers, T. (2013). Multidrug resistance: Physiological principles and nanomedical solutions. *Adv Drug Deliv Rev* 65, 1852-1865.

Lampidis, T.J., Bernal, S.D., Summerhayes, I.C., and Chen, L.B. (1983). Selective toxicity of rhodamine 123 in carcinoma cells in vitro. *Cancer Res* 43, 716-720.

Lampidis, T.J., Hasin, Y., Weiss, M.J., and Chen, L.B. (1985). Selective killing of carcinoma cells "in vitro" by lipophilic-cationic compounds: a cellular basis. *Biomed Pharmacother* 39, 220-226.

Lampidis, T.J., Johnson, L.V., and Israel, M. (1981). Effects of adriamycin on rat heart cells in culture: increased accumulation and nucleoli fragmentation in cardiac muscle v. non-muscle cells. *J Mol Cell Cardiol* 13, 913-924.

Lampidis, T.J., Salet, C., Moreno, G., and Chen, L.B. (1984). Effects of the mitochondrial probe rhodamine 123 and related analogs on the function and viability of pulsating myocardial cells in culture. *Agents Actions* 14, 751-757.

Landau, B.R., Laszlo, J., Stengle, J., and Burk, D. (1958). Certain metabolic and pharmacologic effects in cancer patients given infusions of 2-deoxy-D-glucose. *J Natl Cancer Inst* 21, 485-494.

Lemmon, M.A., and Schlessinger, J. (2010). Cell signaling by receptor tyrosine kinases. *Cell* 141, 1117-1134.

Leone, G., Voso, M.T., Sica, S., Morosetti, R., and Pagano, L. (2001). Therapy related leukemias: susceptibility, prevention and treatment. *Leuk Lymphoma* 41, 255-276.

Levkau, B., Herren, B., Koyama, H., Ross, R., and Raines, E.W. (1998). Caspase-mediated cleavage of focal adhesion kinase pp125FAK and disassembly of focal adhesions in human endothelial cell apoptosis. *J Exp Med* 187, 579-586.

Li, X., Colvin, T., Rauch, J.N., Acosta-Alvear, D., Kampmann, M., Dunyak, B., Hann, B., Aftab, B.T., Murnane, M., Cho, M., *et al.* (2015). Validation of the Hsp70-Bag3 protein-protein interaction as a potential therapeutic target in cancer. *Mol Cancer Ther* 14, 642-648.

Li, X., Srinivasan, S.R., Connarn, J., Ahmad, A., Young, Z.T., Kabza, A.M., Zuiderweg, E.R., Sun, D., and Gestwicki, J.E. (2013). Analogs of the Allosteric Heat Shock Protein 70 (Hsp70) Inhibitor, MKT-077, as Anti-Cancer Agents. *ACS Med Chem Lett* 4.

Lin, T.S., Naumovski, L., Lecane, P.S., Lucas, M.S., Moran, M.E., Cheney, C., Lucas, D.M., Phan, S.C., Miller, R.A., and Byrd, J.C. (2009). Effects of motexafin gadolinium in a phase II trial in refractory chronic lymphocytic leukemia. *Leuk Lymphoma* 50, 1977-1982.

Liu, J., Weiss, A., Durrant, D., Chi, N.W., and Lee, R.M. (2004). The cardiolipin-binding domain of Bid affects mitochondrial respiration and enhances cytochrome c release. *Apoptosis* 9, 533-541.

Liu, J., Zhang, C., Hu, W., and Feng, Z. (2015). Tumor suppressor p53 and its mutants in cancer metabolism. *Cancer Lett* 356, 197-203.

Liu, T., Wu, L.Y., Choi, J.K., and Berkman, C.E. (2010). Targeted photodynamic therapy for prostate cancer: inducing apoptosis via activation of the caspase-8/-3 cascade pathway. *Int J Oncol* 36, 777-784.

Liu, X., Kim, C.N., Yang, J., Jemmerson, R., and Wang, X. (1996). Induction of apoptotic program in cell-free extracts: requirement for dATP and cytochrome c. *Cell* 86, 147-157.

Liu, Y., Fiskum, G., and Schubert, D. (2002). Generation of reactive oxygen species by the mitochondrial electron transport chain. *J Neurochem* 80, 780-787.

Lock, R., Carol, H., Houghton, P.J., Morton, C.L., Kolb, E.A., Gorlick, R., Reynolds, C.P., Maris, J.M., Keir, S.T., Wu, J., *et al.* (2008). Initial testing (stage 1) of the BH3 mimetic ABT-263 by the pediatric preclinical testing program. *Pediatr Blood Cancer* 50, 1181-1189.

Longley, D.B., Harkin, D.P., and Johnston, P.G. (2003). 5-Fluorouracil: mechanisms of action and clinical strategies. *Nat Rev Cancer* 3, 330-338.

Lopez-Rios, F., Sanchez-Arago, M., Garcia-Garcia, E., Ortega, A.D., Berrendero, J.R., Pozo-Rodriguez, F., Lopez-Encuentra, A., Ballestin, C., and Cuezva, J.M. (2007). Loss of the mitochondrial bioenergetic capacity underlies the glucose avidity of carcinomas. *Cancer Res* 67, 9013-9017.

Lu, J., Chew, E.H., and Holmgren, A. (2007). Targeting thioredoxin reductase is a basis for cancer therapy by arsenic trioxide. *Proc Natl Acad Sci U S A* 104, 12288-12293.

Lunt, S.Y., and Vander Heiden, M.G. (2011). Aerobic glycolysis: meeting the metabolic requirements of cell proliferation. *Annu Rev Cell Dev Biol* 27, 441-464.

Luo, X., Budihardjo, I., Zou, H., Slaughter, C., and Wang, X. (1998). Bid, a Bcl2 interacting protein, mediates cytochrome c release from mitochondria in response to activation of cell surface death receptors. *Cell* 94, 481-490.

Lutter, M., Fang, M., Luo, X., Nishijima, M., Xie, X., and Wang, X. (2000). Cardiolipin provides specificity for targeting of tBid to mitochondria. *Nat Cell Biol* 2, 754-761.

Madak, J.T., and Neamati, N. (2015). Membrane permeable lipophilic cations as mitochondrial directing groups. *Curr Top Med Chem* 15, 745-766.

Madesh, M., and Hajnoczky, G. (2001). VDAC-dependent permeabilization of the outer mitochondrial membrane by superoxide induces rapid and massive cytochrome c release. *J Cell Biol* 155, 1003-1015.

Marino, G., and Kroemer, G. (2013). Mechanisms of apoptotic phosphatidylserine exposure. *Cell Res* 23, 1247-1248.

Martinez-Reyes, I., and Cuezva, J.M. (2014). The H(+)-ATP synthase: a gate to ROS-mediated cell death or cell survival. *Biochim Biophys Acta* 1837, 1099-1112.

Martinou, J.-C., and Youle, R.J. (2011). Mitochondria in Apoptosis: Bcl-2 family Members and Mitochondrial Dynamics. *Developmental cell* 21, 92-101.

Mathupala, S.P., Ko, Y.H., and Pedersen, P.L. (2009). Hexokinase-2 bound to mitochondria: cancer's stygian link to the "Warburg Effect" and a pivotal target for effective therapy. *Semin Cancer Biol* 19, 17-24.

Mattiazzi, M., Vijayvergiya, C., Gajewski, C.D., DeVivo, D.C., Lenaz, G., Wiedmann, M., and Manfredi, G. (2004). The mtDNA T8993G (NARP) mutation results in an impairment of oxidative phosphorylation that can be improved by antioxidants. *Hum Mol Genet* 13, 869-879.

Maynard, S., Schurman, S.H., Harboe, C., de Souza-Pinto, N.C., and Bohr, V.A. (2009). Base excision repair of oxidative DNA damage and association with cancer and aging. *Carcinogenesis* 30, 2-10.

Mehta, M.P., Shapiro, W.R., Phan, S.C., Gervais, R., Carrie, C., Chabot, P., Patchell, R.A., Glantz, M.J., Recht, L., Langer, C., *et al.* (2009). Motexafin gadolinium combined with prompt whole brain radiotherapy prolongs time to neurologic progression in non-small-cell lung cancer patients with brain metastases: results of a phase III trial. *Int J Radiat Oncol Biol Phys* 73, 1069-1076.

Metallo, C.M., Gameiro, P.A., Bell, E.L., Mattaini, K.R., Yang, J., Hiller, K., Jewell, C.M., Johnson, Z.R., Irvine, D.J., Guarente, L., *et al.* (2012). Reductive glutamine metabolism by IDH1 mediates lipogenesis under hypoxia. *Nature* 481, 380-384.

Michelakis, E.D., Sutendra, G., Dromparis, P., Webster, L., Haromy, A., Niven, E., Maguire, C., Gammer, T.L., Mackey, J.R., Fulton, D., *et al.* (2010). Metabolic modulation of glioblastoma with dichloroacetate. *Sci Transl Med* 2, 31ra34.

Michor, F., Iwasa, Y., and Nowak, M.A. (2004). Dynamics of cancer progression. *Nat Rev Cancer* 4, 197-205.

Miquel, C., Borrini, F., Grandjouan, S., Auperin, A., Viguier, J., Velasco, V., Duvillard, P., Praz, F., and Sabourin, J.C. (2005). Role of bax mutations in apoptosis in colorectal cancers with microsatellite instability. *Am J Clin Pathol* 123, 562-570.

Miyata, Y., Li, X., Lee, H.F., Jinwal, U.K., Srinivasan, S.R., Seguin, S.P., Young, Z.T., Brodsky, J.L., Dickey, C.A., Sun, D., *et al.* (2013a). Synthesis and initial evaluation of YM-08, a blood-brain barrier permeable derivative of the heat shock protein 70 (Hsp70) inhibitor MKT-077, which reduces tau levels. *ACS Chem Neurosci* 4, 930-939.

Miyata, Y., Nakamoto, H., and Neckers, L. (2013b). The therapeutic target Hsp90 and cancer hallmarks. *Curr Pharm Des* 19, 347-365.

Moan, J., Berg, K., Kvam, E., Western, A., Malik, Z., Ruck, A., and Schneckenburger, H. (1989). Intracellular localization of photosensitizers. *Ciba Found Symp* 146, 95-107; discussion 107-111.

Modi, S., Sugarman, S., Stopeck, A., Linden, H., Ma, W., Kersy, K., Johnson, R.G., Rosen, N., Hannah, A.L., and Hudis, C.A. (2008). Phase II trial of the Hsp90 inhibitor tanespimycin (Tan) + trastuzumab (T) in patients (pts) with HER2-positive metastatic breast cancer (MBC) *Journal of Clinical Oncology* 26.

Modica-Napolitano, J.S., and Aprille, J.R. (1987). Basis for the selective cytotoxicity of rhodamine 123. *Cancer Res* 47, 4361-4365.

Modica-Napolitano, J.S., and Aprille, J.R. (2001). Delocalized lipophilic cations selectively target the mitochondria of carcinoma cells. *Adv Drug Deliv Rev* 49, 63-70.

Modica-Napolitano, J.S., Koya, K., Weisberg, E., Brunelli, B.T., Li, Y., and Chen, L.B. (1996). Selective damage to carcinoma mitochondria by the rhodacyanine MKT-077. *Cancer Res* 56, 544-550.

Modica-Napolitano, J.S., Kulawiec, M., and Singh, K.K. (2007). Mitochondria and human cancer. *Curr Mol Med* 7, 121-131.

Moghissi, K., Dixon, K., Stringer, M., Freeman, T., Thorpe, A., and Brown, S. (1999). The place of bronchoscopic photodynamic therapy in advanced unresectable lung cancer: experience of 100 cases. *Eur J Cardiothorac Surg* 15, 1-6.

Moserova, I., and Kralova, J. (2012). Role of ER stress response in photodynamic therapy: ROS generated in different subcellular compartments trigger diverse cell death pathways. *PLoS One* 7, e32972.

Mukai, H., Saeki, T., Shimada, K., Naito, Y., Matsubara, N., Nakanishi, T., Obaishi, H., Namiki, M., and Sasaki, Y. (2015). Phase 1 combination study of Eribulin mesylate with trastuzumab for advanced or recurrent human epidermal growth factor receptor 2 positive breast cancer. *Investigational New Drugs* 33, 119-127.

Mukherjee, S. (2010). *The Emperor of All Maladies: A Biography of Cancer* (Scribner).

Mullen, A.R., Wheaton, W.W., Jin, E.S., Chen, P.-H., Sullivan, L.B., Cheng, T., Yang, Y., Linehan, W.M., Chandel, N.S., and DeBerardinis, R.J. (2012). Reductive carboxylation supports growth in tumour cells with defective mitochondria. *Nature* 481, 385-388.

Muller, P.A., and Vousden, K.H. (2013). p53 mutations in cancer. *Nat Cell Biol* 15, 2-8.

Murgo, A.J. (2001). Clinical trials of arsenic trioxide in hematologic and solid tumors: overview of the National Cancer Institute Cooperative Research and Development Studies. *Oncologist* 6 *Suppl 2*, 22-28.

Murphy, M.P. (2009). How mitochondria produce reactive oxygen species. *Biochem J* 417, 1-13.

Murphy, M.P., and Smith, R.A. (2000). Drug delivery to mitochondria: the key to mitochondrial medicine. *Adv Drug Deliv Rev* 41, 235-250.

Nagata, S. (2000). Apoptotic DNA fragmentation. *Exp Cell Res* 256, 12-18.

Nagata, S., Suzuki, J., Segawa, K., and Fujii, T. (2016). Exposure of phosphatidylserine on the cell surface. *Cell Death Differ* 23, 952-961.

Nahleh, Z., Tfayli, A., Najm, A., El Sayed, A., and Nahle, Z. (2012). Heat shock proteins in cancer: targeting the 'chaperones'. *Future Med Chem* 4, 927-935.

Nahta, R., Yu, D., Hung, M.C., Hortobagyi, G.N., and Esteva, F.J. (2006). Mechanisms of disease: understanding resistance to HER2-targeted therapy in human breast cancer. *Nat Clin Pract Oncol* 3, 269-280.

Ndozangue-Touriguine, O., Hamelin, J., and Breard, J. (2008). Cytoskeleton and apoptosis. *Biochem Pharmacol* 76, 11-18.

Neugut, A.I., Robinson, E., Nieves, J., Murray, T., and Tsai, W.Y. (1990). Poor survival of treatment-related acute nonlymphocytic leukemia. *JAMA* 264, 1006-1008.

Nie, C., Tian, C., Zhao, L., Petit, P.X., Mehrpour, M., and Chen, Q. (2008). Cysteine 62 of Bax is critical for its conformational activation and its proapoptotic activity in response to H<sub>2</sub>O<sub>2</sub>-induced apoptosis. *J Biol Chem* 283, 15359-15369.

Nishida, N., Yano, H., Nishida, T., Kamura, T., and Kojiro, M. (2006). Angiogenesis in Cancer. *Vascular Health and Risk Management* 2, 213-219.

Nonaka, M., Ikeda, H., and Inokuchi, T. (2004). Inhibitory effect of heat shock protein 70 on apoptosis induced by photodynamic therapy in vitro. *Photochem Photobiol* 79, 94-98.

Noriko Yasuhara, S.S., Shinji Kamada, Yutaka Eguchi and Yoshihide Tsujimoto (1997). Evidence against a functional site for Bcl-2 downstream of caspase cascade in preventing apoptosis. *Oncogene* 15, 7.

Nowell, P.C., and Hungerford, D.A. (1960). Chromosome studies on normal and leukemic human leukocytes. *J Natl Cancer Inst* 25, 85-109.

O'Connor, A.E., Gallagher, W.M., and Byrne, A.T. (2009). Porphyrin and nonporphyrin photosensitizers in oncology: preclinical and clinical advances in photodynamic therapy. *Photochem Photobiol* 85, 1053-1074.

Octavia, Y., Tocchetti, C.G., Gabrielson, K.L., Janssens, S., Crijns, H.J., and Moens, A.L. (2012). Doxorubicin-induced cardiomyopathy: from molecular mechanisms to therapeutic strategies. *J Mol Cell Cardiol* 52, 1213-1225.

Ogrunc, M., Di Micco, R., Liontos, M., Bombardelli, L., Mione, M., Fumagalli, M., Gorgoulis, V.G., and d'Adda di Fagagna, F. (2014). Oncogene-induced reactive oxygen species fuel hyperproliferation and DNA damage response activation. *Cell Death Differ* 21, 998-1012.

Oleinick, N.L., Morris, R.L., and Belichenko, I. (2002). The role of apoptosis in response to photodynamic therapy: what, where, why, and how. *Photochem Photobiol Sci* 1, 1-21.

Oltersdorf, T., Elmore, S.W., Shoemaker, A.R., Armstrong, R.C., Augeri, D.J., Belli, B.A., Bruncko, M., Deckwerth, T.L., Dinges, J., Hajduk, P.J., *et al.* (2005). An inhibitor of Bcl-2 family proteins induces regression of solid tumours. *Nature* 435, 677-681.

Ow, Y.-L.P., Green, D.R., Hao, Z., and Mak, T.W. (2008). Cytochrome c: functions beyond respiration. *Nat Rev Mol Cell Biol* 9, 532-542.

Padayatty, S.J., Katz, A., Wang, Y., Eck, P., Kwon, O., Lee, J.H., Chen, S., Corpe, C., Dutta, A., Dutta, S.K., *et al.* (2003). Vitamin C as an antioxidant: evaluation of its role in disease prevention. *J Am Coll Nutr* 22, 18-35.

Paradies, G., Petrosillo, G., Pistolese, M., and Ruggiero, F.M. (2002). Reactive oxygen species affect mitochondrial electron transport complex I activity through oxidative cardiolipin damage. *Gene* 286, 135-141.

Park, G.B., Choi, Y., Kim, Y.S., Lee, H.K., Kim, D., and Hur, D.Y. (2014). ROS-mediated JNK/p38-MAPK activation regulates Bax translocation in Sorafenib-induced apoptosis of EBV-transformed B cells. *Int J Oncol* 44, 977-985.

Pelicano, H., Carney, D., and Huang, P. (2004). ROS stress in cancer cells and therapeutic implications. *Drug Resist Updat* 7, 97-110.

Pelicano, H., Feng, L., Zhou, Y., Carew, J.S., Hileman, E.O., Plunkett, W., Keating, M.J., and Huang, P. (2003). Inhibition of mitochondrial respiration: a novel strategy to enhance drug-induced apoptosis in human leukemia cells by a reactive oxygen species-mediated mechanism. *J Biol Chem* 278, 37832-37839.

Perry, G., Raina, A.K., Nunomura, A., Wataya, T., Sayre, L.M., and Smith, M.A. (2000). How important is oxidative damage? Lessons from Alzheimer's disease. *Free Radic Biol Med* 28, 831-834.

Perry, S.W., Norman, J.P., Barbieri, J., Brown, E.B., and Gelbard, H.A. (2011). Mitochondrial membrane potential probes and the proton gradient: a practical usage guide. *Biotechniques* 50, 98-115.

Petrosillo, G., Ruggiero, F.M., and Paradies, G. (2003). Role of reactive oxygen species and cardiolipin in the release of cytochrome c from mitochondria. *FASEB J* 17, 2202-2208.

Pollak, M. (2012). The insulin and insulin-like growth factor receptor family in neoplasia: an update. *Nat Rev Cancer* 12, 159-169.

Polyak, K., Xia, Y., Zweier, J.L., Kinzler, K.W., and Vogelstein, B. (1997). A model for p53-induced apoptosis. *Nature* 389, 300-305.

Porporato, P.E., Payen, V.L., Perez-Escuredo, J., De Saedeleer, C.J., Danhier, P., Copetti, T., Dhup, S., Tardy, M., Vazeille, T., Bouzin, C., *et al.* (2014). A mitochondrial switch promotes tumor metastasis. *Cell Rep* 8, 754-766.

Portt, L., Norman, G., Clapp, C., Greenwood, M., and Greenwood, M.T. (2011). Anti-apoptosis and cell survival: a review. *Biochim Biophys Acta* 1813, 238-259.

Powers, M.V., Valenti, M., Miranda, S., Maloney, A., Eccles, S.A., Thomas, G., Clarke, P.A., and Workman, P. (2013). Mode of cell death induced by the HSP90 inhibitor 17-AAG (tanespimycin) is dependent on the expression of pro-apoptotic BAX. *Oncotarget* 4, 1963-1975.

Propper, D.J., Braybrooke, J.P., Taylor, D.J., Lodi, R., Styles, P., Cramer, J.A., Collins, W.C., Levitt, N.C., Talbot, D.C., Ganesan, T.S., *et al.* (1999). Phase I trial of the selective mitochondrial toxin MKT077 in chemo-resistant solid tumours. *Ann Oncol* 10, 923-927.

Quinlan, C.L., Perevoshchikova, I.V., Hey-Mogensen, M., Orr, A.L., and Brand, M.D. (2013). Sites of reactive oxygen species generation by mitochondria oxidizing different substrates. *Redox Biol* 1, 304-312.

Quintas-Cardama, A., Kantarjian, H.M., and Cortes, J.E. (2009). Mechanisms of primary and secondary resistance to imatinib in chronic myeloid leukemia. *Cancer Control* 16, 122-131.

Raez, L.E., Papadopoulos, K., Ricart, A.D., Chiorean, E.G., Dipaola, R.S., Stein, M.N., Rocha Lima, C.M., Schlesselman, J.J., Tolba, K., Langmuir, V.K., *et al.* (2013). A phase I dose-escalation trial of 2-deoxy-D-glucose alone or combined with docetaxel in patients with advanced solid tumors. *Cancer Chemother Pharmacol* 71, 523-530.

Ray, P.D., Huang, B.-W., and Tsuji, Y. (2012). Reactive oxygen species (ROS) homeostasis and redox regulation in cellular signaling. *Cellular signalling* 24, 981-990.

Ricci, C., Pastukh, V., Leonard, J., Turrens, J., Wilson, G., Schaffer, D., and Schaffer, S.W. (2008). Mitochondrial DNA damage triggers mitochondrial-superoxide generation and apoptosis. *Am J Physiol Cell Physiol* 294, C413-422.

Richardson, P.G., Chanan-Khan, A.A., Lonial, S., Krishnan, A.Y., Carroll, M.P., Albitar, M., Kopit, J., Berman, D., and Anderson, K.C. (2009). Tanespimycin + Bortezomib Demonstrates Safety, Activity, and Effective Target Inhibition in Relapsed/Refractory Myeloma Patients: Updated Results of a Phase 1/2 Study. *Blood* 114, 2890-2890.

Riddle, S.R., Ahmad, A., Ahmad, S., Deeb, S.S., Malkki, M., Schneider, B.K., Allen, C.B., and White, C.W. (2000). Hypoxia induces hexokinase II gene expression in human lung cell line A549. *Am J Physiol Lung Cell Mol Physiol* 278, L407-416.

Roberts, A.W., Seymour, J.F., Brown, J.R., Wierda, W.G., Kipps, T.J., Khaw, S.L., Carney, D.A., He, S.Z., Huang, D.C., Xiong, H., *et al.* (2012). Substantial susceptibility of chronic lymphocytic leukemia to BCL2 inhibition: results of a phase I study of navitoclax in patients with relapsed or refractory disease. *J Clin Oncol* 30, 488-496.

Roberts, P.J., and Der, C.J. (2007). Targeting the Raf-MEK-ERK mitogen-activated protein kinase cascade for the treatment of cancer. *Oncogene* 26, 3291-3310.

Rodriguez-Enriquez, S., Gallardo-Perez, J.C., Hernandez-Resendiz, I., Marin-Hernandez, A., Pacheco-Velazquez, S.C., Lopez-Ramirez, S.Y., Rumjanek, F.D., and Moreno-Sanchez, R. (2014). Canonical and new generation anticancer drugs also target energy metabolism. *Arch Toxicol* 88, 1327-1350.

Romani, A.A., Crafa, P., Desenzani, S., Graiani, G., Lagrasta, C., Sianesi, M., Soliani, P., and Borghetti, A.F. (2007). The expression of HSP27 is associated with poor clinical outcome in intrahepatic cholangiocarcinoma. *BMC Cancer* 7, 1-10.

Rosati, A., Ammirante, M., Gentilella, A., Basile, A., Festa, M., Pascale, M., Marzullo, L., Belisario, M.A., Tosco, A., Franceschelli, S., *et al.* (2007). Apoptosis inhibition in cancer cells: a novel molecular pathway that involves BAG3 protein. *Int J Biochem Cell Biol* 39, 1337-1342.

Rousaki, A., Miyata, Y., Jinwal, U.K., Dickey, C.A., Gestwicki, J.E., and Zuiderweg, E.R. (2011). Allosteric drugs: the interaction of antitumor compound MKT-077 with human Hsp70 chaperones. *J Mol Biol* 411, 614-632.

Sabharwal, S.S., and Schumacker, P.T. (2014). Mitochondrial ROS in cancer: initiators, amplifiers or an Achilles' heel? *Nat Rev Cancer* 14, 709-721.

Sakahira, H., Takemura, Y., and Nagata, S. (2001). Enzymatic active site of caspase-activated DNase (CAD) and its inhibition by inhibitor of CAD. *Arch Biochem Biophys* 388, 91-99.

Salesse, S., and Verfaillie, C.M. (2002). BCR/ABL: from molecular mechanisms of leukemia induction to treatment of chronic myelogenous leukemia. *Oncogene* 21, 8547-8559.

Sankari, S.L., Masthan, K.M., Babu, N.A., Bhattacharjee, T., and Elumalai, M. (2012). Apoptosis in cancer--an update. *Asian Pac J Cancer Prev* 13, 4873-4878.

Sasaki, H., Kotsuji, F., and Tsang, B.K. (2002). Caspase 3-mediated focal adhesion kinase processing in human ovarian cancer cells: possible regulation by X-linked inhibitor of apoptosis protein. *Gynecol Oncol* 85, 339-350.

Saydam, N., Kirb, A., Demir, Ö., Hazan, E., Oto, Ö., Saydam, O., and Güner, G. (1997). Determination of glutathione, glutathione reductase, glutathione peroxidase and glutathione S-transferase levels in human lung cancer tissues. *Cancer Letters* 119, 13-19.

Sborov, D.W., Haverkos, B.M., and Harris, P.J. (2015). Investigational cancer drugs targeting cell metabolism in clinical development. *Expert Opin Investig Drugs* 24, 79-94.

Schieber, M., and Chandel, N.S. (2014). ROS function in redox signaling and oxidative stress. *Curr Biol* 24, R453-462.

Semenza, G.L. (2003). Targeting HIF-1 for cancer therapy. *Nat Rev Cancer* 3, 721-732.

Semenza, G.L. (2013). HIF-1 mediates metabolic responses to intratumoral hypoxia and oncogenic mutations. *J Clin Invest* 123, 3664-3671.

Seymour, J.F., Davids, M.S., Pagel, J.M., Kahl, B.S., Wierda, W.G., Miller, T.P., Gerecitano, J.F., Kipps, T.J., Anderson, M.A., and Huang, D. (2013). Updated results of a phase I first-in-human study of the BCL-2 inhibitor ABT-199 (GDC-0199) in patients with relapsed/refractory (R/R) chronic lymphocytic leukemia (CLL). Paper presented at: ASCO Annual Meeting Proceedings.

Sgarbi, G., Baracca, A., Lenaz, G., Valentino, L.M., Carelli, V., and Solaini, G. (2006). Inefficient coupling between proton transport and ATP synthesis may be the pathogenic mechanism for NARP and Leigh syndrome resulting from the T8993G mutation in mtDNA. *Biochem J* 395, 493-500.

Shaw, R.J., Lamia, K.A., Vasquez, D., Koo, S.H., Bardeesy, N., Depinho, R.A., Montminy, M., and Cantley, L.C. (2005). The kinase LKB1 mediates glucose homeostasis in liver and therapeutic effects of metformin. *Science* 310, 1642-1646.

Shi, Y. (2002). Mechanisms of Caspase Activation and Inhibition during Apoptosis. *Molecular Cell* 9, 459-470.

Sibani, S.A., McCarron, P.A., Woolfson, A.D., and Donnelly, R.F. (2008). Photosensitizer delivery for photodynamic therapy. Part 2: systemic carrier platforms. *Expert Opin Drug Deliv* 5, 1241-1254.

Siddik, Z.H. (2003). Cisplatin: mode of cytotoxic action and molecular basis of resistance. *Oncogene* 22, 7265-7279.

Sidera, K., and Patsavoudi, E. (2014). HSP90 inhibitors: current development and potential in cancer therapy. *Recent Pat Anticancer Drug Discov* 9, 1-20.

Slamon, D.J., Clark, G.M., Wong, S.G., Levin, W.J., Ullrich, A., and McGuire, W.L. (1987). Human breast cancer: correlation of relapse and survival with amplification of the HER-2/neu oncogene. *Science* 235, 177-182.

Slamon, D.J., Leyland-Jones, B., Shak, S., Fuchs, H., Paton, V., Bajamonde, A., Fleming, T., Eiermann, W., Wolter, J., Pegram, M., *et al.* (2001). Use of chemotherapy plus a monoclonal antibody against HER2 for metastatic breast cancer that overexpresses HER2. *N Engl J Med* 344, 783-792.

Smiley, S.T., Reers, M., Mottola-Hartshorn, C., Lin, M., Chen, A., Smith, T.W., Steele, G.D., Jr., and Chen, L.B. (1991). Intracellular heterogeneity in mitochondrial membrane potentials revealed by a J-aggregate-forming lipophilic cation JC-1. *Proc Natl Acad Sci U S A* 88, 3671-3675.

Smith, R.E., Bryant, J., DeCillis, A., and Anderson, S. (2003). Acute myeloid leukemia and myelodysplastic syndrome after doxorubicin-cyclophosphamide adjuvant therapy for operable breast cancer: the National Surgical Adjuvant Breast and Bowel Project Experience. *J Clin Oncol* 21, 1195-1204.

Snyder, J.W., Greco, W.R., Bellnier, D.A., Vaughan, L., and Henderson, B.W. (2003). Photodynamic therapy: a means to enhanced drug delivery to tumors. *Cancer Res* 63, 8126-8131.

Souers, A.J., Levenson, J.D., Boghaert, E.R., Ackler, S.L., Catron, N.D., Chen, J., Dayton, B.D., Ding, H., Enschede, S.H., Fairbrother, W.J., *et al.* (2013). ABT-199, a potent and selective BCL-2 inhibitor, achieves antitumor activity while sparing platelets. *Nat Med* 19, 202-208.

Stein, M., Lin, H., Jeyamohan, C., Dvorzhinski, D., Gounder, M., Bray, K., Eddy, S., Goodin, S., White, E., and Dipaola, R.S. (2010). Targeting tumor metabolism with 2-deoxyglucose in patients with castrate-resistant prostate cancer and advanced malignancies. *Prostate* 70, 1388-1394.

Stratton, M.R. (2011). Exploring the genomes of cancer cells: progress and promise. *Science* 331, 1553-1558.

Strum, S.B., Adalsteinsson, O., Black, R.R., Segal, D., Peress, N.L., and Waldenfels, J. (2013). Case report: Sodium dichloroacetate (DCA) inhibition of the "Warburg Effect" in a human cancer patient: complete response in non-Hodgkin's lymphoma after disease progression with rituximab-CHOP. *J Bioenerg Biomembr* 45, 307-315.

Subbarayan, P.R., and Ardalan, B. (2014). In the war against solid tumors arsenic trioxide needs partners. *J Gastrointest Cancer* 45, 363-371.

Sukumar, M., Liu, J., Mehta, G.U., Patel, S.J., Roychoudhuri, R., Crompton, J.G., Klebanoff, C.A., Ji, Y., Li, P., Yu, Z., *et al.* (2016). Mitochondrial Membrane Potential Identifies Cells with Enhanced Stemness for Cellular Therapy. *Cell Metab* 23, 63-76.

Summerhayes, I.C., Lampidis, T.J., Bernal, S.D., Nadakavukaren, J.J., Nadakavukaren, K.K., Shepherd, E.L., and Chen, L.B. (1982). Unusual retention of rhodamine 123 by mitochondria in muscle and carcinoma cells. *Proc Natl Acad Sci U S A* 79, 5292-5296.

Sun, X., Wong, J.R., Song, K., Hu, J., Garlid, K.D., and Chen, L.B. (1994). AA1, a newly synthesized monovalent lipophilic cation, expresses potent in vivo antitumor activity. *Cancer Res* 54, 1465-1471.

Sur, B.W., Nguyen, P., Sun, C.H., Tromberg, B.J., and Nelson, E.L. (2008). Immunophototherapy using PDT combined with rapid intratumoral dendritic cell injection. *Photochem Photobiol* 84, 1257-1264.

Suryani, S., Carol, H., Chonghaile, T.N., Frismantas, V., Sarmah, C., High, L., Bornhauser, B., Cowley, M.J., Szymanska, B., Evans, K., *et al.* (2014). Cell and molecular determinants of in vivo efficacy of the BH3 mimetic ABT-263 against pediatric acute lymphoblastic leukemia xenografts. *Clin Cancer Res* 20, 4520-4531.

Susin, S.A., Lorenzo, H.K., Zamzami, N., Marzo, I., Snow, B.E., Brothers, G.M., Mangion, J., Jacotot, E., Costantini, P., Loeffler, M., *et al.* (1999). Molecular characterization of mitochondrial apoptosis-inducing factor. *Nature* 397, 441-446.

Svensson, J., Johansson, A., Grafe, S., Gitter, B., Trebst, T., Bendsoe, N., Andersson-Engels, S., and Svanberg, K. (2007). Tumor selectivity at short times

following systemic administration of a liposomal temoporfin formulation in a murine tumor model. *Photochem Photobiol* 83, 1211-1219.

Szatrowski, T.P., and Nathan, C.F. (1991). Production of large amounts of hydrogen peroxide by human tumor cells. *Cancer Res* 51, 794-798.

Takeuchi, K., and Ito, F. (2011). Receptor tyrosine kinases and targeted cancer therapeutics. *Biol Pharm Bull* 34, 1774-1780.

Taylor, R.C., Cullen, S.P., and Martin, S.J. (2008). Apoptosis: controlled demolition at the cellular level. *Nat Rev Mol Cell Biol* 9, 231-241.

Thomas, S.R., and Khuntia, D. (2011). Motexafin gadolinium: a promising radiation sensitizer in brain metastasis. *Expert Opin Drug Discov* 6, 195-203.

Thornberry, N.A. (1999). Caspases: a decade of death research. *Cell Death Differ* 6, 1023-1027.

Touzeau, C., Dousset, C., Le Gouill, S., Sampath, D., Levenson, J.D., Souers, A.J., Maiga, S., Bene, M.C., Moreau, P., Pellat-Deceunynck, C., *et al.* (2014). The Bcl-2 specific BH3 mimetic ABT-199: a promising targeted therapy for t(11;14) multiple myeloma. *Leukemia* 28, 210-212.

Townsend, D.M., and Tew, K.D. (2003). The role of glutathione-S-transferase in anti-cancer drug resistance. *Oncogene* 22, 7369-7375.

Toyokuni, S., Okamoto, K., Yodoi, J., and Hiai, H. (1995). Persistent oxidative stress in cancer. *FEBS Lett* 358, 1-3.

Traber, M.G., and Atkinson, J. (2007). Vitamin E, antioxidant and nothing more. *Free Radic Biol Med* 43, 4-15.

Trachootham, D., Alexandre, J., and Huang, P. (2009). Targeting cancer cells by ROS-mediated mechanisms: a radical therapeutic approach? *Nat Rev Drug Discov* 8, 579-591.

Travis, L.B., Fossa, S.D., Schonfeld, S.J., McMaster, M.L., Lynch, C.F., Storm, H., Hall, P., Holowaty, E., Andersen, A., Pukkala, E., *et al.* (2005). Second cancers among 40,576 testicular cancer patients: focus on long-term survivors. *J Natl Cancer Inst* 97, 1354-1365.

Trepel, J., Mollapour, M., Giaccone, G., and Neckers, L. (2010). Targeting the dynamic HSP90 complex in cancer. *Nat Rev Cancer* 10, 537-549.

Tseng, M.T., Reed, M.W., Ackermann, D.M., Schuschke, D.A., Wieman, T.J., and Miller, F.N. (1988). Photodynamic therapy induced ultrastructural alterations in microvasculature of the rat cremaster muscle. *Photochem Photobiol* 48, 675-681.

Tsujimoto, Y. (1998). Role of Bcl-2 family proteins in apoptosis: apoptosomes or mitochondria? *Genes Cells* 3, 697-707.

Tsujimoto, Y., Gorham, J., Cossman, J., Jaffe, E., and Croce, C.M. (1985). The t(14;18) chromosome translocations involved in B-cell neoplasms result from mistakes in VDJ joining. *Science* 229, 1390-1393.

Tsujimoto, Y., and Shimizu, S. (2007). Role of the mitochondrial membrane permeability transition in cell death. *Apoptosis* 12, 835-840.

Umeki, S., Niki, Y., and Soejima, R. (1989). Anticancer chemotherapy accelerates scalp hair loss with no androgenic involvement. *Chemotherapy* 35, 54-57.

Umesh, K.J., Grover, A., Narayan, M., Hirani, A., and Sutariya, V. (2014). Preparation and Characterization of MKT-077 Nanoparticles for Treatment of Alzheimer's Disease and Other Tauopathies. *Pharmaceutical Nanotechnology* 2, 10.

Usmani, S.Z., Bona, R., and Li, Z. (2009). 17 AAG for HSP90 inhibition in cancer--from bench to bedside. *Curr Mol Med* 9, 654-664.

Usuda, J., Azizuddin, K., Chiu, S.M., and Oleinick, N.L. (2003). Association between the photodynamic loss of Bcl-2 and the sensitivity to apoptosis caused by phthalocyanine photodynamic therapy. *Photochem Photobiol* 78, 1-8.

Vafa, O., Wade, M., Kern, S., Beeche, M., Pandita, T.K., Hampton, G.M., and Wahl, G.M. (2002). c-Myc can induce DNA damage, increase reactive oxygen species, and mitigate p53 function: a mechanism for oncogene-induced genetic instability. *Mol Cell* 9, 1031-1044.

van Engeland, M., Nieland, L.J., Ramaekers, F.C., Schutte, B., and Reutelingsperger, C.P. (1998). Annexin V-affinity assay: a review on an apoptosis detection system based on phosphatidylserine exposure. *Cytometry* 31, 1-9.

Vandenberg, C.J., and Cory, S. (2013). ABT-199, a new Bcl-2-specific BH3 mimetic, has in vivo efficacy against aggressive Myc-driven mouse lymphomas without provoking thrombocytopenia. *Blood* 121, 2285-2288.

Vanlangenakker, N., Vanden Berghe, T., Krysko, D.V., Festjens, N., and Vandenamele, P. (2008). Molecular mechanisms and pathophysiology of necrotic cell death. *Curr Mol Med* 8, 207-220.

- Vieira, H.L., Haouzi, D., El Hamel, C., Jacotot, E., Belzacq, A.S., Brenner, C., and Kroemer, G. (2000). Permeabilization of the mitochondrial inner membrane during apoptosis: impact of the adenine nucleotide translocator. *Cell Death Differ* 7, 1146-1154.
- Villamor, N., Montserrat, E., and Colomer, D. (2003). Mechanism of action and resistance to monoclonal antibody therapy. *Semin Oncol* 30, 424-433.
- Viollet, B., Guigas, B., Sanz Garcia, N., Leclerc, J., Foretz, M., and Andreelli, F. (2012). Cellular and molecular mechanisms of metformin: an overview. *Clinical Science (London, England : 1979)* 122, 253-270.
- Vogel, C.L., Cobleigh, M.A., Tripathy, D., Gutheil, J.C., Harris, L.N., Fehrenbacher, L., Slamon, D.J., Murphy, M., Novotny, W.F., Burchmore, M., *et al.* (2002). Efficacy and safety of trastuzumab as a single agent in first-line treatment of HER2-overexpressing metastatic breast cancer. *J Clin Oncol* 20, 719-726.
- Vrouenraets, M.B., Visser, G.W., Snow, G.B., and van Dongen, G.A. (2003). Basic principles, applications in oncology and improved selectivity of photodynamic therapy. *Anticancer Res* 23, 505-522.
- Vu, T., and Claret, F.X. (2012). Trastuzumab: Updated Mechanisms of Action and Resistance in Breast Cancer. *Frontiers in Oncology* 2, 62.
- Wadhwa, R., Sugihara, T., Yoshida, A., Nomura, H., Reddel, R.R., Simpson, R., Maruta, H., and Kaul, S.C. (2000). Selective toxicity of MKT-077 to cancer cells is mediated by its binding to the hsp70 family protein mot-2 and reactivation of p53 function. *Cancer Res* 60, 6818-6821.
- Wang, C., and Youle, R.J. (2009). The role of mitochondria in apoptosis\*. *Annu Rev Genet* 43, 95-118.
- Wang, L., Du, F., and Wang, X. (2008). TNF-alpha induces two distinct caspase-8 activation pathways. *Cell* 133, 693-703.
- Warburg, O., Posener, K., and Negelein, E. (1924). Uber den Stoffwechsel der Tumoren. *Biochem Z* 152, 25.
- Ward, P.S., and Thompson, C.B. (2012). Metabolic reprogramming: a cancer hallmark even warburg did not anticipate. *Cancer Cell* 21, 297-308.
- Wei, M.C., Zong, W.X., Cheng, E.H., Lindsten, T., Panoutsakopoulou, V., Ross, A.J., Roth, K.A., MacGregor, G.R., Thompson, C.B., and Korsmeyer, S.J. (2001). Proapoptotic BAX and BAK: a requisite gateway to mitochondrial dysfunction and death. *Science* 292, 727-730.

Weinberg, F., Hamanaka, R., Wheaton, W.W., Weinberg, S., Joseph, J., Lopez, M., Kalyanaraman, B., Mutlu, G.M., Budinger, G.R., and Chandel, N.S. (2010). Mitochondrial metabolism and ROS generation are essential for Kras-mediated tumorigenicity. *Proc Natl Acad Sci U S A* 107, 8788-8793.

Wenner, C.E. (2012). Targeting mitochondria as a therapeutic target in cancer. *J Cell Physiol* 227, 450-456.

Wong, R.S. (2011). Apoptosis in cancer: from pathogenesis to treatment. *J Exp Clin Cancer Res* 30, 87.

Woo, D.K., Green, P.D., Santos, J.H., D'Souza, A.D., Walther, Z., Martin, W.D., Christian, B.E., Chandel, N.S., and Shadel, G.S. (2012). Mitochondrial genome instability and ROS enhance intestinal tumorigenesis in APC(Min/+) mice. *Am J Pathol* 180, 24-31.

Wu, W.S. (2006). The signaling mechanism of ROS in tumor progression. *Cancer Metastasis Rev* 25, 695-705.

Xu, L., Voloboueva, L.A., Ouyang, Y., Emery, J.F., and Giffard, R.G. (2009). Overexpression of mitochondrial Hsp70/Hsp75 in rat brain protects mitochondria, reduces oxidative stress, and protects from focal ischemia. *J Cereb Blood Flow Metab* 29, 365-374.

Xuan, Y., Hur, H., Ham, I.H., Yun, J., Lee, J.Y., Shim, W., Kim, Y.B., Lee, G., Han, S.U., and Cho, Y.K. (2014). Dichloroacetate attenuates hypoxia-induced resistance to 5-fluorouracil in gastric cancer through the regulation of glucose metabolism. *Exp Cell Res* 321, 219-230.

Xue, L.Y., Chiu, S.M., and Oleinick, N.L. (2001). Photochemical destruction of the Bcl-2 oncoprotein during photodynamic therapy with the phthalocyanine photosensitizer Pc 4. *Oncogene* 20, 3420-3427.

Yamaguchi, R., Janssen, E., Perkins, G., Ellisman, M., Kitada, S., and Reed, J.C. (2011). Efficient elimination of cancer cells by deoxyglucose-ABT-263/737 combination therapy. *PLoS One* 6, e24102.

Yamamoto, K., Ichijo, H., and Korsmeyer, S.J. (1999). BCL-2 Is Phosphorylated and Inactivated by an ASK1/Jun N-Terminal Protein Kinase Pathway Normally Activated at G(2)/M. *Molecular and Cellular Biology* 19, 8469-8478.

Yan, M., Schwaederle, M., Arguello, D., Millis, S.Z., Gatalica, Z., and Kurzrock, R. (2015). HER2 expression status in diverse cancers: review of results from 37,992 patients. *Cancer Metastasis Rev* 34, 157-164.

Yang, N., and Goping, I.S. (2013). Apoptosis (Morgan & Claypool Life Sciences).

Yarden, Y., and Sliwkowski, M.X. (2001). Untangling the ErbB signalling network. *Nat Rev Mol Cell Biol* 2, 127-137.

Zahreddine, H., and Borden, K.L. (2013). Mechanisms and insights into drug resistance in cancer. *Front Pharmacol* 4, 28.

Zhang, R., Humphreys, I., Sahu, R.P., Shi, Y., and Srivastava, S.K. (2008). In vitro and in vivo induction of apoptosis by capsaicin in pancreatic cancer cells is mediated through ROS generation and mitochondrial death pathway. *Apoptosis* 13, 1465-1478.

Zhang, T.D., Chen, G.Q., Wang, Z.G., Wang, Z.Y., Chen, S.J., and Chen, Z. (2001). Arsenic trioxide, a therapeutic agent for APL. *Oncogene* 20, 7146-7153.

Zhou, S., Kachhap, S., Sun, W., Wu, G., Chuang, A., Poeta, L., Grumbine, L., Mithani, S.K., Chatterjee, A., Koch, W., *et al.* (2007). Frequency and phenotypic implications of mitochondrial DNA mutations in human squamous cell cancers of the head and neck. *Proc Natl Acad Sci U S A* 104, 7540-7545.

Zhu, Z.L., Zhang, J., Chen, M.L., and Li, K. (2013). Efficacy and safety of Trastuzumab added to standard treatments for HER2-positive metastatic breast cancer patients. *Asian Pac J Cancer Prev* 14, 7111-7116.

Zigman, S., and Gilman, P., Jr. (1980). Inhibition of cell division and growth by a redox series of cyanine dyes. *Science* 208, 188-191.

Zu, X.L., and Guppy, M. (2004). Cancer metabolism: facts, fantasy, and fiction. *Biochem Biophys Res Commun* 313, 459-465.

**CHAPTER 2**  
**METHODS AND MATERIALS**

## 2.1 Reagents

D112 (unknown purity) was provided by Dr. Paul Gilman.

Caspase inhibitors z-VAD-fmk, z-IETD-fmk and z-DEVD-fmk were purchased from BD Pharmingen (Mississauga, ON, Canada). SYTOX Green death stain, Alexa Fluor 647 Annexin V conjugate, CellRox Green, CM-H<sub>2</sub>DCFDA were all obtained from Invitrogen (Carlsbad, CA, USA). All chemicals were purchased from Sigma-Aldrich (St Louis, MO, USA) unless indicated otherwise.

Antibody against caspase 3 (#ADI-AAP-13) was from Enzo Life Science (Farmingdale, NY, USA); Bid antibody (#2002), Puma antibody (#12450), Bim antibody (#2819), cleaved caspase 8 antibody (#9496), caspase 9 antibody (#9502), Bax antibody (#2774) and Bcl-2 (#2872) antibody were from Cell Signaling (Boston, MA, USA); Bak antibody (#06-536) was from EMD Millipore (Burlington, ON, CA); Bik (sc1710) antibody and Tom-20 antibody (#SC-11415) were from Santa Cruz (Dallas, TX, USA); Cytochrome c antibody (#556433) was from BD Pharmingen (San Diego, CA, USA) and antibodies against  $\alpha$ -tubulin (#T5168) and Bax 6A7 (#B8429) were from Sigma-Aldrich. Noxa antibody (#ab13654) was from Abcam (Toronto, ON, CA).

## 2.2 Cell culture and treatments

### 2.2.1 Mammalian cell culture

All cell lines were cultured in RPMI-1640 medium (ThermoFisher Scientific, #11875127) with 10% FCS (Thermo Fisher Scientific, #10371029) unless described otherwise. Stable transfected human T-cell leukemia Jurkat cell lines Jneo, JBcl2

and Spi2 were kindly provided by Dr. Chris Bleackley (University of Alberta) (Goping et al., 2003), JR cells were kindly provided by Dr. Hannah Rabinowich (University of Pittsburgh). Jurkat cells were cultured in RPMI-1640 medium (ThermoFisher Scientific, #22400089) with 10% FCS and 0.05  $\mu$ M 2-mercaptoethanol (2-ME). Cell lines MCF-10A (#CRL-10317), hTERT-HME1 (#CRL-4-10), B16-F0 (#CRL-6322), B16-F10 (#CRL-6475), Hs578BST (#HTB-125) and Hs578T (#HTB-126) were all obtained from ATCC (Manassas, VA, USA). MCF-10A was maintained in DMEM/F12 (Invitrogen, #11965-118) with 5% horse serum (Invitrogen, #16050-122); 20 ng/ml EGF (Peprotech, #AF-100-15); 0.5 mg/ml hydrocortisone (Sigma Aldrich, #H-0888); 100 ng/ml cholera toxin (Sigma Aldrich, #C-8052) and 10  $\mu$ g/ml insulin (Sigma Aldrich, #I-1882). hTERT-HME1 was cultured in MEGM (#CC-3150) from Lonza Corporation (Allendale, NJ, USA). B16-F0, B16-F10 and Hs578T were maintained in DMEM (ThermoFisher Scientific, #11995040), high glucose, with 10% FCS; Hs578BST was maintained in DMEM, high glucose, with 10% FCS and 30 ng/ml EGF. All cell lines were tested routinely using MycoAlert™ Mycoplasma Detection Kit (Lonza, #LT07-318). Cells were mycoplasma free.

### 2.2.2 Yeast cell culture

Yeast cells were propagated in YPD medium (1 L medium contains 10 g yeast extract, 20 g peptone, 100 ml 20% dextrose and 20 g agar). For respiratory deficient cells, 0.25 mg/ml G418 was added to the medium. All strains were obtained from the MAT  $\alpha$  yeast deletion collection (Giaever et al., 2002).

### 2.2.3 D112 treatment

D112 was diluted in DMSO to achieve a stock concentration of 1 mg/ml (~1.4 mM) and stored in the dark at -20°C. The DMSO concentration during cell treatment conditions was kept consistently at 0.4%. For Jurkat cells treatment, including Jneo, JBcl-2 and JR, cells were harvested and re-suspended in fresh medium at a density of  $2 \times 10^5$  cells/ml. D112 was added directly to the medium and mixed well. For adherent cells,  $2 \times 10^5$  cells were seeded in 24-well plates overnight. D112 was added to the medium when cells reached 80-90% confluence on the second day.

## 2.3 Cell viability assays in mammalian cells

### 2.3.1 Determination of apoptosis

#### 2.3.1.1 Measurement of phosphatidylserine exposure

PS exposure was measured by flow cytometry using Alexa Fluor 647 conjugated to Annexin V (ThermoFisher Scientific, #A23204). Briefly, cells were harvested and washed 3 times with PBS.  $\sim 7 \times 10^4$  cells were then re-suspended in 100  $\mu$ L Annexin-binding buffer (10 mM HEPES, 140 mM NaCl, and 2.5 mM  $\text{CaCl}_2$ , pH 7.4) with 2.5  $\mu$ L Alexa Fluor 647 Annexin V conjugate, and incubated for 15 min at room temperature in the dark. After washing with PBS, the percentage of cells binding Alexa Fluor 647 Annexin V was determined using an Accuri C6 flow cytometer (BD Accuri, Ann Arbor, MI, USA) in the FL-4 channel.

#### 2.3.1.2 Measurement of mitochondrial membrane potential

Loss of mitochondrial membrane potential was detected using the cationic

dye DiOC6 (3,3'-dihexyloxacarbocyanine iodide) purchased from ThermoFisher (#D273) (Perry et al., 2011). Cells were harvested and washed twice with PBS, and then cells were stained with 40 ng/ml DiOC6 in PBS for 10 min at room temperature in the dark. After staining, cells were rinsed gently in PBS and loss of membrane potential was determined by loss of DiOC6 fluorescence in the FL-1 channel as measured by flow cytometry. To measure the basal level of mitochondrial membrane potential, cells were stained with 10 ng/ml DiOC6 in PBS and fluorescence was quantitated as indicated above.

#### 2.3.1.3 Caspase enzymatic activation assay

To measure caspase 3 activation,  $2 \times 10^7$  cells were treated with D112 at indicated concentrations for 24 h. All cells (floating and adherent) were harvested and washed twice with PBS, then re-suspended in 100  $\mu$ L cell lysis buffer (50 mM HEPES, 100 mM NaCl, 0.1% CHAPS, 1 mM DTT, 100 mM EDTA, pH 7.4) on ice for 20 min. Protein concentration was measured by a Pierce BCA protein assay kit (ThermoFisher Scientific, #23225) according to the manufacturer's instructions. 100  $\mu$ g of protein from each assay was diluted in 50  $\mu$ L cell lysis buffer and mixed with 50  $\mu$ L of 2X Reaction Buffer (50 mM HEPES, 100 mM NaCl, 0.1% CHAPS, 10 mM DTT, 100 mM EDTA, 10% glycerol, pH 7.4). 5  $\mu$ L of the 4 mM DEVD-AFC substrate (200  $\mu$ M final concentration) (Walsh et al., 2008) was added to the mixture and incubated at 37°C for 1 h in the dark. Caspase 3 activity was determined at Ex/Em 405/492 nm in a 96-well plate on a Multiskan Ascent plate reader (ThermoFisher Scientific).

#### 2.3.1.4 DNA fragmentation assay

Jneo cells were treated with D112 at indicated concentrations for 24 h. Genomic DNA was extracted using the Mammalian Genomic DNA Miniprep Kit (Sigma Aldrich, #G1N70), according to the manufacturer's instructions. An equal amount of DNA (1  $\mu$ g) was loaded in an agarose electrophoresis gel and visualized using SYBR Safe DNA Gel Stain (1:10,000 dilution in TBE, #s33102, Invitrogen).

#### 2.3.1.5 Subcellular fractionation to enrich for mitochondrial fractions

In order to examine whether mitochondrial resident cytochrome c was released to the cytoplasm in D112-treated cells, mitochondria and cytoplasm were biochemically separated using the following protocol. Jneo cells were treated with D112 at indicated concentrations for 24 h.  $2 \times 10^6$  cells per sample were harvested and cell pellets were then re-suspended in 100  $\mu$ l of digitonin lysis buffer (75 mM NaCl, 1 mM  $\text{NaH}_2\text{PO}_4$ , 8 mM  $\text{Na}_2\text{HPO}_4$ , 250 mM sucrose, 1% digitonin, pH 8) and incubated on ice for 10 min. The lysate was centrifuged for 5 min at 18,000 g at 4°C. The supernatant (cytosolic fraction) was transferred to another tube and pellet containing heavy membrane, including mitochondria, was re-suspended in 200  $\mu$ l of Triton X-100 lysis buffer (0.1% Triton X-100, 25 mM Tris pH 8.0). Both supernatant and pellet were mixed with SDS loading buffer (250 mM Tris-HCL pH 6.8, 4% SDS, 30% glycerol, 0.003% bromphenol blue and 10% 2-mercaptoethanol) and subjected to SDS/PAGE followed by western blotting. Additionally, in this experiment, 2.5  $\mu$ M staurosporine (STS) purchased from Sigma (#S5921) was used as a positive control (Scarlett et al., 2000), and cells were incubated with STS for 4 h before being processed as above.

### 2.3.2 Detection of cellular plasma membrane damage (necrosis)

Cells were harvested and washed twice with PBS, and re-suspended in binding buffer (10 mM HEPES, 140 mM NaCl, 2.5 mM CaCl<sub>2</sub>, pH 7.4) containing 30 nM SYTOX Green stain solution (ThermoFisher Scientific, #S7020). Cells were incubated for 20 min at room temperature in the dark. Cells were washed twice with PBS, and SYTOX Green-positive cells were quantitated in the FL-1 channel as measured by flow cytometry.

### 2.3.3 Cell proliferation

Cell viability was determined by exclusion of the vital dye, trypan blue. Jneo, JBcl-2, JR cells were treated with 62.5 ng/ml D112 for 24 h. All cells were washed and re-suspended in fresh medium. 10<sup>4</sup> cells (per well) were seeded in 24-well plates. The total cell numbers were recorded every 24 h. In brief, an aliquot of cells were stained with 0.4% trypan blue solution (ThermoFisher Scientific, #15250061) at a 1:1 (v/v) ratio. The percent of trypan blue-positive cells was determined using a Bio-Rad TC20 Automated Cell Counter (Bio-Rad, #1450102).

### 2.3.4 Single colony formation

Equal number of cells for each cell line were treated with D112 at indicated concentrations for 24 h. All cells (floating and adherent) were harvested and seeded in 12-well plates and propagated in appropriate culture conditions. Due to differing proliferation rates, cell lines were plated as follows: for MCF-10A cells, 500 cells were seeded, while for SK-BR-3, MDA-MB-468, B16-F0 and B16-F10 cell lines, 100 cells were seeded. Cells were incubated for 7–14 days. Culture media was removed,

and colonies were fixed and stained with crystal violet solution of 0.05% (w/v) crystal violet (Sigma Aldrich, #C3886), 4% formaldehyde (ThermoFisher Scientific, #28906) in 1 X PBS for 30 min. The plates were washed in water until a clear background was obtained. The number of colonies was counted manually.

## **2.4 Protein assays**

### **2.4.1 Western blotting**

Jurkat cells were treated with 0, 0.25, 0.5, 1, 2 or 4  $\mu\text{g/ml}$  D112 for 24 h. All cells were harvested, washed twice in cold PBS and lysed in lysis buffer (50 mM Tris pH 8, 150 mM NaCl, 1% NP-40, 0.5% sodium deoxycholate, 1 mM  $\beta$ -mercaptoethanol), on ice for 20 min. Cell lysate was centrifuged at 12,000 x g for 10 min at 4°C. Protein concentration was measured using a Pierce BCA protein assay kit (ThermoFisher Scientific, #23225). Cell lysates were then mixed with SDS-PAGE gel loading buffer (250 mM Tris-HCL pH 6.8, 4% SDS, 30% glycerol, 0.003% bromphenol blue and 10% 2-mercaptoethanol) to achieve a final concentration of 1 mg/ml protein in 1xSDS loading buffer and boiled for 10 min. 15  $\mu\text{g}$  of protein were loaded onto 8 or 14% SDS polyacrylamide gels (SDS-PAGE), along with 3  $\mu\text{L}$  of PageRuler Prestained Protein Ladder (ThermoFisher Scientific, #26616), and subjected to SDS-PAGE analysis. Proteins were resolved at 100 V and subsequently transferred to PVDF membranes (EMD Millipore, #IPVH00010) using a Bio-Rad Mini-Gel Box Electrotransfer apparatus (Bio-Rad, #1703930) for 1 h at 300 mA. Membranes were blocked in Tris-buffered saline (50 mM Tris-HCl, 150 mM NaCl, pH 7.5) containing 0.1% Tween-20 and 5% skimmed milk for 1 h at room

temperature. Proteins were incubated with specific primary antibodies overnight at 4 °C. After washing 3 times in TBS, membranes were incubated with goat anti-mouse (ThermoFisher Scientific, #31430) or anti-rabbit HRP-conjugated (BD Pharmingen, #554021) secondary antibodies at room temperature for 1 h. Specific immunoreactive proteins were detected using ECL Prime Western Blotting Detection Reagent Kit (GE Healthcare Life Science, Mississauga, CA).

#### 2.4.2 Immunoprecipitation for identification of activated Bax

$2 \times 10^6$  cells were harvested after treatment and lysed in 200  $\mu$ L cold CHAPS lysis buffer (1% CHAPS; 150 mM NaCl; 50 mM Tris; 2 mM EDTA; pH 7.4). Protease inhibitor cocktail (Sigma Aldrich, #11836153001) and Phosphatase inhibitor cocktail (Roche, #4906845001) were added according to the manufacturer's instructions. The lysate was centrifuged at 10,000 g, for 5 min at 4°C. 75  $\mu$ L of the supernatant was incubated with mouse anti-Bax 6A7 antibody (Sigma Aldrich, # B8429) at a 1:10 dilution and incubated at 4°C overnight. Bax 6A7 is conformation specific antibody recognizing activated Bax (Upton et al., 2007). For a negative control, mouse anti-vimentin antibody (Sigma Aldrich, #V2238) was included in a separate reaction with 75  $\mu$ L supernatant. The remaining 50  $\mu$ L of supernatant served as the total cell lysate input control. Protein A-coupled sepharose beads (Abcam, #ab193256) were washed with CHAPS buffer, and 15  $\mu$ L of a 50% bead slurry was added to the antibody/lysate mixtures and incubated for 1 h at 4°C with gentle agitation. After incubation, beads were centrifuged and the supernatant was removed. Beads were washed in lysis buffer three times. Beads were resuspended in 6X SDS-PAGE gel loading buffer (250 mM Tris-HCl pH 6.8, 4% SDS, 30% glycerol, 0.003%

bromphenol blue and 10% 2-mercaptoethanol) and boiled for 10 min.

Immunoprecipitated products were loaded onto 14% SDS polyacrylamide gels and subjected to SDS-PAGE analysis. 7.5  $\mu$ L of the total cell lysate was also loaded, representing a 10% input control. Proteins were resolved at 100 V and subsequently transferred to PVDF membranes (EMD Millipore, #IPVH00010) using a Bio-Rad Mini-Gel Box Electrotransfer apparatus (Bio-Rad, #1703930) for 1 h at 300 mA. Membranes were blocked in Tris-buffered saline (50 mM Tris-HCl, 150 mM NaCl, pH 7.5) containing 0.1% Tween 20 and 5% skimmed milk for 1 h. Bax species that were immunoprecipitated by the active Bax 6A7 antibody were visualized by western blotting with a pan anti-Bax primary antibody (Cell Signaling, #2774), followed by goat anti-rabbit HRP-conjugated secondary antibody (Bio-Rad, #170-6515).

## **2.5 Analysis of D112 fluorescence**

### **2.5.1 D112 spectra**

Fluorescent spectral scans were performed using a model 814 photomultiplier detection system (Photon Technology International, London, Ontario, Can). All data was collected by digital mode on PTI FeliX32 software. The cuvette used was a disposable cuvette (ThermoFisher Scientific, #14-955-125), which contained 0.25  $\mu$ g/ml D112 diluted in phosphate buffer pH 7.4. To acquire a full spectral scan, D112 was excited from 340 nm to 620 nm with interval wavelengths of 20 nm. For each excitation wavelength, the corresponding emission spectra were collected from excitation wavelength +20 nm to 750 nm.

### 2.5.2 D112 spectra with nucleic acids

25 ng/ml DNA/RNA was mixed with 0.25  $\mu$ g/ml D112, and incubated at room temperature for 15 min in the dark. Then the fluorescent spectra was collected as described above.

### 2.5.3 Measurement of D112 fluorescence in tissue culture medium

Equal numbers of cells from each cell line were seeded in 6-well plates and cultured in RPMI-1640 medium (with 10% FCS) overnight. The next day, the media was replaced with fresh media containing 0.25  $\mu$ g/ml D112 for 1 h. The medium was then transferred into a disposable cuvette and D112 fluorescence was assessed as described in 2.5.1 with excitation at 515 nm. D112 intensity was normalized to control medium (0.25  $\mu$ g/ml D112 in the absence of cells).

## 2.6 Examination of D112 Localization

### 2.6.1 Plasmids

mEmerald-Tom 20 plasmid (Addgene, #54282) was kindly supplied by Dr. Robert. E. Campbell (University of Alberta). Rab5-GFP and Rab7-GFP plasmids were generously provided by Dr. Nicolas Touret (University of Alberta).

### 2.6.2 Transient transfections

SK-BR-3 cells were seeded in an 8-well Nunc Lab-Tek chambered coverglass (ThermoFisher Scientific, #155411) and grown to 70% confluence for transfection. To form the transfection complex, 10  $\mu$ L pre-warmed Opti-MEMI Reduced-Serum Medium (Life Technologies, #31985088) with 0.2  $\mu$ g plasmid DNA was mixed with

an equal volume of Opti-MEM1 Reduced-Serum Medium with 0.4  $\mu$ L TransIT-LT1 reagent (Mirus, #MIR 2300). After 20 min incubation at room temperature, the complex was dropped to different areas of the wells and the cells were incubated for 6 h for plasmid delivery. Complex was then replaced by fresh complete growth medium. Transfected cells were cultured for 24 h to allow gene expression and membrane recovery before the next treatment.

### 2.6.3 Confocal microscopy

D112 fluorescence was quenched upon fixation, so all localization studies were performed on live cells. Images were acquired on a Zeiss LSM 710 inverted confocal microscope fitted with a 40x 1.4 NA Oil DIC Plan-Apochromat objective (Toronto, ON, Canada). After acquisition, images were visualized using ZEN 2009 Light Edition (Carl Zeiss) and MetaXpress (Version 5.2) (Molecular Devices) software. Image analysis and processing was performed on Fiji (online open-source, <http://fiji.sc/Fiji> ). Linescan analysis was performed on MetaXpress. For the calculation of Mander' s correlation coefficient for co-localization, a region of interest (ROI) was applied to transfected cells. A manual threshold was applied to each channel using 'dark background' and the Mander' s correlation calculation was run by Coloc 2 method on Fiji Software ([http://fiji.sc/Colocalization\\_Analysis#Colocalization\\_analysis\\_using\\_Coloc\\_2](http://fiji.sc/Colocalization_Analysis#Colocalization_analysis_using_Coloc_2)).

## 2.7 Localization and viability assays in yeast

### 2.7.1 D112 localization in yeast

$3 \times 10^6$  yeast cells were treated with 5  $\mu$ g/ml D112 for 30 min, 1 h, 2 h, 3 h or 4

h. Yeast cells were centrifuged (3,000 x g for 5 min), re-suspended in 100  $\mu$ L fresh YPD medium and 50  $\mu$ L of the cell suspension was spotted onto Concanavalin A (0.1 mg/ml) pre-coated coverslips (Pemberton, 2014), and imaged using a Zeiss AxioObserver.Z1 Microscope fitted with a 40 x objective lens. D112 fluorescence was detected using the Chroma Filter Set 49005 (Cy3, excitation 545/30, emission 620/60).

### 2.7.2 Yeast growth curves

Yeast cells were cultured in 24-well flat-bottomed clear plates with DMSO or D112 at the indicated concentrations in YPD (1L: 10 g yeast extract, 20 g peptone, 100 ml 20% dextrose) or YPG (1L: 10 g yeast extract, 20 g peptone, 100 ml 30% glycerol) medium. Cell growth was performed at 30°C with orbital shaking at 200 rpm using a CLARIOstar Microplate Reader (BMG LABTECH, Ortenberg, Germany) starting from an OD<sub>600</sub> of 0.1. Measurements were recorded every 5 min, preceded by 1 min of shaking at 300 rpm. Doubling time was determined using CLARIOstar data analysis software where the maximal slope of a consecutive 12 point sample during exponential growth was used and entered into the equation  $f(x)=\ln(2)/x$ ; where  $f(x)$ = the slope and  $x$  is the doubling time as derived from the doubling time formula  $P = P_0(2^{t/x})$ .

### 2.7.3 Yeast recovery assay

Yeast cells were seeded in fresh YPD at OD<sub>600</sub> 0.1 in culture tube. D112 at 5  $\mu$ g/ml (in YPD) or 0.625  $\mu$ g/ml (in YPG) was added and incubated at 30°C with orbital shaking at 300 rpm for 24 h. Cells were then washed 3 times and re-

suspended in fresh YPD medium at OD<sub>600</sub> 0.3 (~3 x 10<sup>6</sup> cells/ml). Two-fold serial dilutions were spotted on YPD plates and grown for 3 days at 30°C. For quantification of viability, equal number of yeast cells (300 cells in YPD) or (600 cells in YPG) after treatment were spread on YPD plates, and the number of single colonies was counted after 3~4 days of growth at 30°C.

## **2.8 Assays for ROS detection**

### 2.8.1 Measurement of ROS levels

ROS generation was examined by two cell-permeant oxidative stress indicators, CM-H<sub>2</sub>DCFDA (ThermoFisher Scientific, #C6827) and CellROX Green (ThermoFisher Scientific, #C10444). Cells were treated with D112 at indicated concentrations for 1 h, and 2.5 μM CellRox Green reagent was added and incubated for 30 min at 37°C. Cells were harvested and washed 2 x with PBS. Oxidation of CellROX green yields a bright fluorescent, DNA binding product that was detected in the FL-1 channel using flow cytometry. ROS production was also examined using CM-H<sub>2</sub>DCFDA. Cells were harvested and washed in PBS. 1.5 μM CM-H<sub>2</sub>DCFDA was incubated with cells for 15 min, and then cells were incubated with D112 at indicated concentration for 1 h. Oxidation of CM-H<sub>2</sub>DCFDA yields a fluorescent DCF adduct that was trapped inside the cells and detected in the FL-1 channel using flow cytometry. Peroxide TBHP at 200 μM (*tert*-Butyl hydroperoxide) was used as a positive control. For ROS detection by microscopy, 2.5 μM CellROX green was added to the live cell chamber and incubated at 37°C for 30 min. Images

were acquired using a Zeiss AxioObserver Z1 Microscope with 20 x objective lens. After acquisition, images were visualized using ZEN 2009 Light Edition (Carl Zeiss).

In yeast cells,  $1 \times 10^6$  ( $OD_{600}$  0.1) yeast cells were treated with 5  $\mu\text{g}/\text{ml}$  D112 for 4 h and 5  $\mu\text{M}$  CellROX green was added directly to the medium and incubated at 30°C for 20 min. Yeast cells were spun down, re-suspended in 100  $\mu\text{L}$  fresh YPD medium, spotted to Concanavalin A (0.1 mg/ml) pre-coated glass coverslips and imaged using a Zeiss AxioObserver Z1 Microscope with a 40x objective lens. CellROX Green was detected using Chroma filter set 49002 (GFP, excitation 470/40 nm, emission 525/50 nm).

### 2.8.2 NAC treatment

ROS scavenger NAC (N-acetylcysteine) was freshly prepared (Zafarullah et al., 2003). 1M NAC was dissolved in ddH<sub>2</sub>O and pH was adjusted to 7.4 using NaOH by pH Meter. For ROS scavenger experiments, cells were pre-treated with NAC (10 mM) for 1 h, and ROS production was evaluated as described above.

### 2.8.3 Hypoxia treatment

Cells were incubated in a hypoxia chamber (Xvivo closed incubation system, Biospherix, NY, USA), with 0% oxygen present. All cells were placed in the chamber 4 h before adding D112. After 24 h incubation, apoptosis was determined by analyzing phosphatidylserine exposure as described in 2.3.1.1.

## 2.9 Assays examining D112 interaction with DNA

### 2.9.1 D112 electrophoretic gel-shift assay

0.025  $\mu\text{g/ml}$  D112 was mixed with 0.5  $\mu\text{g}$  or 1  $\mu\text{g}$  DNA ladder and incubated for 30 min at room temperature in the dark. The mixture was loaded onto a 1% agarose gel and run at 100 V for 1 h. The gel was first exposed at 550/570 nm to capture the D112 fluorescent signal. The same gel was then stained with SYBR safe (Sigma Aldrich, # S33102,) to visualize the DNA at 492/510 nm.

### 2.9.2 mtDNA damage assay

Jneo cells were treated with 0.25 or 2  $\mu\text{g/ml}$  D112 for 1 h. Genomic DNA was extracted using the Mammalian Genomic DNA Miniprep Kit (Sigma Aldrich, #G1N70), according to the manufacturer's instructions. PCR was performed using Elongase Enzyme kit (ThermoFisher Scientific, #10480028). The reaction was set up as below:

Component	Volume per 50 $\mu\text{l}$ reaction
<b>Mix 1</b>	
10 mM dNTP mix	1 $\mu\text{l}$
Forward primers, 10 $\mu\text{M}$	1 $\mu\text{l}$
Reverse primers, 10 $\mu\text{M}$	1 $\mu\text{l}$
Template DNA	15 ng
Water	to 20 $\mu\text{l}$
<b>Mix 2</b>	
5X Buffer A	7 $\mu\text{l}$
5X Buffer B	3 $\mu\text{l}$
Elongase Enzyme Mix	1 $\mu\text{l}$
Water	to 30 $\mu\text{l}$

Reactions were performed on the Bio-Rad C1000 Touch Thermal Cycler. The primers for large mtDNA fragment (8.9 kb) (Solesio et al., 2013) were 5'-TTTCATCATGCGGAGATGTTGGATGG-3' and 5'-TCTAAGCCTCCTTATTCGAGCCGA-3'; the primers for small mtDNA fragment (Solesio et al., 2013) (212 bp) were 5'-TTTCATCATGCGGAGATGTTGGATGG-3' and 5'-CCCCACAAACCCCATTAATAACCCA-3'. The PCR program for the large mtDNA fragment was: cycle 1(1X), 94°C for 30 sec; cycle 2 (20X), step 1 at 94.0°C for 30 sec; step 2 at 64.0°C for 30 sec; step 3 at 68°C for 9 min; cycle 3 (1X). The PCR program for the small mtDNA fragment: cycle 1(1X), 94°C for 30 sec; cycle 2 (20X), step 1 at 94.0°C for 30 sec; step 2 at 64.0°C for 30 sec; step 3 at 72°C for 30 sec; cycle 3 (1X). Equal volumes of the PCR reactions were electrophoresed on an agarose gel and visualized by SYBR safe staining. A 15% agarose gel was used for the small mtDNA fragment detection, whereas an 8% agarose gel was used for detection of the large mtDNA fragment.

### 2.9.3 Assay to test for the induction of the petite phenotype

An overnight culture of the W303-1A yeast strain was subcultured into fresh YPD at OD<sub>600</sub> 0.1. Two or 5 µg/ml D112 was added to the cell culture and incubated at 30°C with orbital shaking at 200 rpm for 4 h. Cells were diluted and counted under microscopy. ~300 cells were plated on YPD plates and incubated for 3 days at 30°C. The number of red and white colonies was manually counted. Ethidium bromide (EB, 20 µM) was used as a positive control.

## **2.10 Photodynamic therapy treatment**

Cells were plated in an 8-well Nunc Lab-Tek chambered coverglass (Thermo Fisher Scientific, #155411), D112 was added to the indicated concentrations, incubated for 1 h in the dark, then cells were rinsed twice with fresh medium. Cells were placed in a temperature-controlled humidified live cell chamber (with 5% CO<sub>2</sub>) attached to an inverted Zeiss AxioObserver.Z1 microscope. Cells were exposed to red light (excitation 541/30 nm) for the indicated times. Bright field images were taken every 30 min for 24 h using a 20 or 40X objective. Cell death morphology was manually recorded.

## **2.11 Statistical analysis**

Data are presented as the mean of three independent experiments, with error bars indicating the SD. Statistical significance was determined using a two-tailed Student's t-test for two means with equal variance. For statistical analysis of multiple groups, the one-way Analysis of Variance (ANOVA) test was performed and p-values were obtained by Tukey' s Post Hoc test.

## Reference

Giaever, G., Chu, A.M., Ni, L., Connelly, C., Riles, L., Veronneau, S., Dow, S., Lucau-Danila, A., Anderson, K., Andre, B., *et al.* (2002). Functional profiling of the *Saccharomyces cerevisiae* genome. *Nature* *418*, 387-391.

Goping, I.S., Barry, M., Liston, P., Sawchuk, T., Constantinescu, G., Michalak, K.M., Shostak, I., Roberts, D.L., Hunter, A.M., Korneluk, R., *et al.* (2003). Granzyme B-induced apoptosis requires both direct caspase activation and relief of caspase inhibition. *Immunity* *18*, 355-365.

Pemberton, L.F. (2014). Preparation of yeast cells for live-cell imaging and indirect immunofluorescence. *Methods Mol Biol* *1205*, 79-90.

Perry, S.W., Norman, J.P., Barbieri, J., Brown, E.B., and Gelbard, H.A. (2011). Mitochondrial membrane potential probes and the proton gradient: a practical usage guide. *Biotechniques* *50*, 98-115.

Scarlett, J.L., Sheard, P.W., Hughes, G., Ledgerwood, E.C., Ku, H.H., and Murphy, M.P. (2000). Changes in mitochondrial membrane potential during staurosporine-induced apoptosis in Jurkat cells. *FEBS Lett* *475*, 267-272.

Solesio, M.E., Prime, T.A., Logan, A., Murphy, M.P., del Mar Arroyo-Jimenez, M., Jordán, J., and Galindo, M.F. (2013). The mitochondria-targeted anti-oxidant MitoQ reduces aspects of mitochondrial fission in the 6-OHDA cell model of Parkinson's disease. *Biochimica et Biophysica Acta (BBA) - Molecular Basis of Disease* *1832*, 174-182.

Upton, J.P., Valentijn, A.J., Zhang, L., and Gilmore, A.P. (2007). The N-terminal conformation of Bax regulates cell commitment to apoptosis. *Cell Death Differ* *14*, 932-942.

Walsh, J.G., Cullen, S.P., Sheridan, C., Lüthi, A.U., Gerner, C., and Martin, S.J. (2008). Executioner caspase-3 and caspase-7 are functionally distinct proteases. *Proceedings of the National Academy of Sciences* *105*, 12815-12819.

Zafarullah, M., Li, W.Q., Sylvester, J., and Ahmad, M. (2003). Molecular mechanisms of N-acetylcysteine actions. *Cell Mol Life Sci* *60*, 6-20.

## **CHAPTER 3**

**D112 INDUCES THE MITOCHONDRIAL-APOPTOTIC PATHWAY AND  
SHOWS HIGHER SELECTIVITY FOR TRANSFORMED CELLS**

### 3.1 Introduction

Despite enormous efforts that have been put in anticancer drug development, cancer remains a leading cause of death in North America (American Cancer Society, 2014; Canadian Cancer Society, 2013). A major contributor to treatment failure is the lack of the apoptotic response in cancer cells (Zahreddine and Borden, 2013). Apoptosis is widely blocked in cancer, and moreover the inactivation of apoptosis is central to the development of cancer (Portt et al., 2011; Wong, 2011). Therefore, targeting the apoptotic machinery is a potential therapeutic approach (Bai and Wang, 2014).

The cyanine dye D112, was initially developed by Kodak Laboratories as a photosensitizer for use in photographic emulsions. An interest in therapeutic applications for these dyes triggered the company to initiate a drug-screening program with the Dana Farber Institute in 1970's (Gilman et al., 2006). In this program, the cytotoxicity of photography compounds was evaluated by examining their inhibitory effect on cell proliferation *in vitro* by measuring colony formation. Approximately 2000 dyes were evaluated in this program, and D112 emerged as a lead compound based on the observation that treatment of cells *in vitro* with D112 induced a 900-fold reduction of colony numbers for the CX-1 human colon cancer cell line (IC<sub>50</sub> of 0.01  $\mu\text{g}/\text{ml}$ ) relative to the CV-1 normal monkey kidney epithelial (IC<sub>50</sub> of 9  $\mu\text{g}/\text{ml}$ ). A particular shortcoming of these studies, however, was the comparison of a single pair of non-isogenic cell lines from different species. Further studies were not reported and in the absence of information, it is unclear whether the decision to drop D112 studies was due to scientific or financial reasons. Therefore,

we decided to revive studies on D112 with the goal to determine whether D112 indeed had therapeutic potential. In this chapter, I investigated the cytotoxicity of D112 in cancer cells, characterized D112-induced apoptosis, and further explored its possible selective activity against cancer cells in comparison to normal cells.

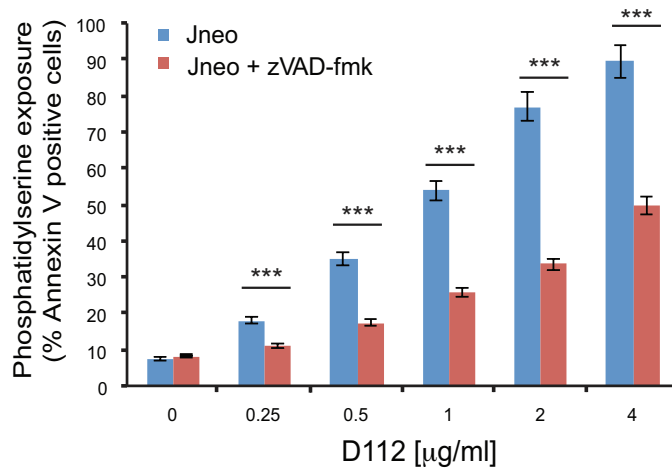
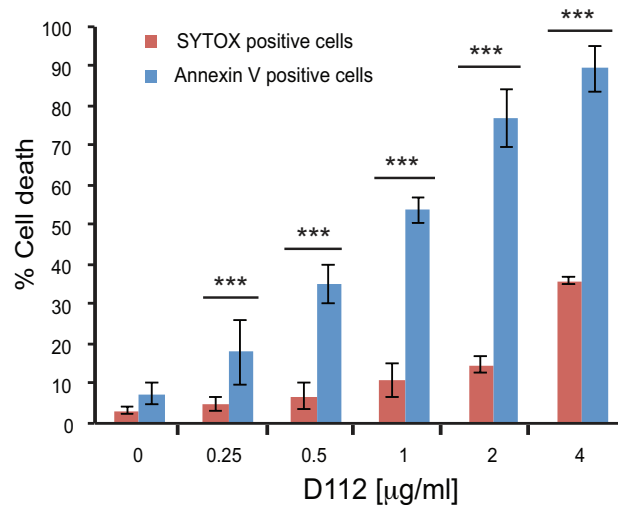
### **3.2 D112 induces apoptosis in Jurkat cells**

I first investigated the mechanism of D112-induced cytotoxicity and hypothesized that D112 induced apoptosis. I tested this hypothesis using a Jurkat human T-cell leukemia cell line as a model system because it had a well-characterized apoptotic response and isogenic cell lines were available to test molecular regulators of the apoptotic pathway (Goping et al., 2003). To investigate whether D112 induced apoptosis, I treated a Jurkat sub-line, named Jneo (Goping et al., 2003) with D112 at increasing concentrations ( $1 \mu\text{g/ml} = 1.4 \mu\text{M}$ ) for 24 h and measured the apoptotic hallmarks of phosphatidylserine externalization, mitochondrial depolarization, caspase activation, and DNA fragmentation.

#### **3.2.1 D112 causes phosphatidylserine exposure**

We first assessed cell death with the apoptotic marker of phosphatidylserine (PS) exposure. PS is normally restricted to the inner leaflet of the plasma membrane bilayer, and is externalized in response to caspase activation (Borisenko et al., 2003). To measure whether D112 induced PS exposure, I harvested cells after D112 treatment and measured fluorescent-annexin V binding by flow cytometry. The addition of D112 increased Annexin V positive cells in a dose-dependent manner

(Fig. 3.1A). To determine whether PS exposure was caspase-dependent, I co-incubated cells with the pan-caspase inhibitor zVAD-fmk and established that D112-mediated PS externalization was caspase-dependent. Of note, at higher concentrations of D112, a significant amount of PS exposure was observed in the presence of zVAD-fmk, relative to non-D112-treated cells. These results suggested that D112 either induced an alternative caspase-independent necrotic pathway, or that secondary necrosis (*in vitro* membrane damage) accounted for Annexin V positivity at higher concentrations of D112. To distinguish between these two possibilities, we measured plasma membrane disruption through uptake of the vital DNA-binding dye, SYTOX green (Fig. 3.1B). Non-specific membrane damage was only evident at D112 concentrations that were higher than the amount required to detect PS exposure indicating that apoptosis and not necrosis was the initiating event. To directly measure secondary necrosis, we simultaneously labeled D112-treated cells with fluorescent Annexin V and SYTOX green in a time course experiment (Fig. 3.2). SYTOX green-only positive cells were undetectable. Instead, cells became Annexin V positive first and only at later time points became double positive for Annexin V and SYTOX green. Moreover, addition of the pan caspase inhibitor zVAD-fmk, reduced the proportion of SYTOX green positive cells indicating that D112 did not induce primary necrosis and SYTOX green positive cells came from secondary necrosis (Vercammen et al., 1998).

**A****B**

**Figure 3.1 D112 causes phosphatidylserine exposure in Jurkat cells. A.** Jneo cells were treated with the indicated concentrations of D112 for 24 h in the presence or absence of the pan-caspase inhibitor zVAD-fmk (20 µM). Phosphatidylserine exposure indicated by Alexa Fluor 647-annexin V positive cells is shown as a percent of total cells as determined by flow cytometry. Mean ± SD of three independent experiments performed in triplicate were shown, statistical significance was determined using a two-tailed Student's t-test for two means with equal variance. \*P<0.05, \*\*P<0.01, \*\*\*P<0.001. **B.** Necrosis detection. Cells were treated as above and were incubated with SYTOX Green stain or Alexa Fluor 647-annexin V. Mean ± SD of three independent experiments performed in triplicate were shown, statistical significance was determined using a two-tailed Student's t-test for two means with equal variance. \*P<0.05, \*\*P<0.01, \*\*\*P<0.001.

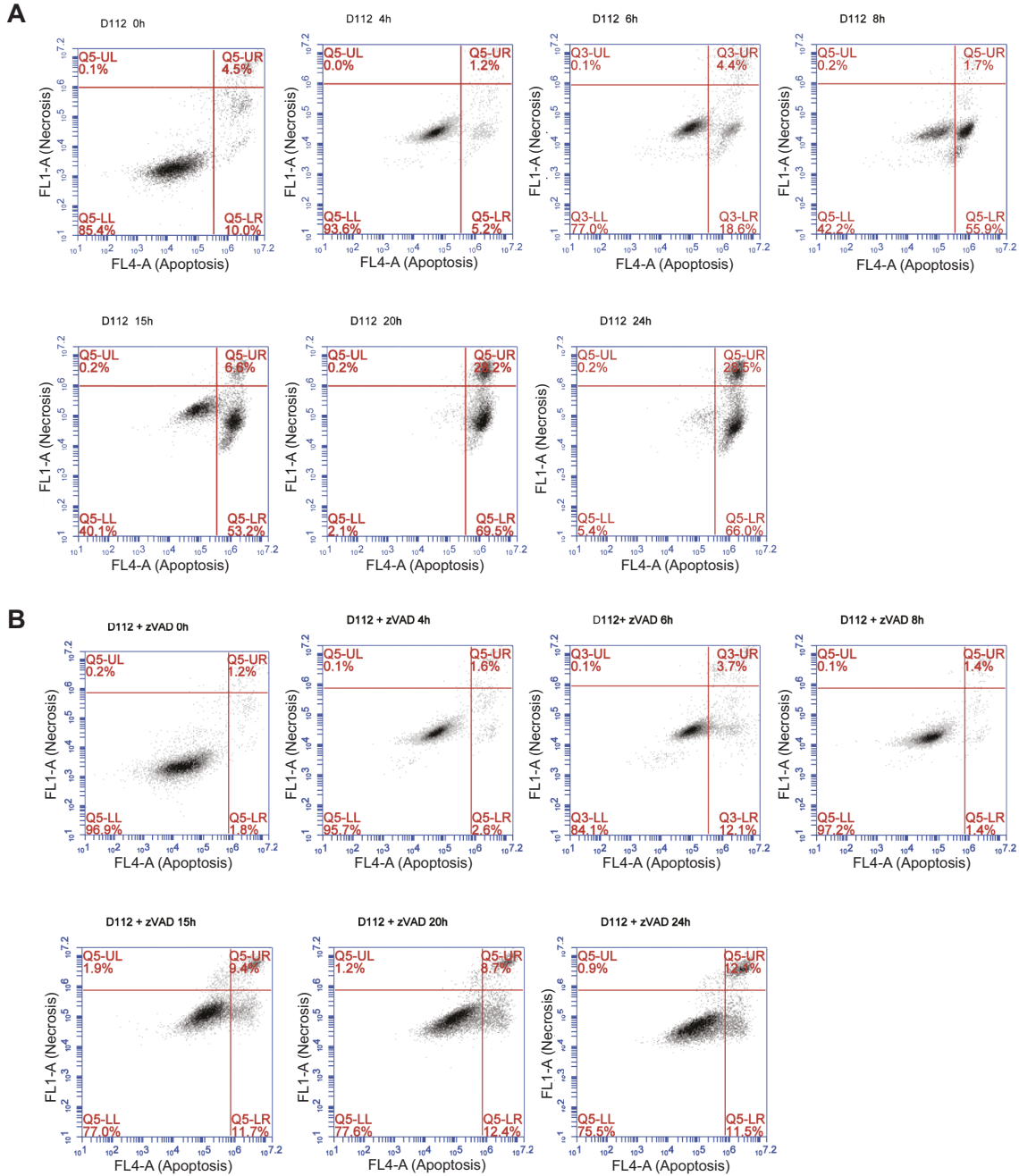


**Figure 3.2 D112 induces apoptosis and secondary necrosis.** Jneo cells were treated with 2  $\mu$ g/ml of D112 in the absence **A.** or presence **B.** of zVAD-fmk (20  $\mu$ M) for the indicated time points and then double labeled with SYTOX green and Alexa Fluro 647 Annexin V. All cells were analyzed by flow cytometry. Shown is a representative of one of three experiments performed in triplicate.

### 3.2.2 D112 causes mitochondrial dysfunction and caspases activation

Since mitochondria are central regulators of the apoptotic pathway, we also examined mitochondrial electrochemical depolarization (loss of electrochemical difference across the inner membrane) in response to D112 treatment. Mitochondrial depolarization was measured by the loss of fluorescence of the potentiometric dye DiOC<sub>6</sub> (3) (3,3'-Dihexyloxacarbocyanine Iodide) (Fig. 3.3 A). Our study showed that the proportion of DiOC<sub>6</sub> negative cells increased in response to D112 treatment. Furthermore, incubation with zVAD-fmk inhibited D112-induced mitochondrial depolarization, indicating that mitochondrial electrochemical potential loss was downstream of caspase activation. Even though mitochondrial depolarization was a late event, we wanted to test whether D112 induced cytochrome c release. In normal condition, cytochrome c residents in intermembrane space, and in response to apoptotic stimuli, it is translocated from the mitochondria to cytoplasm through Bax/Bak pore formed on mitochondrial outer membrane. We incubated cells with increasing concentrations of D112 and fractionated cell components into heavy membrane and cytosolic fractions (Fig. 3.3B). D112 induced the release of cytochrome c from the mitochondrial pellet fraction into the cytosolic supernatant fraction. Mitochondrial involvement and release of cytochrome c suggested that D112 would induce activation of the initiator caspase 9. In support of this, we observed activation-associated cleavage of caspase 9 in response to D112 incubation (Fig. 3.3C). These results are consistent with a model whereby D112 induces cell death via the mitochondrial intrinsic apoptotic pathway.

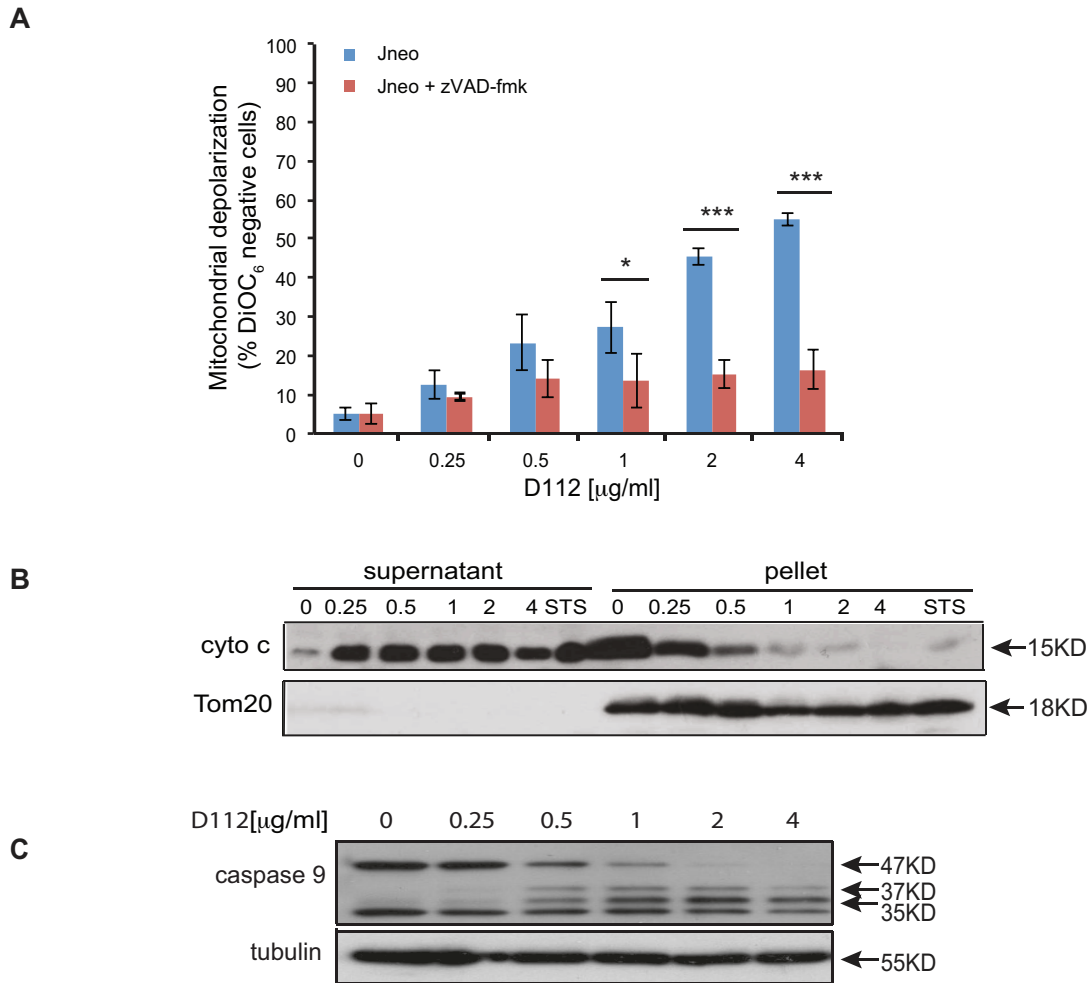


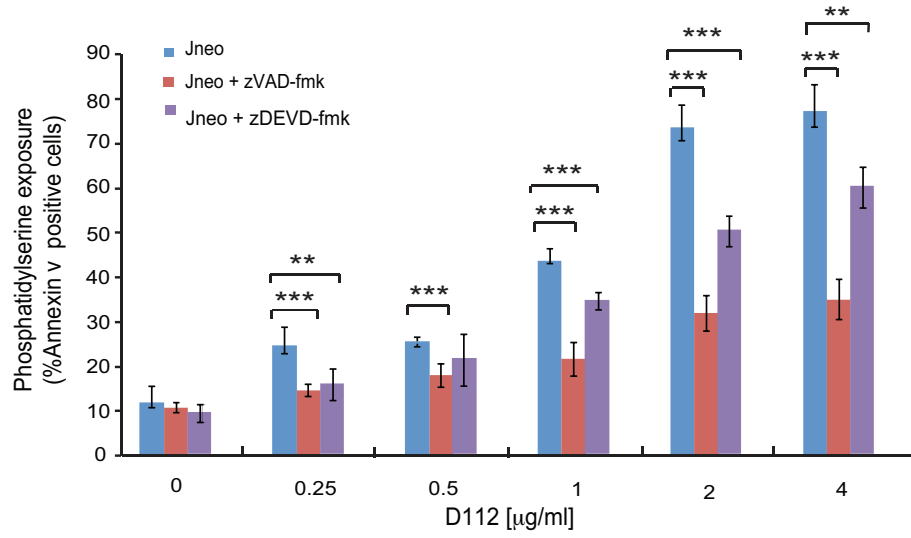
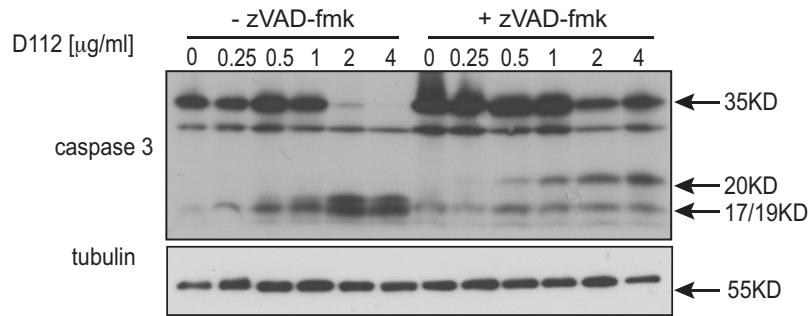
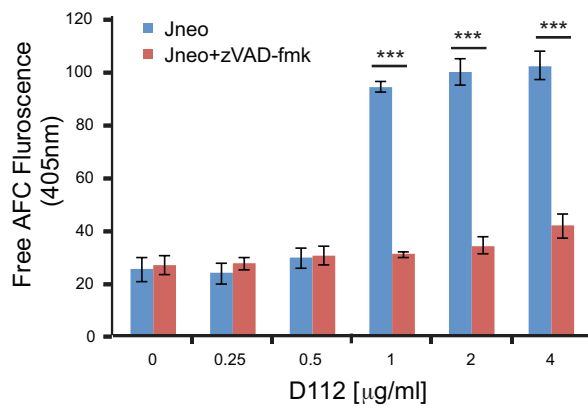
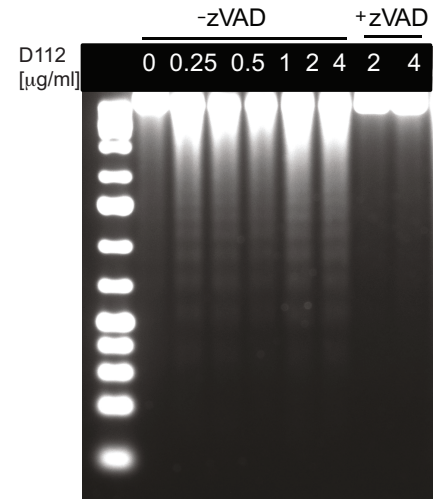
**Figure 3.3 D112 induces mitochondrial dysfunction in Jurkat cells. A.** Mitochondria dysfunction. Cells were treated as above and incubated with DiOC<sub>6</sub>. Loss of electrochemical potential was determined by loss of fluorescence in the FL-1 channel as measured by flow cytometry. Mean  $\pm$  SD of three independent experiments performed in triplicate were shown, statistical significance was determined using a two-tailed Student's t-test for two means with equal variance. \* $P < 0.05$ , \*\* $P < 0.01$ , \*\*\* $P < 0.001$ . **B.** Cytochrome c release. Cells were incubated with D112 at indicated concentrations for 24 h and then harvested and fractionated. Supernatant and pellet were loaded separately and subjected to western blot analysis. Tom 20 was translocase of mitochondrial membrane 20, a mitochondrial specific marker. The experiment was performed independently three times and a representative blot was shown. **C.** Caspase 9 cleavage. Cells were incubated for 24 h with increasing concentrations of D112 as indicated. Whole cell lysates were subjected to western blot analysis with the indicated antibodies. The experiment was performed independently three times and a representative blot was shown.

### 3.2.3 D112 causes caspases activation

Since caspase 9 activation classically leads to executioner caspase 3 activation, we tested the requirement for caspase 3. Incubation with the caspase 3-selective inhibitor zDEVD-fmk significantly reduced D112 induced apoptosis (Fig. 3.4A). We then assessed the activation profile for caspase 3. Caspases are present as inactive pro-enzymes and are activated by proteolytic cleavage. In response to increasing concentrations of D112, we observed the cleavage of pro-caspase 3 from 35 KD to the subunits p17/19 (Fig. 3.4B). Addition of zVAD-fmk inhibited the D112-dependent production of p17/19 and instead produced an intermediate p20 fragment. To assess whether the p20 subunit was associated with enzymatic activity, we incubated cell lysates with the caspase 3 fluorogenic substrate Ac-DEVD-AFC and measured fluorescence of free AFC (Fig. 3.4C). D112-treated cells harbored significantly increased caspase 3 enzymatic activity, while cells that had also been co-incubated with zVAD-fmk had background levels of enzymatic activity. These results indicated that D112 induced the cleavage of caspase 3 to p20. However, the p20 product was not catalytically active, as was evidenced by the absence of AFC fluorescence in enzymatic activity assay.

### 3.2.4 D112 induced DNA fragmentation

We next tested whether D112 induced DNA double-strand breaks consistent with activation of the apoptotic pathway (Fig.3.4D). A DNA ladder was observed in the electrophoretic separation of DNA from D112-treated cells. The production of

**A****B****C****D**

**Figure 3.4 D112 induces caspase activation and DNA fragmentation in Jurkat cells. A.** Phosphatidylserine exposure. Jneo cells were treated with indicated concentrations of D112 for 24 h in the presence or absence of the caspase 3 inhibitor z-DEVD-fmk (20  $\mu$ M), stained as indicated and analyzed by flow cytometry. Mean  $\pm$  SD of three independent experiments performed in triplicate were shown. For statistical analysis, the one-way Analysis of Variance (ANOVA) test was performed and p-values were obtained by Tukey' s Post Hoc test. \*P<0.05, \*\*P<0.01, \*\*\*P<0.001. **B.** Caspase cleavage. Cells were incubated for 24 h with increasing concentrations of D112 as indicated. Whole cell lysates were subjected to western blot analysis with the indicated antibodies. The experiment was performed independently three times and a representative blot is shown. **C.** Caspase 3 enzymatic activation. Jneo cells were treated with D112 in the presence or absence of z-VAD-fmk (20  $\mu$ M) for 24 h prior to lysis. Cell lysates were incubated with the caspase 3 specific fluorometric substrate, Ac-DEVD-AFC, for 1 h and caspase 3 activity was measured at 405 nm. Mean  $\pm$  SD of three independent experiments performed in triplicate were shown, statistical significance was determined using a two-tailed Student's t-test for two means with equal variance. \*P<0.05, \*\*P<0.01, \*\*\*P<0.001. **D.** Jneo cells were treated with D112 in the absence or presence of caspase inhibitor z-VAD-fmk (20  $\mu$ M). Genomic DNA was extracted and separated by agarose gel electrophoresis. DNA fragments were visualized by SYBR safe staining.

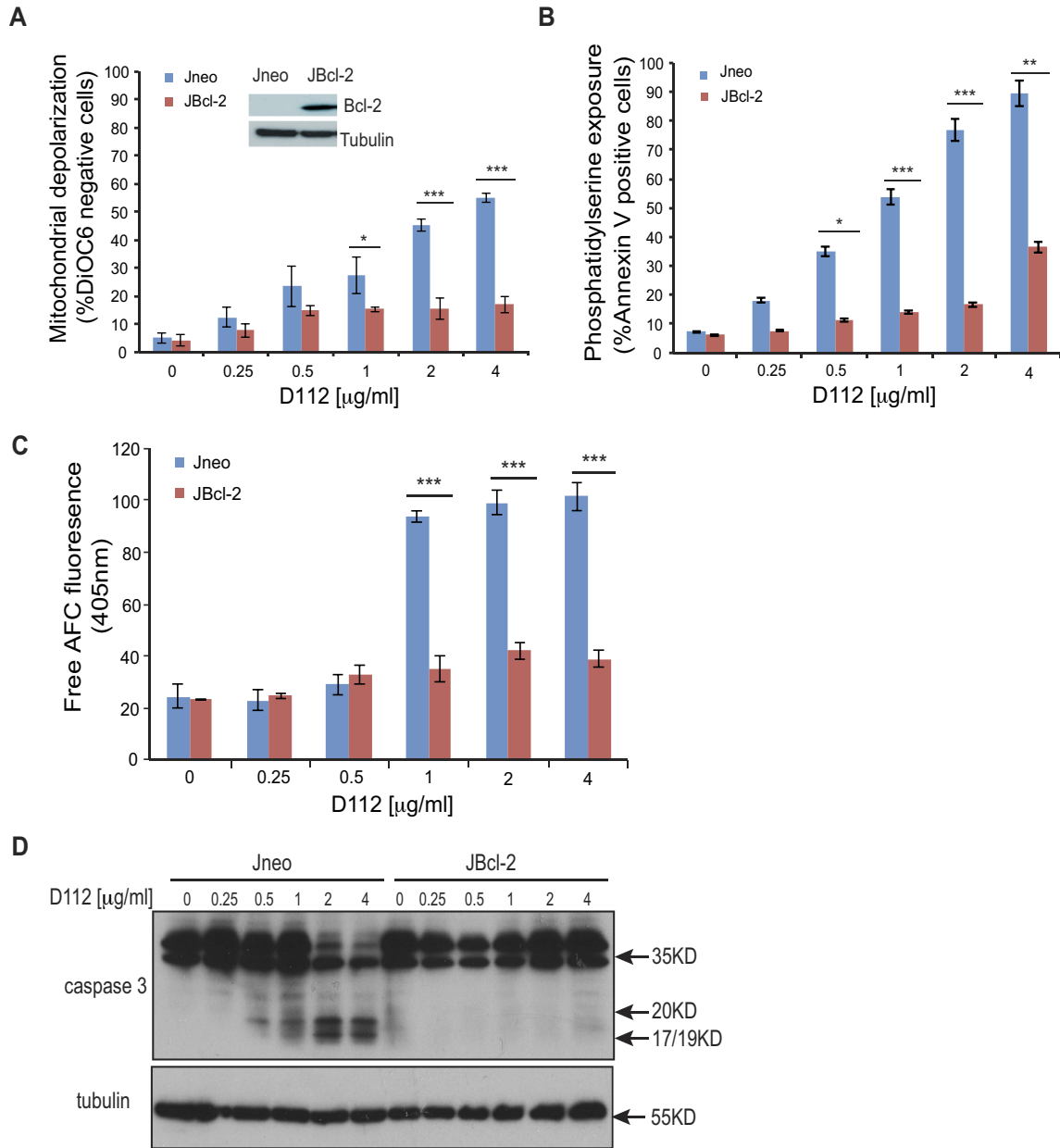
this DNA ladder was caspase dependent as demonstrated by pre-treatment of cells with the caspase inhibitor zVAD-fmk.

All together, our results indicated that D112 induced apoptosis as evidenced by PS externalization, mitochondrial dysfunction, caspase activation and DNA fragmentation. Therefore, we next assessed the functional requirement of mitochondrial dysfunction for D112-induced cytotoxicity.

### **3.3 Mitochondria play a critical role in D112-induced cell death**

#### **3.3.1 Anti-apoptotic Bcl-2 blocks D112-induced cell death**

To explore the functional contribution of mitochondrial dysfunction in D112-induced apoptosis, we examined D112 sensitivity in Jurkat cells ectopically expressing Bcl-2 (JBcl-2) (Goping et al., 2003). We observed that both D112-induced mitochondrial depolarization (Fig. 3.5A) and PS exposure (Fig. 3.5B) were significantly inhibited in JBcl-2 cells. Since caspase activation was critically important for PS exposure and mitochondrial depolarization, we directly measured enzymatic activity. As expected, we found that D112-treated JBcl-2 cells had background levels of caspase 3 activity (Fig. 3.5C). Further, analysis of caspase cleavage patterns demonstrated that JBcl-2 cells showed no production of active subunits of caspase 3 (Fig. 3.5D). These results confirmed that the mitochondrial pathway was critical to induce caspase activation in response to D112.

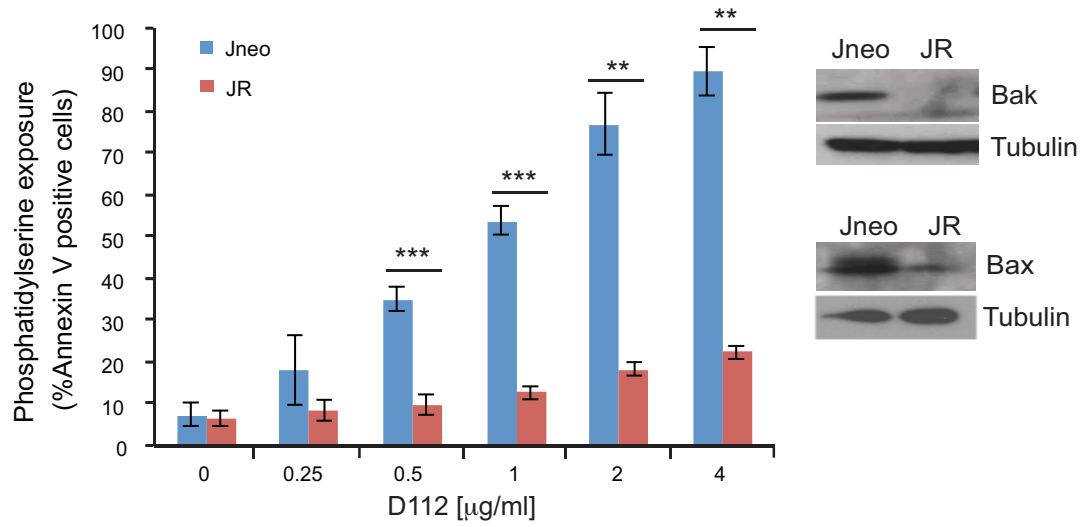
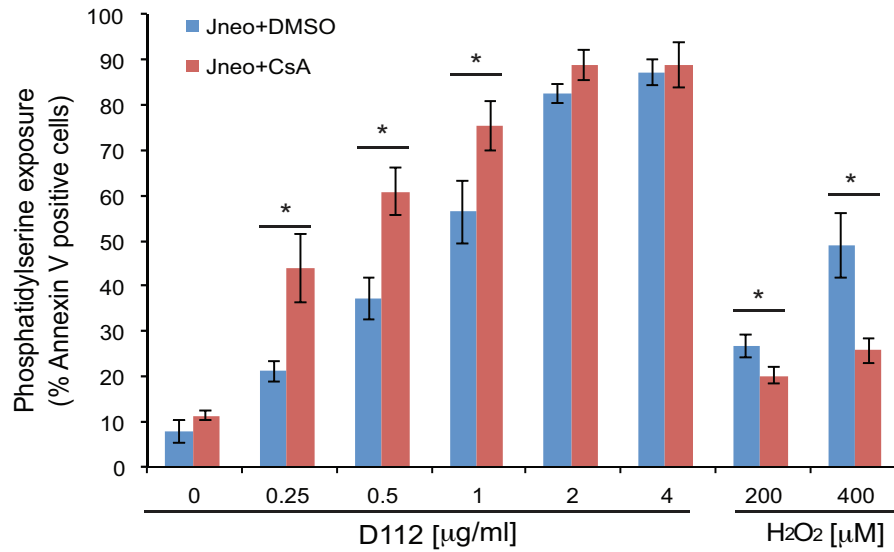
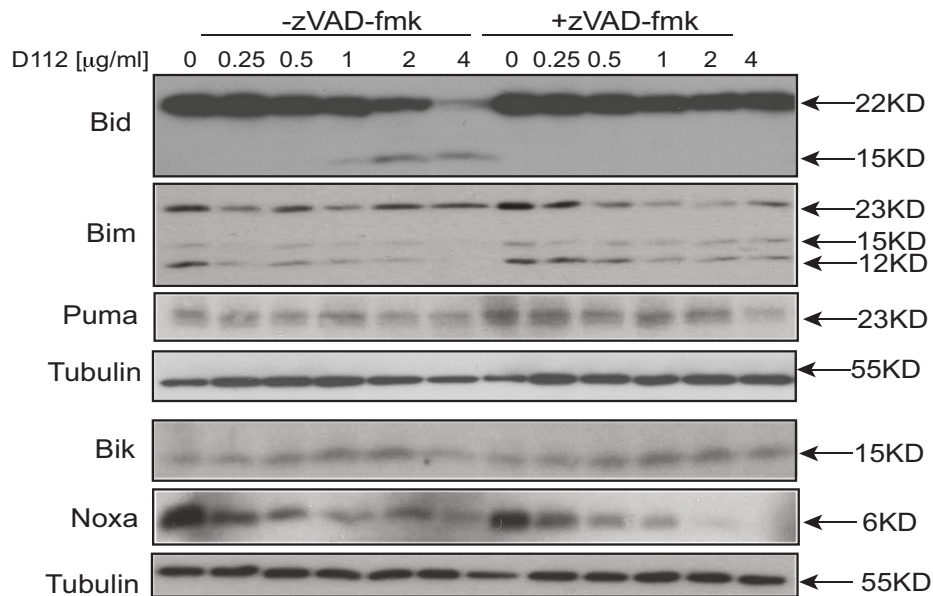


**Figure 3.5 D112-induced apoptosis is blocked by Bcl-2.** Jneo and JBcl-2 cells were treated with the indicated amounts of D112 for 24 h. Apoptotic cell death was measured by **A.** mitochondrial dysfunction, **B.** phosphatidylserine exposure, **C.** caspase 3 enzymatic activation, and **D.** caspase cleavage. All of these apoptotic hallmarks were quantitated as described previously. Mean  $\pm$  SD of three independent experiments performed in triplicate were shown, statistical significance was determined using a two-tailed Student's t-test for two means with equal variance. \* $P < 0.05$ , \*\* $P < 0.01$ , \*\*\* $P < 0.001$ .

### 3.3.2 Bax/Bak deficient cells are resistant to D112-induced cell death

As a complementary approach, the involvement of mitochondrial dysfunction in D112-induced apoptosis was also confirmed by examining PS exposure in a sub-line of Jurkat cells (named JR) with diminished levels of Bax and Bak proteins (Han et al., 2004; Wang et al., 2001). In response to apoptotic stimuli, pro-apoptotic proteins Bax and Bak form pores in the mitochondrial outer membrane, causing the release of mitochondrial proteins inducing apoptosis (Karch et al., 2013; Wei et al., 2001). Given that Bcl-2 blocked D112-induced cytotoxicity, we reasoned that loss-of-function of the pro-apoptotic proteins Bax and Bak would have a similar effect. Indeed in JR cells, PS exposure was not induced by D112, indicating that Bax/Bak was required for D112-induced cell death (Fig. 3.6A). D112 did not appear to require the Permeability Transition Pore (PTP), as cyclosporin A did not inhibit D112-induced cell death (Fig. 3.6B). These results confirmed the crucial role of mitochondrial dysfunction in D112-induced apoptosis and more specifically, that D112 induced a Bax/Bak-dependent mitochondrial apoptotic pathway.

We also assessed the BH3-only class of Bcl-2 family proteins to query upstream transducers of D112 toxicity (Fig. 3.6C). Bid was cleaved in D112 treated cells, but this event was inhibited by zVAD-fmk, indicating that Bid cleavage potentially acted as an amplification mechanism of D112 toxicity, downstream of caspase activation. Puma, Bik, Noxa, and Bim levels did not increase in response to D112. Thus, whether BH3-only proteins were required to transmit the D112-apoptotic signal was not clear.

**A****B****C**

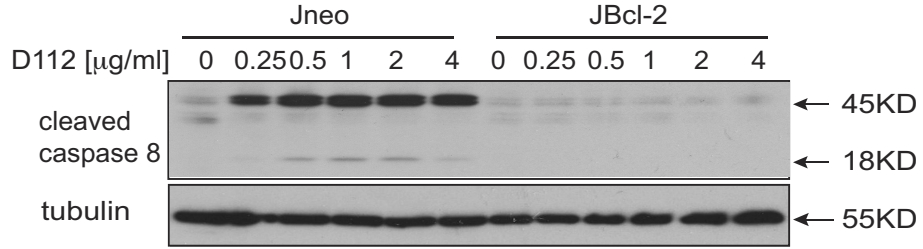
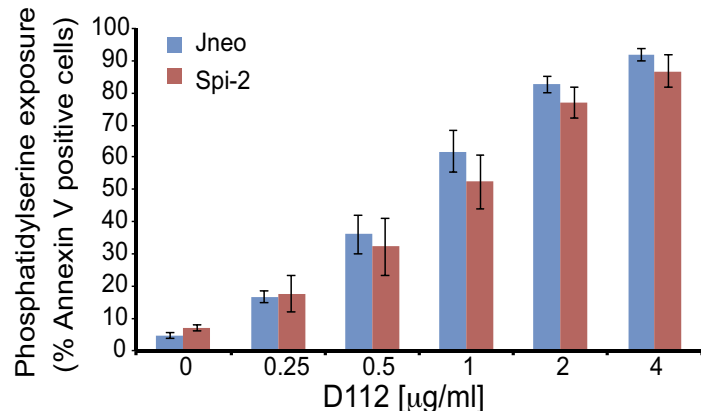
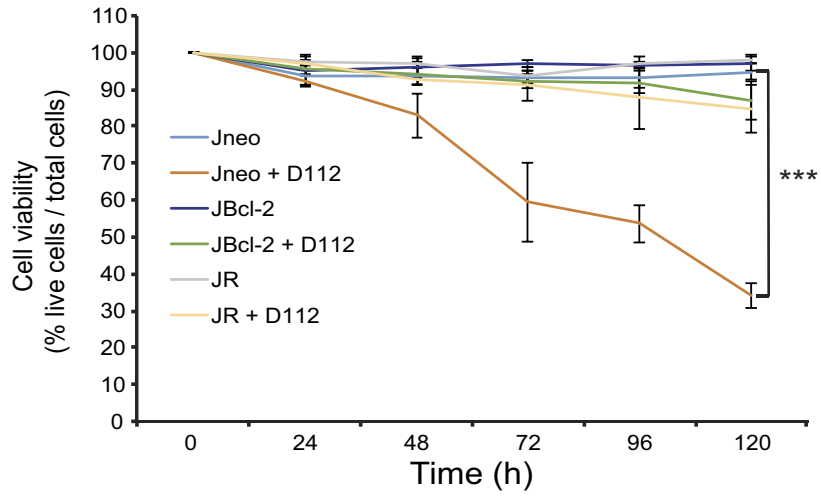
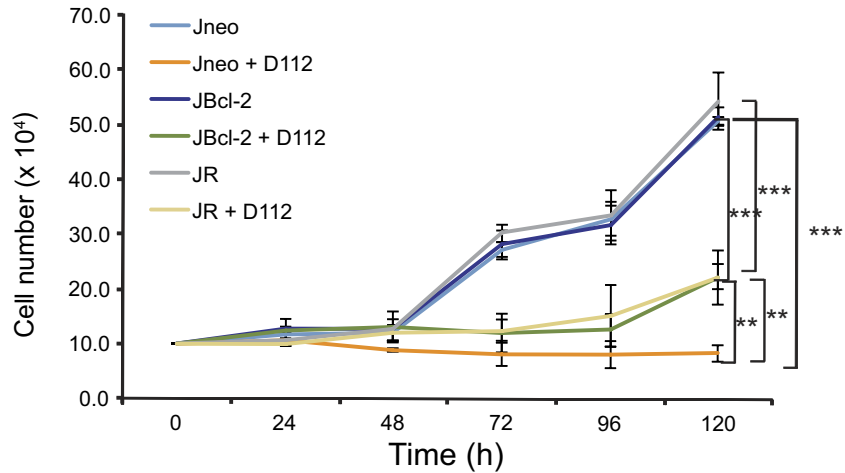
**Figure 3.6 Bax/Bak expression is required for D112-induced cell death. A.** Jneo and JR cells were treated with indicated concentrations of D112 for 24 h and phosphatidylserine positivity was recorded as done previously. The expression of Bax and Bak were verified in western blot insets. **B.** Permeability Transition Pore was not involved in D112-induced cell death. Jneo cells were treated with the indicated concentrations of D112 in the presence or absence of 5  $\mu$ M cyclosporine A (CsA) for 24 h. Jneo cells were treated with H<sub>2</sub>O<sub>2</sub> (200  $\mu$ M and 400  $\mu$ M) for 4 hours, as a positive control. Phosphatidylserine exposure indicated by Alexa Fluor 647-annexin V positive cells is shown as a percent of total cells as determined by flow cytometry. In all experiments, the mean  $\pm$  SD of three independent experiments performed in triplicate were shown, statistical significance was determined using a two-tailed Student's t-test for two means with equal variance. \*P<0.05, \*\*P<0.01, \*\*\*P<0.001. **C.** BH3-only proteins in response to D112 treatment. Jneo cells were incubated for 24 h with increasing concentrations of D112 as indicated. Whole cell lysates were subjected to western blotting analysis with the indicated antibodies. The experiment was performed independently three times and a representative blot is shown.

### 3.3.3 Extrinsic pathway does not contribute to D112-induced cell death

To determine whether the extrinsic pathway contributed to D112-induced apoptosis, we examined caspase 8 activation by western blotting using a caspase 8 cleavage-specific antibody. D112 induced caspase 8 cleavage (Fig. 3.7A), however, this was blocked by Bcl-2, indicating that caspase 8 activation was downstream of mitochondrial dysfunction and not dependent on extrinsic apoptotic mediators. To assess whether caspase 8 activation contributed to D112-induced apoptosis, we assayed Jurkat cells that stably expressed the rabbitpox virus-encoded caspase inhibitor SPI-2 that are resistant to extrinsic-mediated apoptosis (Barry et al., 2000). These cells were equally sensitive to D112 treatment as control cells indicating that caspase 8 was dispensable for D112-mediated apoptosis (Fig. 3.7B).

### 3.3.4 D112 inhibits long-term cell viability

We next assessed the effects of D112 treatment on cell viability. A four-fold lower dose than was used in the previous apoptosis assays showed a gradual decrease in viability of Jneo cells over 5 days, as determined by trypan blue staining (Fig. 3.7C). In contrast, both the presence of Bcl-2 or the depletion of Bax/Bak preserved cell viability. To assess whether D112 also affected proliferation, I counted the total number of live cells daily. As expected, the Jneo cells did not proliferate in the presence of D112. Additionally, D112 significantly inhibited the proliferation of the JBcl-2 and JR cells as compared to untreated cells (Fig. 3.7D). Therefore, low doses of D112 induced cell death dependent on mitochondrial

**A****B****C****D**

**Figure 3.7 The extrinsic pathway does not contribute to D112-induced apoptosis. A.**

Caspase 8 cleavage in response to D112 treatment was examined by western blotting. **B.** Jneo and Spi-2 expressing Jurkat cells were treated with the indicated concentrations of D112 for 24 h. Phosphatidylserine exposure indicated by Alexa Fluor 647-annexin V positive cells is shown as a percent of total cells as determined by flow cytometry. **C.** Inhibition of the apoptosis pathway protects cell from D112-induced cell death. Cells were treated with 62.5 ng/ml D112 for 24 h. Cells then were incubated in fresh medium and counted daily. Cell survival was detected by trypan blue staining. **D.** Cell proliferation is inhibited by D112. Cells were treated with 62.5 ng/ml D112 for 24 h. Cells then were incubated in fresh medium and total live cell number was counted. In all experiments, the mean  $\pm$  SD of three independent experiments performed in triplicate were shown. Statistical significance was determined using a two-tailed Student's t-test for two means with equal variance. For statistical analysis of multiple groups, the one-way Analysis of Variance (ANOVA) test was performed and p-values were obtained by Tukey's Post Hoc test. \*P<0.05, \*\*P<0.01, \*\*\*P<0.001.

dysfunction and inhibited cell proliferation that was relatively independent of mitochondria.

### 3.3.5 Lysosomes do not appear to be involved in D112 toxicity.

Apart from mitochondria, organelles, such as lysosomes, can also contribute to apoptosis. For example, in response to apoptotic stimuli such as staurosporine (STS), death receptor-activation, growth factor-deprivation (Brunk and Svensson, 1999) and oxidative stress (Roberg and Ollinger, 1998), lysosome protease cathepsin B or/and D is released to the cytosol and triggers the apoptotic program by either activating Bax and releasing apoptosis-inducing factor (AIF) to the cytoplasm (Bidere et al., 2003), releasing cytochrome c and activating caspase 3 and 9 (Guicciardi et al., 2000; Johansson et al., 2003; Kagedal et al., 2001), or cleaving and activating Bid (Cirman et al., 2004). To examine the possible involvement of lysosomes, I pretreated cells with the lysosome inhibitor E64 before adding D112. E64 did not rescue D112-induced apoptosis (Fig. 3.8). Therefore, I did not observe strong evidence to suggest that lysosomes were involved in D112 toxicity.

### **3.4 D112 co-localizes with mitochondria**

Given that D112 induced the mitochondrial apoptotic pathway, I wanted to investigate the interaction between D112 and mitochondria. As described previously, D112 is a delocalized lipophilic cation (DLC) and if similar to other DLCs, would be expected to localize to the mitochondria (Madak and Neamati, 2015). Therefore, I

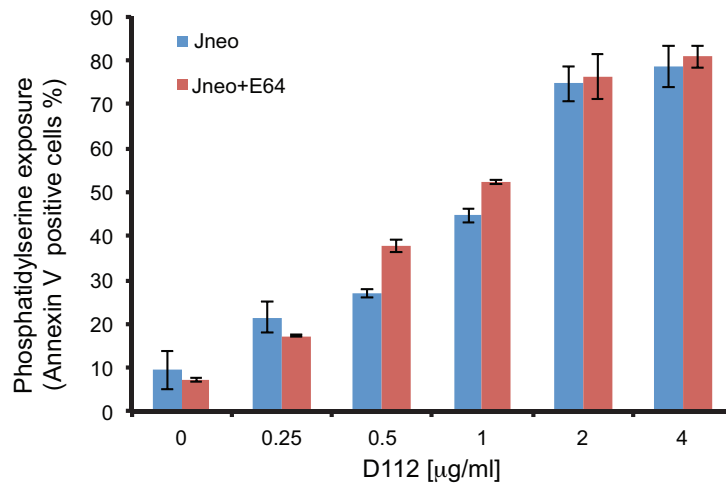


**Figure 3.8 Lysosomes do not contribute to D112-induced cell death.** Jneo cells were treated with the indicated concentrations of D112 in the presence or absence of 10  $\mu\text{M}$  E64 inhibitor for 24 h. Phosphatidylserine exposure indicated by Alexa Fluor 647-annexin V positive cells is shown as a percent of total cells as determined by flow cytometry. In all experiments, the mean  $\pm$  SD of three independent experiments performed in triplicate were shown, statistical significance was determined using a two-tailed Student's t-test for two means with equal variance. \* $P < 0.05$ , \*\* $P < 0.01$ , \*\*\* $P < 0.001$ .

first characterized the fluorescent characteristics of D112 and took advantage of this property to identify D112 intracellular localization.

#### 3.4.1 D112 spectral scan

D112 has a positive charge delocalizing between two nitrogens that gives D112 a visible purple color. In order to gain a better understanding of D112 properties, I performed a spectral scan on D112. I determined that D112 had two excitation peaks (380-410 nm and 510-530 nm) and one emission peak at 615 nm. I thus took advantage of these properties to visualize D112 within the cell (Fig. 3.9).

#### 3.4.2 D112 co-localized with mitochondria

Adherent SK-BR-3 breast cancer cells were used for these experiments as non-adherent Jurkat cells have minimal cytoplasmic space that is not ideal for morphological studies. I attempted to use indirect immunofluorescence to co-localize D112 staining with organelle markers, however D112 fluorescence was lost upon cellular fixation and permeabilization. Therefore, I conducted live cell confocal imaging in cells transiently expressing fluorescently tagged organellar markers. I first asked whether D112 entered the cell via endocytosis, since endocytosis is a common pathway by which cells take up extracellular molecules (Bareford and Swaan, 2007; Doherty and McMahon, 2009). To this aim, I examined the co-localization of D112 with two endosomal markers (Bareford and Swaan, 2007). The early endosome marker Rab5-GFP and late endosome marker Rab7-GFP were transiently transfected into SK-BR-3 cells, respectively. The transfected cells were

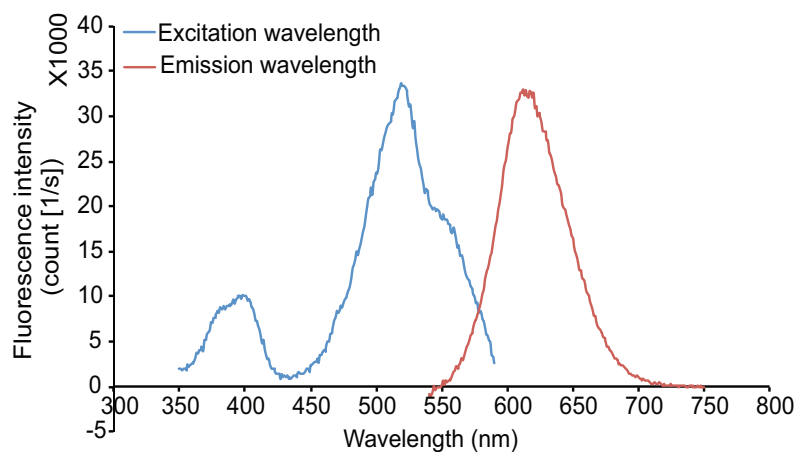
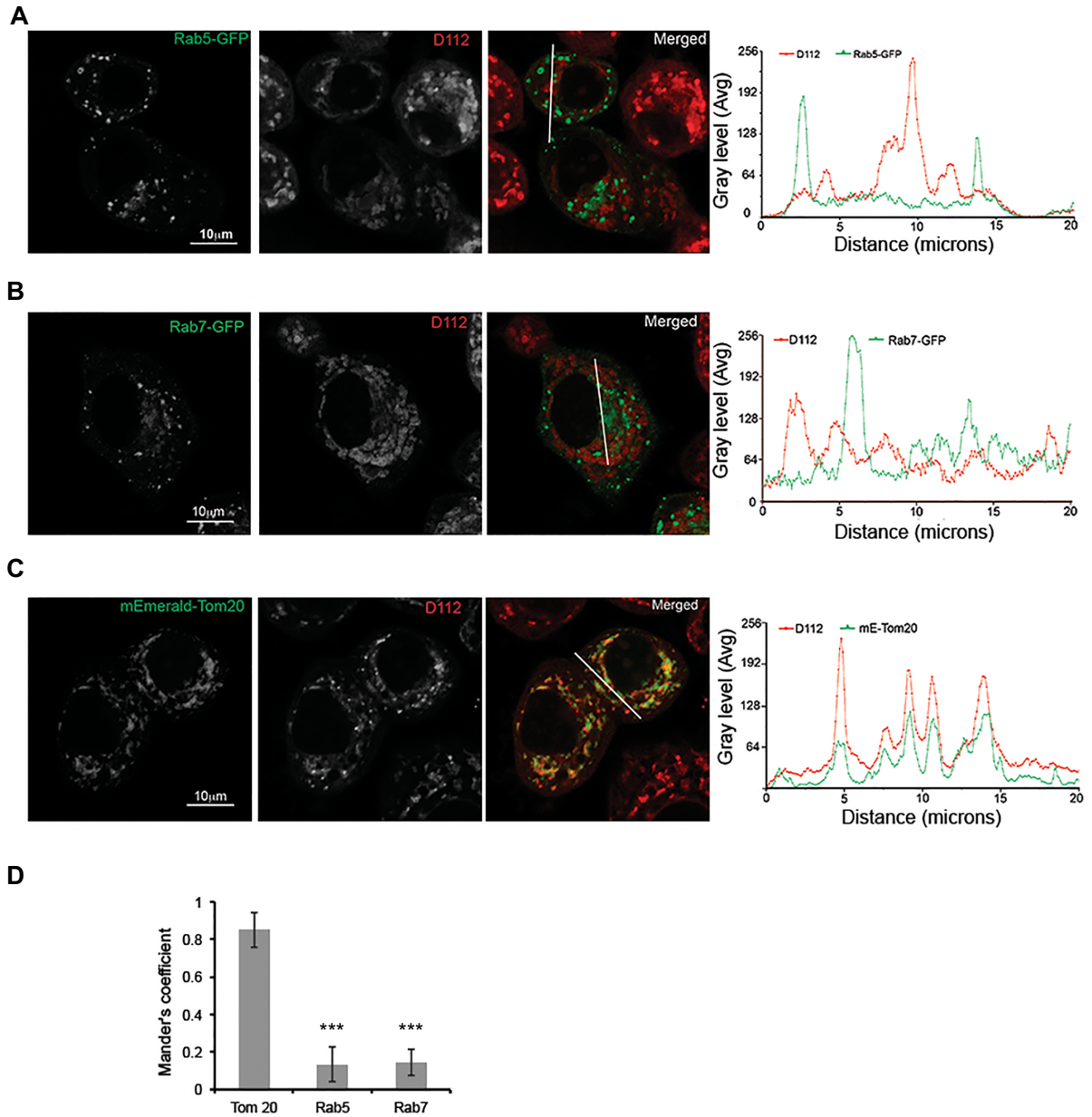


**Figure 3.9 D112 spectra.** D112 excitation and emission spectra. The excitation of 0.25  $\mu\text{g/mL}$  D112 in phosphate buffer (pH7.4) was examined from 340 nm to 620 nm. The corresponding emission spectra were collected from wavelength 540 nm to 750 nm with excitation at 515 nm.

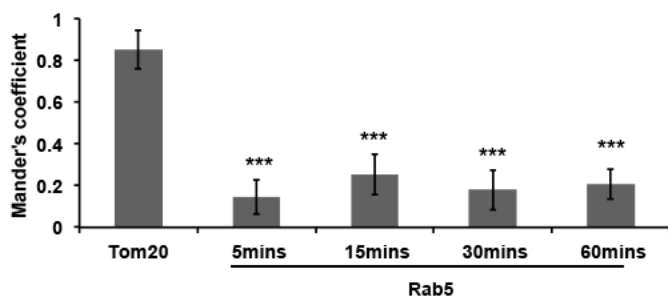
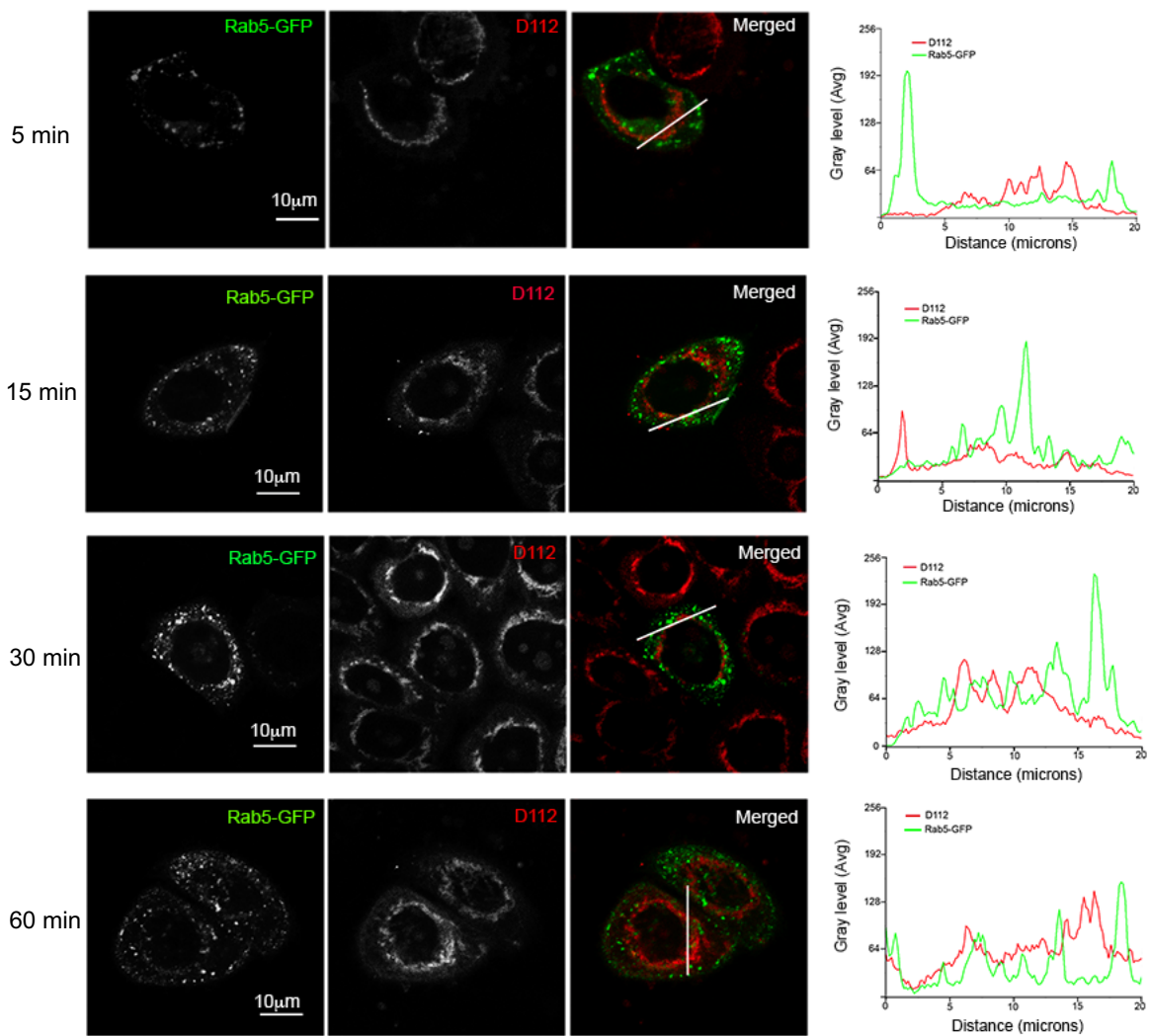
incubated with D112 for 4 h, and live images were captured with a confocal microscope. I observed that D112 co-localized with neither Rab5 (Fig. 3.10A) nor Rab7 (Fig. 3.10B), suggesting that endocytosis was not responsible for D112 cellular uptake. Because endocytosis is an early event, I also recorded D112 localization at earlier time points (Fig. 3.11 and 3.12). Even at the 5-minute time point, D112 was not significantly localized with either endosomal marker. I next analyzed D112 localization with respect to the mitochondrial outer membrane fusion protein mEmerald-Tom 20 (Fig. 3.10C). I observed that the D112 signal strongly overlapped with the mitochondrial marker. Linescan analysis of each fluorescent channel indicated an association of D112 with mitochondria and this co-localization was confirmed as statistically significant by Mander's correlation analysis (Fig. 3.10D). Thus D112 associates with mitochondria suggesting that D112 directly triggers components of the mitochondrial apoptotic pathway.

#### 3.4.3 Mitochondrial electrochemical potential is responsible for D112 accumulation in the mitochondria

Cellular uptake of other DLCs is facilitated by the mitochondrial electrochemical potential (Modica-Napolitano and Weissig, 2015). I decided to examine the contribution of mitochondrial potential for D112 internalization. Treatment of SK-BR-3 cells with the mitochondrial uncoupling agent, carbonyl cyanide *m*-chlorophenyl hydrazine (CCCP), diminished D112-intracellular fluorescence (Fig. 3.13). This result demonstrated that the mitochondrial potential is required for D112 intracellular uptake and localization to mitochondria.

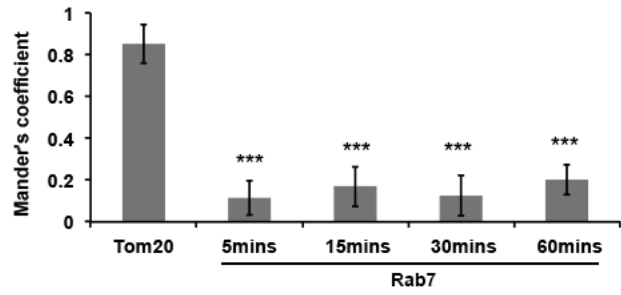
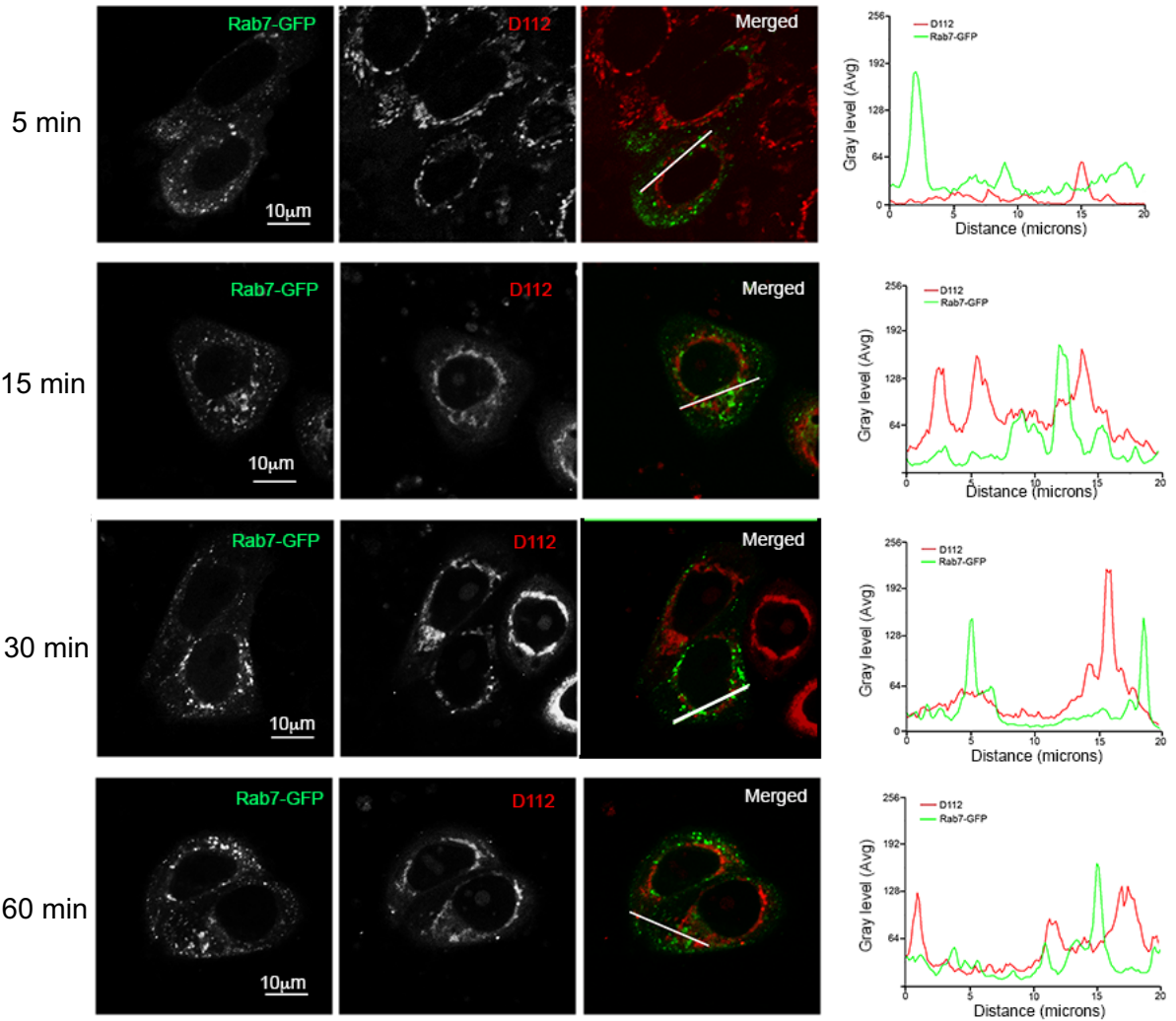


**Figure 3.10 D112 co-localizes with mitochondria.** SK-BR-3 cells were transiently transfected with the indicated plasmids expressing either mEmerald-Tom20, Rab5-GFP or Rab7-GFP. Cells were treated with 0.25  $\mu\text{g/ml}$  D112 for 4 h and then live imaging was performed with confocal microscopy. **A.** D112 did not co-localize with Rab5. **B.** D112 did not co-localize with Rab7. **C.** D112 co-localized with Tom20. The experiment was performed independently twice and representative images are shown. **D.** Summary of the Mander's correlation coefficients of Rab5, Rab7 or Tom20 and D112 in ten SK-BR-3 cells. In all experiments, the mean  $\pm$  SD of three independent experiments performed in triplicate were shown. Statistical significance was determined using a two-tailed Student's t-test for two means with equal variance. \* $P < 0.05$ , \*\* $P < 0.01$ , \*\*\* $P < 0.001$ .



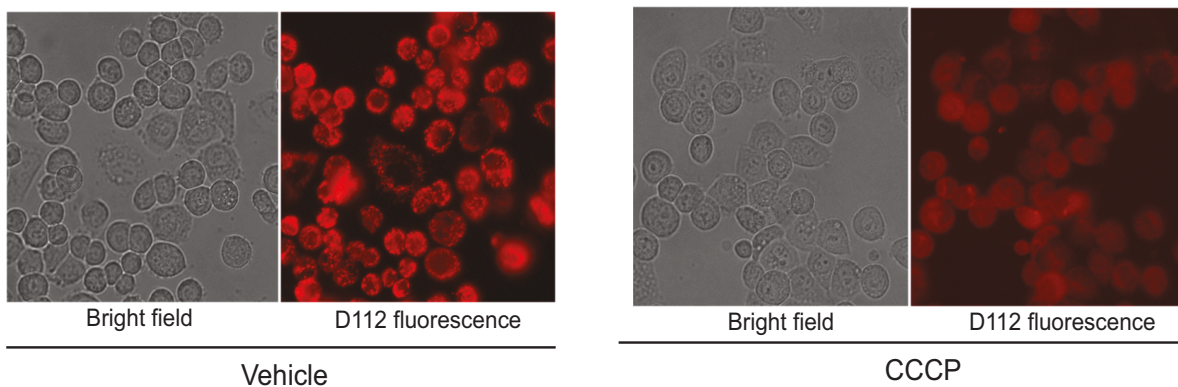
**Figure 3.11 Early endosomes are not associated with D112 intracellular uptake.**

SK-BR-3 cells were transiently transfected with Rab5-GFP. Cells were treated with 0.25  $\mu\text{g/ml}$  D112 for 5 min, 15 min, 30 min or 60 min, and then live imaging was performed with confocal microscopy. Summary of the Mander's correlation coefficients of Rab5 and D112 in ten SK-BR-3 cells is shown at the bottom. The mean  $\pm$  SD of three independent experiments performed in triplicate were shown. Statistical significance was determined using a two-tailed Student's t-test for two means with equal variance. \* $P < 0.05$ , \*\* $P < 0.01$ , \*\*\* $P < 0.001$ .



**Figure 3.12 Late endosomes are not associated with D112 intracellular uptake.**

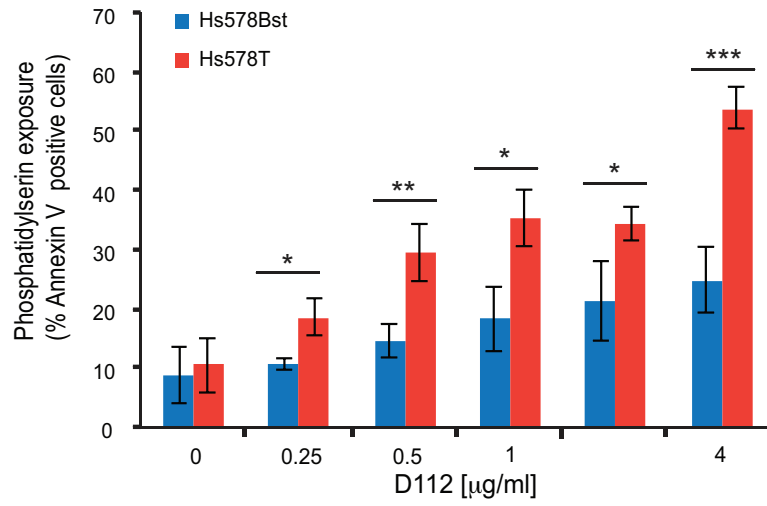
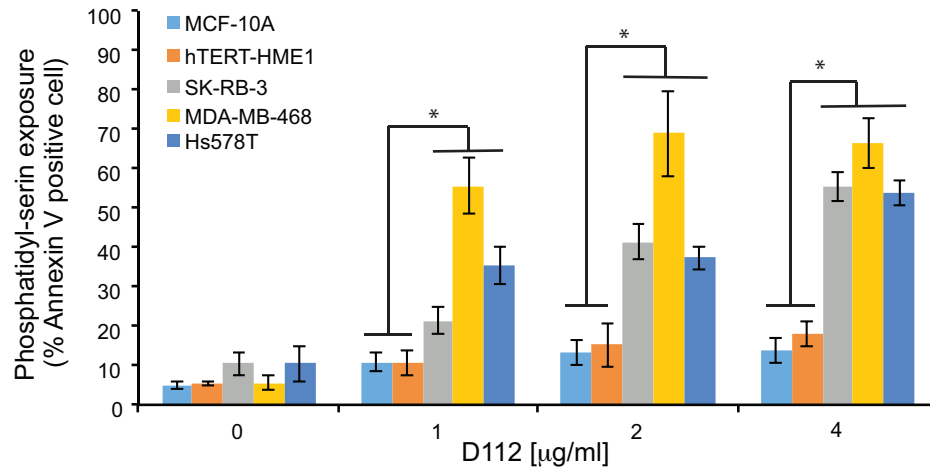
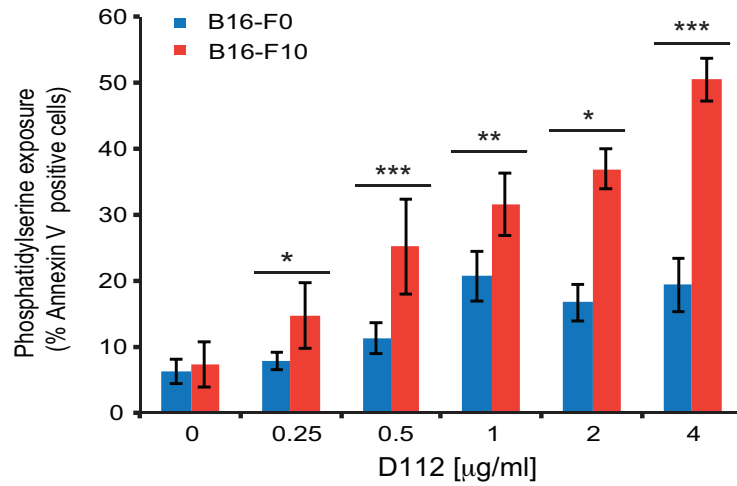
SK-BR-3 cells were transiently transfected with Rab7-GFP. Cells were treated with 0.25  $\mu\text{g/ml}$  D112 for 5 min, 15 min, 30 min or 60 min, and then live imaging was performed with confocal microscopy. Summary of the Mander's correlation coefficients of Rab7 and D112 in ten SK-BR-3 cells is shown at the bottom. The mean  $\pm$  SD of three independent experiments performed in triplicate were shown. Statistical significance was determined using a two-tailed Student's t-test for two means with equal variance. \* $P < 0.05$ , \*\* $P < 0.01$ , \*\*\* $P < 0.001$ .



**Figure 3.13 Mitochondrial membrane potential is required for D112 accumulation.** D112 uptake was dependent on mitochondrial potential. SK-BR-3 cells were pre-treated with carbonyl cyanide m-chlorophenylhydrazone (CCCP, 100  $\mu$ M) for 30 min to abolish membrane potential, then D112 uptake in live cells was examined by microscopy.

### **3.5 D112 shows increased toxicity to breast cancer cells and metastatic melanoma cells**

I first became interested in studying D112 based on the initial reports that D112 had selective toxicity to a human colon cancer cell line in comparison to a normal monkey kidney cell line (Gilman et al., 2006). Additionally, common anti-cancer treatments are less effective against solid tumors versus hematological malignancies (such as exemplified by Jurkat cells) and show a non-apoptotic mechanism of action (Brown and Attardi, 2005; Brown and Wouters, 1999; Mirzayans et al., 2013). Thus I examined whether D112 induced apoptosis in cell lines derived from solid tumors and whether D112 showed any selectivity for transformed or metastatic cancer cells. Accordingly, I first analyzed the paired breast cell lines of Hs 578T and Hs 578Bst (Fig. 3.14A). Hs 578T is a human breast carcinoma cell line and Hs 578Bst is a cell line derived from non-transformed adjacent tissue from the same patient. The carcinoma cell line was significantly more sensitive to D112-induced apoptosis in comparison to the normal cell line. I then expanded this observation to other breast cell lines (Fig. 3.14B). I observed that the non-transformed human mammary epithelial cell line MCF-10A and hTERT-HME1 showed no significant dose-dependent response to D112 treatment. On the other hand, the mammary carcinoma lines, SK-BR-3 and MDA-MB-468, were significantly more sensitive to D112-induced apoptosis. I next took advantage of a progressive metastasis model that had been established in the mouse B16 cell lines (Nakamura et al., 2002). The B16-F0 cell line is a mouse melanoma cell line, while B16-F10 is an aggressive metastatic cell line generated from the B16-F0 line through an

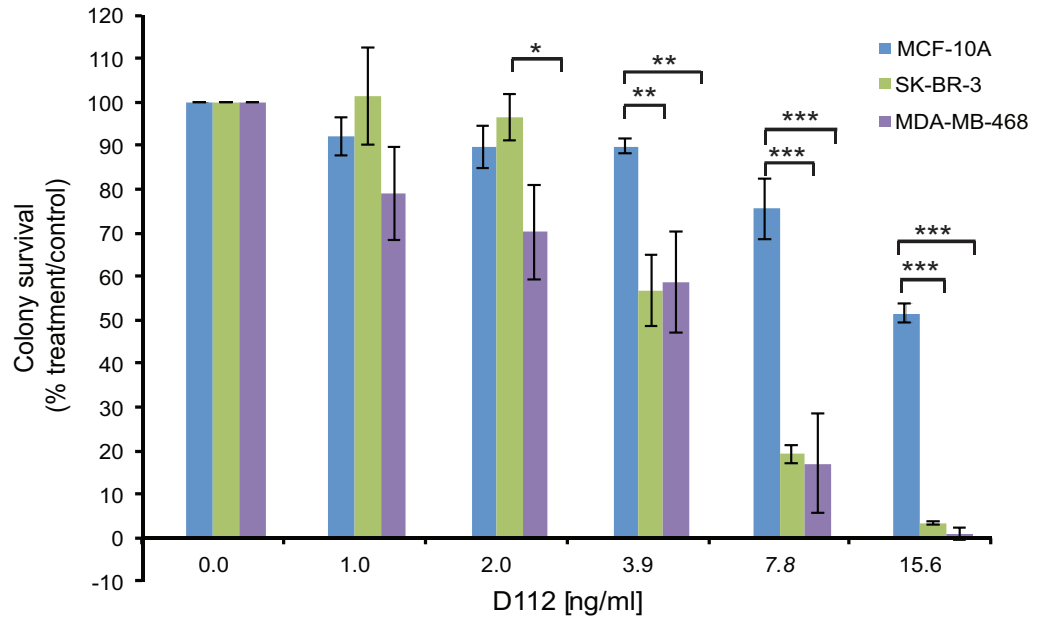
**A****B****C**

**Figure 3.14 D112 shows selective cytotoxicity against transformed cells. A.** Paired human normal breast cell line Hs 578Bst and human breast carcinoma cell line Hs 578T. **B.** Non-transformed human mammary epithelial cell lines MCF-10A and hTERT-HME1 in comparison to the mammary carcinoma cell lines SK-BR-3 and MDA-MB-468. **C.** Melanoma parental cell line B16-F0 and melanoma metastatic cell line B16-F10. All cell lines were treated with the indicated amounts of D112 for 24 h and apoptosis was indicated by PS exposure, which was measured as described previously. Mean  $\pm$  SD of three independent experiments performed in triplicate were shown. Statistical significance was determined using a two-tailed Student's t-test for two means with equal variance. For statistical analysis of multiple groups (in B), the one-way Analysis of Variance (ANOVA) test was performed and p-values were obtained by Tukey's Post Hoc test. \*P<0.05, \*\*P<0.01, \*\*\*P<0.001.

iterative *in vivo* selection procedure. The B16-F0 cells were more resistant to D112-induced apoptosis than the highly metastatic B16-F10 line (Fig. 3.14C). Thus, in the cell lines that I tested, D112 triggered an increased apoptotic response in transformed versus normal cells and increased cytotoxicity to a metastatic versus a weakly metastatic line.

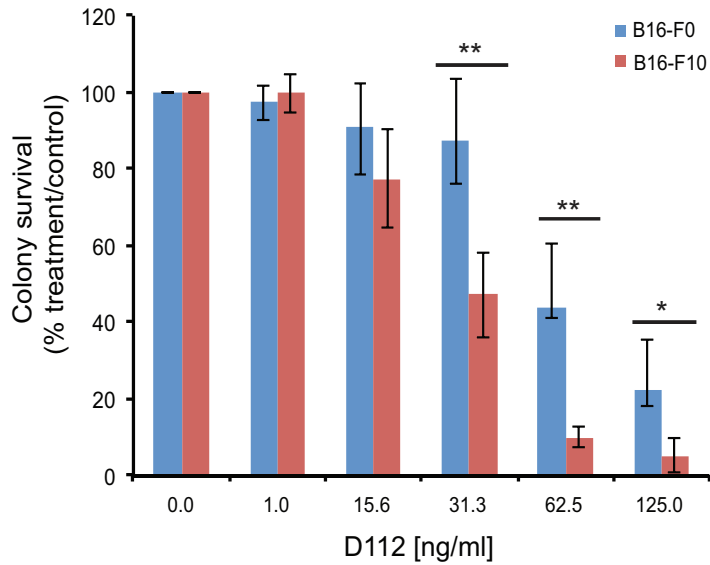
I next evaluated the effect of D112 on these adherent cell lines by the conventional clonogenic survival assay, which provides a read-out of the sum of cytotoxic (e.g. apoptosis) and cytostatic (growth arrest) responses (Brown and Wouters, 1999; Mirzayans et al., 2013). Cell lines were treated with D112 for 24 h and the number of clonal colonies (>50 cells) that formed over a span of 2 weeks was recorded (Fig. 3.15A). MCF-10A cells were three times more resistant to D112 treatment than SK-BR-3 or MDA-MB-468 cells, based on the IC<sub>50</sub> of 15 versus 5 ng/ml. Additionally, weakly-metastatic B16-F0 showed a 2-fold greater resistance than the metastatic B16-F10 cell line (Fig. 3.15B). Since this low dose of D112 was below the threshold to detect apoptosis, it appeared that, similar to Jneo cells, low doses of D112 induced proliferative arrest. Nevertheless, these assays suggest that both high and low doses of D112 have selective activity against the transformed/metastatic cell lines that I tested.

**A**



	IC50
MCF10A	15 ng/ml
SK-BR-3	5 ng/ml
MDA-MB-468	5 ng/ml

**B**



	IC50
B16-F0	52 ng/ml
B16-F10	27 ng/ml

**Figure 3.15 D112 selectively inhibits clonogenic survival of transformed cells. A.**

Long-term colony formation of non-transformed human mammary epithelial cell lines MCF-10A in comparison to the mammary carcinoma cell lines SK-BR-3 and MDA-MB-468. **B.** Long-term colony formation of melanoma cell lines B16-F0 and aggressive metastatic melanoma cell lines B16-F10. Cell lines were treated with the indicated amounts of D112 for 24 h, and all cells were harvested, counted and seeded in 24-well plates. Colonies were stained with crystal blue and counted after 7-14 days incubation. Mean  $\pm$  SD of three independent experiments performed in triplicate were shown. Statistical significance was determined using a two-tailed Student's t-test for two means with equal variance. For statistical analysis of multiple groups (in A), the one-way Analysis of Variance (ANOVA) test was performed and p-values were obtained by Tukey's Post Hoc test. \*P<0.05, \*\*P<0.01, \*\*\*P<0.001.

### 3.6 Discussion

D112 was identified by Kodak as a dye that had higher toxicity against a cancer cell line than a non-transformed cell line (Gilman et al., 2006). Whether this selectivity could be applied to other cancer cell lines was not known. Furthermore, the mechanism of D112-induced killing remained unclear. In this study, I investigated D112-mediated cell killing in a number of cell lines and identified that relatively high doses of D112 triggered the mitochondrial apoptotic pathway and lower doses induced cell cycle arrest.

To determine whether D112 induced apoptosis, I assessed the contribution and activation of the major effector caspase 3. I observed that D112 treatment produced active caspase 3 subunits p19/17. Incubation with caspase inhibitors prevented the generation of active caspase 3 subunits p19/17, and produced p20. It is known that caspase 3 is activated by two cleavage events. The first step of pro-caspase 3 activation, which gives rise to a p20 cleavage product, is mediated mostly by initiator caspases (Fernandes-Alnemri et al., 1994), such as caspase 9 (Han et al., 1997). Non-caspase proteases such as granzyme B (Atkinson et al., 1998) and a wide range of stressors such as ER stress, IL-3-deprivation (Egger et al., 2003) or staurosporine (Johnson et al., 2000) can also produce a p20 fragment that becomes apparent in the presence of zVAD-fmk. In many cases, the enzyme responsible for the generation of p20 is unclear, although in some cases chymotrypsin-like serine proteases can generate a p20 fragment (Egger et al., 2003). Caspase 3 autocatalysis then produces the active subunits p19/17 (Han et al., 1997). As I

observed that D112 produced similar caspase 3 proteolytic products, D112 likely stimulates an apoptotic pathway that is shared with other stress-inducers.

Furthermore, I determined that elevated Bcl-2 levels inhibited not only caspase activity, but also the production of p20, indicating that Bcl-2 functioned upstream of both caspases and the initial caspase 3-protease. As Bcl-2 blocks mitochondrial dysfunction by inhibiting Bax/Bak pore formation, it is possible that the unidentified caspase 3-protease is localized to the mitochondria and is released to the cytosol through a Bax/Bak pore.

The second hallmark of apoptosis that I tested was mitochondrial depolarization. I observed that D112 induced mitochondrial depolarization was downstream of caspase activation. Mitochondrial membrane depolarization has been originally postulated to be an early event in the apoptotic pathway (Gottlieb et al., 2003; Narita et al., 1998; Tsujimoto and Shimizu, 2007). However, more recent evidence suggests that it can also be a subsequent event in the apoptotic pathway, downstream of caspase activation (Ly et al., 2003), and it is not required by the translocation of cytochrome c from mitochondria to cytosol (Bossy-Wetzel et al., 1998). As an example, the mitochondrial potential of Doxorubicin-treated Jurkat cells was only disrupted after the activation of caspases, however, the underlying mechanism remained unclear (Gamen et al., 2000). In another study, Fas-induced loss of mitochondrial potential occurred after the activation of caspase-1-like caspases, and the addition of caspase inhibitors inhibited mitochondrial membrane depolarization (Susin et al., 1997; Wang et al., 2006). Similarly, our study showed that the caspase pan-inhibitor z-VAD-fmk inhibited mitochondrial membrane

depolarization, suggesting that mitochondrial depolarization was a downstream event in our case.

It is noteworthy that mitochondrial membrane depolarization was rescued by caspase inhibitors, whereas PS externalization was only partially protected. For example, in the case of cells treated with 1  $\mu\text{g/ml}$  (equal to 1.4  $\mu\text{M}$ ) D112, 20% more Annexin V-positive cells were detected under this condition even in the presence of zVAD-fmk (Fig.3.1A). Conceivably, other non-caspase-dependent factors, for example Apoptosis-Inducing-Factor (AIF), and/or ATP-depletion may contribute to PS externalization (Susin et al., 1999). In support of this, both caspase- and AIF-mediated PS exposures are dependent on mitochondrial dysfunction and are blocked by Bcl-2. Also, PS exposure is proposed to be a consequence of ATP depletion (Castedo et al., 1996). In healthy cells, ATP-dependent translocases maintain PS on the inside of the cell. During apoptosis, ATP levels decrease and translocase activity diminishes, leading to PS externalization (Bever and Williamson, 2010). In our study, D112 co-localized with mitochondria, and it is possible that D112 inhibits ATP production by interfering with mitochondrial respiration, hence contributing to PS exposure in a caspase-independent manner.

Results from this chapter demonstrated that D112 localizes to mitochondria and induces Bax/Bak-dependent mitochondrial outer membrane permeabilization, cytochrome c release and activation of caspases 9 and 3. Mitochondrial depolarization was dependent on caspase activation, suggesting a positive amplification loop for mitochondrial dysfunction. I speculate that this loop may

involve caspase-cleaved Bid and is unlikely to require Permeability Transition Pore, since preliminary studies with cyclosporin A that blocks PTP activation did not decrease apoptosis. With respect to upstream signaling pathways, it was not clear how D112 triggers mitochondrial effects. I speculate that due to its redox potential, D112 may inhibit the electron transport chain and elevate reactive oxygen species that trigger mitochondrial damage and apoptosis. This is explored further in chapter 4. Furthermore studies that address the mechanism of increased toxicity of the transformed versus non-transformed cell lines shown here will be expanded in chapter 4.

Finally, I observed that D112 displayed enhanced cytotoxicity towards transformed Hs 578T, SK-BR-3 and MDA-MB-468 breast carcinoma cell lines versus non-transformed Hs 578Bst, MCF-10A and hTERT-HME1 normal breast epithelial cell lines. Furthermore, D112 was more cytotoxic to the metastatic melanoma cell line B16-F10 versus the lesser aggressive parental B16-F0 cells. These data suggest that D112 may have potential to be tested as a selective anti-cancer compound that conceivably will cause less off-target toxic side effects. However, the selectivity that I observed was much reduced in comparison to the original study that identified a 900-fold difference in sensitivity between a human colon cancer cell line and non-transformed monkey kidney cell line (Gilman et al., 2006). This is likely because of the difference in cell lines and species differences in the original study. In our current study, I compared cell lines from the same species, of which, one set was originally isolated from tissue from the same patient (Hs578T vs 578 Bst) whereas another set was clonally derived from each other (B16F0 vs B16F10). The

difference in sensitivity that I observed between our cell lines was only 2- and 3-fold. At this time, I am not able to predict whether this difference in sensitivity could translate into a selective anticancer agent. Importantly, incorporation of additional strategies to increase this therapeutic index was explored in Chapter 4. In conclusion, the results from this chapter demonstrate that D112 has properties worthy of further exploration as a potential therapeutic compound. Chapter 4 expands investigations into the molecular mechanism of D112-induced apoptosis and addresses questions raised in this chapter with respect to cancer cell selectivity and strategies to increase cancer cell-selective toxicity.

## Reference

American Cancer Society (2014). *Cancer Facts & Figures 2014*.

Atkinson, E.A., Barry, M., Darmon, A.J., Shostak, I., Turner, P.C., Moyer, R.W., and Bleackley, R.C. (1998). Cytotoxic T lymphocyte-assisted suicide. Caspase 3 activation is primarily the result of the direct action of granzyme B. *J Biol Chem* 273, 21261-21266.

Bai, L., and Wang, S. (2014). Targeting apoptosis pathways for new cancer therapeutics. *Annu Rev Med* 65, 139-155.

Bareford, L.M., and Swaan, P.W. (2007). Endocytic mechanisms for targeted drug delivery. *Adv Drug Deliv Rev* 59, 748-758.

Barry, M., Heibin, J.A., Pinkoski, M.J., Lee, S.F., Moyer, R.W., Green, D.R., and Bleackley, R.C. (2000). Granzyme B short-circuits the need for caspase 8 activity during granule-mediated cytotoxic T-lymphocyte killing by directly cleaving Bid. *Mol Cell Biol* 20, 3781-3794.

Bevers, E.M., and Williamson, P.L. (2010). Phospholipid scramblase: an update. *FEBS Lett* 584, 2724-2730.

Bidere, N., Lorenzo, H.K., Carmona, S., Laforge, M., Harper, F., Dumont, C., and Senik, A. (2003). Cathepsin D triggers Bax activation, resulting in selective apoptosis-inducing factor (AIF) relocation in T lymphocytes entering the early commitment phase to apoptosis. *J Biol Chem* 278, 31401-31411.

Borisenko, G.G., Matsura, T., Liu, S.X., Tyurin, V.A., Jianfei, J., Serinkan, F.B., and Kagan, V.E. (2003). Macrophage recognition of externalized phosphatidylserine and phagocytosis of apoptotic Jurkat cells--existence of a threshold. *Arch Biochem Biophys* 413, 41-52.

Bossy-Wetzel, E., Newmeyer, D.D., and Green, D.R. (1998). Mitochondrial cytochrome c release in apoptosis occurs upstream of DEVD-specific caspase activation and independently of mitochondrial transmembrane depolarization. *EMBO J* 17, 37-49.

Brown, J.M., and Attardi, L.D. (2005). The role of apoptosis in cancer development and treatment response. *Nat Rev Cancer* 5, 231-237.

Brown, J.M., and Wouters, B.G. (1999). Apoptosis, p53, and tumor cell sensitivity to anticancer agents. *Cancer Res* 59, 1391-1399.

Brunk, U.T., and Svensson, I. (1999). Oxidative stress, growth factor starvation and Fas activation may all cause apoptosis through lysosomal leak. *Redox Rep* 4, 3-11. Canadian Cancer Society (2013). National statistics at a glance from Canadian Cancer Statistics.

Castedo, M., Hirsch, T., Susin, S.A., Zamzami, N., Marchetti, P., Macho, A., and Kroemer, G. (1996). Sequential acquisition of mitochondrial and plasma membrane alterations during early lymphocyte apoptosis. *J Immunol* 157, 512-521.

Cirman, T., Oresic, K., Mazovec, G.D., Turk, V., Reed, J.C., Myers, R.M., Salvesen, G.S., and Turk, B. (2004). Selective disruption of lysosomes in HeLa cells triggers apoptosis mediated by cleavage of Bid by multiple papain-like lysosomal cathepsins. *J Biol Chem* 279, 3578-3587.

Doherty, G.J., and McMahon, H.T. (2009). Mechanisms of endocytosis. *Annu Rev Biochem* 78, 857-902.

Egger, L., Schneider, J., Rheme, C., Tapernoux, M., Hacki, J., and Borner, C. (2003). Serine proteases mediate apoptosis-like cell death and phagocytosis under caspase-inhibiting conditions. *Cell Death Differ* 10, 1188-1203.

Fernandes-Alnemri, T., Litwack, G., and Alnemri, E.S. (1994). CPP32, a novel human apoptotic protein with homology to *Caenorhabditis elegans* cell death protein Ced-3 and mammalian interleukin-1 beta-converting enzyme. *J Biol Chem* 269, 30761-30764.

Gamen, S., Anel, A., Perez-Galan, P., Lasierra, P., Johnson, D., Pineiro, A., and Naval, J. (2000). Doxorubicin treatment activates a Z-VAD-sensitive caspase, which causes deltatapsin loss, caspase-9 activity, and apoptosis in Jurkat cells. *Exp Cell Res* 258, 223-235.

Gilman, P., Parton, R.L., and Lenhard, J.R. (2006). Correlation of anti-cancer activity of dyes with redox potential In Patent Application Publication (US: Eastman Kodak Company).

Goping, I.S., Barry, M., Liston, P., Sawchuk, T., Constantinescu, G., Michalak, K.M., Shostak, I., Roberts, D.L., Hunter, A.M., Korneluk, R., *et al.* (2003). Granzyme B-induced apoptosis requires both direct caspase activation and relief of caspase inhibition. *Immunity* 18, 355-365.

Gottlieb, E., Armour, S.M., Harris, M.H., and Thompson, C.B. (2003). Mitochondrial membrane potential regulates matrix configuration and cytochrome c release during apoptosis. *Cell Death Differ* 10, 709-717.

Guicciardi, M.E., Deussing, J., Miyoshi, H., Bronk, S.F., Svingen, P.A., Peters, C., Kaufmann, S.H., and Gores, G.J. (2000). Cathepsin B contributes to TNF-alpha-

mediated hepatocyte apoptosis by promoting mitochondrial release of cytochrome c. *J Clin Invest* 106, 1127-1137.

Han, J., Goldstein, L.A., Gastman, B.R., Rabinovitz, A., Wang, G.Q., Fang, B., and Rabinowich, H. (2004). Differential involvement of Bax and Bak in TRAIL-mediated apoptosis of leukemic T cells. *Leukemia* 18, 1671-1680.

Han, Z., Hendrickson, E.A., Bremner, T.A., and Wyche, J.H. (1997). A sequential two-step mechanism for the production of the mature p17:p12 form of caspase-3 in vitro. *J Biol Chem* 272, 13432-13436.

Johansson, A.C., Steen, H., Ollinger, K., and Roberg, K. (2003). Cathepsin D mediates cytochrome c release and caspase activation in human fibroblast apoptosis induced by staurosporine. *Cell Death Differ* 10, 1253-1259.

Johnson, V.L., Ko, S.C., Holmstrom, T.H., Eriksson, J.E., and Chow, S.C. (2000). Effector caspases are dispensable for the early nuclear morphological changes during chemical-induced apoptosis. *J Cell Sci* 113 ( Pt 17), 2941-2953.

Kagedal, K., Johansson, U., and Ollinger, K. (2001). The lysosomal protease cathepsin D mediates apoptosis induced by oxidative stress. *FASEB J* 15, 1592-1594.

Karch, J., Kwong, J.Q., Burr, A.R., Sargent, M.A., Elrod, J.W., Peixoto, P.M., Martinez-Caballero, S., Osinska, H., Cheng, E.H., Robbins, J., *et al.* (2013). Bax and Bak function as the outer membrane component of the mitochondrial permeability pore in regulating necrotic cell death in mice. *Elife* 2, e00772.

Ly, J.D., Grubb, D.R., and Lawen, A. (2003). The mitochondrial membrane potential ( $\Delta\psi_m$ ) in apoptosis; an update. *Apoptosis* 8, 115-128.

Madak, J.T., and Neamati, N. (2015). Membrane permeable lipophilic cations as mitochondrial directing groups. *Curr Top Med Chem* 15, 745-766.

Mirzayans, R., Andrais, B., Scott, A., Wang, Y.W., and Murray, D. (2013). Ionizing radiation-induced responses in human cells with differing TP53 status. *Int J Mol Sci* 14, 22409-22435.

Modica-Napolitano, J.S., and Weissig, V. (2015). Treatment Strategies that Enhance the Efficacy and Selectivity of Mitochondria-Targeted Anticancer Agents. *Int J Mol Sci* 16, 17394-17421.

Nakamura, K., Yoshikawa, N., Yamaguchi, Y., Kagota, S., Shinozuka, K., and Kunitomo, M. (2002). Characterization of mouse melanoma cell lines by their mortal malignancy using an experimental metastatic model. *Life sciences* 70, 791-798.

Narita, M., Shimizu, S., Ito, T., Chittenden, T., Lutz, R.J., Matsuda, H., and Tsujimoto, Y. (1998). Bax interacts with the permeability transition pore to induce permeability transition and cytochrome c release in isolated mitochondria. *Proc Natl Acad Sci U S A* 95, 14681-14686.

Portt, L., Norman, G., Clapp, C., Greenwood, M., and Greenwood, M.T. (2011). Anti-apoptosis and cell survival: a review. *Biochim Biophys Acta* 1813, 238-259.

Roberg, K., and Ollinger, K. (1998). Oxidative stress causes relocation of the lysosomal enzyme cathepsin D with ensuing apoptosis in neonatal rat cardiomyocytes. *Am J Pathol* 152, 1151-1156.

Susin, S.A., Lorenzo, H.K., Zamzami, N., Marzo, I., Snow, B.E., Brothers, G.M., Mangion, J., Jacotot, E., Costantini, P., Loeffler, M., *et al.* (1999). Molecular characterization of mitochondrial apoptosis-inducing factor. *Nature* 397, 441-446.

Susin, S.A., Zamzami, N., Castedo, M., Daugas, E., Wang, H.G., Geley, S., Fassy, F., Reed, J.C., and Kroemer, G. (1997). The central executioner of apoptosis: multiple connections between protease activation and mitochondria in Fas/APO-1/CD95- and ceramide-induced apoptosis. *J Exp Med* 186, 25-37.

Tsujimoto, Y., and Shimizu, S. (2007). Role of the mitochondrial membrane permeability transition in cell death. *Apoptosis* 12, 835-840.

Vercammen, D., Brouckaert, G., Denecker, G., Van de Craen, M., Declercq, W., Fiers, W., and Vandenabeele, P. (1998). Dual signaling of the Fas receptor: initiation of both apoptotic and necrotic cell death pathways. *J Exp Med* 188, 919-930.

Wang, G.Q., Wieckowski, E., Goldstein, L.A., Gastman, B.R., Rabinovitz, A., Gambotto, A., Li, S., Fang, B., Yin, X.M., and Rabinowich, H. (2001). Resistance to granzyme B-mediated cytochrome c release in Bak-deficient cells. *J Exp Med* 194, 1325-1337.

Wang, L., Kinnear, C., Hammel, J.M., Zhu, W., Hua, Z., Mi, W., and Caldarone, C.A. (2006). Preservation of mitochondrial structure and function after cardioplegic arrest in the neonate using a selective mitochondrial KATP channel opener. *Ann Thorac Surg* 81, 1817-1823.

Wei, M.C., Zong, W.X., Cheng, E.H., Lindsten, T., Panoutsakopoulou, V., Ross, A.J., Roth, K.A., MacGregor, G.R., Thompson, C.B., and Korsmeyer, S.J. (2001). Proapoptotic BAX and BAK: a requisite gateway to mitochondrial dysfunction and death. *Science* 292, 727-730.

Wong, R.S. (2011). Apoptosis in cancer: from pathogenesis to treatment. *J Exp Clin Cancer Res* 30, 87.

Zahreddine, H., and Borden, K.L. (2013). Mechanisms and insights into drug resistance in cancer. *Front Pharmacol* 4, 28.

## **CHAPTER 4**

# **D112-INDUCED ROS PRODUCTION IS SELECTIVELY POTENTIATED IN CANCER CELLS BY PHOTO-ACTIVATION**

## 4.1 Introduction

Delocalized lipophilic compounds selectively accumulate in cancer cell mitochondria and have long been investigated for therapeutic potential (Modica-Napolitano and Aprille, 2001). While targeted effects to cancer cell mitochondria are demonstrated *in vitro*, toxicities identified from *in vivo* studies have precluded further clinical development (Britten et al., 2000). Identifying the molecular mechanisms of toxicity and selectivity are thus necessary next steps for this class of molecules.

In chapter 3, I demonstrated that the delocalized lipophilic cation D112 localized to mitochondria and induced the mitochondrial-centered apoptotic pathway. These results suggested that the molecular mechanism of D112-induced cytotoxicity could involve direct interaction with mitochondrial components. Intriguingly, other DLCs have been shown to inhibit mitochondrial metabolism by binding to components of the electron transport chain or ATP synthase. For instance, Rh123 inhibits  $F_0F_1$ -ATPase (Complex V) activity (Lampidis et al., 1983; Modica-Napolitano and Aprille, 1987) and dequalinium chloride (DECA) interferes with NADH-ubiquinone reductase (Complex I) activity (Weiss et al., 1987). The prediction that D112 affects mitochondrial respiration or oxidative phosphorylation would be consistent with the activity of other DLCs. Therefore I further investigated the link between D112 and mitochondria in this chapter.

Additionally, in Chapter 1, I discussed the potential of enhancing cancer-specific effects through alternative strategies. In Chapter 3, we observed a 2-3-fold selectivity of D112 for cancer cell lines versus non-transformed cell lines. I was interested in exploring avenues with which to enhance this differential selectivity. It is

noteworthy that photo-activation of other DLCs have been shown to enhance the ability to inhibit electron transport *in vitro* (Modica-Napolitano et al., 1998) or tumor growth in a xenograft model (Castro et al., 1988). Moreover, D112 was first developed as a photosensitizer. Whether photo-activation of D112 would affect cytotoxic properties as demonstrated in our assays was unknown.

Thus in this chapter, I explore the contribution of mitochondrial metabolism to D112-induced cytotoxicity. I incorporate a yeast model system to dissect the involvement of oxidative versus fermentative metabolism and expand the results with human cell lines. Additionally, I tested the utility of photo-activation in D112-induced apoptosis with respect to enhancement of its cytotoxicity and selectivity to cancer cells.

## **4.2 D112-induced cell death is enhanced by mitochondrial respiration**

To explore the contribution of mitochondria to D112-induced cytotoxicity, I employed *Saccharomyces cerevisiae* as a model system. To validate yeast as an appropriate model, I first verified that D112 was taken up by yeast using fluorescence microscopy. As shown in Fig 4.1A, D112 fluorescence accumulated in cells over time. The effect of D112 on yeast growth properties was then tested by incubating yeast cells with D112 and monitoring cell growth. D112 (1  $\mu\text{g/ml}$  = 1.4  $\mu\text{M}$ ) inhibited yeast growth in a dose-dependent manner (Fig. 4.1B). To quantitate this effect, I determined yeast doubling times from the maximum slope of the exponential growth curves. D112 significantly decreased yeast proliferative rates (Fig. 4.1C). To assess cell viability, I washed D112-treated cells in fresh media and spotted bulk

serial dilutions on YPD recovery plates (Fig. 4.1D). D112-treated cells showed poor recovery after treatment, indicating that D112 induced cell death. To quantitate this cell-death effect, I plated an equal cell number on YPD recovery plates. D112-treatment induced a four-fold reduction in colony viability (Fig. 4.1E). These data demonstrated that *Saccharomyces cerevisiae* is a useful model for further studies with D112.

Given that yeast mainly utilize fermentative metabolism when cultured in standard glucose-containing medium (YPD as in Fig. 4.1), I was curious as to whether mitochondrial oxidative metabolism affected D112-cytotoxic properties. I propagated yeast in non-fermentable carbon medium (YPG-glycerol) that drives mitochondrial oxidative metabolism and examined yeast growth kinetics. These conditions markedly sensitized yeast cells to D112 with significant growth defects at concentrations as low as 0.157  $\mu\text{g/ml}$  (Fig. 4.2A and B), which was 15-fold lower than the lowest effective dose (2.5  $\mu\text{g/ml}$ ) in YPD (Fig. 4.1C). Moreover, cell viability was reduced by approximately 40-fold in YPG with D112 at 0.625  $\mu\text{g/ml}$  (Fig. 4.2C and D), whereas there was only a 4-fold reduction when treated with 5  $\mu\text{g/ml}$  in YPD (Fig. 4.1D and E), suggesting that mitochondrial respiration is associated with increased D112-toxicity.

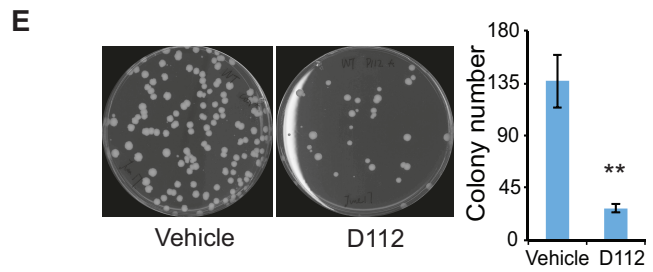
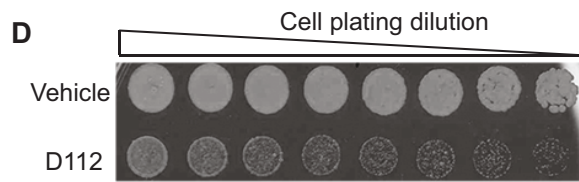
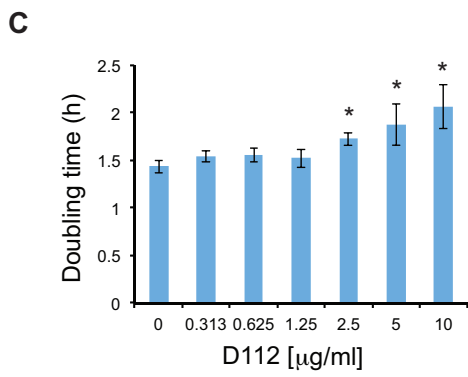
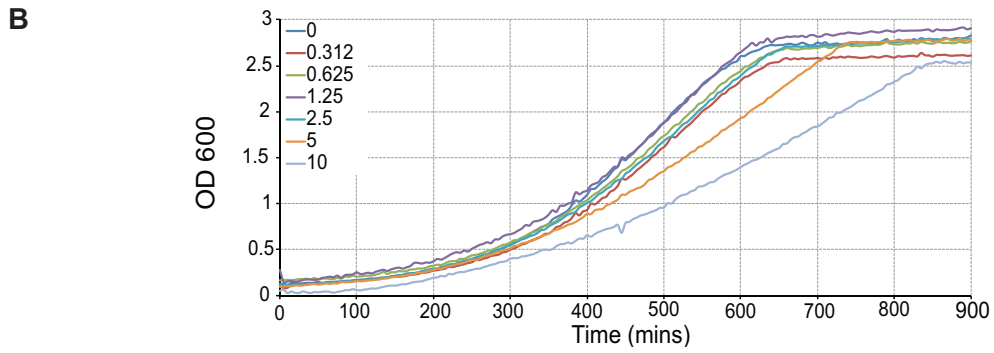
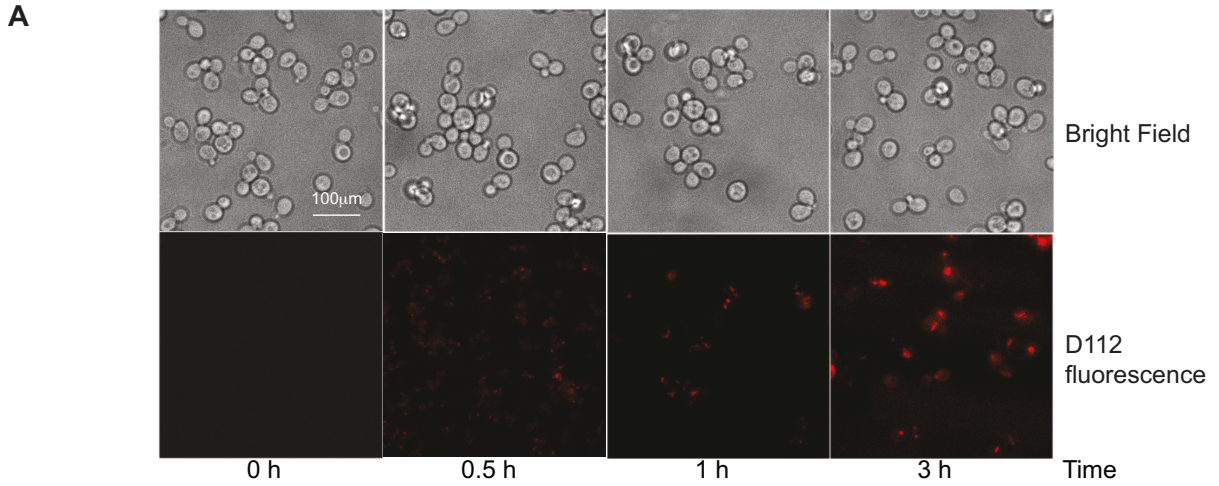


**Figure 4.1 D112 enters yeast cells and inhibits cell growth. A.** D112 intracellular uptake in yeast. Yeast cells were incubated with 5  $\mu\text{g}/\text{mL}$  D112 for the indicated times. Intracellular D112 was observed by fluorescence microscopy. Shown are representative images of 2 independent experiments. Scale bars, 100  $\mu\text{m}$ . **B.** Yeast growth curve in response to D112. Equal numbers of yeast cells were cultured in YPD with indicated concentrations of D112. Yeast proliferation was assessed by optical density (600 nm) over 15 h of growth at 30°C. **C.** Yeast doubling times were determined from the maximum slope of each curve during exponential growth from the graph in figure 4.1B. **D.** Yeast viability following D112 treatment in YPD. After incubation with 5  $\mu\text{g}/\text{mL}$  D112 for 24 hours in YPD medium, 2-fold serial dilutions of the yeast cells were spotted on YPD plates and grown for 3 days at 30°C to assess survival. **E.** Yeast viability following D112 treatment in YPD. After incubation with 5  $\mu\text{g}/\text{mL}$  D112 for 15 h, yeast cells were plated to quantify viability in a colony formation assay. Mean  $\pm$  SD of three independent experiments performed in triplicate were shown (in C.E), statistical significance was determined using a two-tailed Student's t-test for two means with equal variance. \* $P < 0.05$ , \*\* $P < 0.01$ , \*\*\* $P < 0.001$ .

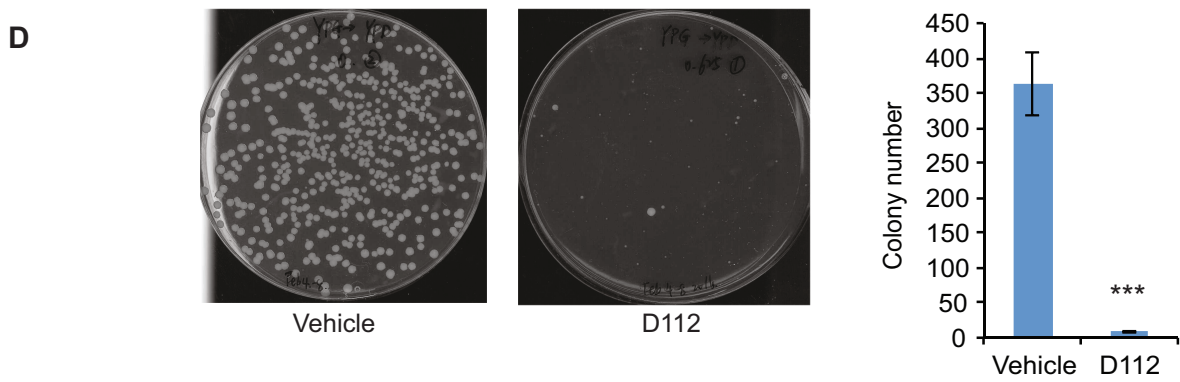
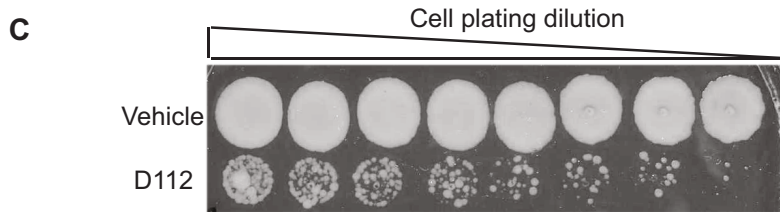
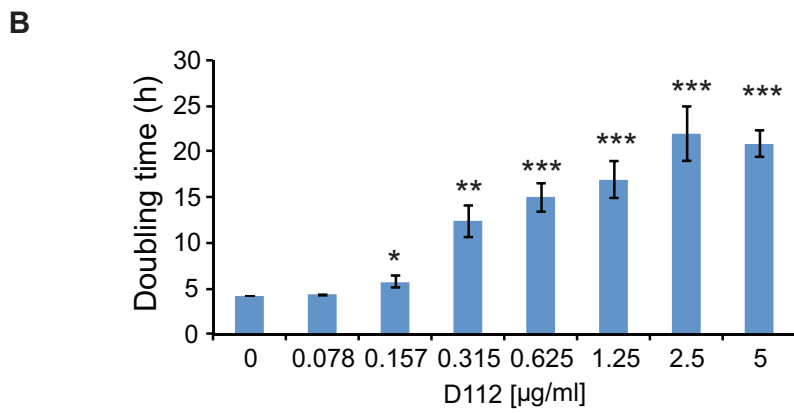
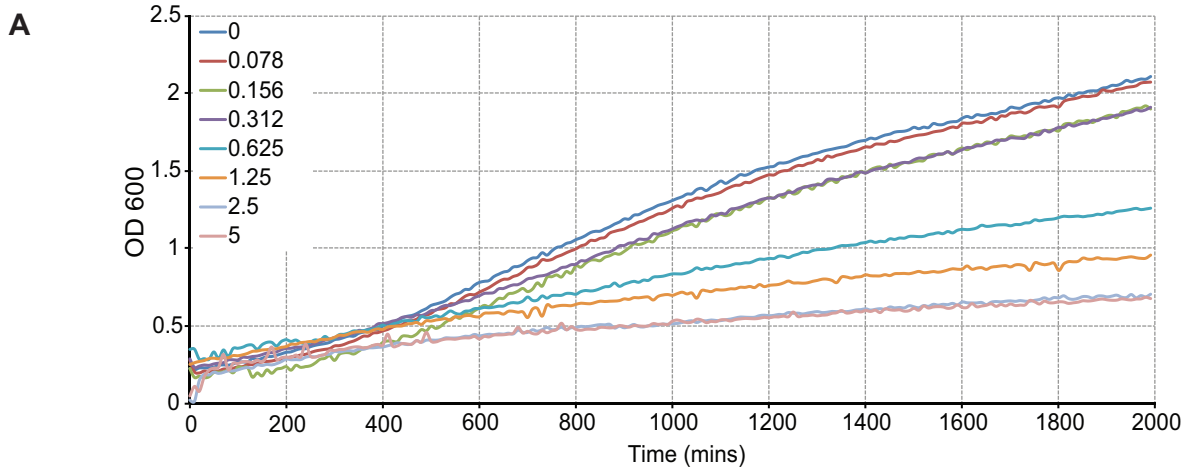


**Figure 4.2 Mitochondrial respiration renders yeast more sensitive to D112 toxicity. A.** Growth curve in YPG medium. Yeast cells were incubated in YPG with indicated concentrations of D112. Yeast proliferation was assessed by optical density (600 nm) over 30 h of growth at 30°C. **B.** Yeast doubling times were determined from the maximum slope of each curve during exponential growth from the graph in figure 4.2A. **C.** Yeast viability following D112 treatment in YPG. After incubation with 0.625 µg/ml D112 for 30 hours, 2-fold serial dilutions of the yeast cells were spotted on YPD plates and grown for 4 days at 30°C to assess survival. **D.** Yeast viability following D112 treatment in YPG. After incubation with 0.625 µg/ml D112 for 30 h, yeast cells were plated to on YPD plates to quantify viability in a colony formation assay. Mean ± SD of three independent experiments performed in triplicate were shown (in B.D), statistical significance was determined using a two-tailed Student's t-test for two means with equal variance. \*P<0.05, \*\*P<0.01, \*\*\*P<0.001.

If mitochondrial respiration was indeed required for D112-toxicity, I would expect that respiration-deficient mutants (petite strains) would be resistant. I tested this postulate using various mutant strains that each lack a gene or genes necessary for oxidative phosphorylation and rely on glycolytic fermentation for growth. I examined 11 petite strains that harbored single gene mutations ( $\rho^-$ ) in electron transport chain (ETC) or  $F_0F_1$  ATP synthase components (Complex I, II, III, and IV), as well as mitochondrial DNA (mtDNA)-deleted mutants ( $\rho^0$ ) that are deficient for multiple genes for electron transport and mitochondrial metabolism (Table 4.1). Each petite strain was treated with 5  $\mu\text{g/ml}$  D112 in YPD, and yeast growth kinetics and cell viability were then determined. Similar to wild-type cells, I found that D112 inhibited cell proliferation in all mutant strains tested as evidenced by increased doubling times (Fig. 4.3A). These results indicated that the growth-arrest effect of D112 was not dependent on a single component of the ETC. In contrast, when assessed for cell viability, the mutants (MTF1, MIP1 and HMI1) that lack mtDNA ( $\rho^0$ ) showed no apparent loss of viability (Fig. 4.3B), while wild-type and other mutant strains showed decreased viability. Thus ablation of individual components of the ETC was not sufficient to protect cells from D112-induced cell death. However, mitochondrial DNA and/or its downstream gene products were necessary for D112-toxicity.

#### **4.3 D112 binds to DNA**

Based on the protective effect of  $\rho^0$  strains (cells that lack mtDNA) and the structure and charge of D112 that may allow binding to nucleic acids, I next

Gene	Description	phenotype
MTF1	Mitochondrial RNA polymerase specificity factor, mtDNA deletion	rho <sup>0</sup>
MIP1	Mitochondrial DNA-directed DNA polymerase, mtDNA deletion	rho <sup>0</sup>
HMI1	Mitochondrial inner membrane localized ATP-dependent DNA helicase , mtDNA deletion	rho <sup>0</sup>
NDI1	NADH: ubiquinone oxidoreductase, Complex I	rho <sup>-</sup>
SDH2	Iron-sulfur protein subunit of succinate dehydrogenase Complex II	rho <sup>-</sup>
CYT1	Cytochrome c1, Complex III	rho <sup>-</sup>
COR1	Ubiquinolcytochrome c reductase core protein 1,Complex III	rho <sup>-</sup>
COX6	Cytochrome c oxidase subunit VI, Complex IV	rho <sup>-</sup>
COX9	Cytochrome c oxidase subunit VIIA, Complex IV	rho <sup>-</sup>
ATP1	Alpha subunit of F1-ATP synthase, F0/F1 ATP synthase	rho <sup>-</sup>
ATP5	Subunit 5 of F0-ATP synthase, F0/F1 ATP synthase	rho <sup>-</sup>

**Table 4.1 Yeast mutant strains. All strains were obtained from the MAT  $\alpha$  yeast deletion collection.**

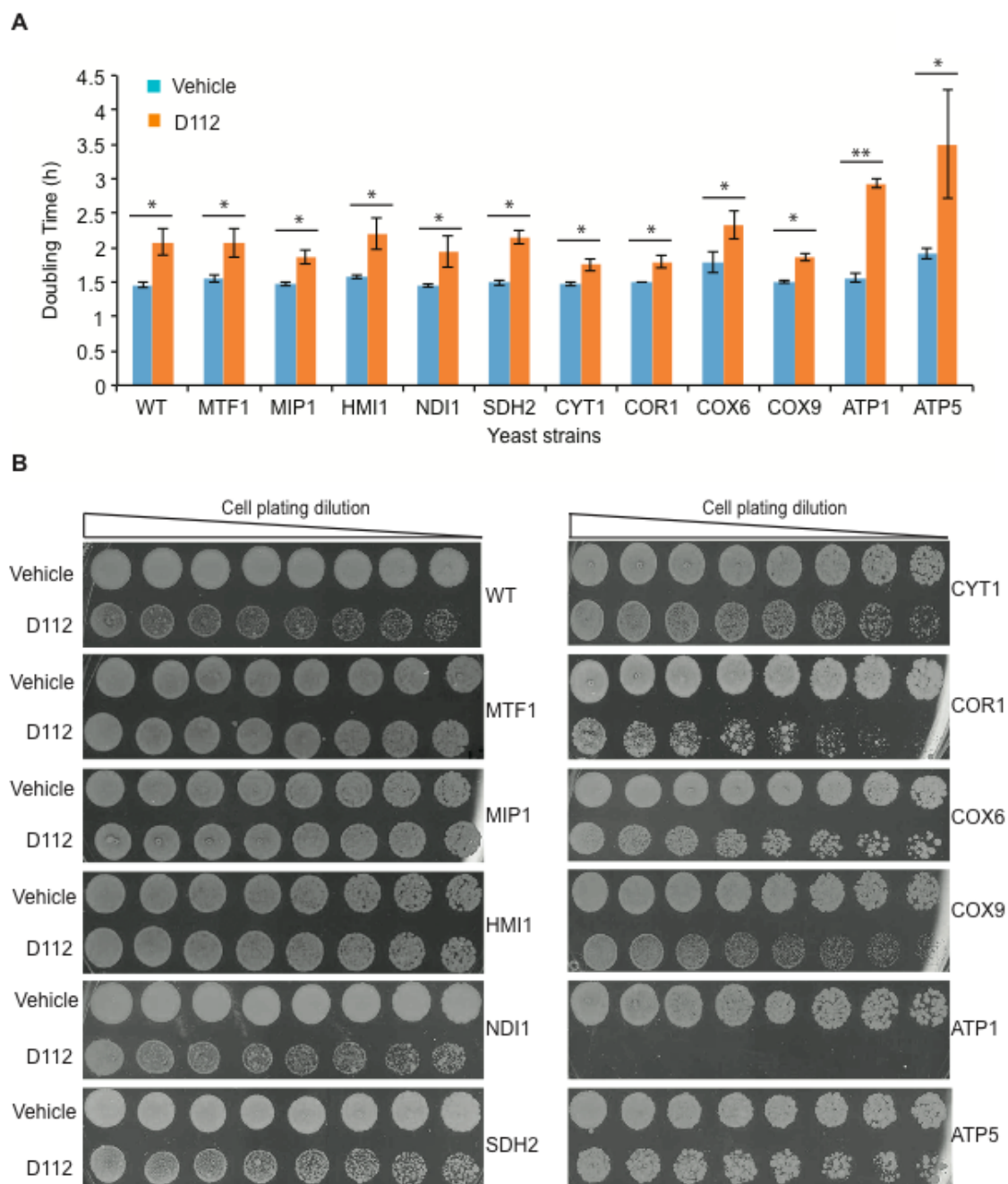


**Figure 4.3 Mitochondrial DNA-deleted mutants are resistant to D112 toxicity.** **A.** Yeast mutant doubling times in the absence or presence of 5  $\mu\text{g}/\text{mL}$  D112 were determined from the maximum slope of each curve (not shown). Mean  $\pm$  SD of three independent experiments performed in triplicate were shown, statistical significance was determined using a two-tailed Student's t-test for two means with equal variance. \* $P < 0.05$ , \*\* $P < 0.01$ , \*\*\* $P < 0.001$ . **B.** Yeast mutant viability following D112 treatment. After incubation with 5  $\mu\text{g}/\text{mL}$  D112 for 24 hours, 2-fold serial dilutions of the yeast cells were spotted on YPD plates and grown for 3 days at 30°C to assess survival.

assessed D112 binding to DNA using an electrophoretic gel-shift assay (Fig. 4.4A). In this assay, D112 was mixed with DNA and loaded onto an agarose gel. D112 alone did not enter the agarose gel, but did migrate partially into the gel when mixed with DNA, which is indicative of DNA-binding. Further, since DNA-binding can alter emission intensity by changing the molecular environment of the fluorophore (Lakowicz, 2006; Olmsted and R.Kearns, 1977), I compared D112 fluorescence in the presence or absence of DNA. To gain a full spectral scan, D112 (+/- DNA) was excited from 340 nm to 620 nm and the corresponding emission spectra to each excitation wavelength were then collected by photomultiplier. D112 alone had two excitation peaks (380-410 nm and 510-530 nm) and one emission peak at 615 nm (Fig. 4.4B). In the presence of DNA, fluorescence emission intensity increased 5-fold from 34,000 to 160,000 counts/s. (Fig. 4.4C). These data demonstrated a direct interaction between D112 and DNA.

This DNA-binding property of D112 is reminiscent of ethidium bromide which is known to damage mitochondrial DNA and generate petite strains in yeast (Olmsted and R.Kearns, 1977). Since the petite phenotype is a function of mitochondrial respiration deficiency, I tested whether D112 induced the petite phenotype. This is easily scored as the W303-1A yeast strain grows as red colonies under normal conditions, but upon becoming petite, grows as white colonies. I treated W303-1A yeast with D112 at the indicated concentrations, or with 20  $\mu$ M EB as a positive control, and I found D112 treatment induced the white-growing petite phenotype (Fig. 4.4D). These data indicate that D112 induced mitochondrial DNA

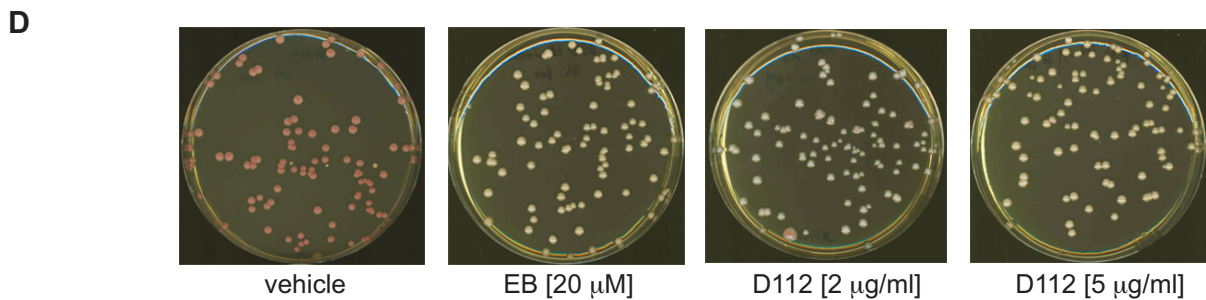
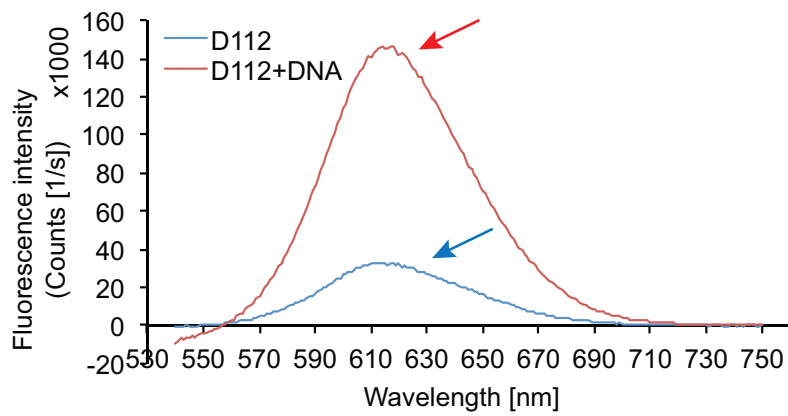
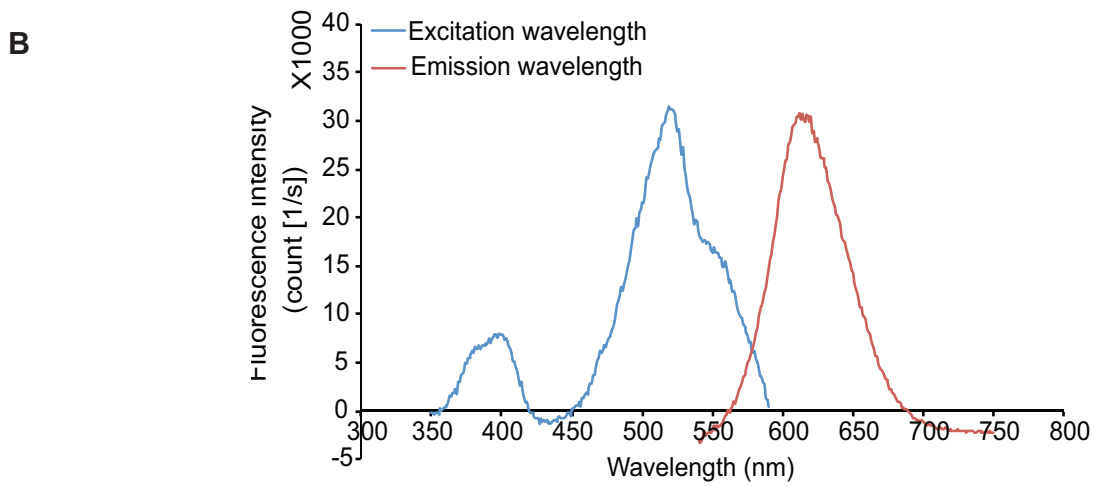
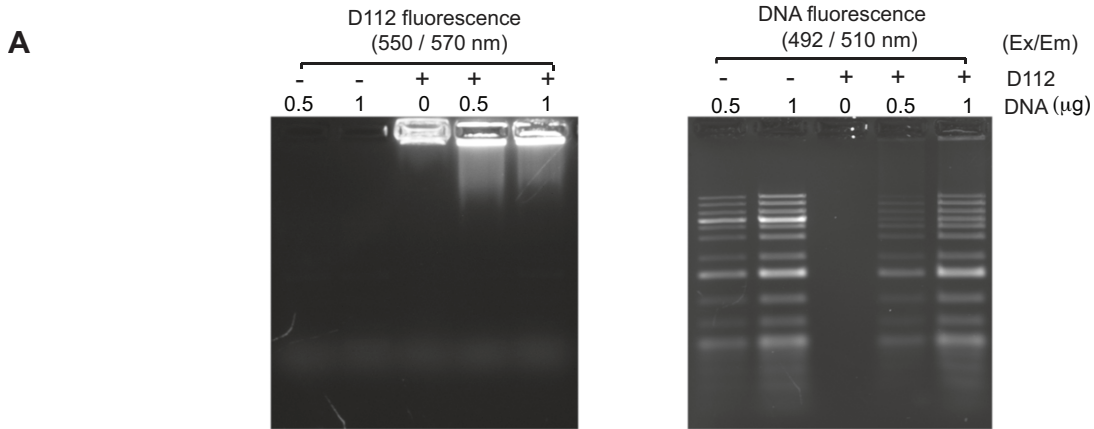


**Figure 4.4 D112 binds to nucleic acid in vitro and induces a petite phenotype in yeast. A.** D112 interaction with DNA in vitro. 0.5  $\mu\text{g}$  (lane 1, 4) or 1  $\mu\text{g}$  of a DNA ladder (lane 2, 5) was incubated without (lane 1, 2) or with 0.025  $\mu\text{g}/\text{mL}$  D112 (lane 4, 5) for 30 min at room temperature. D112 alone (lane 3), DNA alone or DNA-D112 mixtures were separated by 1% agarose gel electrophoresis. The gel was imaged for D112 fluorescence at 550 nm wavelength, and then stained with SYBR safe to visualize the DNA at 492 nm wavelength. **B.** D112 excitation and emission spectra. The excitation of 0.25  $\mu\text{g}/\text{mL}$  D112 in phosphates buffer (pH7.4) was examined from 340 nm to 620 nm. The corresponding emission spectra were collected from wavelength 540 nm to 750 nm with excitation at 515 nm. **C.** D112 emission spectra after binding DNA. 500 ng of DNA was incubated with 0.25  $\mu\text{g}/\text{ml}$  D112 at room temperature for 15 min in dark and the emission spectra recorded at 515 nm excitation wavelength. **D.** A W303-1A yeast strain was treated with D112 at indicated concentration for 4 h. Equal number of cells was plated for single colonies. Ethidium bromide (EB) was used as a positive control.

damage, leading to a petite phenotype, which may involve D112 directly binding mtDNA.

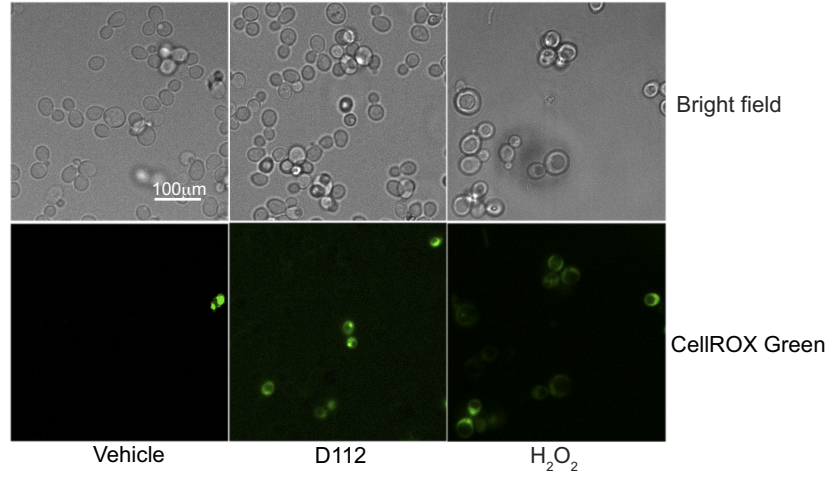
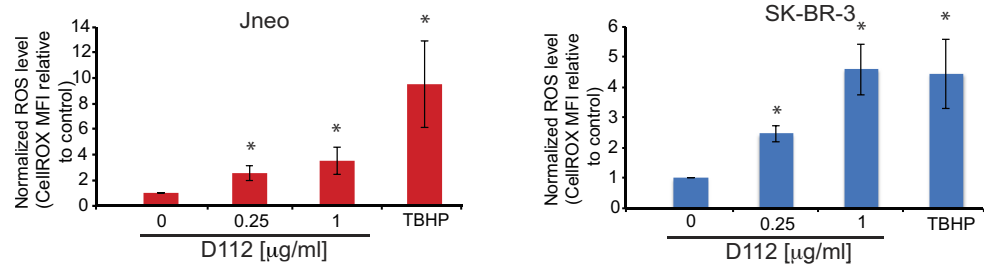
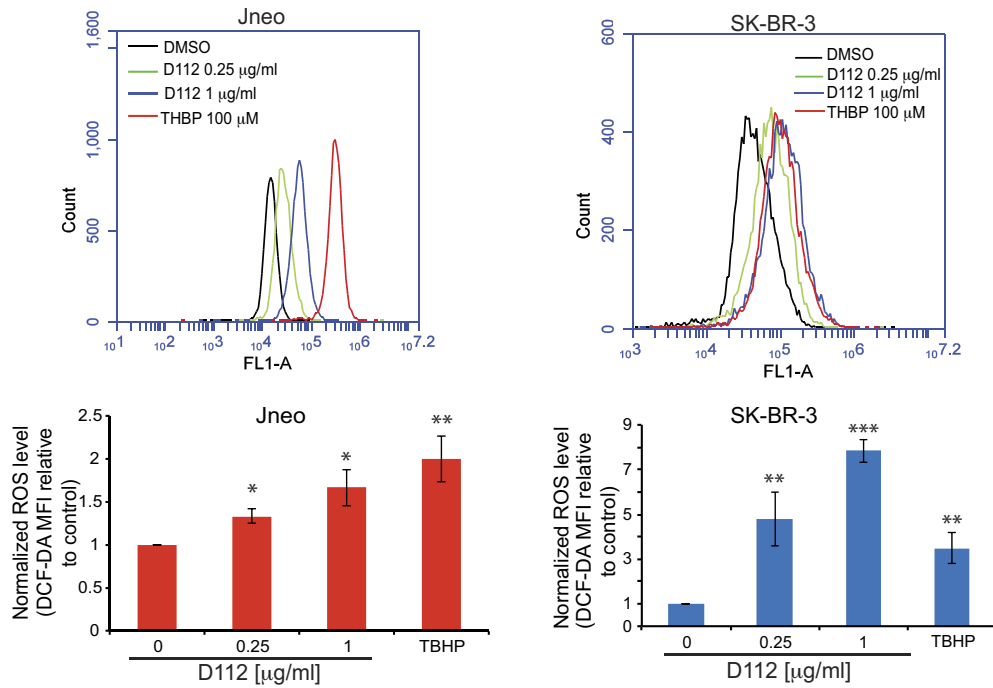
#### **4.4 ROS induction is required for D112-mediated cell death**

While the loss of mtDNA and loss of D112-binding sites may contribute to D112-resistance of rho<sup>0</sup> cells, the lack of mitochondrial-encoded genes could also contribute to the resistant phenotype. The mitochondrial genome encodes components of Complexes I, III, IV and the F<sub>0</sub>F<sub>1</sub> ATP synthase of the ETC (Taanman, 1999). These complexes participate in a series of electron transfer reactions with final electron transfer to oxygen at complex IV. This process is coupled with proton pumping across the inner mitochondrial membrane and the resultant electrochemical gradient provides free energy to drive ATP synthesis. During respiration, a leak of electrons to oxygen from complex I and complex III generates superoxide (Sabharwal and Schumacker, 2014), and this capacity is lost in rho<sup>0</sup> cells (Du et al., 2006; Quinlan et al., 2013). It is well established that sudden rises of ROS induce cell death (Du et al., 2006; Kawanishi et al., 2006; Pelicano et al., 2004; Toyokuni et al., 1995), which could be a mechanism of D112-induced cell death. Thus I explored whether D112 treatment increased ROS production in wild-type cells using the fluorescent indicator CellROX Green. Briefly, wild-type cells were treated with D112 and then CellROX Green was added to the cell culture. Oxidized CellROX Green exhibits bright green fluorescence and subsequent binding to DNA. The fluorescence of CellROX Green was detected using a microscope and I

observed an increase in ROS levels (Fig. 4.5A), suggesting that D112-mediated cell death through ROS production.

To extend this observation and confirm these findings from the yeast system, I tested ROS generation in human cell lines. Specifically, ROS generation was examined in Jurkat (human T lymphoblastoid cell line) and SK-BR-3 (human breast carcinoma) cell lines, both of which show D112 sensitivity in my previous study. ROS was assessed with two different indicators CellROX Green (Fig. 4.5B) and CM-H<sub>2</sub>DCFDA (Fig. 4.5C). In the CellROX Green assay, cells were treated with D112 at the indicated concentrations, or with the ROS inducer *tert*-Butyl hydroperoxide (TBHP) as a positive control. Cells were then stained with CellROX Green, of which fluorescence was quantitated by flow cytometry. D112 significantly increased ROS levels in Jneo and SK-BR-3 cells (3- and 4.5- fold, respectively) (Fig. 4.5B). Similar to CellROX, CM-H<sub>2</sub>DCFDA is another commonly used indicator for intracellular oxidative stress. Oxidation of CM-H<sub>2</sub>DCFDA by ROS yields a green fluorescent adduct that is retained inside cells. D112 treatment increased fluorescence as measured by flow cytometry (Fig. 4.5C, up), and quantitation confirmed that D112 increased ROS levels in both cell lines (Fig. 4.5C, bottom). These results demonstrated that D112 induces ROS generation in human cells.

Next, to test functional relevance, I pre-incubated cells with the ROS scavenger NAC (N-Acetyl-Cysteine) and examined D112-induced apoptosis in both cell lines using flow cytometry. I observed that NAC significantly reduced both D112 and TBHP-induced cell death as evidenced by decreased phosphatidylserine exposure (Fig. 4.6A). NAC had no effect on staurosporine (STS) induced apoptosis,

**A****B****C**

**Figure 4.5 D112 induces ROS production. A.** D112 induced ROS production in yeast. Wild-type yeast cells were treated with 5  $\mu\text{g/ml}$  D112 or 300  $\text{mM}$   $\text{H}_2\text{O}_2$  for 4 h, and then the level of ROS was measured by CellROX Green under microscopy.  $\text{H}_2\text{O}_2$  was used as a positive control. Scale bars, 100  $\mu\text{m}$ . **B.** D112 induced ROS production in mammalian cells. Cancer cells were incubated with D112 or TBHP at indicated concentrations for 1 h. ROS level was measured using CellRox Green or **C.** CM-H2DCF-DA (1.5  $\mu\text{M}$ ) by flow cytometry. DCF-DA fluorescence is shown in representative images (top), and DCF-DA fluorescence intensity in cells was quantified in the bar chart (bottom). Mean  $\pm$  SD of three independent experiments performed in triplicate were shown (in B.C), statistical significance was determined using a two-tailed Student's t-test for two means with equal variance. \* $P < 0.05$ , \*\* $P < 0.01$ , \*\*\* $P < 0.001$ .

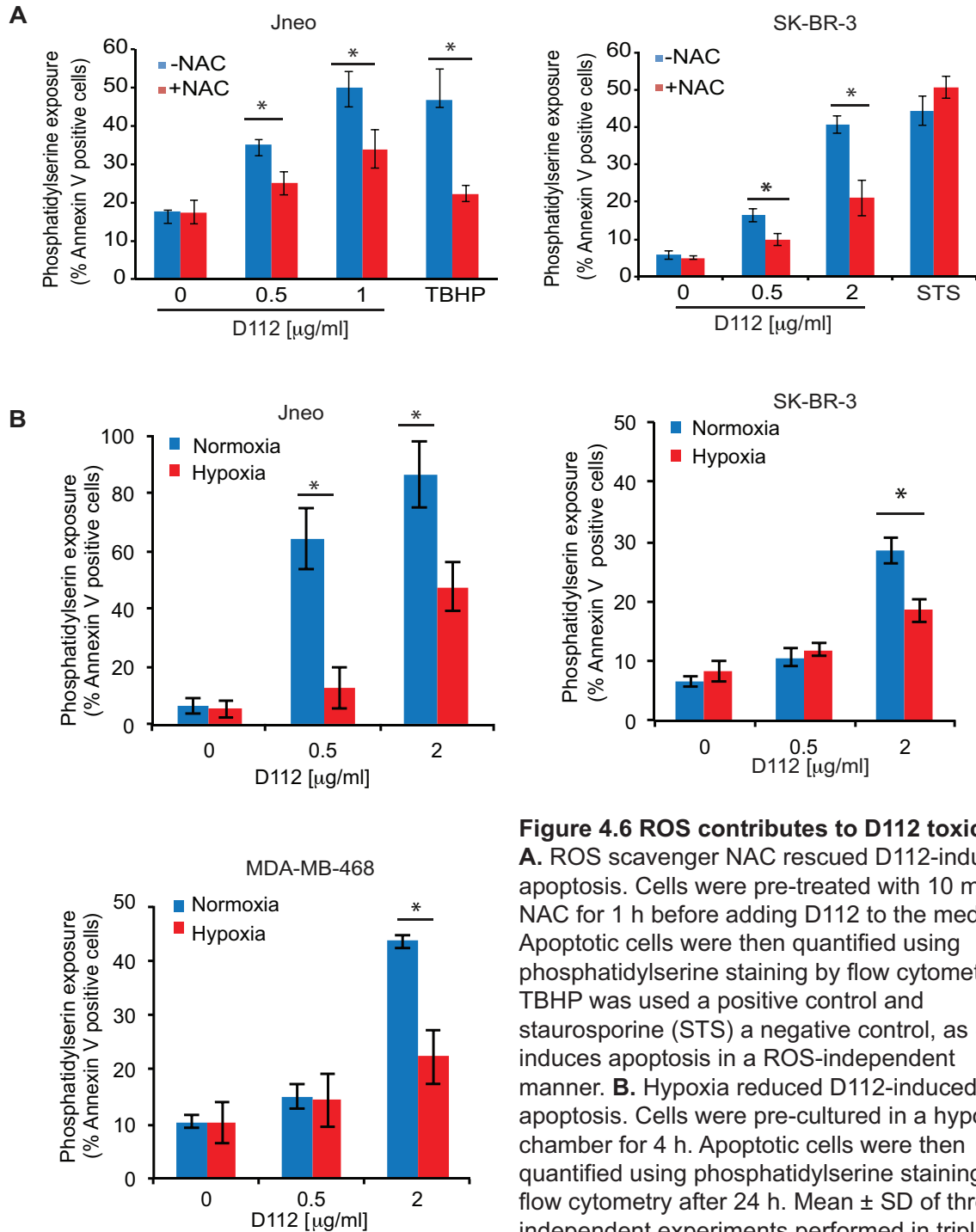


**Figure 4.6 ROS contributes to D12 toxicity.**

**A.** ROS scavenger NAC rescued D12-induced apoptosis. Cells were pre-treated with 10 mM NAC for 1 h before adding D12 to the medium. Apoptotic cells were then quantified using phosphatidylserine staining by flow cytometry. TBHP was used as a positive control and staurosporine (STS) a negative control, as STS induces apoptosis in a ROS-independent manner. **B.** Hypoxia reduced D12-induced apoptosis. Cells were pre-cultured in a hypoxia chamber for 4 h. Apoptotic cells were then quantified using phosphatidylserine staining by flow cytometry after 24 h. Mean  $\pm$  SD of three independent experiments performed in triplicate were shown, statistical significance was determined using a two-tailed Student's t-test for two means with equal variance. \* $P < 0.05$ , \*\* $P < 0.01$ , \*\*\* $P < 0.001$ .

confirming that the protective effect imparted by NAC was ROS-dependent. The involvement of ROS was further confirmed by measuring cell death under hypoxic conditions in the absence of oxygen. Three D112 sensitive cell lines (Jneo, SK-BR-3 and MDA-MB-468) were pre-incubated in a hypoxia chamber and then D112 was added and apoptosis was examined by flow cytometry. Cells incubated in the absence of oxygen were all significantly resistant to D112-induced apoptosis (Fig. 4.6B), indicating the requirement of oxygen for D112-induced cytotoxicity. Together, these observations indicate that ROS generation was necessary for D112-mediated cell death.

I next examined whether ROS production was an initiating event of D112-induced cell death. In chapter 3, I identified that the pro-apoptotic protein BAX was required for D112-induced cell death (Fig. 3.6) and this was inhibited by the anti-apoptotic oncogene Bcl-2 (Fig. 3.5). I was interested to see whether ROS was generated in the Bcl-2 overexpressing cell line (JBcl-2) and BAX/BAK deficient cell line (JR) in response to D112. Therefore, cells were treated with D112 and incubated with the ROS indicator CM-H<sub>2</sub>DCFDA. ROS production was examined by flow cytometry, and I observed that D112 induced a similar increase of ROS in all cell lines (Fig. 4.7A), indicating that ROS production induced by D112 was upstream of Bcl-2 and Bax. As discussed in chapter 1, ROS can induce apoptosis by directly activating Bax (Nie et al., 2008), so I next tested whether Bax was activated in D112-treated cells in a ROS-dependent manner. Structural changes mediate Bax activation, and can be monitored with a conformation-specific antibody, 6A7 (Upton et al., 2007). I treated Jneo cells with increasing concentrations of D112 and

assessed Bax activation in an immunoprecipitation assay. Active Bax was immunoprecipitated from D112-treated cells, but not control cells (Fig. 4.7B, up). Importantly, pre-treatment of cells with NAC ablated Bax immunoprecipitation (Fig. 4.7B, bottom), confirming that ROS was required for Bax activation. We were also curious as to whether ROS contributed to DNA damage. In particular, given that mtDNA is prone to ROS-induced damage (de Grey, 2005; Ishikawa et al., 2008), and that D112 induced mtDNA damage in yeast, we directly tested whether D112-induced ROS contributed to mtDNA damage. I performed a mtDNA double-strand break PCR-based assay in which a decreased production of a large mtDNA fragment (8.9kb) relative to a small mtDNA fragment (220bp) is indicative of mtDNA damage. I identified that D112 caused mtDNA break in a dose-dependent manner, and moreover D112-induced ROS partly contributed to this (Fig. 4.7C, left). The protective effect of NAC on D112-induced mtDNA damage was statistically significant when cells were treated with low dose of D112. Altogether, these data demonstrate that D112 induced ROS production is essential for BAX activation and downstream apoptosis.

#### **4.5 ROS contributes to D112 selective cytotoxicity**

D112 cytotoxicity is selective toward transformed versus non-transformed cell lines (Fig. 3.14A and B) (Yang et al., 2015)., Cancer cells are highly sensitive to ROS-based therapies, due to an elevated oxidative stress environment (Trachootham et al., 2009). This led us to investigate whether ROS production was the mechanism for D112-selectivity. I first measured the base-line level of ROS in

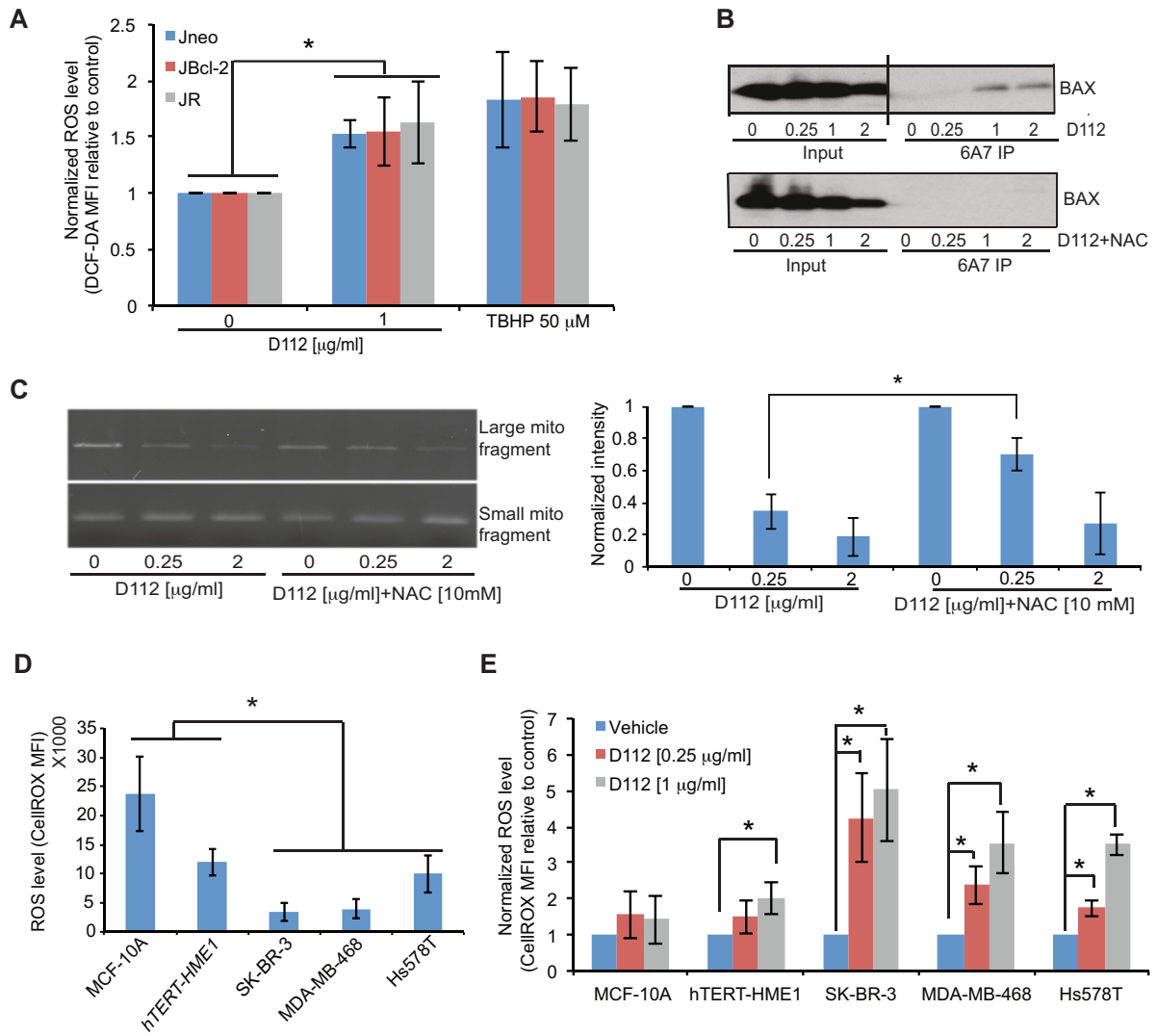


**Figure 4.7 ROS generation contribute to D112 selectivity.** **A.** All cells were incubated with D112 for 1 h. ROS level was measured using CellROX Green (2.5  $\mu$ M) by flow cytometry. **B.** Bax activation in response to D112. Cells were pre-treated with NAC (10 mM) for 1 h. The activated form of Bax was pulled down with the Bax 6A7 antibody and detected by western blotting (top) and quantified by relative intensity of protein bands (bottom). **C.** D112 induces mtDNA damage. Jneo cells were pretreated with 10 mM NAC for 1 h, and then incubated with D112 at indicated concentrations for 1 h. mtDNA damage was evaluated by a PCR-based assay comparing the production of a large mtDNA fragment and a small mtDNA fragment (top). Relative intensity of the large mtDNA fragment was quantified by normalizing treatment to control (bottom). **D.** Basal level of ROS in human cell lines tested. CellROX Green fluorescence of indicated cell lines were quantitated by flow cytometry. **E.** ROS elevation in response to D112 treatment. ROS levels were measured based on CellROX Green staining and are presented as the fold change over untreated cells. In all experiments, Mean  $\pm$  SD of three independent experiments performed in triplicate were shown, statistical significance was determined using a two-tailed Student's t-test for two means with equal variance. \*P<0.05, \*\*P<0.01, \*\*\*P<0.001.

these cells and looked for an association of elevated ROS with D112-sensitivity. Surprisingly, MCF-10A and hTERT-HME1 showed higher basal ROS levels than SK-BR-3, MDA-MB-468 and Hs578T (Fig. 4.7D), inconsistent with a model whereby transformed cells harbor elevated ROS. However, upon addition of D112, the cancer cell lines elevated ROS levels 3-4 fold, whereas the non-transformed cells showed limited ROS induction (Fig. 4.7E). Together, these data support a model where D112 selective cancer cell killing is mediated by a burst in ROS levels.

#### **4.6 D112 is preferentially taken up by cancer cells**

ROS induction in cancer cells may be a consequence of preferential D112 uptake, which would be in line with other cationic DLCs that accumulate selectively in cancer cell mitochondria (Modica-Napolitano and Aprille, 2001; Modica-Napolitano et al., 1996). To directly compare uptake, SK-BR-3 and MCF-10A cells were seeded in the same chamber and incubated with D112. SK-BR-3 and MCF-10A cells were identified by their distinctive morphology. D112 accumulation was then determined using fluorescent microscopy. I observed that D112 accumulated to higher levels in SK-BR-3 cells (smaller round cells, see green arrows) as compared to MCF-10A cells (larger flat cells, see white arrows) (Fig. 4.8A). Given that D112 fluorescence increases upon DNA binding, increased intracellular fluorescence could be due to increased uptake and/or binding of D112 to DNA. Thus, I also measured the fluorescence intensity remaining in the media after treatment (Fig. 4.8B). In this assay, cells were incubated with D112, after which, the medium was removed and D112 fluorescence intensity was measured. There was significantly less

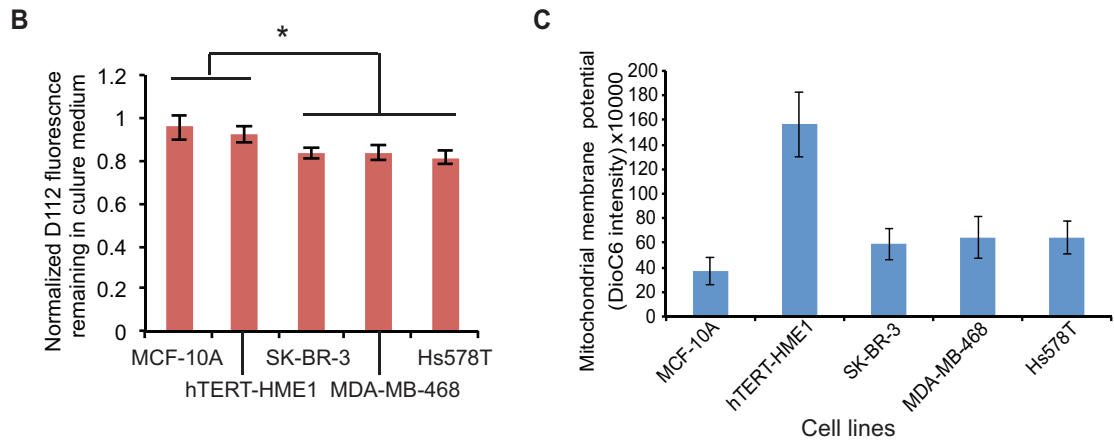
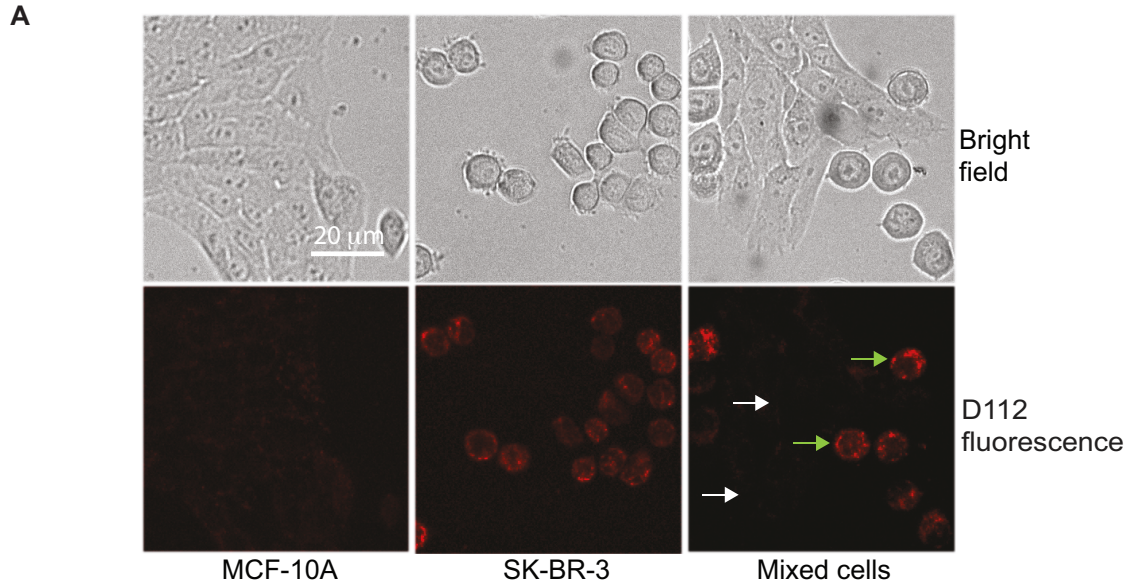


**Figure 4.8 D112 preferentially accumulates in cancer cells. A.** Live images of D112 intracellular uptake in SK-BR-3 and MCF-10A cells. Individual cell line or mixed cell lines were treated with D112 for 1 h and then imaged for D112 fluorescence. White arrows indicated MCF-10A cells and green arrows indicated SK-BR-3 cells. Scale bars, 20  $\mu$ m. **B.** D112 uptake in various cell types. Accumulation of D112 in cells was assessed indirectly by measuring D112 fluorescence intensity remaining in the medium after 1h incubation with D112. D112 fluorescence intensity was normalized to control medium in the absence of cells to exclude the degradation and/or loss of D112 during the procedure. The one-way Analysis of Variance (ANOVA) test was performed and p-values were obtained by Tukey's Post Hoc test. P-value is below 0.05 when comparing non-transformed cell lines with cancer cell lines. **C.** Mitochondrial membrane potential of multiple cell lines. Mean  $\pm$  SD of three independent experiments performed in triplicate were shown. For statistical analysis of multiple groups, the one-way Analysis of Variance (ANOVA) test was performed and p-values were obtained by Tukey's Post Hoc test. \*P<0.05.

fluorescence in the media of the cancer cell lines versus the non-transformed cell lines, suggesting that cancer cells took up more D112. Taken together, these results indicate that D112 accumulated preferentially in the carcinoma versus non-transformed cell lines.

Differential cellular uptake of other DLCs is facilitated by the elevated electrochemical potential ( $\Delta\psi$ ) of cancer cell mitochondria (Madak and Neamati, 2015; Modica-Napolitano and Aprille, 2001), so I tested whether electrochemical potential was also involved in D112 cancer-selectivity. I first confirmed the contribution of mitochondrial membrane potential for D112 internalization. Treatment of SK-BR-3 cells with the mitochondrial uncoupling agent, carbonyl cyanide *m*-chlorophenyl hydrazine (CCCP), diminished intracellular fluorescence (Chapter 3, Fig. 3.13). Given that cancer cells are reported to have hyperpolarized mitochondrial membrane potential, this may explain why cancer cells take up more D112. However, using an electrochemical-sensing dye, DiOC<sub>6</sub>, non-transformed cells showed higher DiOC<sub>6</sub> fluorescent intensity than cancer cells, suggesting that there was no correlation between cellular D112-sensitivity and  $\Delta\psi$  (Fig. 4.8C). Thus, while D112 is preferentially taken up by cancer cells, the mechanism of uptake remains unclear.

#### **4.7 Photo-activation of D112 increases its cytotoxic potential**

Kodak Laboratories originally developed D112 for use as a photosensitizer in photographic emulsions. Photosensitizers produce ROS by transferring light energy to oxygen (Vrouenraets et al., 2003). An exciting application of photosensitizers is their use in photodynamic therapy (PDT) that combines low-dose drug treatment

with targeted activation via light therapy (Snyder et al., 2003). As mentioned in Chapter 1, in principle, a photosensitizer is a light-absorbing compound that is activated upon exposure to specific wavelengths of light. To return to the ground state, the photosensitizer transfers energy or charge to cellular substrates, such as lipid membranes or DNA, or is transferred to oxygen to generate ROS (Vrouenraets et al., 2003). I therefore explored a PDT-application for D112 by investigating whether light activation increased D112 efficacy. The photodynamic therapy usually includes 3 steps: drug administration, drug accumulation and photo-activation (Chapter 1). To follow this standard procedure, SK-BR-3 cells were plated on glass coverslips and incubated with D112 for 1 h, to allow D112 intracellular accumulation. Then cells were rinsed with fresh medium, and exposed to a single pulse (0 s, 10 s, 30 s or 60 s) of 541 nm laser light. Cell morphology was recorded 3 h later (Fig. 4.9). I observed that non-photoactivated D112 did not induce cell death in this short time frame, while photo-activation clearly enhanced D112-induced cell death. In particular, alternate cell death pathways were induced with differing lengths of irradiation based on cell morphology. Specifically, a 10 s treatment led to cell morphology indicative of apoptosis (shrunken and blebbing cells with fragmented bodies, see blue arrows), while a longer photo-activation pretreatment (60 s) induced mostly necrotic cellular morphology (swollen cell body with vacuoles, see red arrows). An intermediate irradiation (30 s) induced mixed apoptotic and necrotic cells (Fig. 4.10A). Importantly, photo-activation alone did not induce cell death in the absence of D112 (Fig. 4.9). To assess the dynamics of photo-activation, cells were

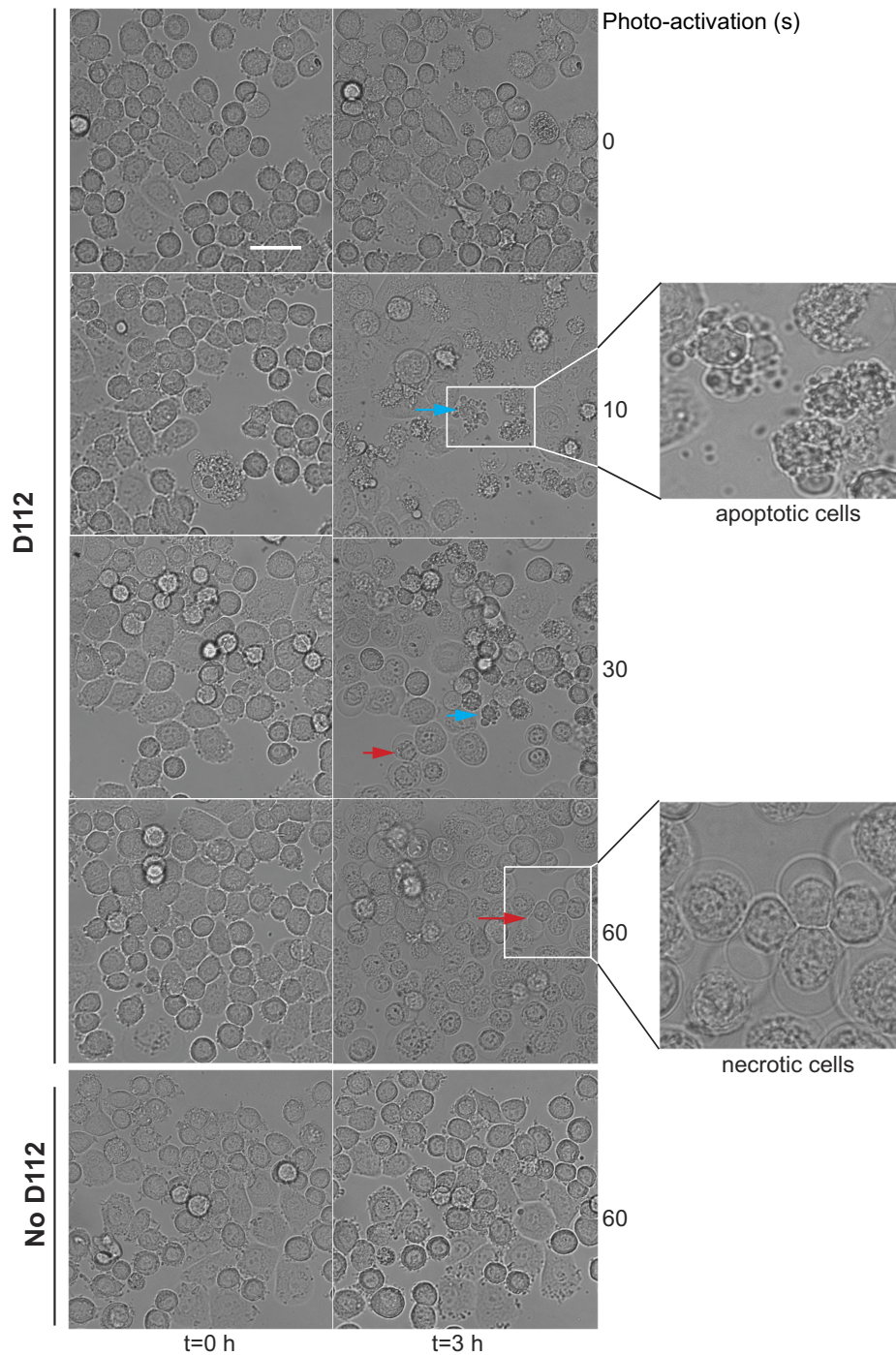


**Figure 4.9 Photo-activation of D112 causes various cell death morphologies in cancer cells.** SK-BR-3 cells were treated with 1  $\mu\text{g/ml}$  D112 for 1 h, washed, exposed to 541 nm light for indicated times, incubated for 3 h after which DIC images were acquired. Cell death by apoptosis (blue arrow) and necrosis (red arrow) was scored morphologically using bright field microscopy. Scale bars, 20  $\mu\text{m}$ .

initially incubated with D112 for 1 h, exposed to light for 10s, followed by morphological monitoring for 24h. Cells treated with light reached half-maximal cell death by 2 hours of D112 treatment, whereas non photo-activated cells required 24 h to reach similar levels of cell death (Fig. 4.10B), indicating that photo-activation enhanced D112 efficacy. Finally, I also examined the effect of D112 dosage on photo-activation properties. Cells were incubated in differing concentrations of D112, rinsed with fresh medium and then exposed to light for 10 sec. Dose response curves demonstrated that photo-activated D112 induced significant cell death at a concentration as low as 0.25  $\mu\text{g/ml}$  and 0.0625  $\mu\text{g/ml}$  in SK-BR-3 and MDA-MB-468 cells, respectively, whereas no cell death was observed at up to 1  $\mu\text{g/ml}$  of non-activated D112 (Fig. 4.10C). Clearly photo-activation greatly increased D112 activity as a cytotoxic agent.

To determine whether the photo-activation of D112 retained selectivity to cancer cell lines, I compared photo-activated D112-induced apoptosis between non-transformed and transformed cell lines. All cells were treated with D112 for 1 h and exposed to light for 10 sec and cell death morphology was observed for 24 h. Under these conditions, photo-activated D112 killed cancer cells while the non-transformed cell lines were spared. I quantified D112-induced apoptosis in the absence or presence of light exposure, and found that photo-activated D112 increased cell death 132-fold for SK-BR-3 and 220-fold for MDA-MB-468 cancer cell lines while

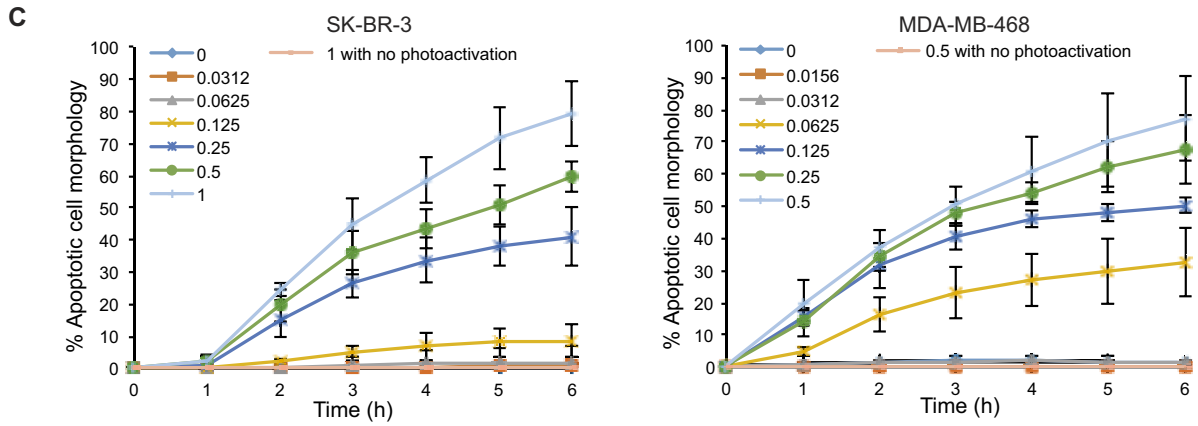
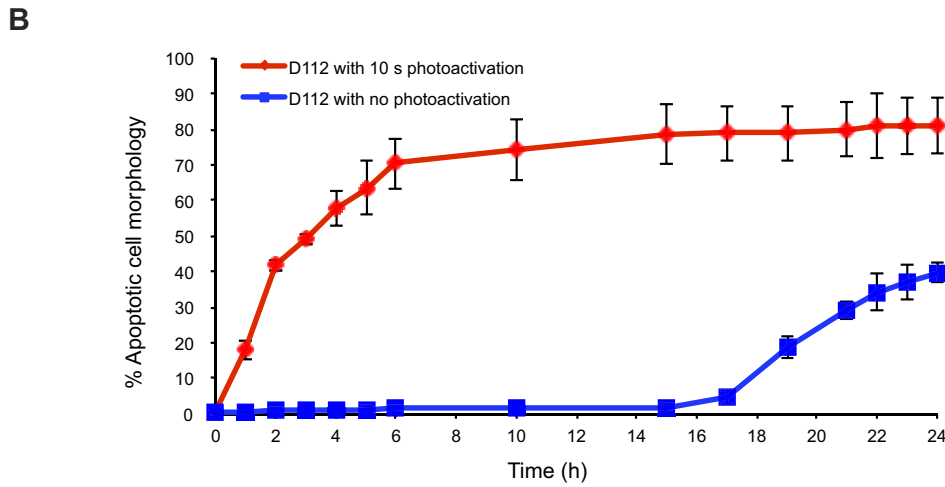
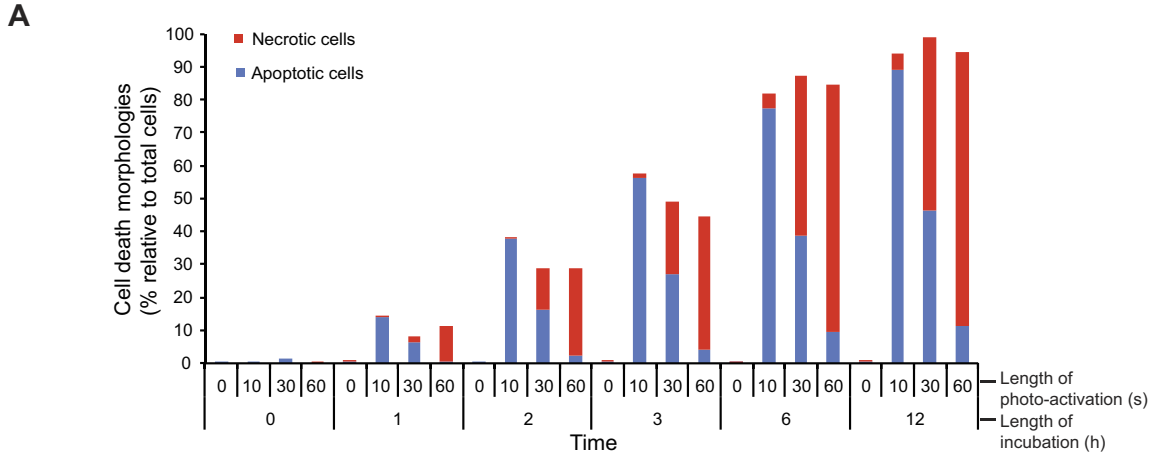


**Figure 4.10 D112 toxicity is enhanced after photo-activation.** **A.** Quantification of cell death after 541 nm light activation. Dead cells were counted based on morphology following D112 treatment and photo-activation as shown in Figure 4.9 at indicated times. **B.** Light exposure enhanced D112 cytotoxicity in cancer cells. Cells were treated with 1  $\mu\text{g/ml}$  D112 for 1 h, exposed to 541 nm light for 10 s, and then left in the D112 containing medium. Cell death was quantified as above at each indicated timepoint. **C.** Cell death occurred in a dose-dependent manner. Cells were treated with D112 at indicated concentrations for 1 h, washed, photo-activated for 10 s with 541 nm light, and then cell death quantified at the indicated timepoint. All values are mean  $\pm$  SD of three independent experiments.

non-transformed MCF-10A and hTERT-HME1 cells were only induced 9 and 5-fold, respectively (Fig. 4.11A and B). This data demonstrated that the photo-activation of D112 potentiates the selectivity of D112 against cancer cells.

Finally, I examined whether enhanced cytotoxicity was associated with ROS production. I observed elevated ROS upon photo-activation, indicating that enhanced cell death was associated with PDT-based ROS production (Fig. 4.12A). I further compared the intracellular level of ROS between the two cell types under PDT conditions (Fig. 4.12B). SK-BR-3 and MCF-10A cells were seeded in the same chamber and then incubated with D112 for 1 h, followed by 10 sec light exposure. SK-BR-3 cells (see red arrows) showed greater intensity of CellROX fluorescence than MCF-10A cells (see white arrows) in response to photo-activation. Thus, D112 selective toxicity was associated with ROS production in PDT. All together, the data indicate that photo-activation of D112 greatly increases its cytotoxic action and potentiates the selectivity of D112 against cancer cells.

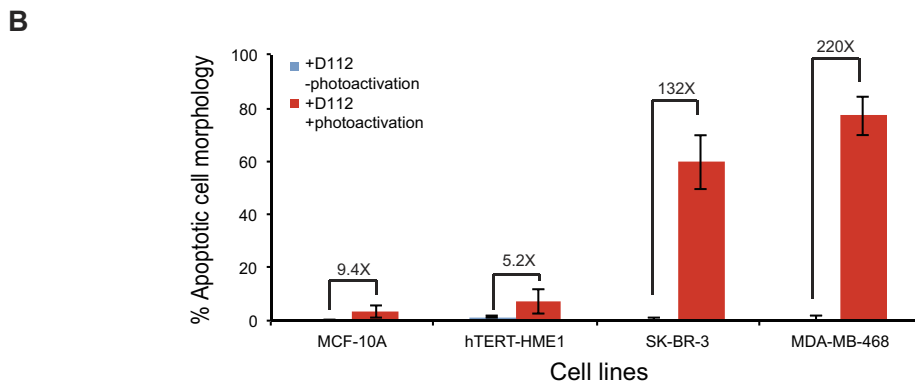
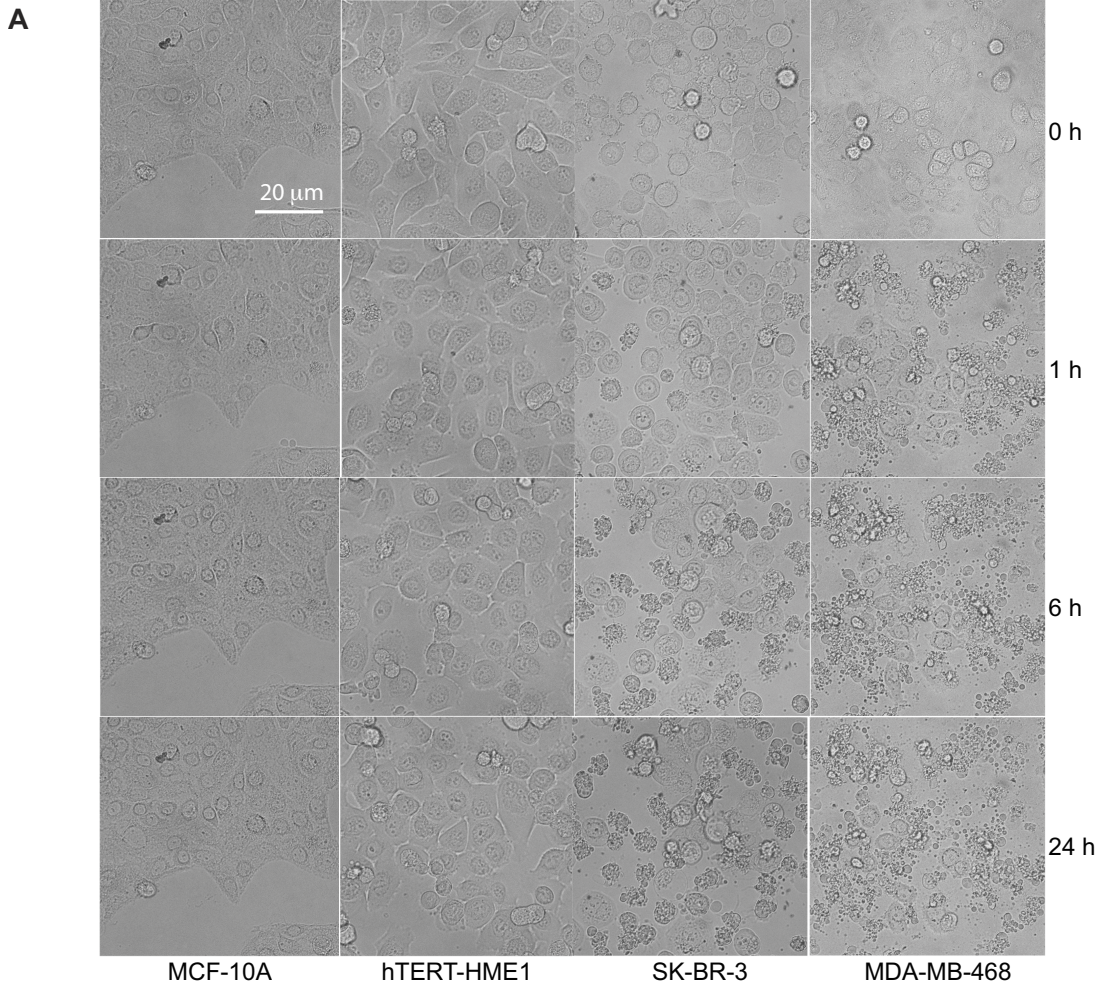


**Figure 4.11 D112 photo-activation is selectively toxic to cancer cells. A.** All cells were pre-treated with 0.5  $\mu$ g/ml D112 for 1 h and then D112 was photo-activated for 10 s using 541 nm light. Cell death was determined based on morphology using bright field microscopy. **B.** Quantification of cell death in multiple cell lines at the 6 h timepoint. Percentage of cell death was compared between non photo-activation and photo-activation treatments.

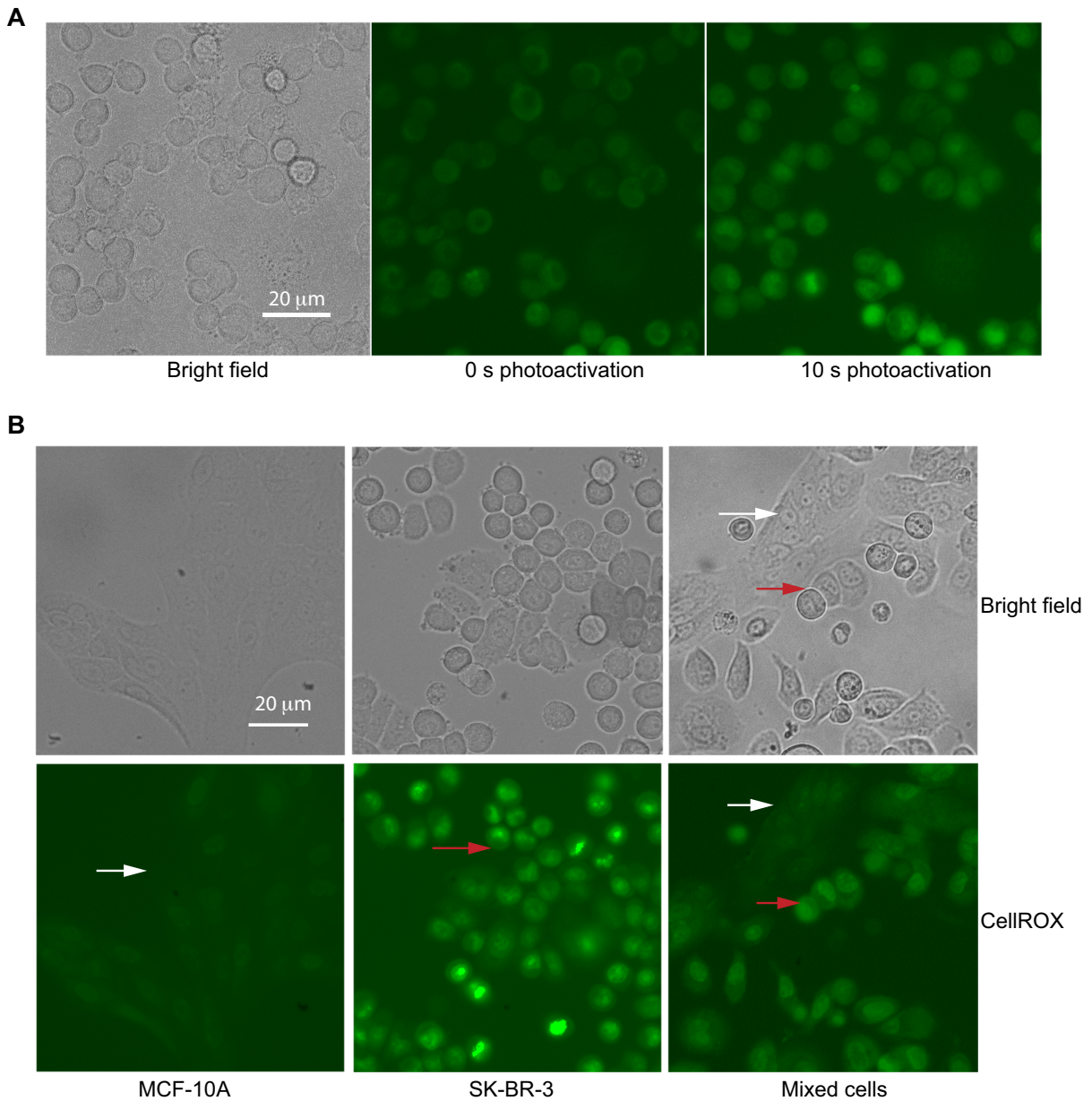


**Figure 4.12 Photo-activation increases ROS production in cancer cells. A.** Photo-activation increases ROS production in SK-BR-3 cells. Cells were pretreated with D112 for 1 h, and ROS generation was then detected in the presence or absence of photo-activation. Scale bars, 20 μm. **B.** ROS elevation in SK-BR-3 and MCF-10A cells after photo-activation. Individual cell line or mixed cell lines were treated with 0.5 μg/ml D112 for 1 h and D112 was photo-activated for 10 s using 541 nm light. ROS was examined by CellROX Green staining by fluorescence microscopy. Scale bars, 20 μm.

## 4.8 Discussion

Based on the properties of DLCs and the data presented in this study, we propose a model for D112-induced cytotoxicity, where D112 enters cells and localizes to mitochondria in a  $\Delta\psi$ -dependent manner. Cancer cells take up D112 more efficiently than non-transformed cell lines although the mechanism of this selectivity is unclear. Once in the mitochondria, D112 may bind mtDNA and/or inhibit multiple components of the ETC, leading to ROS production and mtDNA damage. Photo-activation potentiates the ability of D112 to produce ROS either by direct transfer of electrons to oxygen, or via ETC-mediated ROS generation. The resultant ROS is critical for downstream apoptosis and mediates the functional selectivity of D112.

Given the role of mitochondria in the generation of metabolic energy and regulation of apoptosis, DLCs, such as D112, are of interest as cancer therapeutics because of their role as anti-mitochondrial agents. DLCs have been shown to accumulate more efficiently in the mitochondria of cancer versus normal cells (Madak and Neamati, 2015; Modica-Napolitano and Aprille, 2001). For example, the differential uptake of Rhodamine 123 and MKT-077 is attributed to a 60 mV difference in  $\Delta\psi$  between carcinoma and normal mitochondria from the cells analyzed in those studies (Madak and Neamati, 2015; Modica-Napolitano and Aprille, 2001). While there was differential uptake for D112, we did not observe elevated electrochemical potential of carcinoma mitochondria versus normal mitochondria in our study, leaving the mechanism of selective D112 uptake unclear.

Once DLCs enter the mitochondria, they block ETC function through distinct

mechanisms (Modica-Napolitano and Aprille, 2001). The DLC compound, dequalinium chloride (DECA), binds to the ubiquinone and inhibitor binding pocket of complex I (Fendel et al., 2008), whereas MKT-077 inhibition of electron transfer involved complexes I-IV and is due to a more generalized disruption of membrane-bound ETC components (Modica-Napolitano et al., 1996). I speculate that D112, with its high negative reduction potential (-1.1V) (Gilman et al., 2006) might similarly occupy electron donor sites in the ETC. Yeast mutants that were individually deficient in specific subunits of complexes I-IV showed similar sensitivity to D112 as wild-type cells, indicating that D112 toxicity was not dependent on a single ETC complex. ETC inhibition produces ROS (Chen et al., 2003), and I observed that ROS levels were indeed elevated in cells exposed to D112. Increasing respiration and elevating ROS by culturing yeast cells in YPG medium sensitized cells to D112 toxicity, whereas down-regulation of ROS by growth in hypoxic conditions and analysis of rho<sup>0</sup> cells decreased sensitivity to D112. All together these results indicated that D112-induced ROS production was dependent on ETC and was necessary for D112-mediated cell death.

The resistance of rho<sup>0</sup> cells also suggested the involvement of mitochondrial DNA (mtDNA) in D112 cytotoxicity. MtDNA is more susceptible to chemical attack than the nuclear genome, including damage caused by ROS (Singh et al., 1999; Taanman, 1999). Several DLC agents, such as DECA (Schneider-Berlin et al., 2005) and MKT-077 (Singh et al., 1999) induce mtDNA damage in cells. We determined that D112 could also bind to DNA, induce mtDNA strand breaks and generate petite strains in yeast. Interestingly, the ROS scavenger NAC partially

rescued D112-mediated DNA damage, suggesting that a 'vicious cycle' occurred in D112 treated cells. Potentially, the production of ROS-induced mtDNA damage initially leads to progressive respiratory chain dysfunction and further increases ROS production. Additional studies are needed to clarify whether ROS-mediated mtDNA damage potentiates D112 cytotoxicity and/or whether loss of mtDNA leads to resistance to D112-cytotoxic effects.

D112 preferentially elevated ROS levels in transformed cells. Intracellular ROS dictates opposing cellular responses, depending on levels, with moderate increases promoting cell proliferation and differentiation, whereas excessive levels of ROS cause oxidative damage to lipids, proteins and DNA leading to cell death (Kimura et al., 2005). During respiration, a leak of electrons to oxygen, mostly from complex I and complex III, generates superoxide making mitochondria the major source of ROS (Murphy, 2009). Inhibitors that block electron transport elevate ROS (Liu et al., 2002) and this is a likely mechanism for D112 induced ROS. In support of this another DLC (FPB) that blocks ETC, also induces ROS (He et al., 2015). Compared to normal cells, cancer cells have increased levels of ROS due to their rapid proliferation rate (Kawanishi et al., 2006; Toyokuni et al., 1995), although we did not observe this trend in the cell lines in our study. Nevertheless cancer cells are documented to have a diminished capacity to deal with ROS, which sensitizes them to exogenous agents (Pelicano et al., 2004; Trachootham et al., 2009). In line with this, we observed that D112 treatment elevated ROS levels in transformed cells, which is a key component of D112-induced cell death, since NAC-treatment was

protective. This suggests that transformed cells may be limited in their capacity to buffer against bursts in ROS making them sensitive to ROS-inducers, such as D112.

I demonstrated in Chapter 3 that Bax was critical for D112 function (Yang et al., 2015). In response to apoptotic stimuli, Bax undergoes conformational changes, oligomerization, and insertion into the mitochondrial outer membrane to create pores that release death factors from the mitochondria (Goping et al., 1998). In further examining the molecular link between D112-induced ROS production and cell death, in this chapter, I show that D112-induced Bax activation was dependent on ROS. Previous studies have demonstrated that ROS or perturbation of the intracellular redox causes Bax translocation and oligomerization via distinct pathways (Hsieh and Papaconstantinou, 2006; Park et al., 2014). Moreover, ROS could also activate Bax by direct oxidation on Cys62 (Nie et al., 2008). Further investigation is needed to elucidate the mechanism(s) specifically involved in D112-induced Bax activation by ROS.

Finally, I found that D112-induced ROS production and cell killing was potentiated by photoactivation, indicating that D112 may have applications in PDT. PDT spares normal tissue by delivering non-toxic doses of a photosensitizer that is subsequently light-activated at targeted tumor sites (Dolmans et al., 2003). To date, several PDT drugs have been approved for oncological applications (Dolmans et al., 2003). Limitations of PDT include skin sensitivity and light source challenges and ongoing efforts are underway to identify new photosensitizers with more selective uptake by tumor cells and stronger absorption at longer wavelengths. Of particular interest are photosensitizers that localize to mitochondria promoting apoptosis, since

photosensitizers targeting the plasma membrane or lysosomes may block the apoptotic program (Buytaert et al., 2007). Thus, photo-activatable DLCs may be ideally suited for PDT. In particular, photo-activation of MKT-077 enhanced its ability to block electron-transport in mitochondria *in vitro* (Modica-Napolitano et al., 1998), and photo-activation of Rh-123-treated cells inhibited growth after injection as xenograft transplants in mice (Castro et al., 1989; Shea et al., 1989). Hence my study is not the first to demonstrated enhanced effects of photo-activation on DLCs. However, I believe that our report is the first to demonstrate that photo-activation potentiates DLC-cancer cell-selective killing. I propose that this is due to selective D112 uptake that leads to selective ROS production, which is amplified by photo-activation to trigger Bax-dependent apoptotic pathways. Thus D112 may be an ideal prototype for further evaluation in a PDT setting.

## Reference

- Britten, C.D., Rowinsky, E.K., Baker, S.D., Weiss, G.R., Smith, L., Stephenson, J., Rothenberg, M., Smetzer, L., Cramer, J., Collins, W., *et al.* (2000). A phase I and pharmacokinetic study of the mitochondrial-specific rhodacyanine dye analog MKT 077. *Clin Cancer Res* 6, 42-49.
- Buytaert, E., Dewaele, M., and Agostinis, P. (2007). Molecular effectors of multiple cell death pathways initiated by photodynamic therapy. *Biochim Biophys Acta* 1776, 86-107.
- Castro, D.J., Saxton, R.E., Fetterman, H.R., Castro, D.J., and Ward, P.H. (1988). Phototherapy with the argon laser on human melanoma cells "sensitized" with rhodamine-123: a new method for tumor growth inhibition. *Laryngoscope* 98, 369-376.
- Castro, D.J., Saxton, R.E., Rodgerson, D.O., Fu, Y.S., Bhuta, S.M., Fetterman, H.R., Castro, D.J., Tartell, P.B., and Ward, P.H. (1989). Rhodamine-123 as a new laser dye: in vivo study of dye effects on murine metabolism, histology and ultrastructure. *Laryngoscope* 99, 1057-1062.
- Chen, Q., Vazquez, E.J., Moghaddas, S., Hoppel, C.L., and Lesnefsky, E.J. (2003). Production of reactive oxygen species by mitochondria: central role of complex III. *J Biol Chem* 278, 36027-36031.
- de Grey, A.D. (2005). Reactive oxygen species production in the mitochondrial matrix: implications for the mechanism of mitochondrial mutation accumulation. *Rejuvenation Res* 8, 13-17.
- Dolmans, D.E., Fukumura, D., and Jain, R.K. (2003). Photodynamic therapy for cancer. *Nat Rev Cancer* 3, 380-387.
- Du, J., Daniels, D.H., Asbury, C., Venkataraman, S., Liu, J., Spitz, D.R., Oberley, L.W., and Cullen, J.J. (2006). Mitochondrial production of reactive oxygen species mediate dicumarol-induced cytotoxicity in cancer cells. *J Biol Chem* 281, 37416-37426.
- Fendel, U., Tocilescu, M.A., Kerscher, S., and Brandt, U. (2008). Exploring the inhibitor binding pocket of respiratory complex I. *Biochim Biophys Acta* 1777, 660-665.
- Gilman, P., Parton, R.L., and Lenhard, J.R. (2006). Correlation of anti-cancer activity of dyes with redox potential In Patent Application Publication (US: Eastman Kodak Company).

- Goping, I.S., Gross, A., Lavoie, J.N., Nguyen, M., Jemmerson, R., Roth, K., Korsmeyer, S.J., and Shore, G.C. (1998). Regulated targeting of BAX to mitochondria. *J Cell Biol* 143, 207-215.
- He, H., Li, D.W., Yang, L.Y., Fu, L., Zhu, X.J., Wong, W.K., Jiang, F.L., and Liu, Y. (2015). A novel bifunctional mitochondria-targeted anticancer agent with high selectivity for cancer cells. *Sci Rep* 5, 13543.
- Hsieh, C.C., and Papaconstantinou, J. (2006). Thioredoxin-ASK1 complex levels regulate ROS-mediated p38 MAPK pathway activity in livers of aged and long-lived Snell dwarf mice. *FASEB J* 20, 259-268.
- Ishikawa, K., Takenaga, K., Akimoto, M., Koshikawa, N., Yamaguchi, A., Imanishi, H., Nakada, K., Honma, Y., and Hayashi, J. (2008). ROS-generating mitochondrial DNA mutations can regulate tumor cell metastasis. *Science* 320, 661-664.
- Kawanishi, S., Hiraku, Y., Pinlaor, S., and Ma, N. (2006). Oxidative and nitrative DNA damage in animals and patients with inflammatory diseases in relation to inflammation-related carcinogenesis. *Biol Chem* 387, 365-372.
- Kimura, H., Sawada, T., Oshima, S., Kozawa, K., Ishioka, T., and Kato, M. (2005). Toxicity and roles of reactive oxygen species. *Curr Drug Targets Inflamm Allergy* 4, 489-495.
- Lakowicz, J.R. (2006). *Principles of Fluorescence Spectroscopy*, Third Edition (Springer ).
- Lampidis, T.J., Bernal, S.D., Summerhayes, I.C., and Chen, L.B. (1983). Selective toxicity of rhodamine 123 in carcinoma cells in vitro. *Cancer Res* 43, 716-720.
- Liu, Y., Fiskum, G., and Schubert, D. (2002). Generation of reactive oxygen species by the mitochondrial electron transport chain. *J Neurochem* 80, 780-787.
- Madak, J.T., and Neamati, N. (2015). Membrane permeable lipophilic cations as mitochondrial directing groups. *Curr Top Med Chem* 15, 745-766.
- Modica-Napolitano, J.S., and Aprille, J.R. (1987). Basis for the selective cytotoxicity of rhodamine 123. *Cancer Res* 47, 4361-4365.
- Modica-Napolitano, J.S., and Aprille, J.R. (2001). Delocalized lipophilic cations selectively target the mitochondria of carcinoma cells. *Adv Drug Deliv Rev* 49, 63-70.
- Modica-Napolitano, J.S., Brunelli, B.T., Koya, K., and Chen, L.B. (1998). Photoactivation enhances the mitochondrial toxicity of the cationic rhodacyanine MKT-077. *Cancer Res* 58, 71-75.

Modica-Napolitano, J.S., Koya, K., Weisberg, E., Brunelli, B.T., Li, Y., and Chen, L.B. (1996). Selective damage to carcinoma mitochondria by the rhodacyanine MKT-077. *Cancer Res* 56, 544-550.

Murphy, M.P. (2009). How mitochondria produce reactive oxygen species. *Biochem J* 417, 1-13.

Nie, C., Tian, C., Zhao, L., Petit, P.X., Mehrpour, M., and Chen, Q. (2008). Cysteine 62 of Bax is critical for its conformational activation and its proapoptotic activity in response to H<sub>2</sub>O<sub>2</sub>-induced apoptosis. *J Biol Chem* 283, 15359-15369.

Olmsted, J., and R.Kearns, D. (1977). Mechanism of Ethidium Bromide Fluorescence Enhancement on Binding to Nucleic Acids. *Biochemistry* 16, 8.

Park, G.B., Choi, Y., Kim, Y.S., Lee, H.K., Kim, D., and Hur, D.Y. (2014). ROS-mediated JNK/p38-MAPK activation regulates Bax translocation in Sorafenib-induced apoptosis of EBV-transformed B cells. *Int J Oncol* 44, 977-985.

Pelicano, H., Carney, D., and Huang, P. (2004). ROS stress in cancer cells and therapeutic implications. *Drug Resist Updat* 7, 97-110.

Quinlan, C.L., Pervoshchikova, I.V., Hey-Mogensen, M., Orr, A.L., and Brand, M.D. (2013). Sites of reactive oxygen species generation by mitochondria oxidizing different substrates. *Redox Biol* 1, 304-312.

Sabharwal, S.S., and Schumacker, P.T. (2014). Mitochondrial ROS in cancer: initiators, amplifiers or an Achilles' heel? *Nat Rev Cancer* 14, 709-721.

Schneider-Berlin, K.R., Bonilla, T.D., and Rowe, T.C. (2005). Induction of petite mutants in yeast *Saccharomyces cerevisiae* by the anticancer drug dequalinium. *Mutat Res* 572, 84-97.

Shea, C.R., Chen, N., Wimberly, J., and Hasan, T. (1989). Rhodamine Dyes as Potential Agents for Photochemotherapy of Cancer in Human Bladder Carcinoma Cells. *Cancer Research* 49, 5.

Singh, K.K., Russell, J., Sigala, B., Zhang, Y., Williams, J., and Keshav, K.F. (1999). Mitochondrial DNA determines the cellular response to cancer therapeutic agents. *Oncogene* 18, 6641-6646.

Snyder, J.W., Greco, W.R., Bellnier, D.A., Vaughan, L., and Henderson, B.W. (2003). Photodynamic therapy: a means to enhanced drug delivery to tumors. *Cancer Res* 63, 8126-8131.

Taanman, J.W. (1999). The mitochondrial genome: structure, transcription, translation and replication. *Biochim Biophys Acta* 1410, 103-123.

Toyokuni, S., Okamoto, K., Yodoi, J., and Hiai, H. (1995). Persistent oxidative stress in cancer. *FEBS Lett* 358, 1-3.

Trachootham, D., Alexandre, J., and Huang, P. (2009). Targeting cancer cells by ROS-mediated mechanisms: a radical therapeutic approach? *Nat Rev Drug Discov* 8, 579-591.

Upton, J.P., Valentijn, A.J., Zhang, L., and Gilmore, A.P. (2007). The N-terminal conformation of Bax regulates cell commitment to apoptosis. *Cell Death Differ* 14, 932-942.

Vrouenraets, M.B., Visser, G.W., Snow, G.B., and van Dongen, G.A. (2003). Basic principles, applications in oncology and improved selectivity of photodynamic therapy. *Anticancer Res* 23, 505-522.

Weiss, M.J., Wong, J.R., Ha, C.S., Bleday, R., Salem, R.R., Steele, G.D., Jr., and Chen, L.B. (1987). Dequalinium, a topical antimicrobial agent, displays anticarcinoma activity based on selective mitochondrial accumulation. *Proc Natl Acad Sci U S A* 84, 5444-5448.

Yang, N., Gilman, P., Mirzayans, R., Sun, X., Touret, N., Weinfeld, M., and Goping, I.S. (2015). Characterization of the apoptotic response induced by the cyanine dye D112: a potentially selective anti-cancer compound. *PLoS One* 10, e0125381.

## CHAPTER 5 DISCUSSION

## **5.1 Introduction**

Prior to my thesis studies, D112 had been proposed as a potential anti-cancer drug based on its reduction potential and higher toxicity towards a human cancer colon cell line versus a non-transformed monkey kidney cell line. These observations were not sufficient to claim that D112 had potential for further anti-cancer drug development. Specifically, the claim that D112 was selective against cancer cells had not been rigorously tested. Whether this selectivity was applicable across multiple cancer cell lines versus appropriate non-transformed counterparts needed to be determined. Further, the mechanism of D112-induced cell death was unclear. It was not known whether D112 induced non-specific cell death, cell proliferation arrest or apoptosis. Finally, strategies to enhance D112-targeted killing of cancer cells had not been done. Therefore, in this thesis, I addressed these questions and determined that D112 properties, mechanism of cell death and strategies to enhance cancer cell apoptosis revealed a potential for D112 as a compound suitable for further testing along the drug development pipeline.

## **5.2 D112 properties**

The supportive properties of D112 as a potential anticancer drug are summarized as follows: (i) D112 is lipophilic and positively charged. As proposed in other DLCs studies, both of these properties likely facilitate D112's selective accumulation in carcinoma mitochondria, in response to a higher, negative mitochondrial membrane potential (Modica-Napolitano and Aprille, 2001; Modica-Napolitano and Weissig, 2015). (ii) D112 possesses a large negative (-1.1 V)

reduction potential. Zigman and Gilman (Zigman and Gilman, 1980) were the first to observe that the reduction potential of a cyanine dye was related to its ability to inhibit cell growth. Dyes with reduction potentials that were more negative than -1.0 V were able to penetrate cells and cause cell growth inhibition (Zigman and Gilman, 1980). (iii) D112 is a fluorescent compound. D112's fluorescent spectra distinguishes it from some other chemotherapeutic compounds, allowing traceability in biological systems and potential for photo-activation (Fig. 5.1). The drawbacks for D112 potential drug development are as follows: as mentioned earlier, D112 is hydrophobic, and is poorly soluble in aqueous environments. Additionally, its relatively large molecular weight is not a favorable drug property. Thus structure-activity-relationship (SAR) approaches to generate chemical variants of smaller size and increased solubility could be considered.

### **5.3 The mechanisms of D112-induced cytotoxicity**

Based on the data in Chapter 3 and 4, we propose a model for D112-induced cytotoxicity (Fig.5.2) in which D112 enters cells and localizes to mitochondria in a  $\Delta\psi$ -dependent manner. Interestingly, although the mechanism is unclear, I found that cancer cells take up D112 more efficiently than non-transformed cells, at least in the cell lines used in my study. Once inside the mitochondria, D112 binds to mtDNA and likely inhibits multiple components of the ETC, leading to ROS production and mtDNA damage. The resultant ROS is required for Bax activation (Fig. 5.2A). Given

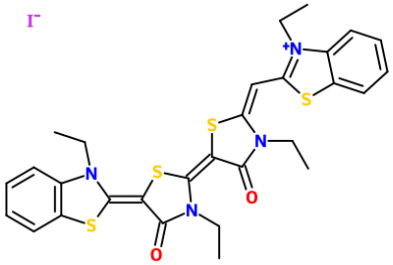
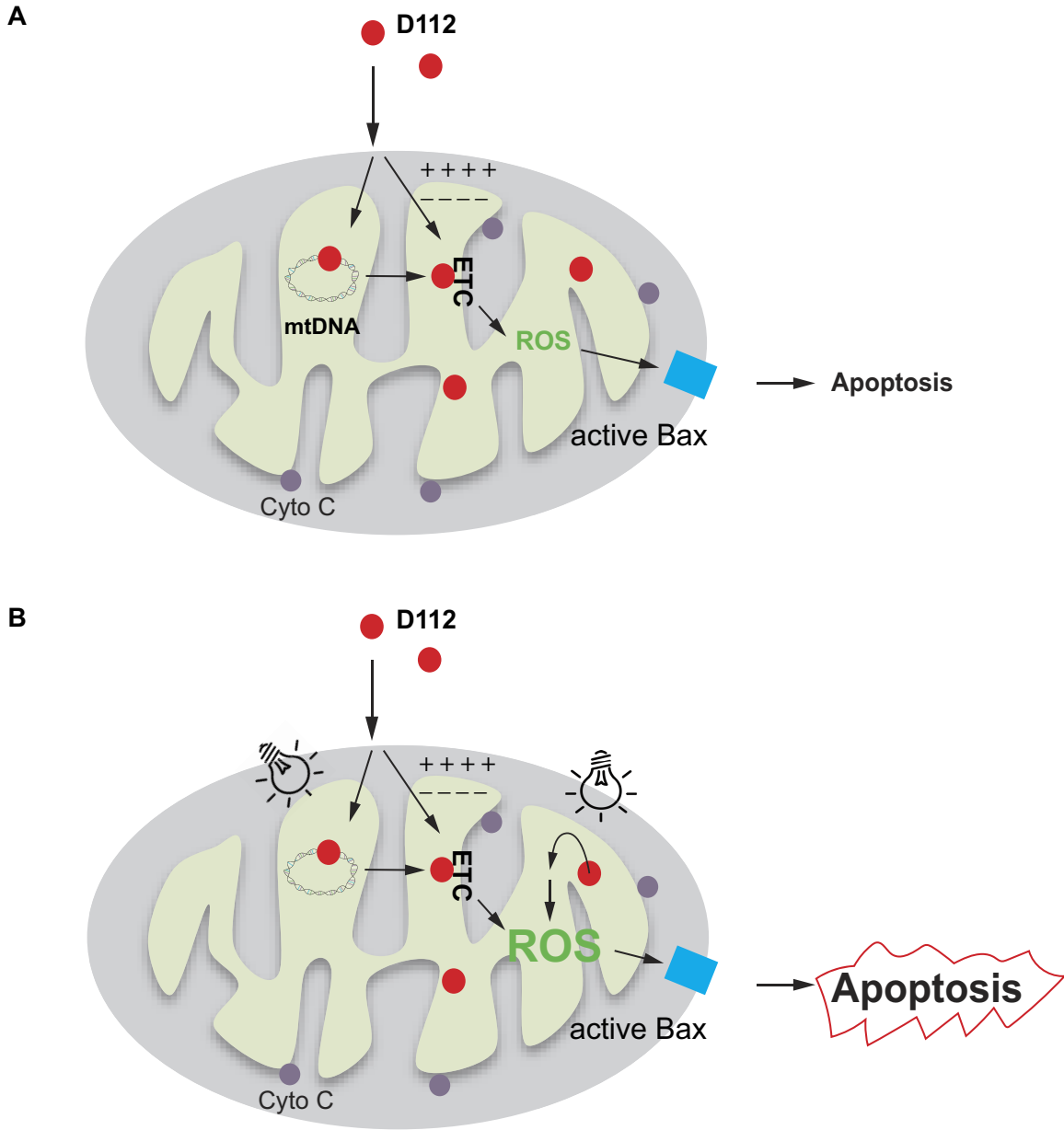
	<b>Name</b>	D112
	<b>Company</b>	Eastman Kodak
	<b>Molecular formula</b>	C <sub>29</sub> H <sub>29</sub> N <sub>4</sub> S <sub>4</sub> O <sub>2</sub> I
	<b>Molecular weight</b>	720.7
	<b>Color</b>	Purple
	<b>Ex/Em</b>	515/620 nm
	<b>Reduction potential</b>	-1.1 V
	<b>Charge</b>	Positive
	<b>IC50</b>	0.5~4 μg/ml (0.7~5.6 μM)

Figure 5.1 Physical properties of D112.

that Bax/Bak deficient cells are resistant to D112-induced cell death, ROS plays a critical role in Bax activation and D112-induced apoptotic cell death. Moreover, cancer cells produce more ROS than non-transformed cells after D112 treatment, leading us to speculate that ROS mediates the functional selectivity of D112. This cancer-selective burst in ROS production is likely a combination of initial selective uptake of D112 in cancer cell lines in addition to a diminished ability of cancer cells to eliminate ROS. Furthermore, Bcl-2 overexpression strongly diminishes D112-induced cell death; necrosis and extrinsic apoptotic pathways are therefore not involved in D112-mediated apoptosis. I determined that, the IC 50 of D112 to cancer cells is  $\sim 0.5\text{-}4\ \mu\text{g/ml}$  ( $0.7\text{-}5.6\ \mu\text{M}$ ). The IC 50 in normal cells is greater than this by approximately 2 to 3-fold, but not clearly identified, as the amounts of D112 needed to induce maximal cell death in non-transformed cells was unachievable due to the low solubility of D112. Intriguingly, this 2 to 3-fold difference was greatly enhanced by photo-activation to an 8.3 to 22.5-fold difference using  $0.5\ \mu\text{g/ml}$  of D112. I propose that in a PDT setting, photo-activation potentiates D112-induced ROS accumulation, either by direct transfer of electrons to oxygen, or via ETC-inhibition leading to ROS generation (Fig. 5.2B). As a result, boosted ROS generation kills cancer cells more effectively. In summary, my study determined that D112 selectively kills cancer cells by enhancing mitochondrial-generated ROS, and demonstrated D112's potential application as a photosensitizer in a PDT setting.



**Figure 5.2 Proposed model of D112-induced mitochondrial dysfunction. A.** In response to mitochondrial electrochemical potential, positively-charged D112 accumulates in mitochondria and binds mtDNA. D112 damages mtDNA and inhibits the ETC, generating ROS. ROS targets BAX, leading to mitochondrial outer membrane permeabilization that triggers downstream apoptosis. **B.** In response to photo-activation, D112 generates increased ROS as a result of direct ROS production, enhanced mtDNA damage and enhanced inhibition of the ETC.

## 5.4 D112 in chemotherapy

### 5.4.1 Application of DLCs

DLC applications in oncology have been investigated for more than 20 years (Modica-Napolitano and Aprille, 2001). Although no DLCs have yet been approved for clinical use, this group of compounds is of interest for drug development due to their targeting of cancer mitochondria. Previous studies have demonstrated DLCs' potential in oncologic applications (Bernal et al., 1983; Davis et al., 1985; Modica-Napolitano and Aprille, 1987; Modica-Napolitano et al., 1996; Tikoo et al., 2000), and insights into their mechanisms suggest use in other fields as well (Baracca et al., 2003; Wadhwa et al., 2000).

One promising application of DLCs in cancer treatment lies in their potential as chemotherapeutic drugs. As discussed in chapter 1, favorable properties of DLCs, such as mitochondrial-targeting and selective toxicity to cancer cells, have fueled investigations into this specific group of compounds. The two most well studied examples are DLCs MKT-077 (Chiba et al., 1998; Koya et al., 1996; Modica-Napolitano et al., 1996) and Rh-123 (Bernal et al., 1983; Davis et al., 1985). Based on evidence of selective toxicity to cancer cells in both cell culture and animal models, both MKT-077 and Rh-123 were approved for evaluations in phase I clinical trials. In the study of MKT-077, two independent clinical trials were conducted in small-scale settings with less than 15 patients. In one clinical trial conducted in 1999, ten patients with advanced, chemo-resistant solid cancers, including kidney (3), prostate (1), lung (1), melanoma (1) and colon cancer (3), were treated with three dose levels (30, 40 and 50 mg/m<sup>2</sup>) of MKT-077 daily for 5 days by infusion (Propper

et al., 1999) and each treatment cycle took 21 days. The results were disappointing, with only one renal cancer patient attaining disease stability, and the majority of patients showing little or no response. In tolerability assessment, recurrent renal toxicity was of primary concern. However, during the trial period, the toxicity level was considered manageable and reversible. Because irreversible renal toxicity was observed in animal models, further recruitment to clinical trials was discontinued. In 2000, another independent clinical trial was conducted in 13 patients with advanced solid malignancies refractory to standard therapy, including colon cancer, melanoma cancer, renal cancer, thymoma and unknown primary adenocarcinoma (Britten et al., 2000). In this trial, MKT-077 was administered to patients weekly for 4 weeks every 6 weeks at doses ranging from 42 to 126 mg/m<sup>2</sup>. Consistently, the principle toxicity was found to be renal magnesium wasting, although this nephrotoxicity could be managed by administering magnesium supplementation. Two out of 4 patients treated with 126 mg/m<sup>2</sup> MKT-077 showed progressive disease during treatment, however, the overall efficiency of MKT-077 on disease progression was not fully addressed in the report. It is noteworthy that beyond the temporary adverse effects, both studies confirmed the preferential accumulation of MKT-077 in tumor sites, providing proof of the specific localization of this class of compounds. MKT-077 currently serves as a prototype for the synthesis of new yet related compounds with enhanced cytotoxicity.

In contrast to MKT-077 studies, wherein patients with different types of advanced diseases were enrolled in clinical trials, the phase I clinical trial of Rh-123 was performed specifically on patients with hormone refractory prostate cancer

(Jones et al., 2005). Rh-123 was administered to patients at a single dose, ranging from 12 to 134 mg/m<sup>2</sup>. The study found the maximum tolerated dose was 96 mg/m<sup>2</sup> and noted that transient and variable toxicities occurred following Rh-123 administration—hypertension being the most severe one—but only in 2/10 patients. The adverse effects were overall minimal and manageable. Promisingly, the study found that the doubling time of prostate specific antigen (PSA), an acceptable clinical biomarker for prostate cancer, was increased in 8/10 patients after Rh-123 treatment. Although the results were not statistically significant with a P value of 0.055, they did suggest a favorable trend. Furthermore, Rh-123 was also selectively persistent in prostatic tumor tissue. To my knowledge, follow-up clinical trials of Rh 123 have not been conducted due to a lack of positive data.

Taken together, clinical studies on MKT-077 and Rh-123 validated their tumor-targeting properties. Significant efficacies were not fully achieved, indicating that DLCs show potential as anticancer agents although toxicities were a major barrier. Thus, strategies to increase drug effectiveness with lower doses or combination may make DLCs more attractive for development, in the future.

Another beneficial use of DLCs in oncology is as mitochondrial-directing groups (Madak and Neamati, 2015). It is believed that mitochondrial membrane potential can supply the force to deliver DLC-linked chemotherapeutic drugs into cancer cells. The first attempt to conjugate DLCs with a therapeutic drug took place in the 1980s. In the study, Rh-123 was conjugated with a platinum (II) tetrachlorodianion. Platinum compounds are known for their anticancer activity (Ali et al., 2013). Fluorescence was then measured to examine the delivery efficiency.

Conjugation with Rh-123 increased the amount of intracellular platinum ~70-fold more than platinum alone. However, the DLC-platinum complex was not selectively taken up by tumor cells due to the loss of the positive charge, which compromised its tumor selectivity (Teicher et al., 1986). Whether a modified complex that retains the cationic properties of the complex has been tested, is unknown at this time. However, in a more recent development, conjugations with the DLC triphenylphosphonium (TPP) have shown promising results. TPP conjugation maintains its positive charge and the small molecular weight of TPP (<300) suggests that TPP can be attached to a variety of drugs (Madak and Neamati, 2015). As described in Chapter 1, TPP successfully directed antioxidant and oxidant compounds into mitochondria in tumor sites and enhanced their activity (Madak and Neamati, 2015; Smith et al., 2003). In addition to chemical conjugations, some DLCs form liposome-like structures that facilitate drug delivery. One example is dequalinium, which forms liposome-like structures called DQAsomes (Vaidya and Vyas, 2012; Weissig et al., 1998). Since they were first described in the 1990s, DQAsomes have been successfully used to deliver small compounds, such as paclitaxel, to tumor sites. Studies have shown the selective tumor cell killing activity of paclitaxel in mouse xenograft models was enhanced after being loaded with DQAsomes (Li et al., 2014; Vaidya and Vyas, 2012; Weissig, 2015). Nowadays, DQAsomes are considered one of the prototypes for mitochondria-targeted vesicular systems (Weissig, 2015). Thus, in addition to inhibiting cancer mitochondria directly, some DLCs are being developed as drug delivery agents to facilitate the intracellular uptake of other widely-used anti-cancer compounds.

Alternatively, mechanistic studies of DLCs have extended their application to fields outside of oncology. Rh 123, as mentioned in chapter 1, has been commercially used as a probe to assay mitochondrial membrane potential in apoptotic cells (Baracca et al., 2003). MKT-077 has been shown to inhibit Hsp70 and thus is being investigated for therapeutic purposes in this regard. Hsp70 is a molecular chaperone that normally assists in the folding of newly synthesized proteins and the degradation of unfolded proteins (Chiang et al., 1989; Mayer and Bukau, 2005). Under stress conditions, Hsp70 binds to its protein substrates and stabilizes them against denaturation or aggregation until the stress is ameliorated. Hsp70 is involved in several central nervous system (CNS) disorders, for instance, Alzheimer's disease (AD) (Burbulla et al., 2010; Yang et al., 2011). Hsp70 inhibition by MKT-077 led to a rapid increase in ubiquitination and degradation of the AD related protein—tau (Rousaki et al., 2011). As the positive charge in MKT-077 is not necessary for its Hsp70-binding, and usually makes the compound more toxic to the kidney than neutral compounds (Vegt et al., 2010), the study suggested that a conversion of MKT-077 into a neutralized compound might take MKT-077 out of contention as an anticancer drug but allow it to be used in the treatment of CNS disorders such as AD. Currently efforts are underway to develop nanoparticles to help MKT-077 overcome the blood-brain barrier, and therefore make MKT-077 more suitable for treatment of AD and other tauopathies (Umesh et al., 2014).

Due to their structural heterogeneities, the molecular targets and biological effects of DLCs vary. In some cases, alternative applications in addition to cancer treatment are more successful, especially when anticancer efficiency is limited. Rh-

123 and MKT-077 are two such representative examples. Of note, the cancer mitochondrial-targeting property of DLCs retain them as promising candidates in cancer therapy. Accordingly, DLCs, such as MKT-077, currently serve as prototypes for further structure-activity relationship (SAR) studies (Li et al., 2015; Li et al., 2013).

#### 5.4.2. D112 as a chemotherapeutic compound

Our study provided evidence supporting the potential of D112 as a chemotherapeutic drug candidate: (i) D112 selectively killed cells derived from both solid tumors and hematological malignancies, suggesting applicability in the treatment of a variety of cancer types. Though the mechanism of its selectivity is not yet clear, the preferential accumulation of D112 in cancer cells, at least in part, contributes to D112 selectivity. (ii) The mitochondrial apoptotic pathway is triggered by D112 and *in vitro*, is blocked by Bcl-2 and loss of Bax/Bak. This result suggests that D112 may have minimal off-target inflammatory-related side effects; (iii) ROS plays an essential role in D112-induced cell death. This likely contributes an additional layer to D112-selectivity as dysfunctional redox balance in cancer cells renders them more vulnerable to additional ROS insults (Trachootham et al., 2009); (iv) Similar to other DLCs, D112's inherent fluorescence facilitated evaluation of intracellular localization and uptake. In future *in vivo* studies, D112 biodistribution, accumulation and metabolism may be easily traced and evaluated by measuring D112 fluorescence. Thus, our data to date, support D112's potential as an anticancer compound, warranting further investigation.

Our current study was conducted on cell lines, and the next logical experiments to test the therapeutic potential of D112 are *in vivo* efficacy and toxicity assays. Although we cannot precisely predict *in vivo* toxicity and efficacy from our *in vitro* studies, given that D112 shares 82% structural similarity with the well-studied MKT-077 (determined by the online program ChemSpider), we can speculate on D112's *in vivo* properties. MKT-077 was tested in mouse pre-clinical models and human phase I clinical trials, both of which revealed renal toxicity (Britten et al., 2000). With the aim of improving therapeutic functionality, Li et al (Li et al., 2013) performed SAR studies of MKT-077 and synthesized a second generation of MKT-077 analogues (Figure 5.3). While the target-binding property remained unaffected, MKT-077 structural variants with a hydrophobic group (such as a benzyl group) added to the R3 position showed 2-fold elevated cytotoxicity to cancer cells. Further modification of R2 and R3 by adding an ethyl and benzyl group respectively, exemplified by the compound JG 98, showed enhanced anticancer activity by 10-20 fold (Li et al., 2013; Rousaki et al., 2011). Interestingly, these newer MKT-077 analogues are more structurally similar to D112 than MKT-077 itself, implying that D112 might already display higher efficiency and accordingly less toxicity, than MKT-077 in *in vivo* applications. In any case, the examination of D112's activity in animal models is a necessary step for future studies.

With regards to testing the *in vivo* efficacy of D112, research on Rh-123 and MKT-077 demonstrated the importance of choosing a proper tumor model (Britten et al., 2000; Jones et al., 2005; Propper et al., 1999) For instance, Rh-123 exhibited anticancer activity in mice bearing Ehrlich ascites tumors or bladder carcinoma, but it

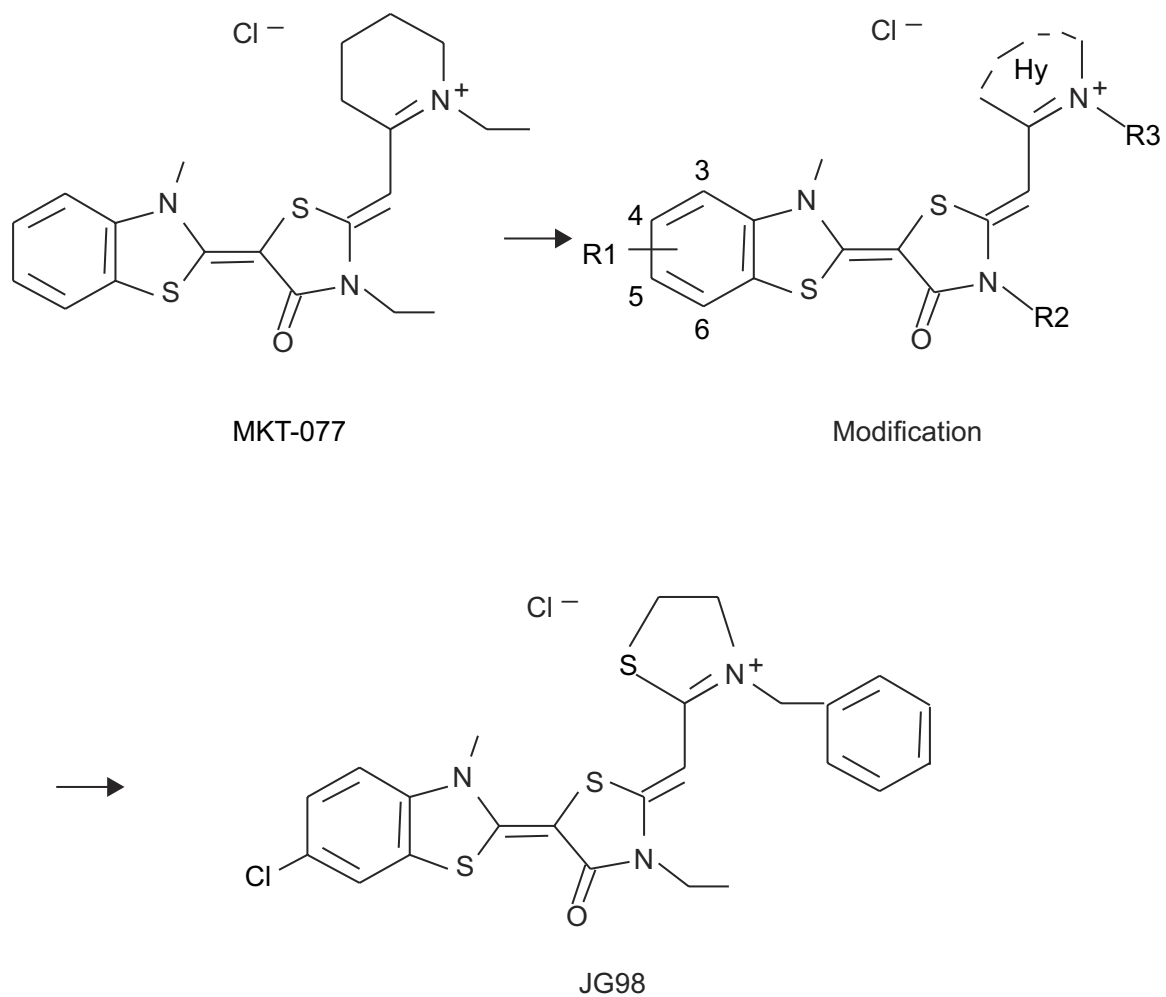


**Figure 5.3 Structures of MKT-077 and JG98.** Analogues of MKT-077 were synthesized with chemical modifications on R1, R2 and R3 position. JG98 is shown as a representative example.

failed to prolong survival of mice implanted with leukemia, melanoma or lung carcinoma (Bernal et al., 1983). This difference may have been due to the capacities of these cell lines to retain Rh-123 in mitochondria. Similar results were observed in MKT-077 studies, where not all carcinoma cell lines (3 out of 5) tested *in vivo* were sensitive to MKT-077 (Starenki and Park, 2015). Even though our studies utilized breast cancer, T-cell lymphoma and melanoma cell lines, a large-scale cancer cell screen, such as the NCI-60 cell screen, would be informative to target the appropriate cancer types. By measuring the IC<sub>50</sub> of D112 to a large panel of cancer cell lines, one would be able to determine which cancer types are more sensitive to D112, and would be used for further *in vivo* studies.

In addition, the structural similarity between D112 and MKT-077 suggests that: (i) Hsp70, especially mitochondrial HSP70, is a possible target of D112. It has been shown that the nonpyridinium moieties of the MKT-077 (benzothiazole ring and thiazolyl ring) are buried in the HSP70 pocket (Fig. 5.4). This structural region is shared by D112, suggesting that D112 can also bind to HSP70. The D112-HSP70 binding could be evaluated *in silico* using computer software, such as AUTODOCK. Functional assays, such as loss-of-function siRNA-mediated knock-down studies of Hsp70 in a cell line model would evaluate the contribution of HSP70 to D112-induced apoptosis. Clearly, the application of D112 as an HSP70 inhibitor warrants future investigation. (ii) On the negative side, D112 might cause renal toxicity *in vivo*, as renal toxicity was reported in MKT-077 clinical trials. In addition, due to its mitochondrial-targeting property, D112 might cause adverse effects on mitochondrial function in skeletal muscle. The postulation of possible toxicities would help us

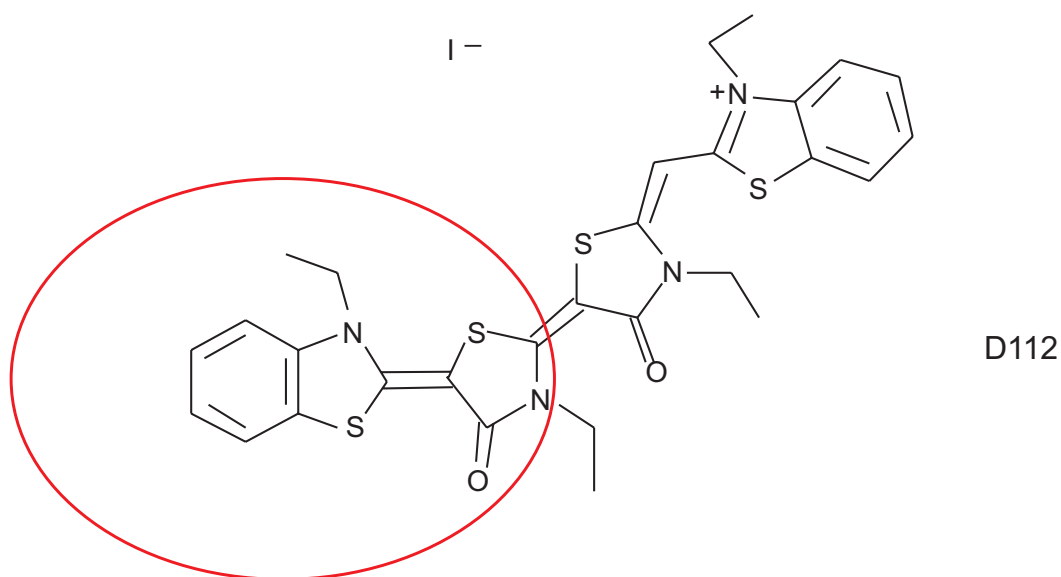
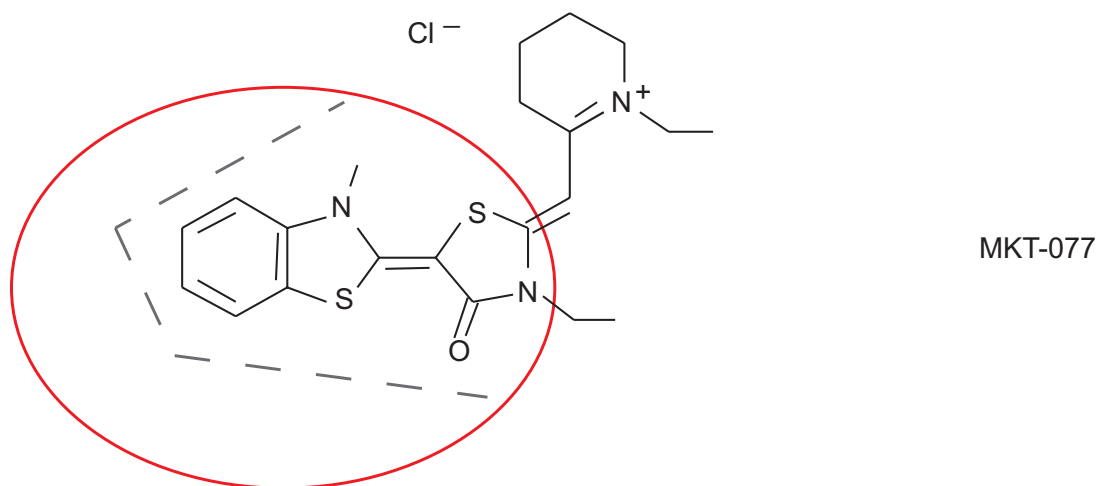


**Figure 5.4 Structures of MKT-077 and D112.** (Upper) The benzothiazole ring and thiazolone ring of MKT-077 are shown (red circle). These moieties have been shown to bind within the HSP70 pocket (Indicated by dashed line). (Lower) A similar structure is shared with D112 (red circle).

design a reasonable protocol for animal studies. For example, as reported from MKT-077 clinical studies (Britten et al., 2000), to prevent and manage renal toxicity, magnesium supplementation could be administered to animals before or after drug injection.

As toxicity is usually a result of off-target effects due to high dosage, a strategy to prevent side effects would be to collaborate with chemists to develop and modify D112 in order to generate more efficient drugs. Alternatively, therapeutic benefits could be achieved through drug combination. As a matter of fact, DLCs have long been evaluated in drug combination. For example, Rh-123 pretreatment dramatically reduced the dosage of docetaxel required to achieve half-maximal growth inhibition in prostate and breast cancer cell lines (Riggins et al., 2007). An understanding of D112-induced cell death suggests that combining D112 with other chemotherapeutic compounds might have synergistic effects as well. For example, Bcl-2 reduced D112-induced apoptosis; thus, Bcl-2 inhibitors such as the BH3-only protein mimetic ABT-199 (Souers et al., 2013) would be expected to enhance D112 toxicity by neutralizing Bcl-2 activity in cancer cells. In addition, when yeast cells were inhibited from fermentative metabolism by culturing in YPG media, cells became more sensitive to D112-induced cell death. This observation suggests that the glycolysis inhibitor 2-deoxyglucose (2-DG) (Pelicano et al., 2006) might be an appropriate adjunct for D112 combination therapy. In support of this, it has been shown that the anticancer activity of Rh-123 was potentiated by 2-deoxyglucose in several animal models (Bernal et al., 1983). Alternatively, considering the involvement of mtDNA in D112-induced cell death, inhibitors that interfere with

mtDNA repair machinery (Kazak et al., 2012) might enhance D112 toxicity. All together, these studies indicate that combination cocktails containing D112 may be strategies to increase *in vivo* efficacy and decrease toxicity.

## **5.5 D112 potential in photodynamic therapy**

### 5.5.1 Photodynamic therapy in oncology

The first experimental study of PDT was carried out in 1903 (Dolmans et al., 2003), and although the therapeutic application of PDT was slow to develop, recently increasing PDT applications are being adopted for clinical use. Compared to chemotherapy, this drug-device combination shows an extraordinarily high response ratio in cancer treatment. For example, photofrin-based PDT is currently being used to successfully treat patients with different cancer types (Brown et al., 2004). Photofrin, also known as Porfimer sodium, was the first photosensitizer to be approved for cancer treatment. In its early clinical trial, it was reported that 12 out of 13 patients with non-small cell lung cancer attained a complete response following PDT treatments (Schuitmaker et al., 1996). Even in patients with inoperable non-small cell lung cancer, the success rate was higher than chemotherapy, with 10/11 patients achieving complete remission (Sutedja et al., 1992). A high response ratio was achieved in other cancer types as well, including esophageal cancer, lung cancer, endobronchial cancer, bladder cancer and cervical cancer (Brown et al., 2004). Indeed, its high therapeutic efficiency makes photofrin the most commonly used photosensitizer to date (Dougherty, 1984). Yet despite photofrin's status as the "gold standard" in PDT oncologic application, it is still far from being an ideal

photosensitizer. First of all, photofrin is a mixture of more than 60 components and the precise composition remains unclear, thus the active compound has not yet been identified (O'Connor et al., 2009). In addition, photofrin has low cancer cell selectivity, necessitating a relatively high dose administration. The normal dosing concentration of 2 mg/kg induces side effects such as skin photosensitivity (Allison et al., 2006; Bellnier and Dougherty, 1996). To overcome the unfavorable properties of photofrin, second-generation photosensitizers were developed based on the structure of photofrin. Foscan/Temoporfin was developed and derived from photofrin through chemical modification (Senge and Brandt, 2011). The advantage of Foscan is its high efficacy: the drug doses and light intensity required to achieve the same response by Foscan are 100 times lower than photofrin (Mitra and Foster, 2005). In addition, the selectivity is improved. One study showed that Foscan preferentially accumulated in tumor cells, with a tumor to normal tissue ratio of 100:1 (Zimmermann et al., 2001). Foscan was approved in Europe for the treatment of head and neck cancer in 2001 (O'Connor et al., 2009). However, this compound still presents some drawbacks such as skin photosensitivity and slow optimal activity, which in turn requires prolonged light treatment. In addition to Foscan, other photosensitizers have been approved for oncology indications (O'Connor et al., 2009). Although these photosensitizers are promising in terms of efficiency and safety, their major drawbacks are low selectivity, skin photosensitivity and limited penetration to tumor tissue (Fig 5.5). Thus, identification of novel photosensitizers for oncologic applications is an emerging area of interest.

Photosensitizer	Approved indications	Localization	Effect	Disadvantages
Photofrin	Esophageal, lung, bladder and cervical cancer	Golgi apparatus, plasma membrane	Vascular damage and necrotic cell death	<ol style="list-style-type: none"> <li>1. Mixture</li> <li>2. Low selectivity</li> <li>3. Long-lasting photosensitivity</li> </ol>
Levulan	Actinic keratosis	Mitochondria, cytosol, cytosolic membranes	Direct tumor killing	<ol style="list-style-type: none"> <li>1. Pain</li> <li>2. Limited Penetration, only use in topical treatment</li> </ol>
Metvix	Actinic keratosis basal cell carcinoma	Mitochondria, cytosol, cytosolic membranes	Direct tumor killing	<ol style="list-style-type: none"> <li>1. Pain</li> </ol>
Foscan	Head and neck cancer (Europe)	Endoplasmic reticulum, mitochondria	Vascular damage and direct tumor killing	<ol style="list-style-type: none"> <li>1. Prolonged skin photosensitivity</li> <li>2. Optimal activity require long light exposure</li> </ol>
NPe6	Early lung cancer (Japan)	Lysosome, endosome	Vascular damage and direct tumor killing	<ol style="list-style-type: none"> <li>1. Not effective at low doses</li> </ol>

**Figure 5.5 Summary of FDA-approved photosensitizers.**

To refine PDT application in oncology, considerable efforts have been made in two directions: combination therapy and novel photosensitizer development. It has been proposed that the efficiency and selectivity of current photosensitizers could be improved by conjugation to delivery biomolecules, such as tumor-targeted antibodies, liposomes or other nanoparticles (Lin et al., 2015; Rosenkranz et al., 2000). Studies on Photofrin-conjugation showed that several delivery systems have successfully directed photofrin to tumor cells, thus increasing its cytotoxicity and selectivity (Kano et al., 2013; Lamch et al., 2014). Alternatively, new photosensitizers have been synthesized and investigated. Notably, the new generation of photosensitizers is no longer exclusive to porphyrin-based compounds. Compounds, such as hypericin, chalcogenopyrylium, methylene blue, cyanine MC540 and tetr-aryl-azadipyrrromethenes, have also been studied in an expanded panel of cancer types, including breast cancer, colon cancer, prostate cancer and lymphoma (O'Connor et al., 2009). In comparison to porphyrin-based photosensitizers, non-porphyrin photosensitizers possess several favorable features, such as proper drug-light interval time (time between drug administration and light irradiation), low skin sensitivity and high selectivity to tumor cells. To date, most of the non-porphyrin compounds have not received clinical approval, for various reasons. Take cyanine MC540 and methylene blue for examples. Although MC540-based PDT is well tolerated by normal hematopoietic stem and progenitor cells and is highly effective against leukemia and lymphoma cells (Itoh et al., 1993), it is not effective to cells derived from solid tumors (Anderson et al., 2002). Methylene blue, on the other hand, successfully destroyed tumor cells after light exposure when it

was administrated intralesionally (Orth et al., 1995), however, no response was observed in patients when it was injected intravenously (Williams et al., 1989). It was later determined that the absence of response was due to its poor tumor localization caused by high hydrophobicity (Mellish et al., 2002). It is noteworthy that despite these limitations, the development of non-porphyrin photosensitizers emerges as an exciting new approach for the field of PDT, with the aim of identifying photosensitizers with a short half-life and reduced toxicity to normal cells.

### 5.5.2 The consideration of D112 in PDT

As described in Chapter 1, DLCs preferentially accumulate in cancer mitochondria and this property renders them good candidates as PDT-based molecules. As a matter of fact, DLC compounds MKT-077 and Rh 123 have been evaluated as photosensitizers. Photo-activation enhanced the *in vitro* mitochondrial toxicity of MKT-077 by 6-fold (Modica-Napolitano et al., 1998), and in a mouse model, Rh 123 successfully eradicated superficial tumors (Castro et al., 1988). Therefore, photodynamic therapy might be an alternative approach to improve D112 anticancer efficiency as well. This hypothesis is supported by my observations that D112 possesses characteristics of an “ideal” photosensitizer. First, an ideal photosensitizer has no mutagenicity or carcinogenicity. D112 mainly accumulates in mitochondria, thus D112 is unlikely to be strongly mutagenic. D112's safety was also examined using Osiris Property Predictor (a computer program available through the Organic Chemistry Portal: [www.organic-chemistry.org/prog/peo](http://www.organic-chemistry.org/prog/peo)) as described in Chapter 1. Second, an ideal photosensitizer has high selectivity. The low selectivity of photofrin was an obstacle to its clinical application (O'Connor et al., 2009). In our

study, we demonstrated that D112 shows preferable accumulation in cancer mitochondria *in vitro*. Other DLCs, such as Rh-123 and MKT-077, selectively localize in tumor tissue (Britten et al., 2000; Jones et al., 2005), suggesting that selective localization is a shared feature among DLC compounds. The third consideration is a photosensitizer's absorption, distribution, metabolism and excretion properties (ADME). Tookad is a photosensitizer that was shown to have unfavorable metabolism, which was suggested as the reason why clinical trial results showed little or no response in prostate cancer patients (Chen et al., 2002). Tookad was cleared from the circulation of mice in 15 minutes, preventing the accumulation in tissue, which is necessary for tumor and metastases treatment. No such *in vivo* data has been obtained for D112 so far, but it has been shown that the similarly-structured MKT-077 was absorbed and distributed quickly in clinical trials (Britten et al., 2000), implying that D112 might exhibit a similar behavior *in vivo*. Moreover, even though manageable renal toxicity was encountered in MKT-077 clinical studies, the administered drug dose in PDT applications of D112 would be much lower and conceivably circumvent renal toxicity. In my study, I found that photo-activation enhanced D112 toxicity to cancer cells ~100-fold and selectivity 8.3~22.5-fold, suggesting that combined with a proper photo-activation step, low doses of D112 would retain anti-cancer activity and spare toxicity of normal tissue. Solubility is another factor that must be considered in the development of photosensitizers. For instance, as mentioned above, methylene blue is limited in PDT applications due to its poor solubility. D112 is also not a water-soluble compound. However, this disadvantage could be overcome by two strategies. One is the modification of its

structure. Cyanine has a simple structure; as such, significant numbers of derivatives can be synthesized through straightforward modifications around the core structure. The absorbance wavelength of D112 can also be changed by chemical modification with the intention of shifting the excitation wavelength further into the red region of the spectrum. Another way to overcome the poor solubility is to inject D112 directly into the tumor site. As mentioned above, methylene blue successfully eliminated tumor cells after light exposure when it was administered intralesionally (Orth et al., 1995). The fourth important characteristic is purity. Most photosensitizers are a single pure substance of known composition, except Photofrin. The purity of a drug contributes to its storage stability. D112 is a synthesized compound; therefore a highly purified product is achievable. Lastly, penetration must be considered. Owing to their poor penetration, the photosensitizers Metvix and Levulan can only be used in skin cancer by topical treatment (O'Connor et al., 2009). The hydrophobicity of D112 may favor its penetration. Clearly further work must be done to assess the pharmacokinetics, pharmacodynamics and safety profile of D112, in order to determine whether D112 should be tested as a photosensitizer *in vivo*.

In future, to test D112 potential in PDT, we first need to establish the administration dose. Antitumor activity is positively correlated with exposure time and drug concentration. However, high doses usually cause toxicity. In nude mice, the maximum tolerated dose of MKT-077 was 20 mg/kg of body weight (Chiba et al., 1998), while Rh-123 had significant toxicity in mice injected at doses higher than 10 mg/kg (Castro et al., 1992). We predict that the maximum tolerated dose of D112 will

between 10~40 mg/kg, as the molecular weight of D112 is larger than MKT-077 and Rh-123. Importantly, the drug dosage will be lower in PDT applications as compared to standard chemotherapy. For example, 10 mg/kg of Rh-123 was used in chemotherapy, and only 0.1~1 mg/kg of Rh-123 was administered in PDT (Castro et al., 1992). Therefore, I predict that the lowered dose of D112 for PDT applications will significantly decrease non-specific toxicity.

In addition, a precise drug-light interval is important to achieve the maximum selectivity of photosensitizer in PDT. Evidenced by the differential retention of Rh-123 in human breast carcinoma and normal mammary surgical tissue (Dairkee and Hackett, 1991), and rat glioma and normal brain tissue (Beckman et al., 1987), Rh-123 did show selectivity to tumors. However, although the peak intensity appeared between 8 and 12 post-administration, the most distinct differences in fluorescence intensity between normal tissue and malignant tumor were observed after 24 hours of dye exposure (Castro et al., 1989). Since the elimination of Rh-123 was rapid, the ideal drug-light interval in Rh-123-PDT would be 12~24 hours post-administration. To optimize D112-therapeutic effects, drug biodistribution, accumulation and metabolism would need to be examined primarily in animal models.

Additionally, some other factors need to be considered for future D112 PDT studies, such as light intensity and specific animal model. Currently, light intensity at 25~120 J/cm<sup>2</sup> is commonly used *in vivo* (Silva et al., 2015). Light intensity in this range is sufficient to activate photosensitizers, without unacceptable adverse effects. On the other hand, the animal model should be chosen from the D112-sensitive

cancer types. Finally, advances in light delivery technologies, such as the invention of the fiber optic diffuser, makes PDT applicable for most cancer types.

In sum, we are not aware of ongoing clinical trials on DLCs as photosensitizers. Despite some drawbacks discussed above, DLCs still represent promising candidates for PDT application in oncology, especially cyanine dyes (Kassab, 2002). Their most promising features are higher selectivity and specificity to cancer mitochondria.

## **5.6 Concluding remarks**

Based on the selective toxicity against a human colon cell line in comparison to a normal monkey kidney epithelial cell line, the cyanine dye D112 was first proposed as a potential anticancer drug in the 1970's. However, due to changing industry priorities, no further investigation had been pursued to verify this finding. The research in this thesis provides the preliminary evidence to support D112's potential as an anticancer drug prototype and might bring attention back to this group of compounds. First, I identified that D112 was a mitochondrial-targeted DLC that preferentially accumulated in cancer mitochondria. Second, I confirmed D112 selectivity in other cell lines. Moreover, insight into the molecular mechanism suggested that D112-induced ROS triggered apoptosis. Thus selectivity was likely a function of both selective cancer cell uptake and selective cancer cell sensitivity to oxidative stress. Finally, the exciting finding that photo-activation increased D112 toxicity to cancer cells ~100-fold revealed a strategy to enhance D112 effectiveness. Finally, by comparing the properties of D112 with other well-studied DLCs, my thesis

work presents fundamental information for the next series of studies to determine the utility and applicability of D112 as a therapeutic agent.

## Reference

Ali, I., Wani, W.A., Saleem, K., and Haque, A. (2013). Platinum compounds: a hope for future cancer chemotherapy. *Anticancer Agents Med Chem* 13, 296-306.

Allison, R.R., Bagnato, V.S., Cuenca, R., Downie, G.H., and Sibata, C.H. (2006). The future of photodynamic therapy in oncology. *Future Oncol* 2, 53-71.

Anderson, G.S., Miyagi, K., Sampson, R.W., and Sieber, F. (2002). Anti-tumor effect of Merocyanine 540-mediated photochemotherapy combined with Edelfosine: potential implications for the ex vivo purging of hematopoietic stem cell grafts from breast cancer patients. *J Photochem Photobiol B* 68, 101-108.

Baracca, A., Sgarbi, G., Solaini, G., and Lenaz, G. (2003). Rhodamine 123 as a probe of mitochondrial membrane potential: evaluation of proton flux through F<sub>0</sub> during ATP synthesis. *Biochim Biophys Acta* 1606, 137-146.

Beckman, W.C., Jr., Powers, S.K., Brown, J.T., Gillespie, G.Y., Bigner, D.D., and Camps, J.L., Jr. (1987). Differential retention of rhodamine 123 by avian sarcoma virus-induced glioma and normal brain tissue of the rat in vivo. *Cancer* 59, 266-270.

Bellnier, D.A., and Dougherty, T.J. (1996). A preliminary pharmacokinetic study of intravenous Photofrin in patients. *J Clin Laser Med Surg* 14, 311-314.

Bernal, S.D., Lampidis, T.J., Mclsaac, R.M., and Chen, L.B. (1983). Anticarcinoma activity in vivo of rhodamine 123, a mitochondrial-specific dye. *Science* 222, 169-172.

Britten, C.D., Rowinsky, E.K., Baker, S.D., Weiss, G.R., Smith, L., Stephenson, J., Rothenberg, M., Smetzer, L., Cramer, J., Collins, W., *et al.* (2000). A phase I and pharmacokinetic study of the mitochondrial-specific rhodacyanine dye analog MKT 077. *Clin Cancer Res* 6, 42-49.

Brown, S.B., Brown, E.A., and Walker, I. (2004). The present and future role of photodynamic therapy in cancer treatment. *Lancet Oncol* 5, 497-508.

Burbulla, L.F., Schelling, C., Kato, H., Rapaport, D., Voitalla, D., Schiesling, C., Schulte, C., Sharma, M., Illig, T., Bauer, P., *et al.* (2010). Dissecting the role of the mitochondrial chaperone mortalin in Parkinson's disease: functional impact of disease-related variants on mitochondrial homeostasis. *Hum Mol Genet* 19, 4437-4452.

Castro, D.J., Haghghat, S., Saxton, R.E., Reisler, E., Jongwaard, N., Castro, D.J., Ward, P.H., and Lufkin, R.B. (1992). Biodistribution of rhodamine-123 in nude mice

heterotransplanted with human squamous cell carcinomas. *Laryngoscope* 102, 868-874.

Castro, D.J., Saxton, R.E., Fetterman, H.R., Castro, D.J., and Ward, P.H. (1988). Phototherapy with argon lasers and Rhodamine-123 for tumor eradication. *Otolaryngol Head Neck Surg* 98, 581-588.

Castro, D.J., Saxton, R.E., Rodgerson, D.O., Fu, Y.S., Bhuta, S.M., Fetterman, H.R., Castro, D.J., Tartell, P.B., and Ward, P.H. (1989). Rhodamine-123 as a new laser dye: in vivo study of dye effects on murine metabolism, histology and ultrastructure. *Laryngoscope* 99, 1057-1062.

Chen, Q., Huang, Z., Luck, D., Beckers, J., Brun, P.H., Wilson, B.C., Scherz, A., Salomon, Y., and Hetzel, F.W. (2002). Preclinical studies in normal canine prostate of a novel palladium-bacteriopheophorbide (WST09) photosensitizer for photodynamic therapy of prostate cancers. *Photochem Photobiol* 76, 438-445.

Chiang, H.L., Terlecky, S.R., Plant, C.P., and Dice, J.F. (1989). A role for a 70-kilodalton heat shock protein in lysosomal degradation of intracellular proteins. *Science* 246, 382-385.

Chiba, Y., Kubota, T., Watanabe, M., Matsuzaki, S.W., Otani, Y., Teramoto, T., Matsumoto, Y., Koya, K., and Kitajima, M. (1998). MKT-077, localized lipophilic cation: antitumor activity against human tumor xenografts serially transplanted into nude mice. *Anticancer Res* 18, 1047-1052.

Dairkee, S.H., and Hackett, A.J. (1991). Differential retention of rhodamine 123 by breast carcinoma and normal human mammary tissue. *Breast Cancer Res Treat* 18, 57-61.

Davis, S., Weiss, M.J., Wong, J.R., Lampidis, T.J., and Chen, L.B. (1985). Mitochondrial and plasma membrane potentials cause unusual accumulation and retention of rhodamine 123 by human breast adenocarcinoma-derived MCF-7 cells. *J Biol Chem* 260, 13844-13850.

Dolmans, D.E., Fukumura, D., and Jain, R.K. (2003). Photodynamic therapy for cancer. *Nat Rev Cancer* 3, 380-387.

Dougherty, T.J. (1984). Photodynamic therapy (PDT) of malignant tumors. *Crit Rev Oncol Hematol* 2, 83-116.

Itoh, T., Messner, H.A., Jamal, N., Tweeddale, M., and Sieber, F. (1993). Merocyanine 540-sensitized photoinactivation of high-grade non-Hodgkin's lymphoma cells: potential application in autologous BMT. *Bone Marrow Transplant* 12, 191-196.

- Jones, L.W., Narayan, K.S., Shapiro, C.E., and Sweatman, T.W. (2005). Rhodamine-123: therapy for hormone refractory prostate cancer, a phase I clinical trial. *J Chemother* 17, 435-440.
- Kano, A., Taniwaki, Y., Nakamura, I., Shimada, N., Moriyama, K., and Maruyama, A. (2013). Tumor delivery of Photofrin(R) by PLL-g-PEG for photodynamic therapy. *J Control Release* 167, 315-321.
- Kassab, K. (2002). Photophysical and photosensitizing properties of selected cyanines. *J Photochem Photobiol B* 68, 15-22.
- Kazak, L., Reyes, A., and Holt, I.J. (2012). Minimizing the damage: repair pathways keep mitochondrial DNA intact. *Nat Rev Mol Cell Biol* 13, 659-671.
- Koya, K., Li, Y., Wang, H., Ukai, T., Tatsuta, N., Kawakami, M., Shishido, and Chen, L.B. (1996). MKT-077, a novel rhodacyanine dye in clinical trials, exhibits anticarcinoma activity in preclinical studies based on selective mitochondrial accumulation. *Cancer Res* 56, 538-543.
- Lamch, L., Bazylińska, U., Kulbacka, J., Pietkiewicz, J., Biezunska-Kusiak, K., and Wilk, K.A. (2014). Polymeric micelles for enhanced Photofrin II (R) delivery, cytotoxicity and pro-apoptotic activity in human breast and ovarian cancer cells. *Photodiagnosis Photodyn Ther* 11, 570-585.
- Li, X., Colvin, T., Rauch, J.N., Acosta-Alvear, D., Kampmann, M., Duniak, B., Hann, B., Aftab, B.T., Murnane, M., Cho, M., *et al.* (2015). Validation of the Hsp70-Bag3 protein-protein interaction as a potential therapeutic target in cancer. *Mol Cancer Ther* 14, 642-648.
- Li, X., Srinivasan, S.R., Connarn, J., Ahmad, A., Young, Z.T., Kabza, A.M., Zuiderweg, E.R., Sun, D., and Gestwicki, J.E. (2013). Analogs of the Allosteric Heat Shock Protein 70 (Hsp70) Inhibitor, MKT-077, as Anti-Cancer Agents. *ACS Med Chem Lett* 4.
- Li, X.Y., Zhao, Y., Sun, M.G., Shi, J.F., Ju, R.J., Zhang, C.X., Li, X.T., Zhao, W.Y., Mu, L.M., Zeng, F., *et al.* (2014). Multifunctional liposomes loaded with paclitaxel and artemether for treatment of invasive brain glioma. *Biomaterials* 35, 5591-5604.
- Lin, L., Xiong, L., Wen, Y., Lei, S., Deng, X., Liu, Z., Chen, W., and Miao, X. (2015). Active Targeting of Nano-Photosensitizer Delivery Systems for Photodynamic Therapy of Cancer Stem Cells. *J Biomed Nanotechnol* 11, 531-554.
- Madak, J.T., and Neamati, N. (2015). Membrane permeable lipophilic cations as mitochondrial directing groups. *Curr Top Med Chem* 15, 745-766.

Mayer, M.P., and Bukau, B. (2005). Hsp70 chaperones: cellular functions and molecular mechanism. *Cell Mol Life Sci* 62, 670-684.

Mellish, K.J., Cox, R.D., Vernon, D.I., Griffiths, J., and Brown, S.B. (2002). In vitro photodynamic activity of a series of methylene blue analogues. *Photochem Photobiol* 75, 392-397.

Mitra, S., and Foster, T.H. (2005). Photophysical parameters, photosensitizer retention and tissue optical properties completely account for the higher photodynamic efficacy of meso-tetra-hydroxyphenyl-chlorin vs Photofrin. *Photochem Photobiol* 81, 849-859.

Modica-Napolitano, J.S., and Aprille, J.R. (1987). Basis for the selective cytotoxicity of rhodamine 123. *Cancer Res* 47, 4361-4365.

Modica-Napolitano, J.S., and Aprille, J.R. (2001). Delocalized lipophilic cations selectively target the mitochondria of carcinoma cells. *Adv Drug Deliv Rev* 49, 63-70.

Modica-Napolitano, J.S., Brunelli, B.T., Koya, K., and Chen, L.B. (1998). Photoactivation enhances the mitochondrial toxicity of the cationic rhodacyanine MKT-077. *Cancer Res* 58, 71-75.

Modica-Napolitano, J.S., Koya, K., Weisberg, E., Brunelli, B.T., Li, Y., and Chen, L.B. (1996). Selective damage to carcinoma mitochondria by the rhodacyanine MKT-077. *Cancer Res* 56, 544-550.

Modica-Napolitano, J.S., and Weissig, V. (2015). Treatment Strategies that Enhance the Efficacy and Selectivity of Mitochondria-Targeted Anticancer Agents. *Int J Mol Sci* 16, 17394-17421.

O'Connor, A.E., Gallagher, W.M., and Byrne, A.T. (2009). Porphyrin and nonporphyrin photosensitizers in oncology: preclinical and clinical advances in photodynamic therapy. *Photochem Photobiol* 85, 1053-1074.

Orth, K., Ruck, A., Stanescu, A., and Beger, H.G. (1995). Intraluminal treatment of inoperable oesophageal tumours by intralesional photodynamic therapy with methylene blue. *Lancet* 345, 519-520.

Pelicano, H., Martin, D.S., Xu, R.H., and Huang, P. (2006). Glycolysis inhibition for anticancer treatment. *Oncogene* 25, 4633-4646.

Propper, D.J., Braybrooke, J.P., Taylor, D.J., Lodi, R., Styles, P., Cramer, J.A., Collins, W.C., Levitt, N.C., Talbot, D.C., Ganesan, T.S., *et al.* (1999). Phase I trial of the selective mitochondrial toxin MKT077 in chemo-resistant solid tumours. *Ann Oncol* 10, 923-927.

Riggins, J., Narayan, K.S., and Jones, L. (2007). Rhodamine-123 reduces the dosage of docetaxel necessary to achieve maximal cell growth inhibition in prostate and breast cancer cell lines in vitro. *Cancer Research AACR Annual Meeting*.

Rosenkranz, A.A., Jans, D.A., and Sobolev, A.S. (2000). Targeted intracellular delivery of photosensitizers to enhance photodynamic efficiency. *Immunol Cell Biol* 78, 452-464.

Rousaki, A., Miyata, Y., Jinwal, U.K., Dickey, C.A., Gestwicki, J.E., and Zuiderweg, E.R. (2011). Allosteric drugs: the interaction of antitumor compound MKT-077 with human Hsp70 chaperones. *J Mol Biol* 411, 614-632.

Schuitmaker, J.J., Baas, P., van Leengoed, H.L., van der Meulen, F.W., Star, W.M., and van Zandwijk, N. (1996). Photodynamic therapy: a promising new modality for the treatment of cancer. *J Photochem Photobiol B* 34, 3-12.

Senge, M.O., and Brandt, J.C. (2011). Temoporfin (Foscan(R), 5,10,15,20-tetra(m-hydroxyphenyl)chlorin)--a second-generation photosensitizer. *Photochem Photobiol* 87, 1240-1296.

Silva, Z.S., Jr., Bussadori, S.K., Fernandes, K.P., Huang, Y.Y., and Hamblin, M.R. (2015). Animal models for photodynamic therapy (PDT). *Biosci Rep* 35.

Smith, R.A., Porteous, C.M., Gane, A.M., and Murphy, M.P. (2003). Delivery of bioactive molecules to mitochondria in vivo. *Proc Natl Acad Sci U S A* 100, 5407-5412.

Souers, A.J., Levenson, J.D., Boghaert, E.R., Ackler, S.L., Catron, N.D., Chen, J., Dayton, B.D., Ding, H., Enschede, S.H., Fairbrother, W.J., *et al.* (2013). ABT-199, a potent and selective BCL-2 inhibitor, achieves antitumor activity while sparing platelets. *Nat Med* 19, 202-208.

Starenki, D., and Park, J.I. (2015). Selective Mitochondrial Uptake of MKT-077 Can Suppress Medullary Thyroid Carcinoma Cell Survival In Vitro and In Vivo. *Endocrinol Metab (Seoul)* 30, 593-603.

Sutedja, T., Baas, P., Stewart, F., and van Zandwijk, N. (1992). A pilot study of photodynamic therapy in patients with inoperable non-small cell lung cancer. *Eur J Cancer* 28A, 1370-1373.

Teicher, B.A., Holden, S.A., Jacobs, J.L., Abrams, M.J., and Jones, A.G. (1986). Intracellular distribution of a platinum-rhodamine 123 complex in cis-platinum sensitive and resistant human squamous carcinoma cell lines. *Biochem Pharmacol* 35, 3365-3369.

Tikoo, A., Shakri, R., Connolly, L., Hirokawa, Y., Shishido, T., Bowers, B., Ye, L.H., Kohama, K., Simpson, R.J., and Maruta, H. (2000). Treatment of ras-induced cancers by the F-actin-bundling drug MKT-077. *Cancer J* 6, 162-168.

Trachootham, D., Alexandre, J., and Huang, P. (2009). Targeting cancer cells by ROS-mediated mechanisms: a radical therapeutic approach? *Nat Rev Drug Discov* 8, 579-591.

Umesh, K.J., Grover, A., Narayan, M., Hirani, A., and Sutariya, V. (2014). Preparation and Characterization of MKT-077 Nanoparticles for Treatment of Alzheimer's Disease and Other Tauopathies. *Pharmaceutical Nanotechnology* 2, 10.

Vaidya, B., and Vyas, S.P. (2012). Transferrin coupled vesicular system for intracellular drug delivery for the treatment of cancer: development and characterization. *J Drug Target* 20, 372-380.

Vegt, E., de Jong, M., Wetzels, J.F., Masereeuw, R., Melis, M., Oyen, W.J., Gotthardt, M., and Boerman, O.C. (2010). Renal toxicity of radiolabeled peptides and antibody fragments: mechanisms, impact on radionuclide therapy, and strategies for prevention. *J Nucl Med* 51, 1049-1058.

Wadhwa, R., Sugihara, T., Yoshida, A., Nomura, H., Reddel, R.R., Simpson, R., Maruta, H., and Kaul, S.C. (2000). Selective toxicity of MKT-077 to cancer cells is mediated by its binding to the hsp70 family protein mot-2 and reactivation of p53 function. *Cancer Res* 60, 6818-6821.

Weissig, V. (2015). DQAsomes as the prototype of mitochondria-targeted pharmaceutical nanocarriers: preparation, characterization, and use. *Methods Mol Biol* 1265, 1-11.

Weissig, V., Lasch, J., Erdos, G., Meyer, H.W., Rowe, T.C., and Hughes, J. (1998). DQAsomes: a novel potential drug and gene delivery system made from Dequalinium. *Pharm Res* 15, 334-337.

Williams, J.L., Stamp, J., Devonshire, R., and Fowler, G.J. (1989). Methylene blue and the photodynamic therapy of superficial bladder cancer. *J Photochem Photobiol B* 4, 229-232.

Yang, H., Zhou, X., Liu, X., Yang, L., Chen, Q., Zhao, D., Zuo, J., and Liu, W. (2011). Mitochondrial dysfunction induced by knockdown of mortalin is rescued by Parkin. *Biochem Biophys Res Commun* 410, 114-120.

Zigman, S., and Gilman, P., Jr. (1980). Inhibition of cell division and growth by a redox series of cyanine dyes. *Science* 208, 188-191.

Zimmermann, A., Ritsch-Marte, M., and Kostron, H. (2001). mTHPC-mediated photodynamic diagnosis of malignant brain tumors. *Photochem Photobiol* 74, 611-616.

## BIBLIOGRAPHY

- Abdul, M., and Hoosein, N. (2003). Potentiation of the antiproliferative activity of MKT-077 by loperamide, diltiazem and tamoxifen. *Oncol Rep* 10, 2023-2026.
- Aft, R.L., Zhang, F.W., and Gius, D. (2002). Evaluation of 2-deoxy-D-glucose as a chemotherapeutic agent: mechanism of cell death. *Br J Cancer* 87, 805-812.
- Agostinis, P., Berg, K., Cengel, K.A., Foster, T.H., Girotti, A.W., Gollnick, S.O., Hahn, S.M., Hamblin, M.R., Juzeniene, A., Kessel, D., *et al.* (2011). Photodynamic therapy of cancer: an update. *CA Cancer J Clin* 61, 250-281.
- Akopova, O.V., Kolchinskaya, L.I., Nosar, V.I., Bouryi, V.A., Mankovska, I.N., and Sagach, V.F. (2012). Cytochrome C as an amplifier of ROS release in mitochondria. *Fiziol Zh* 58, 3-12.
- Alam, J.J. (2003). Apoptosis: target for novel drugs. *Trends Biotechnol* 21, 479-483.
- Ali, I., Wani, W.A., Saleem, K., and Haque, A. (2013). Platinum compounds: a hope for future cancer chemotherapy. *Anticancer Agents Med Chem* 13, 296-306.
- Allison, R.R., and Sibata, C.H. (2010). Oncologic photodynamic therapy photosensitizers: a clinical review. *Photodiagnosis Photodyn Ther* 7, 61-75.
- American Cancer Society (2014). *Cancer Facts & Figures 2014*.
- Anderson, G.S., Miyagi, K., Sampson, R.W., and Sieber, F. (2002). Anti-tumor effect of Merocyanine 540-mediated photochemotherapy combined with Edelfosine: potential implications for the ex vivo purging of hematopoietic stem cell grafts from breast cancer patients. *J Photochem Photobiol B* 68, 101-108.
- Andre, M., Mounier, N., Leleu, X., Sonet, A., Brice, P., Henry-Amar, M., Tilly, H., Coiffier, B., Bosly, A., Morel, P., *et al.* (2004). Second cancers and late toxicities after treatment of aggressive non-Hodgkin lymphoma with the ACVBP regimen: a GELA cohort study on 2837 patients. *Blood* 103, 1222-1228.
- Andreyev, A.Y., Kushnareva, Y.E., and Starkov, A.A. (2005). Mitochondrial metabolism of reactive oxygen species. *Biochemistry (Mosc)* 70, 200-214.
- Armstrong, G.T., Liu, W., Leisenring, W., Yasui, Y., Hammond, S., Bhatia, S., Neglia, J.P., Stovall, M., Srivastava, D., and Robison, L.L. (2011). Occurrence of multiple subsequent neoplasms in long-term survivors of childhood cancer: a report from the childhood cancer survivor study. *J Clin Oncol* 29, 3056-3064.

- Arner, E.S., and Holmgren, A. (2000). Physiological functions of thioredoxin and thioredoxin reductase. *Eur J Biochem* 267, 6102-6109.
- Assimon, V.A., Gillies, A.T., Rauch, J.N., and Gestwicki, J.E. (2013). Hsp70 protein complexes as drug targets. *Curr Pharm Des* 19, 404-417.
- Atkinson, E.A., Barry, M., Darmon, A.J., Shostak, I., Turner, P.C., Moyer, R.W., and Bleackley, R.C. (1998). Cytotoxic T lymphocyte-assisted suicide. Caspase 3 activation is primarily the result of the direct action of granzyme B. *J Biol Chem* 273, 21261-21266.
- Azzouzi, A.R., Barret, E., Moore, C.M., Villers, A., Allen, C., Scherz, A., Muir, G., de Wildt, M., Barber, N.J., Lebdai, S., *et al.* (2013). TOOKAD((R)) Soluble vascular-targeted photodynamic (VTP) therapy: determination of optimal treatment conditions and assessment of effects in patients with localised prostate cancer. *BJU Int* 112, 766-774.
- Bai, L., and Wang, S. (2014). Targeting apoptosis pathways for new cancer therapeutics. *Annu Rev Med* 65, 139-155.
- Baines, C.P., Kaiser, R.A., Purcell, N.H., Blair, N.S., Osinska, H., Hambleton, M.A., Brunskill, E.W., Sayen, M.R., Gottlieb, R.A., Dorn, G.W., *et al.* (2005). Loss of cyclophilin D reveals a critical role for mitochondrial permeability transition in cell death. *Nature* 434, 658-662.
- Bang, Y.-J., Van Cutsem, E., Feyereislova, A., Chung, H.C., Shen, L., Sawaki, A., Lordick, F., Ohtsu, A., Omuro, Y., Satoh, T., *et al.* Trastuzumab in combination with chemotherapy versus chemotherapy alone for treatment of HER2-positive advanced gastric or gastro-oesophageal junction cancer (ToGA): a phase 3, open-label, randomised controlled trial. *The Lancet* 376, 687-697.
- Baracca, A., Sgarbi, G., Solaini, G., and Lenaz, G. (2003). Rhodamine 123 as a probe of mitochondrial membrane potential: evaluation of proton flux through F(0) during ATP synthesis. *Biochim Biophys Acta* 1606, 137-146.
- Bareford, L.M., and Swaan, P.W. (2007). Endocytic mechanisms for targeted drug delivery. *Adv Drug Deliv Rev* 59, 748-758.
- Barry, M., Heibein, J.A., Pinkoski, M.J., Lee, S.F., Moyer, R.W., Green, D.R., and Bleackley, R.C. (2000). Granzyme B short-circuits the need for caspase 8 activity during granule-mediated cytotoxic T-lymphocyte killing by directly cleaving Bid. *Mol Cell Biol* 20, 3781-3794.
- Bean, G.R., Ganesan, Y.T., Dong, Y., Takeda, S., Liu, H., Chan, P.M., Huang, Y., Chodosh, L.A., Zambetti, G.P., Hsieh, J.J., *et al.* (2013). PUMA and BIM are required for oncogene inactivation-induced apoptosis. *Sci Signal* 6, ra20.

Beckman, W.C., Jr., Powers, S.K., Brown, J.T., Gillespie, G.Y., Bigner, D.D., and Camps, J.L., Jr. (1987). Differential retention of rhodamine 123 by avian sarcoma virus-induced glioma and normal brain tissue of the rat in vivo. *Cancer* 59, 266-270.

Behrend, L., Henderson, G., and Zwacka, R.M. (2003). Reactive oxygen species in oncogenic transformation. *Biochem Soc Trans* 31, 1441-1444.

Bellance, N., Lestienne, P., and Rossignol, R. (2009). Mitochondria: from bioenergetics to the metabolic regulation of carcinogenesis. *Front Biosci (Landmark Ed)* 14, 4015-4034.

Bellnier, D.A., and Dougherty, T.J. (1996). A preliminary pharmacokinetic study of intravenous Photofrin in patients. *J Clin Laser Med Surg* 14, 311-314.

Bernal, S.D., Lampidis, T.J., Mclsaac, R.M., and Chen, L.B. (1983). Anticarcinoma activity in vivo of rhodamine 123, a mitochondrial-specific dye. *Science* 222, 169-172.

Berns, K., Horlings, H.M., Hennessy, B.T., Madiredjo, M., Hijmans, E.M., Beelen, K., Linn, S.C., Gonzalez-Angulo, A.M., Stemke-Hale, K., Hauptmann, M., *et al.* (2007). A functional genetic approach identifies the PI3K pathway as a major determinant of trastuzumab resistance in breast cancer. *Cancer Cell* 12, 395-402.

Bervers, E.M., and Williamson, P.L. (2010). Phospholipid scramblase: an update. *FEBS Lett* 584, 2724-2730.

Bleday, R., Weiss, M.J., Salem, R.R., Wilson, R.E., Chen, L.B., and Steele, G., Jr. (1986). Inhibition of rat colon tumor isograft growth with dequalinium chloride. *Arch Surg* 121, 1272-1275.

Bidere, N., Lorenzo, H.K., Carmona, S., Laforge, M., Harper, F., Dumont, C., and Senik, A. (2003). Cathepsin D triggers Bax activation, resulting in selective apoptosis-inducing factor (AIF) relocation in T lymphocytes entering the early commitment phase to apoptosis. *J Biol Chem* 278, 31401-31411.

Blume-Jensen, P., and Hunter, T. (2001). Oncogenic kinase signalling. *Nature* 411, 355-365.

Boland, M.L., Chourasia, A.H., and Macleod, K.F. (2013). Mitochondrial dysfunction in cancer. *Front Oncol* 3, 292.

Bonadonna, G., and Monfardini, S. (1969). Cardiac toxicity of daunorubicin. *Lancet* 1, 837.

Boonstra, J., and Post, J.A. (2004). Molecular events associated with reactive oxygen species and cell cycle progression in mammalian cells. *Gene* 337, 1-13.

Borden, E.C., Kluger, H., and Crowley, J. (2008). Apoptosis: a clinical perspective. *Nat Rev Drug Discov* 7, 959-959.

Borisenko, G.G., Matsura, T., Liu, S.X., Tyurin, V.A., Jianfei, J., Serinkan, F.B., and Kagan, V.E. (2003). Macrophage recognition of externalized phosphatidylserine and phagocytosis of apoptotic Jurkat cells--existence of a threshold. *Arch Biochem Biophys* 413, 41-52.

Bossy-Wetzel, E., Newmeyer, D.D., and Green, D.R. (1998). Mitochondrial cytochrome c release in apoptosis occurs upstream of DEVD-specific caspase activation and independently of mitochondrial transmembrane depolarization. *EMBO J* 17, 37-49.

Botchkarev, V.A., Komarova, E.A., Siebenhaar, F., Botchkareva, N.V., Komarov, P.G., Maurer, M., Gilchrest, B.A., and Gudkov, A.V. (2000). p53 is essential for chemotherapy-induced hair loss. *Cancer Res* 60, 5002-5006.

Brahimi-Horn, M.C., Chiche, J., and Pouyssegur, J. (2007). Hypoxia signalling controls metabolic demand. *Curr Opin Cell Biol* 19, 223-229.

Britten, C.D., Rowinsky, E.K., Baker, S.D., Weiss, G.R., Smith, L., Stephenson, J., Rothenberg, M., Smetzer, L., Cramer, J., Collins, W., *et al.* (2000). A phase I and pharmacokinetic study of the mitochondrial-specific rhodacyanine dye analog MKT 077. *Clin Cancer Res* 6, 42-49.

Brown, J.M., and Attardi, L.D. (2005). The role of apoptosis in cancer development and treatment response. *Nat Rev Cancer* 5, 231-237.

Brown, J.M., and Wouters, B.G. (1999). Apoptosis, p53, and tumor cell sensitivity to anticancer agents. *Cancer Res* 59, 1391-1399.

Brown, S.B., Brown, E.A., and Walker, I. (2004). The present and future role of photodynamic therapy in cancer treatment. *Lancet Oncol* 5, 497-508.

Bruey, J.M., Ducasse, C., Bonniaud, P., Ravagnan, L., Susin, S.A., Diaz-Latoud, C., Gurbuxani, S., Arrigo, A.P., Kroemer, G., Solary, E., *et al.* (2000). Hsp27 negatively regulates cell death by interacting with cytochrome c. *Nat Cell Biol* 2, 645-652.

Brunk, U.T., and Svensson, I. (1999). Oxidative stress, growth factor starvation and Fas activation may all cause apoptosis through lysosomal leak. *Redox Rep* 4, 3-11.

Burbulla, L.F., Schelling, C., Kato, H., Rapaport, D., Voitalla, D., Schiesling, C., Schulte, C., Sharma, M., Illig, T., Bauer, P., *et al.* (2010). Dissecting the role of the mitochondrial chaperone mortalin in Parkinson's disease: functional impact of

disease-related variants on mitochondrial homeostasis. *Hum Mol Genet* 19, 4437-4452.

Buytaert, E., Dewaele, M., and Agostinis, P. (2007). Molecular effectors of multiple cell death pathways initiated by photodynamic therapy. *Biochim Biophys Acta* 1776, 86-107.

Canadian Cancer Society (2013). National statistics at a glance from Canadian Cancer Statistics.

Cang, S., Iragavarapu, C., Savooji, J., Song, Y., and Liu, D. (2015). ABT-199 (venetoclax) and BCL-2 inhibitors in clinical development. *J Hematol Oncol* 8, 129.

Capdeville, R., Buchdunger, E., Zimmermann, J., and Matter, A. (2002). Glivec (STI571, imatinib), a rationally developed, targeted anticancer drug. *Nat Rev Drug Discov* 1, 493-502.

Castedo, M., Hirsch, T., Susin, S.A., Zamzami, N., Marchetti, P., Macho, A., and Kroemer, G. (1996). Sequential acquisition of mitochondrial and plasma membrane alterations during early lymphocyte apoptosis. *J Immunol* 157, 512-521.

Castro, D.J., Haghghat, S., Saxton, R.E., Reisler, E., Jongwaard, N., Castro, D.J., Ward, P.H., and Lufkin, R.B. (1992). Biodistribution of rhodamine-123 in nude mice heterotransplanted with human squamous cell carcinomas. *Laryngoscope* 102, 868-874.

Castro, D.J., Saxton, R.E., Fetterman, H.R., Castro, D.J., and Ward, P.H. (1988). Phototherapy with the argon laser on human melanoma cells "sensitized" with rhodamine-123: a new method for tumor growth inhibition. *Laryngoscope* 98, 369-376.

Castro, D.J., Saxton, R.E., Fetterman, H.R., Castro, D.J., and Ward, P.H. (1988). Phototherapy with argon lasers and Rhodamine-123 for tumor eradication. *Otolaryngol Head Neck Surg* 98, 581-588.

Castro, D.J., Saxton, R.E., Rodgerson, D.O., Fu, Y.S., Bhuta, S.M., Fetterman, H.R., Castro, D.J., Tartell, P.B., and Ward, P.H. (1989). Rhodamine-123 as a new laser dye: in vivo study of dye effects on murine metabolism, histology and ultrastructure. *Laryngoscope* 99, 1057-1062.

Cha, Y., Park, D.W., Lee, C.H., Baek, S.H., Kim, S.Y., Kim, J.R., and Kim, J.H. (2006). Arsenic trioxide induces apoptosis in human colorectal adenocarcinoma HT-29 cells through ROS. *Cancer Res Treat* 38, 54-60.

Chance, B., Sies, H., and Boveris, A. (1979). Hydroperoxide metabolism in mammalian organs. *Physiol Rev* 59, 527-605.

Chang, J., Xie, M., Shah, V.R., Schneider, M.D., Entman, M.L., Wei, L., and Schwartz, R.J. (2006). Activation of Rho-associated coiled-coil protein kinase 1 (ROCK-1) by caspase-3 cleavage plays an essential role in cardiac myocyte apoptosis. *Proc Natl Acad Sci U S A* 103, 14495-14500.

Chatterjee, A., Mambo, E., and Sidransky, D. (2006). Mitochondrial DNA mutations in human cancer. *Oncogene* 25, 4663-4674.

Chauhan, D., Velankar, M., Brahmandam, M., Hideshima, T., Podar, K., Richardson, P., Schlossman, R., Ghobrial, I., Raje, N., Munshi, N., *et al.* (2007). A novel Bcl-2/Bcl-X(L)/Bcl-w inhibitor ABT-737 as therapy in multiple myeloma. *Oncogene* 26, 2374-2380.

Chen, B., Pogue, B.W., Luna, J.M., Hardman, R.L., Hoopes, P.J., and Hasan, T. (2006). Tumor vascular permeabilization by vascular-targeting photosensitization: effects, mechanism, and therapeutic implications. *Clin Cancer Res* 12, 917-923.

Chen, G., Chen, Z., Hu, Y., and Huang, P. (2011). Inhibition of mitochondrial respiration and rapid depletion of mitochondrial glutathione by beta-phenethyl isothiocyanate: mechanisms for anti-leukemia activity. *Antioxid Redox Signal* 15, 2911-2921.

Chen, L.B., Summerhayes, I.C., Johnson, L.V., Walsh, M.L., Bernal, S.D., and Lampidis, T.J. (1982). Probing mitochondria in living cells with rhodamine 123. *Cold Spring Harb Symp Quant Biol* 46 Pt 1, 141-155.

Chen, Q., Huang, Z., Luck, D., Beckers, J., Brun, P.H., Wilson, B.C., Scherz, A., Salomon, Y., and Hetzel, F.W. (2002). Preclinical studies in normal canine prostate of a novel palladium-bacteriopheophorbide (WST09) photosensitizer for photodynamic therapy of prostate cancers. *Photochem Photobiol* 76, 438-445.

Chen, Q., Vazquez, E.J., Moghaddas, S., Hoppel, C.L., and Lesnefsky, E.J. (2003). Production of reactive oxygen species by mitochondria: central role of complex III. *J Biol Chem* 278, 36027-36031.

Cherukuri, D.P., and Nelson, M.A. (2008). Role of reactive oxygen species (ROS) and JNKs in selenite-induced apoptosis in HepG2 cells. *Cancer Biol Ther* 7, 697-698.

Chiang, H.L., Terlecky, S.R., Plant, C.P., and Dice, J.F. (1989). A role for a 70-kilodalton heat shock protein in lysosomal degradation of intracellular proteins. *Science* 246, 382-385.

Chiba, Y., Kubota, T., Watanabe, M., Matsuzaki, S.W., Otani, Y., Teramoto, T., Matsumoto, Y., Koya, K., and Kitajima, M. (1998a). MKT-077, localized lipophilic

cation: antitumor activity against human tumor xenografts serially transplanted into nude mice. *Anticancer Res* 18, 1047-1052.

Chiba, Y., Kubota, T., Watanabe, M., Otani, Y., Teramoto, T., Matsumoto, Y., Koya, K., and Kitajima, M. (1998b). Selective antitumor activity of MKT-077, a delocalized lipophilic cation, on normal cells and cancer cells in vitro. *J Surg Oncol* 69, 105-110.

Chung, A.S., Lee, J., and Ferrara, N. (2010). Targeting the tumour vasculature: insights from physiological angiogenesis. *Nat Rev Cancer* 10, 505-514.

Chunta, J.L., Vistisen, K.S., Yazdi, Z., and Braun, R.D. (2012). Uptake rate of cationic mitochondrial inhibitor MKT-077 determines cellular oxygen consumption change in carcinoma cells. *PLoS One* 7, e37471.

Cirman, T., Oresic, K., Mazovec, G.D., Turk, V., Reed, J.C., Myers, R.M., Salvesen, G.S., and Turk, B. (2004). Selective disruption of lysosomes in HeLa cells triggers apoptosis mediated by cleavage of Bid by multiple papain-like lysosomal cathepsins. *J Biol Chem* 279, 3578-3587.

Coleman, M.L., Sahai, E.A., Yeo, M., Bosch, M., Dewar, A., and Olson, M.F. (2001). Membrane blebbing during apoptosis results from caspase-mediated activation of ROCK I. *Nat Cell Biol* 3, 339-345.

Colvin, T.A., Gabai, V.L., Gong, J., Calderwood, S.K., Li, H., Gummuluru, S., Matchuk, O.N., Smirnova, S.G., Orlova, N.V., Zamulaeva, I.A., *et al.* (2014). Hsp70-Bag3 interactions regulate cancer-related signaling networks. *Cancer Res* 74, 4731-4740.

Costantini, P., Belzacq, A.S., Vieira, H.L., Larochette, N., de Pablo, M.A., Zamzami, N., Susin, S.A., Brenner, C., and Kroemer, G. (2000). Oxidation of a critical thiol residue of the adenine nucleotide translocator enforces Bcl-2-independent permeability transition pore opening and apoptosis. *Oncogene* 19, 307-314.

Crystal, A.S., Shaw, A.T., Sequist, L.V., Friboulet, L., Niederst, M.J., Lockerman, E.L., Frias, R.L., Gainor, J.F., Amzallag, A., Greninger, P., *et al.* (2014). Patient-derived models of acquired resistance can identify effective drug combinations for cancer. *Science* 346, 1480-1486.

Cuezva, J.M., Ostronoff, L.K., Ricart, J., Lopez de Heredia, M., Di Liegro, C.M., and Izquierdo, J.M. (1997). Mitochondrial biogenesis in the liver during development and oncogenesis. *J Bioenerg Biomembr* 29, 365-377.

Dai, C., Dai, S., and Cao, J. (2012). Proteotoxic stress of cancer: implication of the heat-shock response in oncogenesis. *J Cell Physiol* 227, 2982-2987.

Dairkee, S.H., and Hackett, A.J. (1991). Differential retention of rhodamine 123 by breast carcinoma and normal human mammary tissue. *Breast Cancer Res Treat* 18, 57-61.

Davids, M.S., Pagel, J.M., Kahl, B.S., Wierda, W.G., Miller, T.P., Gerecitano, J.F., Kipps, T.J., Anderson, M.-A., Huang, D.C.S., Rudersdorf, N.K., *et al.* (2013). Bcl-2 Inhibitor ABT-199 (GDC-0199) Monotherapy Shows Anti-Tumor Activity Including Complete Remissions In High-Risk Relapsed/Refractory (R/R) Chronic Lymphocytic Leukemia (CLL) and Small Lymphocytic Lymphoma (SLL). *Blood* 122, 872-872.

Davids, M.S., Roberts, A.W., Anderson, M.A., Pagel, J.M., Kahl, B.S., Gerecitano, J.F., Darden, D.E., Nolan, C.E., Gressick, L.A., Yang, J., *et al.* (2012). The BCL-2-Specific BH3-Mimetic ABT-199 (GDC-0199) Is Active and Well-Tolerated in Patients with Relapsed Non-Hodgkin Lymphoma: Interim Results of a Phase I Study. *Blood* 120, 304-304.

Davis, S., Weiss, M.J., Wong, J.R., Lampidis, T.J., and Chen, L.B. (1985). Mitochondrial and plasma membrane potentials cause unusual accumulation and retention of rhodamine 123 by human breast adenocarcinoma-derived MCF-7 cells. *J Biol Chem* 260, 13844-13850.

De Giorgi, F., Lartigue, L., Bauer, M.K., Schubert, A., Grimm, S., Hanson, G.T., Remington, S.J., Youle, R.J., and Ichas, F. (2002). The permeability transition pore signals apoptosis by directing Bax translocation and multimerization. *Faseb j* 16, 607-609.

de Grey, A.D. (2005). Reactive oxygen species production in the mitochondrial matrix: implications for the mechanism of mitochondrial mutation accumulation. *Rejuvenation Res* 8, 13-17.

DeBerardinis, R.J., Mancuso, A., Daikhin, E., Nissim, I., Yudkoff, M., Wehrli, S., and Thompson, C.B. (2007). Beyond aerobic glycolysis: transformed cells can engage in glutamine metabolism that exceeds the requirement for protein and nucleotide synthesis. *Proc Natl Acad Sci U S A* 104, 19345-19350.

DeNicola, G.M., Karreth, F.A., Humpton, T.J., Gopinathan, A., Wei, C., Frese, K., Mangal, D., Yu, K.H., Yeo, C.J., Calhoun, E.S., *et al.* (2011). Oncogene-induced Nrf2 transcription promotes ROS detoxification and tumorigenesis. *Nature* 475, 106-109.

Dobbelstein, M., and Moll, U. (2014). Targeting tumour-supportive cellular machineries in anticancer drug development. *Nat Rev Drug Discov* 13, 179-196.

Dolmans, D.E., Fukumura, D., and Jain, R.K. (2003). Photodynamic therapy for cancer. *Nat Rev Cancer* 3, 380-387.

Doherty, G.J., and McMahon, H.T. (2009). Mechanisms of endocytosis. *Annu Rev Biochem* 78, 857-902.

Dolmans, D.E., Fukumura, D., and Jain, R.K. (2003). Photodynamic therapy for cancer. *Nat Rev Cancer* 3, 380-387.

Dougherty, T.J. (1984). Photodynamic therapy (PDT) of malignant tumors. *Crit Rev Oncol Hematol* 2, 83-116.

Druker, B.J., Guilhot, F., O'Brien, S.G., Gathmann, I., Kantarjian, H., Gattermann, N., Deininger, M.W., Silver, R.T., Goldman, J.M., Stone, R.M., *et al.* (2006). Five-year follow-up of patients receiving imatinib for chronic myeloid leukemia. *N Engl J Med* 355, 2408-2417.

Du, J., Daniels, D.H., Asbury, C., Venkataraman, S., Liu, J., Spitz, D.R., Oberley, L.W., and Cullen, J.J. (2006). Mitochondrial production of reactive oxygen species mediate dicumarol-induced cytotoxicity in cancer cells. *J Biol Chem* 281, 37416-37426.

Dussmann, H., Rehm, M., Kogel, D., and Prehn, J.H. (2003). Outer mitochondrial membrane permeabilization during apoptosis triggers caspase-independent mitochondrial and caspase-dependent plasma membrane potential depolarization: a single-cell analysis. *J Cell Sci* 116, 525-536.

Dwarakanath, B.S., Singh, D., Banerji, A.K., Sarin, R., Venkataramana, N.K., Jalali, R., Vishwanath, P.N., Mohanti, B.K., Tripathi, R.P., Kalia, V.K., *et al.* (2009). Clinical studies for improving radiotherapy with 2-deoxy-D-glucose: present status and future prospects. *J Cancer Res Ther* 5 *Suppl* 1, S21-26.

Edelhauser, H.F., Van Horn, D.L., Miller, P., and Pederson, H.J. (1976). Effect of thiol-oxidation of glutathione with diamide on corneal endothelial function, junctional complexes, and microfilaments. *J Cell Biol* 68, 567-578.

Egger, L., Schneider, J., Rheme, C., Tapernoux, M., Hacki, J., and Borner, C. (2003). Serine proteases mediate apoptosis-like cell death and phagocytosis under caspase-inhibiting conditions. *Cell Death Differ* 10, 1188-1203.

Enari, M., Sakahira, H., Yokoyama, H., Okawa, K., Iwamatsu, A., and Nagata, S. (1998). A caspase-activated DNase that degrades DNA during apoptosis, and its inhibitor ICAD. *Nature* 391, 43-50.

Estaquier, J., Vallette, F., Vayssiere, J.L., and Mignotte, B. (2012). The mitochondrial pathways of apoptosis. *Adv Exp Med Biol* 942, 157-183.

European Cancer Organisation. EBCC-10 NEWS: Combination of lapatinib and trastuzumab shrinks HER2 positive breast cancer significantly in 11 days after diagnosis (ECCO).

Evans, C.G., Chang, L., and Gestwicki, J.E. (2010). Heat shock protein 70 (hsp70) as an emerging drug target. *J Med Chem* 53, 4585-4602.

Evans, J.M., Donnelly, L.A., Emslie-Smith, A.M., Alessi, D.R., and Morris, A.D. (2005). Metformin and reduced risk of cancer in diabetic patients. *BMJ* 330, 1304-1305.

Evens, A.M. (2004). Motexafin gadolinium: a redox-active tumor selective agent for the treatment of cancer. *Curr Opin Oncol* 16, 576-580.

Fan, J., Kamphorst, J.J., Mathew, R., Chung, M.K., White, E., Shlomi, T., and Rabinowitz, J.D. (2013). Glutamine-driven oxidative phosphorylation is a major ATP source in transformed mammalian cells in both normoxia and hypoxia. *Mol Syst Biol* 9, 712.

Fan, M., Goodwin, M.E., Birrer, M.J., and Chambers, T.C. (2001). The c-Jun NH(2)-terminal protein kinase/AP-1 pathway is required for efficient apoptosis induced by vinblastine. *Cancer Res* 61, 4450-4458.

Feldmann, G., Haouzi, D., Moreau, A., Durand-Schneider, A.M., Bringuier, A., Berson, A., Mansouri, A., Fau, D., and Pessayre, D. (2000). Opening of the mitochondrial permeability transition pore causes matrix expansion and outer membrane rupture in Fas-mediated hepatic apoptosis in mice. *Hepatology* 31, 674-683.

Fendel, U., Tocilescu, M.A., Kerscher, S., and Brandt, U. (2008). Exploring the inhibitor binding pocket of respiratory complex I. *Biochim Biophys Acta* 1777, 660-665.

Fernald, K., and Kurokawa, M. Evading apoptosis in cancer. *Trends in Cell Biology* 23, 620-633.

Fernandes-Alnemri, T., Litwack, G., and Alnemri, E.S. (1994). CPP32, a novel human apoptotic protein with homology to *Caenorhabditis elegans* cell death protein Ced-3 and mammalian interleukin-1 beta-converting enzyme. *J Biol Chem* 269, 30761-30764.

Formentini, L., Sanchez-Arago, M., Sanchez-Cenizo, L., and Cuezva, J.M. (2012). The mitochondrial ATPase inhibitory factor 1 triggers a ROS-mediated retrograde prosurvival and proliferative response. *Mol Cell* 45, 731-742.

Fulda, S. (2009). Tumor resistance to apoptosis. *Int J Cancer* 124, 511-515.

- Fulda, S. (2010). Exploiting mitochondrial apoptosis for the treatment of cancer. *Mitochondrion* 10, 598-603.
- Fulda, S., and Debatin, K.M. (2006). Extrinsic versus intrinsic apoptosis pathways in anticancer chemotherapy. *Oncogene* 25, 4798-4811.
- Gamen, S., Anel, A., Perez-Galan, P., Laserra, P., Johnson, D., Pineiro, A., and Naval, J. (2000). Doxorubicin treatment activates a Z-VAD-sensitive caspase, which causes deltaprim loss, caspase-9 activity, and apoptosis in Jurkat cells. *Exp Cell Res* 258, 223-235.
- Garon, E.B., Christofk, H.R., Hosmer, W., Britten, C.D., Bahng, A., Crabtree, M.J., Hong, C.S., Kamranpour, N., Pitts, S., Kabbavar, F., *et al.* (2014). Dichloroacetate should be considered with platinum-based chemotherapy in hypoxic tumors rather than as a single agent in advanced non-small cell lung cancer. *J Cancer Res Clin Oncol* 140, 443-452.
- Garrido, C., Brunet, M., Didelot, C., Zermati, Y., Schmitt, E., and Kroemer, G. (2006). Heat shock proteins 27 and 70: anti-apoptotic proteins with tumorigenic properties. *Cell Cycle* 5, 2592-2601.
- Gehrmann, M., Specht, H.M., Bayer, C., Brandstetter, M., Chizzali, B., Duma, M., Breuninger, S., Hube, K., Lehnerer, S., van Phi, V., *et al.* (2014). Hsp70--a biomarker for tumor detection and monitoring of outcome of radiation therapy in patients with squamous cell carcinoma of the head and neck. *Radiat Oncol* 9, 131.
- Gennari, R., Menard, S., Fagnoni, F., Ponchio, L., Scelsi, M., Tagliabue, E., Castiglioni, F., Villani, L., Magalotti, C., Gibelli, N., *et al.* (2004). Pilot study of the mechanism of action of preoperative trastuzumab in patients with primary operable breast tumors overexpressing HER2. *Clin Cancer Res* 10, 5650-5655.
- Giaever, G., Chu, A.M., Ni, L., Connelly, C., Riles, L., Veronneau, S., Dow, S., Lucau-Danila, A., Anderson, K., Andre, B., *et al.* (2002). Functional profiling of the *Saccharomyces cerevisiae* genome. *Nature* 418, 387-391.
- Gilman, P., Parton, R.L., and Lenhard, J.R. (2006). Correlation of anti-cancer activity of dyes with redox potential In Patent Application Publication (US: Eastman Kodak Company).
- Giron-Calle, J., Zwizinski, C.W., and Schmid, H.H. (1994). Peroxidative damage to cardiac mitochondria. II. Immunological analysis of modified adenine nucleotide translocase. *Arch Biochem Biophys* 315, 1-7.

- Gogvadze, V., Orrenius, S., and Zhivotovsky, B. (2008). Mitochondria in cancer cells: what is so special about them? *Trends Cell Biol* 18, 165-173.
- Gollnick, S.O., Vaughan, L., and Henderson, B.W. (2002). Generation of effective antitumor vaccines using photodynamic therapy. *Cancer Res* 62, 1604-1608.
- Goloudina, A.R., Demidov, O.N., and Garrido, C. (2012). Inhibition of HSP70: A challenging anti-cancer strategy. *Cancer Letters* 325, 117-124.
- Gonzalvez, F., Pariselli, F., Dupaigne, P., Budihardjo, I., Lutter, M., Antonsson, B., Diolez, P., Manon, S., Martinou, J.C., Gubern, M., *et al.* (2005). tBid interaction with cardiolipin primarily orchestrates mitochondrial dysfunctions and subsequently activates Bax and Bak. *Cell Death Differ* 12, 614-626.
- Goodman, L.S., Wintrobe, M.M., and *et al.* (1946). Nitrogen mustard therapy; use of methyl-bis (beta-chloroethyl) amine hydrochloride and tris (beta-chloroethyl) amine hydrochloride for Hodgkin's disease, lymphosarcoma, leukemia and certain allied and miscellaneous disorders. *J Am Med Assoc* 132, 126-132.
- Goping, I.S., Barry, M., Liston, P., Sawchuk, T., Constantinescu, G., Michalak, K.M., Shostak, I., Roberts, D.L., Hunter, A.M., Korneluk, R., *et al.* (2003). Granzyme B-induced apoptosis requires both direct caspase activation and relief of caspase inhibition. *Immunity* 18, 355-365.
- Goping, I.S., Gross, A., Lavoie, J.N., Nguyen, M., Jemmerson, R., Roth, K., Korsmeyer, S.J., and Shore, G.C. (1998). Regulated targeting of BAX to mitochondria. *J Cell Biol* 143, 207-215.
- Gottesman, M.M. (2002). Mechanisms of cancer drug resistance. *Annu Rev Med* 53, 615-627.
- Gottlieb, E., Armour, S.M., Harris, M.H., and Thompson, C.B. (2003). Mitochondrial membrane potential regulates matrix configuration and cytochrome c release during apoptosis. *Cell Death Differ* 10, 709-717.
- Grebien, F., Hantschel, O., Wojcik, J., Kaupe, I., Kovacic, B., Wyrzucki, A.M., Gish, G.D., Cerny-Reiterer, S., Koide, A., Beug, H., *et al.* (2011). Targeting the SH2-kinase interface in Bcr-Abl inhibits leukemogenesis. *Cell* 147, 306-319.
- Gross, A., McDonnell, J.M., and Korsmeyer, S.J. (1999). BCL-2 family members and the mitochondria in apoptosis. *Genes Dev* 13, 1899-1911.
- Guicciardi, M.E., Deussing, J., Miyoshi, H., Bronk, S.F., Svingen, P.A., Peters, C., Kaufmann, S.H., and Gores, G.J. (2000). Cathepsin B contributes to TNF-alpha-mediated hepatocyte apoptosis by promoting mitochondrial release of cytochrome c. *J Clin Invest* 106, 1127-1137.

Guzy, R.D., Sharma, B., Bell, E., Chandel, N.S., and Schumacker, P.T. (2008). Loss of the SdhB, but Not the SdhA, subunit of complex II triggers reactive oxygen species-dependent hypoxia-inducible factor activation and tumorigenesis. *Mol Cell Biol* 28, 718-731.

Hahn, S.M., Putt, M.E., Metz, J., Shin, D.B., Rickter, E., Menon, C., Smith, D., Glatstein, E., Fraker, D.L., and Busch, T.M. (2006). Photofrin uptake in the tumor and normal tissues of patients receiving intraperitoneal photodynamic therapy. *Clin Cancer Res* 12, 5464-5470.

Hait, W.N. (2010). Anticancer drug development: the grand challenges. *Nat Rev Drug Discov* 9, 253-254.

Han, J., Goldstein, L.A., Gastman, B.R., Rabinovitz, A., Wang, G.Q., Fang, B., and Rabinowich, H. (2004). Differential involvement of Bax and Bak in TRAIL-mediated apoptosis of leukemic T cells. *Leukemia* 18, 1671-1680.

Han, M., Vakili, M.R., Soleymani Abyaneh, H., Molavi, O., Lai, R., and Lavasanifar, A. (2014). Mitochondrial delivery of doxorubicin via triphenylphosphine modification for overcoming drug resistance in MDA-MB-435/DOX cells. *Mol Pharm* 11, 2640-2649.

Han, Z., Hendrickson, E.A., Bremner, T.A., and Wyche, J.H. (1997). A sequential two-step mechanism for the production of the mature p17:p12 form of caspase-3 in vitro. *J Biol Chem* 272, 13432-13436.

Hanahan, D., and Weinberg, R.A. (2011). Hallmarks of cancer: the next generation. *Cell* 144, 646-674.

Hankins, H.M., Baldrige, R.D., Xu, P., and Graham, T.R. (2015). Role of flippases, scramblases and transfer proteins in phosphatidylserine subcellular distribution. *Traffic* 16, 35-47.

Harries, M., and Smith, I. (2002). The development and clinical use of trastuzumab (Herceptin). *Endocr Relat Cancer* 9, 75-85.

Hayashi, M., Sakata, M., Takeda, T., Yamamoto, T., Okamoto, Y., Sawada, K., Kimura, A., Minekawa, R., Tahara, M., Tasaka, K., *et al.* (2004). Induction of glucose transporter 1 expression through hypoxia-inducible factor 1 $\alpha$  under hypoxic conditions in trophoblast-derived cells. *J Endocrinol* 183, 145-154.

He, H., Li, D.W., Yang, L.Y., Fu, L., Zhu, X.J., Wong, W.K., Jiang, F.L., and Liu, Y. (2015). A novel bifunctional mitochondria-targeted anticancer agent with high selectivity for cancer cells. *Sci Rep* 5, 13543.

He, J., Agarwal, M.L., Larkin, H.E., Friedman, L.R., Xue, L.Y., and Oleinick, N.L. (1996). The induction of partial resistance to photodynamic therapy by the protooncogene BCL-2. *Photochem Photobiol* 64, 845-852.

Henderson, B.W., Waldow, S.M., Mang, T.S., Potter, W.R., Malone, P.B., and Dougherty, T.J. (1985). Tumor destruction and kinetics of tumor cell death in two experimental mouse tumors following photodynamic therapy. *Cancer Res* 45, 572-576.

Higgins, C.F. (2007). Multiple molecular mechanisms for multidrug resistance transporters. *Nature* 446, 749-757.

High, L.M., Szymanska, B., Wilczynska-Kalak, U., Barber, N., O'Brien, R., Khaw, S.L., Vikstrom, I.B., Roberts, A.W., and Lock, R.B. (2010). The Bcl-2 homology domain 3 mimetic ABT-737 targets the apoptotic machinery in acute lymphoblastic leukemia resulting in synergistic in vitro and in vivo interactions with established drugs. *Mol Pharmacol* 77, 483-494.

Hirsch, H.A., Iliopoulos, D., Tsiichlis, P.N., and Struhl, K. (2009). Metformin selectively targets cancer stem cells, and acts together with chemotherapy to block tumor growth and prolong remission. *Cancer Res* 69, 7507-7511.

Hsieh, C.C., and Papaconstantinou, J. (2006). Thioredoxin-ASK1 complex levels regulate ROS-mediated p38 MAPK pathway activity in livers of aged and long-lived Snell dwarf mice. *FASEB J* 20, 259-268.

Hu, Y., Rosen, D.G., Zhou, Y., Feng, L., Yang, G., Liu, J., and Huang, P. (2005). Mitochondrial manganese-superoxide dismutase expression in ovarian cancer: role in cell proliferation and response to oxidative stress. *J Biol Chem* 280, 39485-39492.

Huttemann, M., Pecina, P., Rainbolt, M., Sanderson, T.H., Kagan, V.E., Samavati, L., Doan, J.W., and Lee, I. (2011). The multiple functions of cytochrome c and their regulation in life and death decisions of the mammalian cell: From respiration to apoptosis. *Mitochondrion* 11, 369-381.

Irani, K., Xia, Y., Zweier, J.L., Sollott, S.J., Der, C.J., Fearon, E.R., Sundaresan, M., Finkel, T., and Goldschmidt-Clermont, P.J. (1997). Mitogenic signaling mediated by oxidants in Ras-transformed fibroblasts. *Science* 275, 1649-1652.

Ishikawa, K., Takenaga, K., Akimoto, M., Koshikawa, N., Yamaguchi, A., Imanishi, H., Nakada, K., Honma, Y., and Hayashi, J. (2008). ROS-generating mitochondrial DNA mutations can regulate tumor cell metastasis. *Science* 320, 661-664.

Ishitsuka, K., Kunami, N., Katsuya, H., Nogami, R., Ishikawa, C., Yotsumoto, F., Tanji, H., Mori, N., Takeshita, M., Miyamoto, S., *et al.* (2012). Targeting Bcl-2 family

proteins in adult T-cell leukemia/lymphoma: in vitro and in vivo effects of the novel Bcl-2 family inhibitor ABT-737. *Cancer Lett* 317, 218-225.

Itoh, T., Messner, H.A., Jamal, N., Tweeddale, M., and Sieber, F. (1993). Merocyanine 540-sensitized photoinactivation of high-grade non-Hodgkin's lymphoma cells: potential application in autologous BMT. *Bone Marrow Transplant* 12, 191-196.

Izumi, Y., Xu, L., di Tomaso, E., Fukumura, D., and Jain, R.K. (2002). Tumour biology: herceptin acts as an anti-angiogenic cocktail. *Nature* 416, 279-280.

Jackson, J.R., Patrick, D.R., Dar, M.M., and Huang, P.S. (2007). Targeted anti-mitotic therapies: can we improve on tubulin agents? *Nat Rev Cancer* 7, 107-117.

James, T.H. (1977). *The Theory of the Photographic Process* (New York: The Macmillan Company).

Jiao, D., Smith, T.J., Yang, C.S., Pittman, B., Desai, D., Amin, S., and Chung, F.L. (1997). Chemopreventive activity of thiol conjugates of isothiocyanates for lung tumorigenesis. *Carcinogenesis* 18, 2143-2147.

Johansson, A.C., Steen, H., Ollinger, K., and Roberg, K. (2003). Cathepsin D mediates cytochrome c release and caspase activation in human fibroblast apoptosis induced by staurosporine. *Cell Death Differ* 10, 1253-1259.

Johnson, L.V., Walsh, M.L., and Chen, L.B. (1980). Localization of mitochondria in living cells with rhodamine 123. *Proc Natl Acad Sci U S A* 77, 990-994.

Johnson, V.L., Ko, S.C., Holmstrom, T.H., Eriksson, J.E., and Chow, S.C. (2000). Effector caspases are dispensable for the early nuclear morphological changes during chemical-induced apoptosis. *J Cell Sci* 113 ( Pt 17), 2941-2953.

Jones, L.W., Narayan, K.S., Shapiro, C.E., and Sweatman, T.W. (2005). Rhodamine-123: therapy for hormone refractory prostate cancer, a phase I clinical trial. *J Chemother* 17, 435-440.

Kabingu, E., Vaughan, L., Owczarczak, B., Ramsey, K.D., and Gollnick, S.O. (2007). CD8+ T cell-mediated control of distant tumours following local photodynamic therapy is independent of CD4+ T cells and dependent on natural killer cells. *Br J Cancer* 96, 1839-1848.

Kagedal, K., Johansson, U., and Ollinger, K. (2001). The lysosomal protease cathepsin D mediates apoptosis induced by oxidative stress. *FASEB J* 15, 1592-1594.

Kamb, A., Wee, S., and Lengauer, C. (2007). Why is cancer drug discovery so difficult? *Nat Rev Drug Discov* 6, 115-120.

Kang, Y.H., and Lee, S.J. (2008). The role of p38 MAPK and JNK in Arsenic trioxide-induced mitochondrial cell death in human cervical cancer cells. *J Cell Physiol* 217, 23-33.

Kano, A., Taniwaki, Y., Nakamura, I., Shimada, N., Moriyama, K., and Maruyama, A. (2013). Tumor delivery of Photofrin(R) by PLL-g-PEG for photodynamic therapy. *J Control Release* 167, 315-321.

Karch, J., Kwong, J.Q., Burr, A.R., Sargent, M.A., Elrod, J.W., Peixoto, P.M., Martinez-Caballero, S., Osinska, H., Cheng, E.H., Robbins, J., *et al.* (2013). Bax and Bak function as the outer membrane component of the mitochondrial permeability pore in regulating necrotic cell death in mice. *Elife* 2, e00772.

Kassab, K. (2002). Photophysical and photosensitizing properties of selected cyanines. *J Photochem Photobiol B* 68, 15-22.

Kawanishi, S., Hiraku, Y., Pinlaor, S., and Ma, N. (2006). Oxidative and nitrative DNA damage in animals and patients with inflammatory diseases in relation to inflammation-related carcinogenesis. *Biol Chem* 387, 365-372.

Kazak, L., Reyes, A., and Holt, I.J. (2012). Minimizing the damage: repair pathways keep mitochondrial DNA intact. *Nat Rev Mol Cell Biol* 13, 659-671.

Kessel, D. (2002). Relocalization of cationic porphyrins during photodynamic therapy. *Photochem Photobiol Sci* 1, 837-840.

Kim, J.W., Tchernyshyov, I., Semenza, G.L., and Dang, C.V. (2006). HIF-1-mediated expression of pyruvate dehydrogenase kinase: a metabolic switch required for cellular adaptation to hypoxia. *Cell Metab* 3, 177-185.

Kim, S.H., Bajji, A., Tangallapally, R., Markovitz, B., Trovato, R., Shenderovich, M., Baichwal, V., Bartel, P., Cimbor, D., McKinnon, R., *et al.* (2012). Discovery of (2S)-1-[4-(2-{6-amino-8-[(6-bromo-1,3-benzodioxol-5-yl)sulfonyl]-9H-purin-9-yl}ethyl)piperidin-1-yl]-2-hydroxypropan-1-one (MPC-3100), a purine-based Hsp90 inhibitor. *J Med Chem* 55, 7480-7501.

Kim, T., Keum, G., and Pae, A.N. (2013). Discovery and development of heat shock protein 90 inhibitors as anticancer agents: a review of patented potent geldanamycin derivatives. *Expert Opin Ther Pat* 23, 919-943.

Kimura, H., Sawada, T., Oshima, S., Kozawa, K., Ishioka, T., and Kato, M. (2005). Toxicity and roles of reactive oxygen species. *Curr Drug Targets Inflamm Allergy* 4, 489-495.

Kipps, T.J., Eradat, H., Grosicki, S., Catalano, J., Cosolo, W., Dyagil, I.S., Yalamanchili, S., Chai, A., Sahasranaman, S., Punnoose, E., *et al.* (2015). A phase 2 study of the BH3 mimetic BCL2 inhibitor navitoclax (ABT-263) with or without rituximab, in previously untreated B-cell chronic lymphocytic leukemia. *Leuk Lymphoma* 56, 2826-2833.

Ko, B.-K., Lee, S.-Y., Lee, Y.-H., Hwang, I.-S., Persson, H., Rockberg, J., Borrebaeck, C., Park, D., Kim, K.-T., Uhlen, M., *et al.* (2015). Combination of novel HER2-targeting antibody 1E11 with trastuzumab shows synergistic antitumor activity in HER2-positive gastric cancer. *Molecular Oncology* 9, 398-408.

Kodiha, M., Pié, B., Wang, Y.M., Flamant, E., Boppana, N.B., Young, J.C., Separovic, D., Cooper, E., and Stochaj, U. (2015). Detecting changes in the mitochondrial membrane potential by quantitative fluorescence microscopy. Kong, Q., and Lillehei, K.O. (1998). Antioxidant inhibitors for cancer therapy. *Med Hypotheses* 51, 405-409.

Korbelik, M., Stott, B., and Sun, J. (2007). Photodynamic therapy-generated vaccines: relevance of tumour cell death expression. *Br J Cancer* 97, 1381-1387.

Kousis, P.C., Henderson, B.W., Maier, P.G., and Gollnick, S.O. (2007). Photodynamic therapy enhancement of antitumor immunity is regulated by neutrophils. *Cancer Res* 67, 10501-10510.

Koya, K., Li, Y., Wang, H., Ukai, T., Tatsuta, N., Kawakami, M., Shishido, and Chen, L.B. (1996). MKT-077, a novel rhodacyanine dye in clinical trials, exhibits anticarcinoma activity in preclinical studies based on selective mitochondrial accumulation. *Cancer Res* 56, 538-543.

Krebs, J.J., Hauser, H., and Carafoli, E. (1979). Asymmetric distribution of phospholipids in the inner membrane of beef heart mitochondria. *J Biol Chem* 254, 5308-5316.

Kroemer, G., and Pouyssegur, J. (2008). Tumor cell metabolism: cancer's Achilles' heel. *Cancer Cell* 13, 472-482.

Krosl, G., Korbelik, M., and Dougherty, G.J. (1995). Induction of immune cell infiltration into murine SCCVII tumour by photofrin-based photodynamic therapy. *Br J Cancer* 71, 549-555.

Kunjachan, S., Rychlik, B., Storm, G., Kiessling, F., and Lammers, T. (2013). Multidrug resistance: Physiological principles and nanomedical solutions. *Adv Drug Deliv Rev* 65, 1852-1865.

Lakowicz, J.R. (2006). Principles of Fluorescence Spectroscopy, Third Edition (Springer )

Lamch, L., Bazylińska, U., Kulbacka, J., Pietkiewicz, J., Biezunska-Kusiak, K., and Wilk, K.A. (2014). Polymeric micelles for enhanced Photofrin II (R) delivery, cytotoxicity and pro-apoptotic activity in human breast and ovarian cancer cells. *Photodiagnosis Photodyn Ther* 11, 570-585.

Lampidis, T.J., Bernal, S.D., Summerhayes, I.C., and Chen, L.B. (1983). Selective toxicity of rhodamine 123 in carcinoma cells in vitro. *Cancer Res* 43, 716-720.

Lampidis, T.J., Hasin, Y., Weiss, M.J., and Chen, L.B. (1985). Selective killing of carcinoma cells "in vitro" by lipophilic-cationic compounds: a cellular basis. *Biomed Pharmacother* 39, 220-226.

Lampidis, T.J., Johnson, L.V., and Israel, M. (1981). Effects of adriamycin on rat heart cells in culture: increased accumulation and nucleoli fragmentation in cardiac muscle v. non-muscle cells. *J Mol Cell Cardiol* 13, 913-924.

Lampidis, T.J., Salet, C., Moreno, G., and Chen, L.B. (1984). Effects of the mitochondrial probe rhodamine 123 and related analogs on the function and viability of pulsating myocardial cells in culture. *Agents Actions* 14, 751-757.

Landau, B.R., Laszlo, J., Stengle, J., and Burk, D. (1958). Certain metabolic and pharmacologic effects in cancer patients given infusions of 2-deoxy-D-glucose. *J Natl Cancer Inst* 21, 485-494.

Lemmon, M.A., and Schlessinger, J. (2010). Cell signaling by receptor tyrosine kinases. *Cell* 141, 1117-1134.

Leone, G., Voso, M.T., Sica, S., Morosetti, R., and Pagano, L. (2001). Therapy related leukemias: susceptibility, prevention and treatment. *Leuk Lymphoma* 41, 255-276.

Levkau, B., Herren, B., Koyama, H., Ross, R., and Raines, E.W. (1998). Caspase-mediated cleavage of focal adhesion kinase pp125FAK and disassembly of focal adhesions in human endothelial cell apoptosis. *J Exp Med* 187, 579-586.

Li, X., Colvin, T., Rauch, J.N., Acosta-Alvear, D., Kampmann, M., Duniak, B., Hann, B., Aftab, B.T., Murnane, M., Cho, M., *et al.* (2015). Validation of the Hsp70-Bag3 protein-protein interaction as a potential therapeutic target in cancer. *Mol Cancer Ther* 14, 642-648.

Li, X., Srinivasan, S.R., Connarn, J., Ahmad, A., Young, Z.T., Kabza, A.M., Zuiderweg, E.R., Sun, D., and Gestwicki, J.E. (2013). Analogs of the Allosteric Heat

Shock Protein 70 (Hsp70) Inhibitor, MKT-077, as Anti-Cancer Agents. *ACS Med Chem Lett* 4.

Li, X.Y., Zhao, Y., Sun, M.G., Shi, J.F., Ju, R.J., Zhang, C.X., Li, X.T., Zhao, W.Y., Mu, L.M., Zeng, F., *et al.* (2014). Multifunctional liposomes loaded with paclitaxel and artemether for treatment of invasive brain glioma. *Biomaterials* 35, 5591-5604.

Lin, L., Xiong, L., Wen, Y., Lei, S., Deng, X., Liu, Z., Chen, W., and Miao, X. (2015). Active Targeting of Nano-Photosensitizer Delivery Systems for Photodynamic Therapy of Cancer Stem Cells. *J Biomed Nanotechnol* 11, 531-554.

Lin, T.S., Naumovski, L., Lecane, P.S., Lucas, M.S., Moran, M.E., Cheney, C., Lucas, D.M., Phan, S.C., Miller, R.A., and Byrd, J.C. (2009). Effects of motexafin gadolinium in a phase II trial in refractory chronic lymphocytic leukemia. *Leuk Lymphoma* 50, 1977-1982.

Liu, J., Weiss, A., Durrant, D., Chi, N.W., and Lee, R.M. (2004). The cardiolipin-binding domain of Bid affects mitochondrial respiration and enhances cytochrome c release. *Apoptosis* 9, 533-541.

Liu, J., Zhang, C., Hu, W., and Feng, Z. (2015). Tumor suppressor p53 and its mutants in cancer metabolism. *Cancer Lett* 356, 197-203.

Liu, T., Wu, L.Y., Choi, J.K., and Berkman, C.E. (2010). Targeted photodynamic therapy for prostate cancer: inducing apoptosis via activation of the caspase-8/-3 cascade pathway. *Int J Oncol* 36, 777-784.

Liu, X., Kim, C.N., Yang, J., Jemmerson, R., and Wang, X. (1996). Induction of apoptotic program in cell-free extracts: requirement for dATP and cytochrome c. *Cell* 86, 147-157.

Liu, Y., Fiskum, G., and Schubert, D. (2002). Generation of reactive oxygen species by the mitochondrial electron transport chain. *J Neurochem* 80, 780-787.

Lock, R., Carol, H., Houghton, P.J., Morton, C.L., Kolb, E.A., Gorlick, R., Reynolds, C.P., Maris, J.M., Keir, S.T., Wu, J., *et al.* (2008). Initial testing (stage 1) of the BH3 mimetic ABT-263 by the pediatric preclinical testing program. *Pediatr Blood Cancer* 50, 1181-1189.

Longley, D.B., Harkin, D.P., and Johnston, P.G. (2003). 5-Fluorouracil: mechanisms of action and clinical strategies. *Nat Rev Cancer* 3, 330-338.

Lopez-Rios, F., Sanchez-Arago, M., Garcia-Garcia, E., Ortega, A.D., Berrendero, J.R., Pozo-Rodriguez, F., Lopez-Encuentra, A., Ballestin, C., and Cuezva, J.M. (2007). Loss of the mitochondrial bioenergetic capacity underlies the glucose avidity of carcinomas. *Cancer Res* 67, 9013-9017.

- Lu, J., Chew, E.H., and Holmgren, A. (2007). Targeting thioredoxin reductase is a basis for cancer therapy by arsenic trioxide. *Proc Natl Acad Sci U S A* *104*, 12288-12293.
- Lunt, S.Y., and Vander Heiden, M.G. (2011). Aerobic glycolysis: meeting the metabolic requirements of cell proliferation. *Annu Rev Cell Dev Biol* *27*, 441-464.
- Luo, X., Budihardjo, I., Zou, H., Slaughter, C., and Wang, X. (1998). Bid, a Bcl2 interacting protein, mediates cytochrome c release from mitochondria in response to activation of cell surface death receptors. *Cell* *94*, 481-490.
- Lutter, M., Fang, M., Luo, X., Nishijima, M., Xie, X., and Wang, X. (2000). Cardiolipin provides specificity for targeting of tBid to mitochondria. *Nat Cell Biol* *2*, 754-761.
- Ly, J.D., Grubb, D.R., and Lawen, A. (2003). The mitochondrial membrane potential ( $\Delta\psi_m$ ) in apoptosis; an update. *Apoptosis* *8*, 115-128.
- Madak, J.T., and Neamati, N. (2015). Membrane permeable lipophilic cations as mitochondrial directing groups. *Curr Top Med Chem* *15*, 745-766.
- Madesh, M., and Hajnoczky, G. (2001). VDAC-dependent permeabilization of the outer mitochondrial membrane by superoxide induces rapid and massive cytochrome c release. *J Cell Biol* *155*, 1003-1015.
- Marino, G., and Kroemer, G. (2013). Mechanisms of apoptotic phosphatidylserine exposure. *Cell Res* *23*, 1247-1248.
- Martinez-Reyes, I., and Cuezva, J.M. (2014). The H(+)-ATP synthase: a gate to ROS-mediated cell death or cell survival. *Biochim Biophys Acta* *1837*, 1099-1112.
- Martinou, J.-C., and Youle, R.J. (2011). Mitochondria in Apoptosis: Bcl-2 family Members and Mitochondrial Dynamics. *Developmental cell* *21*, 92-101.
- Mathupala, S.P., Ko, Y.H., and Pedersen, P.L. (2009). Hexokinase-2 bound to mitochondria: cancer's stygian link to the "Warburg Effect" and a pivotal target for effective therapy. *Semin Cancer Biol* *19*, 17-24.
- Mattiazzi, M., Vijayvergiya, C., Gajewski, C.D., DeVivo, D.C., Lenaz, G., Wiedmann, M., and Manfredi, G. (2004). The mtDNA T8993G (NARP) mutation results in an impairment of oxidative phosphorylation that can be improved by antioxidants. *Hum Mol Genet* *13*, 869-879.
- Maynard, S., Schurman, S.H., Harboe, C., de Souza-Pinto, N.C., and Bohr, V.A. (2009). Base excision repair of oxidative DNA damage and association with cancer and aging. *Carcinogenesis* *30*, 2-10.

- Mayer, M.P., and Bukau, B. (2005). Hsp70 chaperones: cellular functions and molecular mechanism. *Cell Mol Life Sci* 62, 670-684.
- Mehta, M.P., Shapiro, W.R., Phan, S.C., Gervais, R., Carrie, C., Chabot, P., Patchell, R.A., Glantz, M.J., Recht, L., Langer, C., *et al.* (2009). Motexafin gadolinium combined with prompt whole brain radiotherapy prolongs time to neurologic progression in non-small-cell lung cancer patients with brain metastases: results of a phase III trial. *Int J Radiat Oncol Biol Phys* 73, 1069-1076.
- Mellish, K.J., Cox, R.D., Vernon, D.I., Griffiths, J., and Brown, S.B. (2002). In vitro photodynamic activity of a series of methylene blue analogues. *Photochem Photobiol* 75, 392-397.
- Metallo, C.M., Gameiro, P.A., Bell, E.L., Mattaini, K.R., Yang, J., Hiller, K., Jewell, C.M., Johnson, Z.R., Irvine, D.J., Guarente, L., *et al.* (2012). Reductive glutamine metabolism by IDH1 mediates lipogenesis under hypoxia. *Nature* 481, 380-384.
- Michelakis, E.D., Sutendra, G., Dromparis, P., Webster, L., Haromy, A., Niven, E., Maguire, C., Gammer, T.L., Mackey, J.R., Fulton, D., *et al.* (2010). Metabolic modulation of glioblastoma with dichloroacetate. *Sci Transl Med* 2, 31ra34.
- Michor, F., Iwasa, Y., and Nowak, M.A. (2004). Dynamics of cancer progression. *Nat Rev Cancer* 4, 197-205.
- Miquel, C., Borrini, F., Grandjouan, S., Auperin, A., Viguier, J., Velasco, V., Duvillard, P., Praz, F., and Sabourin, J.C. (2005). Role of bax mutations in apoptosis in colorectal cancers with microsatellite instability. *Am J Clin Pathol* 123, 562-570.
- Mirzayans, R., Andrais, B., Scott, A., Wang, Y.W., and Murray, D. (2013). Ionizing radiation-induced responses in human cells with differing TP53 status. *Int J Mol Sci* 14, 22409-22435.
- Mitra, S., and Foster, T.H. (2005). Photophysical parameters, photosensitizer retention and tissue optical properties completely account for the higher photodynamic efficacy of meso-tetra-hydroxyphenyl-chlorin vs Photofrin. *Photochem Photobiol* 81, 849-859.
- Miyata, Y., Li, X., Lee, H.F., Jinwal, U.K., Srinivasan, S.R., Seguin, S.P., Young, Z.T., Brodsky, J.L., Dickey, C.A., Sun, D., *et al.* (2013a). Synthesis and initial evaluation of YM-08, a blood-brain barrier permeable derivative of the heat shock protein 70 (Hsp70) inhibitor MKT-077, which reduces tau levels. *ACS Chem Neurosci* 4, 930-939.
- Miyata, Y., Nakamoto, H., and Neckers, L. (2013b). The therapeutic target Hsp90 and cancer hallmarks. *Curr Pharm Des* 19, 347-365.

- Moan, J., Berg, K., Kvam, E., Western, A., Malik, Z., Ruck, A., and Schneckenburger, H. (1989). Intracellular localization of photosensitizers. *Ciba Found Symp* 146, 95-107; discussion 107-111.
- Modi, S., Sugarman, S., Stopeck, A., Linden, H., Ma, W., Kersy, K., Johnson, R.G., Rosen, N., Hannah, A.L., and Hudis, C.A. (2008). Phase II trial of the Hsp90 inhibitor tanespimycin (Tan) + trastuzumab (T) in patients (pts) with HER2-positive metastatic breast cancer (MBC) *Journal of Clinical Oncology* 26.
- Modica-Napolitano, J.S., and Aprille, J.R. (1987). Basis for the selective cytotoxicity of rhodamine 123. *Cancer Res* 47, 4361-4365.
- Modica-Napolitano, J.S., and Aprille, J.R. (2001). Delocalized lipophilic cations selectively target the mitochondria of carcinoma cells. *Adv Drug Deliv Rev* 49, 63-70.
- Modica-Napolitano, J.S., and Weissig, V. (2015). Treatment Strategies that Enhance the Efficacy and Selectivity of Mitochondria-Targeted Anticancer Agents. *Int J Mol Sci* 16, 17394-17421.
- Modica-Napolitano, J.S., Brunelli, B.T., Koya, K., and Chen, L.B. (1998). Photoactivation enhances the mitochondrial toxicity of the cationic rhodacyanine MKT-077. *Cancer Res* 58, 71-75.
- Modica-Napolitano, J.S., Koya, K., Weisberg, E., Brunelli, B.T., Li, Y., and Chen, L.B. (1996). Selective damage to carcinoma mitochondria by the rhodacyanine MKT-077. *Cancer Res* 56, 544-550.
- Modica-Napolitano, J.S., Kulawiec, M., and Singh, K.K. (2007). Mitochondria and human cancer. *Curr Mol Med* 7, 121-131.
- Moghissi, K., Dixon, K., Stringer, M., Freeman, T., Thorpe, A., and Brown, S. (1999). The place of bronchoscopic photodynamic therapy in advanced unresectable lung cancer: experience of 100 cases. *Eur J Cardiothorac Surg* 15, 1-6.
- Mosero, I., and Kralova, J. (2012). Role of ER stress response in photodynamic therapy: ROS generated in different subcellular compartments trigger diverse cell death pathways. *PLoS One* 7, e32972.
- Mukai, H., Saeki, T., Shimada, K., Naito, Y., Matsubara, N., Nakanishi, T., Obaishi, H., Namiki, M., and Sasaki, Y. (2015). Phase 1 combination study of Eribulin mesylate with trastuzumab for advanced or recurrent human epidermal growth factor receptor 2 positive breast cancer. *Investigational New Drugs* 33, 119-127.
- Mukherjee, S. (2010). *The Emperor of All Maladies: A Biography of Cancer* (Scribner).

- Mullen, A.R., Wheaton, W.W., Jin, E.S., Chen, P.-H., Sullivan, L.B., Cheng, T., Yang, Y., Linehan, W.M., Chandel, N.S., and DeBerardinis, R.J. (2012). Reductive carboxylation supports growth in tumour cells with defective mitochondria. *Nature* 481, 385-388.
- Muller, P.A., and Vousden, K.H. (2013). p53 mutations in cancer. *Nat Cell Biol* 15, 2-8.
- Murgo, A.J. (2001). Clinical trials of arsenic trioxide in hematologic and solid tumors: overview of the National Cancer Institute Cooperative Research and Development Studies. *Oncologist* 6 Suppl 2, 22-28.
- Murphy, M.P. (2009). How mitochondria produce reactive oxygen species. *Biochem J* 417, 1-13.
- Murphy, M.P., and Smith, R.A. (2000). Drug delivery to mitochondria: the key to mitochondrial medicine. *Adv Drug Deliv Rev* 41, 235-250.
- Nagata, S. (2000). Apoptotic DNA fragmentation. *Exp Cell Res* 256, 12-18.
- Nagata, S., Suzuki, J., Segawa, K., and Fujii, T. (2016). Exposure of phosphatidylserine on the cell surface. *Cell Death Differ* 23, 952-961.
- Nahleh, Z., Tfayli, A., Najm, A., El Sayed, A., and Nahle, Z. (2012). Heat shock proteins in cancer: targeting the 'chaperones'. *Future Med Chem* 4, 927-935.
- Nahta, R., Yu, D., Hung, M.C., Hortobagyi, G.N., and Esteva, F.J. (2006). Mechanisms of disease: understanding resistance to HER2-targeted therapy in human breast cancer. *Nat Clin Pract Oncol* 3, 269-280.
- Nakamura, K., Yoshikawa, N., Yamaguchi, Y., Kagota, S., Shinozuka, K., and Kunitomo, M. (2002). Characterization of mouse melanoma cell lines by their mortal malignancy using an experimental metastatic model. *Life sciences* 70, 791-798.
- Narita, M., Shimizu, S., Ito, T., Chittenden, T., Lutz, R.J., Matsuda, H., and Tsujimoto, Y. (1998). Bax interacts with the permeability transition pore to induce permeability transition and cytochrome c release in isolated mitochondria. *Proc Natl Acad Sci U S A* 95, 14681-14686.
- Ndozangue-Touriguine, O., Hamelin, J., and Breard, J. (2008). Cytoskeleton and apoptosis. *Biochem Pharmacol* 76, 11-18.
- Neugut, A.I., Robinson, E., Nieves, J., Murray, T., and Tsai, W.Y. (1990). Poor survival of treatment-related acute nonlymphocytic leukemia. *JAMA* 264, 1006-1008.

Nie, C., Tian, C., Zhao, L., Petit, P.X., Mehrpour, M., and Chen, Q. (2008). Cysteine 62 of Bax is critical for its conformational activation and its proapoptotic activity in response to H<sub>2</sub>O<sub>2</sub>-induced apoptosis. *J Biol Chem* 283, 15359-15369.

Nishida, N., Yano, H., Nishida, T., Kamura, T., and Kojiro, M. (2006). Angiogenesis in Cancer. *Vascular Health and Risk Management* 2, 213-219.

Nonaka, M., Ikeda, H., and Inokuchi, T. (2004). Inhibitory effect of heat shock protein 70 on apoptosis induced by photodynamic therapy in vitro. *Photochem Photobiol* 79, 94-98.

Noriko Yasuhara, S.S., Shinji Kamada, Yutaka Eguchi and Yoshihide Tsujimoto (1997). Evidence against a functional site for Bcl-2 downstream of caspase cascade in preventing apoptosis. *Oncogene* 15, 7.

Nowell, P.C., and Hungerford, D.A. (1960). Chromosome studies on normal and leukemic human leukocytes. *J Natl Cancer Inst* 25, 85-109.

O'Connor, A.E., Gallagher, W.M., and Byrne, A.T. (2009). Porphyrin and nonporphyrin photosensitizers in oncology: preclinical and clinical advances in photodynamic therapy. *Photochem Photobiol* 85, 1053-1074.

Octavia, Y., Tocchetti, C.G., Gabrielson, K.L., Janssens, S., Crijns, H.J., and Moens, A.L. (2012). Doxorubicin-induced cardiomyopathy: from molecular mechanisms to therapeutic strategies. *J Mol Cell Cardiol* 52, 1213-1225.

Ogrunc, M., Di Micco, R., Liontos, M., Bombardelli, L., Mione, M., Fumagalli, M., Gorgoulis, V.G., and d'Adda di Fagagna, F. (2014). Oncogene-induced reactive oxygen species fuel hyperproliferation and DNA damage response activation. *Cell Death Differ* 21, 998-1012.

Oleinick, N.L., Morris, R.L., and Belichenko, I. (2002). The role of apoptosis in response to photodynamic therapy: what, where, why, and how. *Photochem Photobiol Sci* 1, 1-21.

Olmsted, J., and R.Kearns, D. (1977). Mechanism of Ethidium Bromide Fluorescence Enhancement on Binding to Nucleic Acids. *Biochemistry* 16, 8.

Oltersdorf, T., Elmore, S.W., Shoemaker, A.R., Armstrong, R.C., Augeri, D.J., Belli, B.A., Bruncko, M., Deckwerth, T.L., Dinges, J., Hajduk, P.J., *et al.* (2005). An inhibitor of Bcl-2 family proteins induces regression of solid tumours. *Nature* 435, 677-681.

Orth, K., Ruck, A., Stanescu, A., and Beger, H.G. (1995). Intraluminal treatment of inoperable oesophageal tumours by intralesional photodynamic therapy with methylene blue. *Lancet* 345, 519-520.

Ow, Y.-L.P., Green, D.R., Hao, Z., and Mak, T.W. (2008). Cytochrome c: functions beyond respiration. *Nat Rev Mol Cell Biol* 9, 532-542.

Padayatty, S.J., Katz, A., Wang, Y., Eck, P., Kwon, O., Lee, J.H., Chen, S., Corpe, C., Dutta, A., Dutta, S.K., *et al.* (2003). Vitamin C as an antioxidant: evaluation of its role in disease prevention. *J Am Coll Nutr* 22, 18-35.

Paradies, G., Petrosillo, G., Pistolese, M., and Ruggiero, F.M. (2002). Reactive oxygen species affect mitochondrial electron transport complex I activity through oxidative cardiolipin damage. *Gene* 286, 135-141.

Park, G.B., Choi, Y., Kim, Y.S., Lee, H.K., Kim, D., and Hur, D.Y. (2014). ROS-mediated JNK/p38-MAPK activation regulates Bax translocation in Sorafenib-induced apoptosis of EBV-transformed B cells. *Int J Oncol* 44, 977-985.

Pelicano, H., Carney, D., and Huang, P. (2004). ROS stress in cancer cells and therapeutic implications. *Drug Resist Updat* 7, 97-110.

Pelicano, H., Feng, L., Zhou, Y., Carew, J.S., Hileman, E.O., Plunkett, W., Keating, M.J., and Huang, P. (2003). Inhibition of mitochondrial respiration: a novel strategy to enhance drug-induced apoptosis in human leukemia cells by a reactive oxygen species-mediated mechanism. *J Biol Chem* 278, 37832-37839.

Pemberton, L.F. (2014). Preparation of yeast cells for live-cell imaging and indirect immunofluorescence. *Methods Mol Biol* 1205, 79-90.

Perry, G., Raina, A.K., Nunomura, A., Wataya, T., Sayre, L.M., and Smith, M.A. (2000). How important is oxidative damage? Lessons from Alzheimer's disease. *Free Radic Biol Med* 28, 831-834.

Perry, S.W., Norman, J.P., Barbieri, J., Brown, E.B., and Gelbard, H.A. (2011). Mitochondrial membrane potential probes and the proton gradient: a practical usage guide. *Biotechniques* 50, 98-115.

Petrosillo, G., Ruggiero, F.M., and Paradies, G. (2003). Role of reactive oxygen species and cardiolipin in the release of cytochrome c from mitochondria. *FASEB J* 17, 2202-2208.

Pollak, M. (2012). The insulin and insulin-like growth factor receptor family in neoplasia: an update. *Nat Rev Cancer* 12, 159-169.

Polyak, K., Xia, Y., Zweier, J.L., Kinzler, K.W., and Vogelstein, B. (1997). A model for p53-induced apoptosis. *Nature* 389, 300-305.

Porporato, P.E., Payen, V.L., Perez-Escuredo, J., De Saedeleer, C.J., Danhier, P., Copetti, T., Dhup, S., Tardy, M., Vazeille, T., Bouzin, C., *et al.* (2014). A mitochondrial switch promotes tumor metastasis. *Cell Rep* 8, 754-766.

Portt, L., Norman, G., Clapp, C., Greenwood, M., and Greenwood, M.T. (2011). Anti-apoptosis and cell survival: a review. *Biochim Biophys Acta* 1813, 238-259.

Powers, M.V., Valenti, M., Miranda, S., Maloney, A., Eccles, S.A., Thomas, G., Clarke, P.A., and Workman, P. (2013). Mode of cell death induced by the HSP90 inhibitor 17-AAG (tanespimycin) is dependent on the expression of pro-apoptotic BAX. *Oncotarget* 4, 1963-1975.

Propper, D.J., Braybrooke, J.P., Taylor, D.J., Lodi, R., Styles, P., Cramer, J.A., Collins, W.C., Levitt, N.C., Talbot, D.C., Ganesan, T.S., *et al.* (1999). Phase I trial of the selective mitochondrial toxin MKT077 in chemo-resistant solid tumours. *Ann Oncol* 10, 923-927.

Quinlan, C.L., Perevoshchikova, I.V., Hey-Mogensen, M., Orr, A.L., and Brand, M.D. (2013). Sites of reactive oxygen species generation by mitochondria oxidizing different substrates. *Redox Biol* 1, 304-312.

Quintas-Cardama, A., Kantarjian, H.M., and Cortes, J.E. (2009). Mechanisms of primary and secondary resistance to imatinib in chronic myeloid leukemia. *Cancer Control* 16, 122-131.

Raez, L.E., Papadopoulos, K., Ricart, A.D., Chiorean, E.G., Dipaola, R.S., Stein, M.N., Rocha Lima, C.M., Schlesselman, J.J., Tolba, K., Langmuir, V.K., *et al.* (2013). A phase I dose-escalation trial of 2-deoxy-D-glucose alone or combined with docetaxel in patients with advanced solid tumors. *Cancer Chemother Pharmacol* 71, 523-530.

Ray, P.D., Huang, B.-W., and Tsuji, Y. (2012). Reactive oxygen species (ROS) homeostasis and redox regulation in cellular signaling. *Cellular signalling* 24, 981-990.

Ricci, C., Pastukh, V., Leonard, J., Turrens, J., Wilson, G., Schaffer, D., and Schaffer, S.W. (2008). Mitochondrial DNA damage triggers mitochondrial-superoxide generation and apoptosis. *Am J Physiol Cell Physiol* 294, C413-422.

Richardson, P.G., Chanan-Khan, A.A., Lonial, S., Krishnan, A.Y., Carroll, M.P., Albitar, M., Kopit, J., Berman, D., and Anderson, K.C. (2009). Tanespimycin + Bortezomib Demonstrates Safety, Activity, and Effective Target Inhibition in Relapsed/Refractory Myeloma Patients: Updated Results of a Phase 1/2 Study. *Blood* 114, 2890-2890.

Riddle, S.R., Ahmad, A., Ahmad, S., Deeb, S.S., Malkki, M., Schneider, B.K., Allen, C.B., and White, C.W. (2000). Hypoxia induces hexokinase II gene expression in human lung cell line A549. *Am J Physiol Lung Cell Mol Physiol* 278, L407-416.

Riggins, J., Narayan, K.S., and Jones, L. (2007). Rhodamine-123 reduces the dosage of docetaxel necessary to achieve maximal cell growth inhibition in prostate and breast cancer cell lines in vitro. *Cancer Research AACR Annual Meeting*.

Roberg, K., and Ollinger, K. (1998). Oxidative stress causes relocation of the lysosomal enzyme cathepsin D with ensuing apoptosis in neonatal rat cardiomyocytes. *Am J Pathol* 152, 1151-1156.

Roberts, A.W., Seymour, J.F., Brown, J.R., Wierda, W.G., Kipps, T.J., Khaw, S.L., Carney, D.A., He, S.Z., Huang, D.C., Xiong, H., *et al.* (2012). Substantial susceptibility of chronic lymphocytic leukemia to BCL2 inhibition: results of a phase I study of navitoclax in patients with relapsed or refractory disease. *J Clin Oncol* 30, 488-496.

Roberts, P.J., and Der, C.J. (2007). Targeting the Raf-MEK-ERK mitogen-activated protein kinase cascade for the treatment of cancer. *Oncogene* 26, 3291-3310.

Rodriguez-Enriquez, S., Gallardo-Perez, J.C., Hernandez-Resendiz, I., Marin-Hernandez, A., Pacheco-Velazquez, S.C., Lopez-Ramirez, S.Y., Rumjanek, F.D., and Moreno-Sanchez, R. (2014). Canonical and new generation anticancer drugs also target energy metabolism. *Arch Toxicol* 88, 1327-1350.

Romani, A.A., Crafa, P., Desenzani, S., Graiani, G., Lagrasta, C., Sianesi, M., Soliani, P., and Borghetti, A.F. (2007). The expression of HSP27 is associated with poor clinical outcome in intrahepatic cholangiocarcinoma. *BMC Cancer* 7, 1-10.

Rosati, A., Ammirante, M., Gentilella, A., Basile, A., Festa, M., Pascale, M., Marzullo, L., Belisario, M.A., Tosco, A., Franceschelli, S., *et al.* (2007). Apoptosis inhibition in cancer cells: a novel molecular pathway that involves BAG3 protein. *Int J Biochem Cell Biol* 39, 1337-1342.

Rosenkranz, A.A., Jans, D.A., and Sobolev, A.S. (2000). Targeted intracellular delivery of photosensitizers to enhance photodynamic efficiency. *Immunol Cell Biol* 78, 452-464.

Rousaki, A., Miyata, Y., Jinwal, U.K., Dickey, C.A., Gestwicki, J.E., and Zuiderweg, E.R. (2011). Allosteric drugs: the interaction of antitumor compound MKT-077 with human Hsp70 chaperones. *J Mol Biol* 411, 614-632.

Sabharwal, S.S., and Schumacker, P.T. (2014). Mitochondrial ROS in cancer: initiators, amplifiers or an Achilles' heel? *Nat Rev Cancer* 14, 709-721.

Sakahira, H., Takemura, Y., and Nagata, S. (2001). Enzymatic active site of caspase-activated DNase (CAD) and its inhibition by inhibitor of CAD. *Arch Biochem Biophys* 388, 91-99.

Salesse, S., and Verfaillie, C.M. (2002). BCR/ABL: from molecular mechanisms of leukemia induction to treatment of chronic myelogenous leukemia. *Oncogene* 21, 8547-8559.

Sankari, S.L., Masthan, K.M., Babu, N.A., Bhattacharjee, T., and Elumalai, M. (2012). Apoptosis in cancer--an update. *Asian Pac J Cancer Prev* 13, 4873-4878.

Sasaki, H., Kotsuji, F., and Tsang, B.K. (2002). Caspase 3-mediated focal adhesion kinase processing in human ovarian cancer cells: possible regulation by X-linked inhibitor of apoptosis protein. *Gynecol Oncol* 85, 339-350.

Saydam, N., Kirb, A., Demir, Ö., Hazan, E., Oto, Ö., Saydam, O., and Güner, G. (1997). Determination of glutathione, glutathione reductase, glutathione peroxidase and glutathione S-transferase levels in human lung cancer tissues. *Cancer Letters* 119, 13-19.

Sborov, D.W., Haverkos, B.M., and Harris, P.J. (2015). Investigational cancer drugs targeting cell metabolism in clinical development. *Expert Opin Investig Drugs* 24, 79-94.

Scarlett, J.L., Sheard, P.W., Hughes, G., Ledgerwood, E.C., Ku, H.H., and Murphy, M.P. (2000). Changes in mitochondrial membrane potential during staurosporine-induced apoptosis in Jurkat cells. *FEBS Lett* 475, 267-272.

Schieber, M., and Chandel, N.S. (2014). ROS function in redox signaling and oxidative stress. *Curr Biol* 24, R453-462.

Schneider-Berlin, K.R., Bonilla, T.D., and Rowe, T.C. (2005). Induction of petite mutants in yeast *Saccharomyces cerevisiae* by the anticancer drug dequalinium. *Mutat Res* 572, 84-97.

Schuitmaker, J.J., Baas, P., van Leengoed, H.L., van der Meulen, F.W., Star, W.M., and van Zandwijk, N. (1996). Photodynamic therapy: a promising new modality for the treatment of cancer. *J Photochem Photobiol B* 34, 3-12.

Semenza, G.L. (2003). Targeting HIF-1 for cancer therapy. *Nat Rev Cancer* 3, 721-732.

Semenza, G.L. (2013). HIF-1 mediates metabolic responses to intratumoral hypoxia and oncogenic mutations. *J Clin Invest* 123, 3664-3671.

Senge, M.O., and Brandt, J.C. (2011). Temoporfin (Foscan(R), 5,10,15,20-tetra(m-hydroxyphenyl)chlorin)--a second-generation photosensitizer. *Photochem Photobiol* 87, 1240-1296.

Seymour, J.F., Davids, M.S., Pagel, J.M., Kahl, B.S., Wierda, W.G., Miller, T.P., Gerecitano, J.F., Kipps, T.J., Anderson, M.A., and Huang, D. (2013). Updated results of a phase I first-in-human study of the BCL-2 inhibitor ABT-199 (GDC-0199) in patients with relapsed/refractory (R/R) chronic lymphocytic leukemia (CLL). Paper presented at: ASCO Annual Meeting Proceedings.

Sgarbi, G., Baracca, A., Lenaz, G., Valentino, L.M., Carelli, V., and Solaini, G. (2006). Inefficient coupling between proton transport and ATP synthesis may be the pathogenic mechanism for NARP and Leigh syndrome resulting from the T8993G mutation in mtDNA. *Biochem J* 395, 493-500.

Shaw, R.J., Lamia, K.A., Vasquez, D., Koo, S.H., Bardeesy, N., Depinho, R.A., Montminy, M., and Cantley, L.C. (2005). The kinase LKB1 mediates glucose homeostasis in liver and therapeutic effects of metformin. *Science* 310, 1642-1646.

Shea, C.R., Chen, N., Wimberly, J., and Hasan, T. (1989). Rhodamine Dyes as Potential Agents for Photochemotherapy of Cancer in Human Bladder Carcinoma Cells. *Cancer Research* 49, 5.

Shi, Y. (2002). Mechanisms of Caspase Activation and Inhibition during Apoptosis. *Molecular Cell* 9, 459-470.

Sibani, S.A., McCarron, P.A., Woolfson, A.D., and Donnelly, R.F. (2008). Photosensitizer delivery for photodynamic therapy. Part 2: systemic carrier platforms. *Expert Opin Drug Deliv* 5, 1241-1254.

Siddik, Z.H. (2003). Cisplatin: mode of cytotoxic action and molecular basis of resistance. *Oncogene* 22, 7265-7279.

Sidera, K., and Patsavoudi, E. (2014). HSP90 inhibitors: current development and potential in cancer therapy. *Recent Pat Anticancer Drug Discov* 9, 1-20.

Silva, Z.S., Jr., Bussadori, S.K., Fernandes, K.P., Huang, Y.Y., and Hamblin, M.R. (2015). Animal models for photodynamic therapy (PDT). *Biosci Rep* 35.

Singh, K.K., Russell, J., Sigala, B., Zhang, Y., Williams, J., and Keshav, K.F. (1999). Mitochondrial DNA determines the cellular response to cancer therapeutic agents. *Oncogene* 18, 6641-6646.

Slamon, D.J., Clark, G.M., Wong, S.G., Levin, W.J., Ullrich, A., and McGuire, W.L. (1987). Human breast cancer: correlation of relapse and survival with amplification of the HER-2/neu oncogene. *Science* 235, 177-182.

Slamon, D.J., Leyland-Jones, B., Shak, S., Fuchs, H., Paton, V., Bajamonde, A., Fleming, T., Eiermann, W., Wolter, J., Pegram, M., *et al.* (2001). Use of chemotherapy plus a monoclonal antibody against HER2 for metastatic breast cancer that overexpresses HER2. *N Engl J Med* 344, 783-792.

Smiley, S.T., Reers, M., Mottola-Hartshorn, C., Lin, M., Chen, A., Smith, T.W., Steele, G.D., Jr., and Chen, L.B. (1991). Intracellular heterogeneity in mitochondrial membrane potentials revealed by a J-aggregate-forming lipophilic cation JC-1. *Proc Natl Acad Sci U S A* 88, 3671-3675.

Smith, R.A., Porteous, C.M., Gane, A.M., and Murphy, M.P. (2003). Delivery of bioactive molecules to mitochondria in vivo. *Proc Natl Acad Sci U S A* 100, 5407-5412.

Smith, R.E., Bryant, J., DeCillis, A., and Anderson, S. (2003). Acute myeloid leukemia and myelodysplastic syndrome after doxorubicin-cyclophosphamide adjuvant therapy for operable breast cancer: the National Surgical Adjuvant Breast and Bowel Project Experience. *J Clin Oncol* 21, 1195-1204.

Snyder, J.W., Greco, W.R., Bellnier, D.A., Vaughan, L., and Henderson, B.W. (2003). Photodynamic therapy: a means to enhanced drug delivery to tumors. *Cancer Res* 63, 8126-8131.

Solesio, M.E., Prime, T.A., Logan, A., Murphy, M.P., del Mar Arroyo-Jimenez, M., Jordán, J., and Galindo, M.F. (2013). The mitochondria-targeted anti-oxidant MitoQ reduces aspects of mitochondrial fission in the 6-OHDA cell model of Parkinson's disease. *Biochimica et Biophysica Acta (BBA) - Molecular Basis of Disease* 1832, 174-182.

Souers, A.J., Levenson, J.D., Boghaert, E.R., Ackler, S.L., Catron, N.D., Chen, J., Dayton, B.D., Ding, H., Enschede, S.H., Fairbrother, W.J., *et al.* (2013). ABT-199, a potent and selective BCL-2 inhibitor, achieves antitumor activity while sparing platelets. *Nat Med* 19, 202-208.

Starenki, D., and Park, J.I. (2015). Selective Mitochondrial Uptake of MKT-077 Can Suppress Medullary Thyroid Carcinoma Cell Survival In Vitro and In Vivo. *Endocrinol Metab (Seoul)* 30, 593-603.

Stein, M., Lin, H., Jeyamohan, C., Dvorzhinski, D., Gounder, M., Bray, K., Eddy, S., Goodin, S., White, E., and Dipaola, R.S. (2010). Targeting tumor metabolism with 2-deoxyglucose in patients with castrate-resistant prostate cancer and advanced malignancies. *Prostate* 70, 1388-1394.

Stratton, M.R. (2011). Exploring the genomes of cancer cells: progress and promise. *Science* 331, 1553-1558.

Strum, S.B., Adalsteinsson, O., Black, R.R., Segal, D., Peress, N.L., and Waldenfels, J. (2013). Case report: Sodium dichloroacetate (DCA) inhibition of the "Warburg Effect" in a human cancer patient: complete response in non-Hodgkin's lymphoma after disease progression with rituximab-CHOP. *J Bioenerg Biomembr* 45, 307-315.

Subbarayan, P.R., and Ardalan, B. (2014). In the war against solid tumors arsenic trioxide needs partners. *J Gastrointest Cancer* 45, 363-371.

Sukumar, M., Liu, J., Mehta, G.U., Patel, S.J., Roychoudhuri, R., Crompton, J.G., Klebanoff, C.A., Ji, Y., Li, P., Yu, Z., *et al.* (2016). Mitochondrial Membrane Potential Identifies Cells with Enhanced Stemness for Cellular Therapy. *Cell Metab* 23, 63-76.

Summerhayes, I.C., Lampidis, T.J., Bernal, S.D., Nadakavukaren, J.J., Nadakavukaren, K.K., Shepherd, E.L., and Chen, L.B. (1982). Unusual retention of rhodamine 123 by mitochondria in muscle and carcinoma cells. *Proc Natl Acad Sci U S A* 79, 5292-5296.

Sun, X., Wong, J.R., Song, K., Hu, J., Garlid, K.D., and Chen, L.B. (1994). AA1, a newly synthesized monovalent lipophilic cation, expresses potent in vivo antitumor activity. *Cancer Res* 54, 1465-1471.

Sur, B.W., Nguyen, P., Sun, C.H., Tromberg, B.J., and Nelson, E.L. (2008). Immunophototherapy using PDT combined with rapid intratumoral dendritic cell injection. *Photochem Photobiol* 84, 1257-1264.

Suryani, S., Carol, H., Chonghaile, T.N., Frismantas, V., Sarmah, C., High, L., Bornhauser, B., Cowley, M.J., Szymanska, B., Evans, K., *et al.* (2014). Cell and molecular determinants of in vivo efficacy of the BH3 mimetic ABT-263 against pediatric acute lymphoblastic leukemia xenografts. *Clin Cancer Res* 20, 4520-4531.

Susin, S.A., Lorenzo, H.K., Zamzami, N., Marzo, I., Snow, B.E., Brothers, G.M., Mangion, J., Jacotot, E., Costantini, P., Loeffler, M., *et al.* (1999). Molecular characterization of mitochondrial apoptosis-inducing factor. *Nature* 397, 441-446.

Susin, S.A., Zamzami, N., Castedo, M., Daugas, E., Wang, H.G., Geley, S., Fassy, F., Reed, J.C., and Kroemer, G. (1997). The central executioner of apoptosis: multiple connections between protease activation and mitochondria in Fas/APO-1/CD95- and ceramide-induced apoptosis. *J Exp Med* 186, 25-37.

Sutedja, T., Baas, P., Stewart, F., and van Zandwijk, N. (1992). A pilot study of photodynamic therapy in patients with inoperable non-small cell lung cancer. *Eur J Cancer* 28A, 1370-1373.

- Svensson, J., Johansson, A., Grafe, S., Gitter, B., Trebst, T., Bendsoe, N., Andersson-Engels, S., and Svanberg, K. (2007). Tumor selectivity at short times following systemic administration of a liposomal temoporfin formulation in a murine tumor model. *Photochem Photobiol* 83, 1211-1219.
- Szatrowski, T.P., and Nathan, C.F. (1991). Production of large amounts of hydrogen peroxide by human tumor cells. *Cancer Res* 51, 794-798.
- Taanman, J.W. (1999). The mitochondrial genome: structure, transcription, translation and replication. *Biochim Biophys Acta* 1410, 103-123.
- Takeuchi, K., and Ito, F. (2011). Receptor tyrosine kinases and targeted cancer therapeutics. *Biol Pharm Bull* 34, 1774-1780.
- Taylor, R.C., Cullen, S.P., and Martin, S.J. (2008). Apoptosis: controlled demolition at the cellular level. *Nat Rev Mol Cell Biol* 9, 231-241.
- Teicher, B.A., Holden, S.A., Jacobs, J.L., Abrams, M.J., and Jones, A.G. (1986). Intracellular distribution of a platinum-rhodamine 123 complex in cis-platinum sensitive and resistant human squamous carcinoma cell lines. *Biochem Pharmacol* 35, 3365-3369.
- Thomas, S.R., and Khuntia, D. (2011). Motexafin gadolinium: a promising radiation sensitizer in brain metastasis. *Expert Opin Drug Discov* 6, 195-203.
- Thornberry, N.A. (1999). Caspases: a decade of death research. *Cell Death Differ* 6, 1023-1027.
- Tikoo, A., Shakri, R., Connolly, L., Hirokawa, Y., Shishido, T., Bowers, B., Ye, L.H., Kohama, K., Simpson, R.J., and Maruta, H. (2000). Treatment of ras-induced cancers by the F-actin-bundling drug MKT-077. *Cancer J* 6, 162-168.
- Touzeau, C., Dousset, C., Le Gouill, S., Sampath, D., Levenson, J.D., Souers, A.J., Maiga, S., Bene, M.C., Moreau, P., Pellat-Deceunynck, C., *et al.* (2014). The Bcl-2 specific BH3 mimetic ABT-199: a promising targeted therapy for t(11;14) multiple myeloma. *Leukemia* 28, 210-212.
- Townsend, D.M., and Tew, K.D. (2003). The role of glutathione-S-transferase in anti-cancer drug resistance. *Oncogene* 22, 7369-7375.
- Toyokuni, S., Okamoto, K., Yodoi, J., and Hiai, H. (1995). Persistent oxidative stress in cancer. *FEBS Lett* 358, 1-3.
- Traber, M.G., and Atkinson, J. (2007). Vitamin E, antioxidant and nothing more. *Free Radic Biol Med* 43, 4-15.

- Trachootham, D., Alexandre, J., and Huang, P. (2009). Targeting cancer cells by ROS-mediated mechanisms: a radical therapeutic approach? *Nat Rev Drug Discov* 8, 579-591.
- Travis, L.B., Fossa, S.D., Schonfeld, S.J., McMaster, M.L., Lynch, C.F., Storm, H., Hall, P., Holowaty, E., Andersen, A., Pukkala, E., *et al.* (2005). Second cancers among 40,576 testicular cancer patients: focus on long-term survivors. *J Natl Cancer Inst* 97, 1354-1365.
- Trepel, J., Mollapour, M., Giaccone, G., and Neckers, L. (2010). Targeting the dynamic HSP90 complex in cancer. *Nat Rev Cancer* 10, 537-549.
- Tseng, M.T., Reed, M.W., Ackermann, D.M., Schuschke, D.A., Wieman, T.J., and Miller, F.N. (1988). Photodynamic therapy induced ultrastructural alterations in microvasculature of the rat cremaster muscle. *Photochem Photobiol* 48, 675-681.
- Tsujimoto, Y. (1998). Role of Bcl-2 family proteins in apoptosis: apoptosomes or mitochondria? *Genes Cells* 3, 697-707.
- Tsujimoto, Y., Gorham, J., Cossman, J., Jaffe, E., and Croce, C.M. (1985). The t(14;18) chromosome translocations involved in B-cell neoplasms result from mistakes in VDJ joining. *Science* 229, 1390-1393.
- Tsujimoto, Y., and Shimizu, S. (2007). Role of the mitochondrial membrane permeability transition in cell death. *Apoptosis* 12, 835-840.
- Umeki, S., Niki, Y., and Soejima, R. (1989). Anticancer chemotherapy accelerates scalp hair loss with no androgenic involvement. *Chemotherapy* 35, 54-57.
- Umesh, K.J., Grover, A., Narayan, M., Hirani, A., and Sutariya, V. (2014). Preparation and Characterization of MKT-077 Nanoparticles for Treatment of Alzheimer's Disease and Other Tauopathies. *Pharmaceutical Nanotechnology* 2, 10.
- Upton, J.P., Valentijn, A.J., Zhang, L., and Gilmore, A.P. (2007). The N-terminal conformation of Bax regulates cell commitment to apoptosis. *Cell Death Differ* 14, 932-942.
- Usmani, S.Z., Bona, R., and Li, Z. (2009). 17 AAG for HSP90 inhibition in cancer--from bench to bedside. *Curr Mol Med* 9, 654-664.
- Usuda, J., Azizuddin, K., Chiu, S.M., and Oleinick, N.L. (2003). Association between the photodynamic loss of Bcl-2 and the sensitivity to apoptosis caused by phthalocyanine photodynamic therapy. *Photochem Photobiol* 78, 1-8.
- Vafa, O., Wade, M., Kern, S., Beeche, M., Pandita, T.K., Hampton, G.M., and Wahl, G.M. (2002). c-Myc can induce DNA damage, increase reactive oxygen species, and

mitigate p53 function: a mechanism for oncogene-induced genetic instability. *Mol Cell* 9, 1031-1044.

Vaidya, B., and Vyas, S.P. (2012). Transferrin coupled vesicular system for intracellular drug delivery for the treatment of cancer: development and characterization. *J Drug Target* 20, 372-380.

van Engeland, M., Nieland, L.J., Ramaekers, F.C., Schutte, B., and Reutelingsperger, C.P. (1998). Annexin V-affinity assay: a review on an apoptosis detection system based on phosphatidylserine exposure. *Cytometry* 31, 1-9.

Vandenberg, C.J., and Cory, S. (2013). ABT-199, a new Bcl-2-specific BH3 mimetic, has in vivo efficacy against aggressive Myc-driven mouse lymphomas without provoking thrombocytopenia. *Blood* 121, 2285-2288.

Vanlangenakker, N., Vanden Berghe, T., Krysko, D.V., Festjens, N., and Vandenaabeele, P. (2008). Molecular mechanisms and pathophysiology of necrotic cell death. *Curr Mol Med* 8, 207-220.

Vegt, E., de Jong, M., Wetzels, J.F., Masereeuw, R., Melis, M., Oyen, W.J., Gotthardt, M., and Boerman, O.C. (2010). Renal toxicity of radiolabeled peptides and antibody fragments: mechanisms, impact on radionuclide therapy, and strategies for prevention. *J Nucl Med* 51, 1049-1058.

Vercammen, D., Brouckaert, G., Denecker, G., Van de Craen, M., Declercq, W., Fiers, W., and Vandenaabeele, P. (1998). Dual signaling of the Fas receptor: initiation of both apoptotic and necrotic cell death pathways. *J Exp Med* 188, 919-930.

Vieira, H.L., Haouzi, D., El Hamel, C., Jacotot, E., Belzacq, A.S., Brenner, C., and Kroemer, G. (2000). Permeabilization of the mitochondrial inner membrane during apoptosis: impact of the adenine nucleotide translocator. *Cell Death Differ* 7, 1146-1154.

Villamor, N., Montserrat, E., and Colomer, D. (2003). Mechanism of action and resistance to monoclonal antibody therapy. *Semin Oncol* 30, 424-433.

Viollet, B., Guigas, B., Sanz Garcia, N., Leclerc, J., Foretz, M., and Andreelli, F. (2012). Cellular and molecular mechanisms of metformin: an overview. *Clinical Science (London, England : 1979)* 122, 253-270.

Vogel, C.L., Cobleigh, M.A., Tripathy, D., Gutheil, J.C., Harris, L.N., Fehrenbacher, L., Slamon, D.J., Murphy, M., Novotny, W.F., Burchmore, M., *et al.* (2002). Efficacy and safety of trastuzumab as a single agent in first-line treatment of HER2-overexpressing metastatic breast cancer. *J Clin Oncol* 20, 719-726.

Vrouenraets, M.B., Visser, G.W., Snow, G.B., and van Dongen, G.A. (2003). Basic principles, applications in oncology and improved selectivity of photodynamic therapy. *Anticancer Res* 23, 505-522.

Vu, T., and Claret, F.X. (2012). Trastuzumab: Updated Mechanisms of Action and Resistance in Breast Cancer. *Frontiers in Oncology* 2, 62.

Wadhwa, R., Sugihara, T., Yoshida, A., Nomura, H., Reddel, R.R., Simpson, R., Maruta, H., and Kaul, S.C. (2000). Selective toxicity of MKT-077 to cancer cells is mediated by its binding to the hsp70 family protein mot-2 and reactivation of p53 function. *Cancer Res* 60, 6818-6821.

Walsh, J.G., Cullen, S.P., Sheridan, C., Lüthi, A.U., Gerner, C., and Martin, S.J. (2008). Executioner caspase-3 and caspase-7 are functionally distinct proteases. *Proceedings of the National Academy of Sciences* 105, 12815-12819.

Wang, C., and Youle, R.J. (2009). The role of mitochondria in apoptosis\*. *Annu Rev Genet* 43, 95-118.

Wang, G.Q., Wieckowski, E., Goldstein, L.A., Gastman, B.R., Rabinovitz, A., Gambotto, A., Li, S., Fang, B., Yin, X.M., and Rabinowich, H. (2001). Resistance to granzyme B-mediated cytochrome c release in Bak-deficient cells. *J Exp Med* 194, 1325-1337.

Wang, L., Du, F., and Wang, X. (2008). TNF-alpha induces two distinct caspase-8 activation pathways. *Cell* 133, 693-703.

Wang, L., Kinnear, C., Hammel, J.M., Zhu, W., Hua, Z., Mi, W., and Caldarone, C.A. (2006). Preservation of mitochondrial structure and function after cardioplegic arrest in the neonate using a selective mitochondrial KATP channel opener. *Ann Thorac Surg* 81, 1817-1823.

Warburg, O., Posener, K., and Negelein, E. (1924). Über den Stoffwechsel der Tumoren. *Biochem Z* 152, 25.

Ward, P.S., and Thompson, C.B. (2012). Metabolic reprogramming: a cancer hallmark even warburg did not anticipate. *Cancer Cell* 21, 297-308.

Wei, M.C., Zong, W.X., Cheng, E.H., Lindsten, T., Panoutsakopoulou, V., Ross, A.J., Roth, K.A., MacGregor, G.R., Thompson, C.B., and Korsmeyer, S.J. (2001). Proapoptotic BAX and BAK: a requisite gateway to mitochondrial dysfunction and death. *Science* 292, 727-730.

Weinberg, F., Hamanaka, R., Wheaton, W.W., Weinberg, S., Joseph, J., Lopez, M., Kalyanaraman, B., Mutlu, G.M., Budinger, G.R., and Chandel, N.S. (2010).

Mitochondrial metabolism and ROS generation are essential for Kras-mediated tumorigenicity. *Proc Natl Acad Sci U S A* 107, 8788-8793.

Weiss, M.J., Wong, J.R., Ha, C.S., Bleday, R., Salem, R.R., Steele, G.D., Jr., and Chen, L.B. (1987). Dequalinium, a topical antimicrobial agent, displays anticarcinoma activity based on selective mitochondrial accumulation. *Proc Natl Acad Sci U S A* 84, 5444-5448.

Weissig, V. (2015). DQAsomes as the prototype of mitochondria-targeted pharmaceutical nanocarriers: preparation, characterization, and use. *Methods Mol Biol* 1265, 1-11.

Weissig, V., Lasch, J., Erdos, G., Meyer, H.W., Rowe, T.C., and Hughes, J. (1998). DQAsomes: a novel potential drug and gene delivery system made from Dequalinium. *Pharm Res* 15, 334-337.

Wenner, C.E. (2012). Targeting mitochondria as a therapeutic target in cancer. *J Cell Physiol* 227, 450-456.

Williams, J.L., Stamp, J., Devonshire, R., and Fowler, G.J. (1989). Methylene blue and the photodynamic therapy of superficial bladder cancer. *J Photochem Photobiol B* 4, 229-232.

Wong, R.S. (2011). Apoptosis in cancer: from pathogenesis to treatment. *J Exp Clin Cancer Res* 30, 87.

Woo, D.K., Green, P.D., Santos, J.H., D'Souza, A.D., Walther, Z., Martin, W.D., Christian, B.E., Chandel, N.S., and Shadel, G.S. (2012). Mitochondrial genome instability and ROS enhance intestinal tumorigenesis in APC(Min/+) mice. *Am J Pathol* 180, 24-31.

Wu, W.S. (2006). The signaling mechanism of ROS in tumor progression. *Cancer Metastasis Rev* 25, 695-705.

Xu, L., Voloboueva, L.A., Ouyang, Y., Emery, J.F., and Giffard, R.G. (2009). Overexpression of mitochondrial Hsp70/Hsp75 in rat brain protects mitochondria, reduces oxidative stress, and protects from focal ischemia. *J Cereb Blood Flow Metab* 29, 365-374.

Xuan, Y., Hur, H., Ham, I.H., Yun, J., Lee, J.Y., Shim, W., Kim, Y.B., Lee, G., Han, S.U., and Cho, Y.K. (2014). Dichloroacetate attenuates hypoxia-induced resistance to 5-fluorouracil in gastric cancer through the regulation of glucose metabolism. *Exp Cell Res* 321, 219-230.

Xue, L.Y., Chiu, S.M., and Oleinick, N.L. (2001). Photochemical destruction of the Bcl-2 oncoprotein during photodynamic therapy with the phthalocyanine photosensitizer Pc 4. *Oncogene* 20, 3420-3427.

Yamaguchi, R., Janssen, E., Perkins, G., Ellisman, M., Kitada, S., and Reed, J.C. (2011). Efficient elimination of cancer cells by deoxyglucose-ABT-263/737 combination therapy. *PLoS One* 6, e24102.

Yamamoto, K., Ichijo, H., and Korsmeyer, S.J. (1999). BCL-2 Is Phosphorylated and Inactivated by an ASK1/Jun N-Terminal Protein Kinase Pathway Normally Activated at G(2)/M. *Molecular and Cellular Biology* 19, 8469-8478.

Yan, M., Schwaederle, M., Arguello, D., Millis, S.Z., Gatalica, Z., and Kurzrock, R. (2015). HER2 expression status in diverse cancers: review of results from 37,992 patients. *Cancer Metastasis Rev* 34, 157-164.

Yang, H., Zhou, X., Liu, X., Yang, L., Chen, Q., Zhao, D., Zuo, J., and Liu, W. (2011). Mitochondrial dysfunction induced by knockdown of mortalin is rescued by Parkin. *Biochem Biophys Res Commun* 410, 114-120.

Yang, N., Gilman, P., Mirzayans, R., Sun, X., Touret, N., Weinfeld, M., and Goping, I.S. (2015). Characterization of the apoptotic response induced by the cyanine dye D112: a potentially selective anti-cancer compound. *PLoS One* 10, e0125381.

Yang, N., and Goping, I.S. (2013). Apoptosis (Morgan & Claypool Life Sciences).  
Yarden, Y., and Sliwkowski, M.X. (2001). Untangling the ErbB signalling network. *Nat Rev Mol Cell Biol* 2, 127-137.

Zafarullah, M., Li, W.Q., Sylvester, J., and Ahmad, M. (2003). Molecular mechanisms of N-acetylcysteine actions. *Cell Mol Life Sci* 60, 6-20.

Zahreddine, H., and Borden, K.L. (2013). Mechanisms and insights into drug resistance in cancer. *Front Pharmacol* 4, 28.

Zhang, R., Humphreys, I., Sahu, R.P., Shi, Y., and Srivastava, S.K. (2008). In vitro and in vivo induction of apoptosis by capsaicin in pancreatic cancer cells is mediated through ROS generation and mitochondrial death pathway. *Apoptosis* 13, 1465-1478.

Zhang, T.D., Chen, G.Q., Wang, Z.G., Wang, Z.Y., Chen, S.J., and Chen, Z. (2001). Arsenic trioxide, a therapeutic agent for APL. *Oncogene* 20, 7146-7153.

Zhou, S., Kachhap, S., Sun, W., Wu, G., Chuang, A., Poeta, L., Grumbine, L., Mithani, S.K., Chatterjee, A., Koch, W., *et al.* (2007). Frequency and phenotypic implications of mitochondrial DNA mutations in human squamous cell cancers of the head and neck. *Proc Natl Acad Sci U S A* 104, 7540-7545.

Zhu, Z.L., Zhang, J., Chen, M.L., and Li, K. (2013). Efficacy and safety of Trastuzumab added to standard treatments for HER2-positive metastatic breast cancer patients. *Asian Pac J Cancer Prev* 14, 7111-7116.

Zigman, S., and Gilman, P., Jr. (1980). Inhibition of cell division and growth by a redox series of cyanine dyes. *Science* 208, 188-191.

Ali, I., Wani, W.A., Saleem, K., and Haque, A. (2013). Platinum compounds: a hope for future cancer chemotherapy. *Anticancer Agents Med Chem* 13, 296-306.

Allison, R.R., Bagnato, V.S., Cuenca, R., Downie, G.H., and Sibata, C.H. (2006). The future of photodynamic therapy in oncology. *Future Oncol* 2, 53-71.

Anderson, G.S., Miyagi, K., Sampson, R.W., and Sieber, F. (2002). Anti-tumor effect of Merocyanine 540-mediated photochemotherapy combined with Edelfosine: potential implications for the ex vivo purging of hematopoietic stem cell grafts from breast cancer patients. *J Photochem Photobiol B* 68, 101-108.

Baracca, A., Sgarbi, G., Solaini, G., and Lenaz, G. (2003). Rhodamine 123 as a probe of mitochondrial membrane potential: evaluation of proton flux through F<sub>0</sub> during ATP synthesis. *Biochim Biophys Acta* 1606, 137-146.

Beckman, W.C., Jr., Powers, S.K., Brown, J.T., Gillespie, G.Y., Bigner, D.D., and Camps, J.L., Jr. (1987). Differential retention of rhodamine 123 by avian sarcoma virus-induced glioma and normal brain tissue of the rat in vivo. *Cancer* 59, 266-270.

Bellnier, D.A., and Dougherty, T.J. (1996). A preliminary pharmacokinetic study of intravenous Photofrin in patients. *J Clin Laser Med Surg* 14, 311-314.

Bernal, S.D., Lampidis, T.J., Mclsaac, R.M., and Chen, L.B. (1983). Anticarcinoma activity in vivo of rhodamine 123, a mitochondrial-specific dye. *Science* 222, 169-172.

Britten, C.D., Rowinsky, E.K., Baker, S.D., Weiss, G.R., Smith, L., Stephenson, J., Rothenberg, M., Smetzer, L., Cramer, J., Collins, W., *et al.* (2000). A phase I and pharmacokinetic study of the mitochondrial-specific rhodacyanine dye analog MKT 077. *Clin Cancer Res* 6, 42-49.

Brown, S.B., Brown, E.A., and Walker, I. (2004). The present and future role of photodynamic therapy in cancer treatment. *Lancet Oncol* 5, 497-508.

Burbulla, L.F., Schelling, C., Kato, H., Rapaport, D., Voitalla, D., Schiesling, C., Schulte, C., Sharma, M., Illig, T., Bauer, P., *et al.* (2010). Dissecting the role of the mitochondrial chaperone mortalin in Parkinson's disease: functional impact of

disease-related variants on mitochondrial homeostasis. *Hum Mol Genet* 19, 4437-4452.

Castro, D.J., Haghghat, S., Saxton, R.E., Reisler, E., Jongwaard, N., Castro, D.J., Ward, P.H., and Lufkin, R.B. (1992). Biodistribution of rhodamine-123 in nude mice heterotransplanted with human squamous cell carcinomas. *Laryngoscope* 102, 868-874.

Castro, D.J., Saxton, R.E., Fetterman, H.R., Castro, D.J., and Ward, P.H. (1988). Phototherapy with argon lasers and Rhodamine-123 for tumor eradication. *Otolaryngol Head Neck Surg* 98, 581-588.

Castro, D.J., Saxton, R.E., Rodgerson, D.O., Fu, Y.S., Bhuta, S.M., Fetterman, H.R., Castro, D.J., Tartell, P.B., and Ward, P.H. (1989). Rhodamine-123 as a new laser dye: in vivo study of dye effects on murine metabolism, histology and ultrastructure. *Laryngoscope* 99, 1057-1062.

Chen, Q., Huang, Z., Luck, D., Beckers, J., Brun, P.H., Wilson, B.C., Scherz, A., Salomon, Y., and Hetzel, F.W. (2002). Preclinical studies in normal canine prostate of a novel palladium-bacteriopheophorbide (WST09) photosensitizer for photodynamic therapy of prostate cancers. *Photochem Photobiol* 76, 438-445.

Chiang, H.L., Terlecky, S.R., Plant, C.P., and Dice, J.F. (1989). A role for a 70-kilodalton heat shock protein in lysosomal degradation of intracellular proteins. *Science* 246, 382-385.

Chiba, Y., Kubota, T., Watanabe, M., Matsuzaki, S.W., Otani, Y., Teramoto, T., Matsumoto, Y., Koya, K., and Kitajima, M. (1998). MKT-077, localized lipophilic cation: antitumor activity against human tumor xenografts serially transplanted into nude mice. *Anticancer Res* 18, 1047-1052.

Dairkee, S.H., and Hackett, A.J. (1991). Differential retention of rhodamine 123 by breast carcinoma and normal human mammary tissue. *Breast Cancer Res Treat* 18, 57-61.

Davis, S., Weiss, M.J., Wong, J.R., Lampidis, T.J., and Chen, L.B. (1985). Mitochondrial and plasma membrane potentials cause unusual accumulation and retention of rhodamine 123 by human breast adenocarcinoma-derived MCF-7 cells. *J Biol Chem* 260, 13844-13850.

Dolmans, D.E., Fukumura, D., and Jain, R.K. (2003). Photodynamic therapy for cancer. *Nat Rev Cancer* 3, 380-387.

Dougherty, T.J. (1984). Photodynamic therapy (PDT) of malignant tumors. *Crit Rev Oncol Hematol* 2, 83-116.

- Itoh, T., Messner, H.A., Jamal, N., Tweeddale, M., and Sieber, F. (1993). Merocyanine 540-sensitized photoinactivation of high-grade non-Hodgkin's lymphoma cells: potential application in autologous BMT. *Bone Marrow Transplant* 12, 191-196.
- Jones, L.W., Narayan, K.S., Shapiro, C.E., and Sweatman, T.W. (2005). Rhodamine-123: therapy for hormone refractory prostate cancer, a phase I clinical trial. *J Chemother* 17, 435-440.
- Kano, A., Taniwaki, Y., Nakamura, I., Shimada, N., Moriyama, K., and Maruyama, A. (2013). Tumor delivery of Photofrin(R) by PLL-g-PEG for photodynamic therapy. *J Control Release* 167, 315-321.
- Kassab, K. (2002). Photophysical and photosensitizing properties of selected cyanines. *J Photochem Photobiol B* 68, 15-22.
- Kazak, L., Reyes, A., and Holt, I.J. (2012). Minimizing the damage: repair pathways keep mitochondrial DNA intact. *Nat Rev Mol Cell Biol* 13, 659-671.
- Koya, K., Li, Y., Wang, H., Ukai, T., Tatsuta, N., Kawakami, M., Shishido, and Chen, L.B. (1996). MKT-077, a novel rhodacyanine dye in clinical trials, exhibits anticarcinoma activity in preclinical studies based on selective mitochondrial accumulation. *Cancer Res* 56, 538-543.
- Lamch, L., Bazylińska, U., Kulbacka, J., Pietkiewicz, J., Biezunska-Kusiak, K., and Wilk, K.A. (2014). Polymeric micelles for enhanced Photofrin II (R) delivery, cytotoxicity and pro-apoptotic activity in human breast and ovarian cancer cells. *Photodiagnosis Photodyn Ther* 11, 570-585.
- Li, X., Colvin, T., Rauch, J.N., Acosta-Alvear, D., Kampmann, M., Duniak, B., Hann, B., Aftab, B.T., Murnane, M., Cho, M., *et al.* (2015). Validation of the Hsp70-Bag3 protein-protein interaction as a potential therapeutic target in cancer. *Mol Cancer Ther* 14, 642-648.
- Li, X., Srinivasan, S.R., Connarn, J., Ahmad, A., Young, Z.T., Kabza, A.M., Zuiderweg, E.R., Sun, D., and Gestwicki, J.E. (2013). Analogs of the Allosteric Heat Shock Protein 70 (Hsp70) Inhibitor, MKT-077, as Anti-Cancer Agents. *ACS Med Chem Lett* 4.
- Li, X.Y., Zhao, Y., Sun, M.G., Shi, J.F., Ju, R.J., Zhang, C.X., Li, X.T., Zhao, W.Y., Mu, L.M., Zeng, F., *et al.* (2014). Multifunctional liposomes loaded with paclitaxel and artemether for treatment of invasive brain glioma. *Biomaterials* 35, 5591-5604.
- Lin, L., Xiong, L., Wen, Y., Lei, S., Deng, X., Liu, Z., Chen, W., and Miao, X. (2015). Active Targeting of Nano-Photosensitizer Delivery Systems for Photodynamic Therapy of Cancer Stem Cells. *J Biomed Nanotechnol* 11, 531-554.

Madak, J.T., and Neamati, N. (2015). Membrane permeable lipophilic cations as mitochondrial directing groups. *Curr Top Med Chem* 15, 745-766.

Mayer, M.P., and Bukau, B. (2005). Hsp70 chaperones: cellular functions and molecular mechanism. *Cell Mol Life Sci* 62, 670-684.

Mellish, K.J., Cox, R.D., Vernon, D.I., Griffiths, J., and Brown, S.B. (2002). In vitro photodynamic activity of a series of methylene blue analogues. *Photochem Photobiol* 75, 392-397.

Mitra, S., and Foster, T.H. (2005). Photophysical parameters, photosensitizer retention and tissue optical properties completely account for the higher photodynamic efficacy of meso-tetra-hydroxyphenyl-chlorin vs Photofrin. *Photochem Photobiol* 81, 849-859.

Modica-Napolitano, J.S., and Aprille, J.R. (1987). Basis for the selective cytotoxicity of rhodamine 123. *Cancer Res* 47, 4361-4365.

Modica-Napolitano, J.S., and Aprille, J.R. (2001). Delocalized lipophilic cations selectively target the mitochondria of carcinoma cells. *Adv Drug Deliv Rev* 49, 63-70.

Modica-Napolitano, J.S., Brunelli, B.T., Koya, K., and Chen, L.B. (1998). Photoactivation enhances the mitochondrial toxicity of the cationic rhodacyanine MKT-077. *Cancer Res* 58, 71-75.

Modica-Napolitano, J.S., Koya, K., Weisberg, E., Brunelli, B.T., Li, Y., and Chen, L.B. (1996). Selective damage to carcinoma mitochondria by the rhodacyanine MKT-077. *Cancer Res* 56, 544-550.

Modica-Napolitano, J.S., and Weissig, V. (2015). Treatment Strategies that Enhance the Efficacy and Selectivity of Mitochondria-Targeted Anticancer Agents. *Int J Mol Sci* 16, 17394-17421.

O'Connor, A.E., Gallagher, W.M., and Byrne, A.T. (2009). Porphyrin and nonporphyrin photosensitizers in oncology: preclinical and clinical advances in photodynamic therapy. *Photochem Photobiol* 85, 1053-1074.

Orth, K., Ruck, A., Stanescu, A., and Beger, H.G. (1995). Intraluminal treatment of inoperable oesophageal tumours by intralesional photodynamic therapy with methylene blue. *Lancet* 345, 519-520.

Pelicano, H., Martin, D.S., Xu, R.H., and Huang, P. (2006). Glycolysis inhibition for anticancer treatment. *Oncogene* 25, 4633-4646.

Propper, D.J., Braybrooke, J.P., Taylor, D.J., Lodi, R., Styles, P., Cramer, J.A., Collins, W.C., Levitt, N.C., Talbot, D.C., Ganesan, T.S., *et al.* (1999). Phase I trial of the selective mitochondrial toxin MKT077 in chemo-resistant solid tumours. *Ann Oncol* 10, 923-927.

Riggins, J., Narayan, K.S., and Jones, L. (2007). Rhodamine-123 reduces the dosage of docetaxel necessary to achieve maximal cell growth inhibition in prostate and breast cancer cell lines in vitro. *Cancer Research AACR Annual Meeting*.

Rosenkranz, A.A., Jans, D.A., and Sobolev, A.S. (2000). Targeted intracellular delivery of photosensitizers to enhance photodynamic efficiency. *Immunol Cell Biol* 78, 452-464.

Rousaki, A., Miyata, Y., Jinwal, U.K., Dickey, C.A., Gestwicki, J.E., and Zuiderweg, E.R. (2011). Allosteric drugs: the interaction of antitumor compound MKT-077 with human Hsp70 chaperones. *J Mol Biol* 411, 614-632.

Schuitmaker, J.J., Baas, P., van Leengoed, H.L., van der Meulen, F.W., Star, W.M., and van Zandwijk, N. (1996). Photodynamic therapy: a promising new modality for the treatment of cancer. *J Photochem Photobiol B* 34, 3-12.

Senge, M.O., and Brandt, J.C. (2011). Temoporfin (Foscan(R), 5,10,15,20-tetra(m-hydroxyphenyl)chlorin)--a second-generation photosensitizer. *Photochem Photobiol* 87, 1240-1296.

Silva, Z.S., Jr., Bussadori, S.K., Fernandes, K.P., Huang, Y.Y., and Hamblin, M.R. (2015). Animal models for photodynamic therapy (PDT). *Biosci Rep* 35.

Smith, R.A., Porteous, C.M., Gane, A.M., and Murphy, M.P. (2003). Delivery of bioactive molecules to mitochondria in vivo. *Proc Natl Acad Sci U S A* 100, 5407-5412.

Souers, A.J., Levenson, J.D., Boghaert, E.R., Ackler, S.L., Catron, N.D., Chen, J., Dayton, B.D., Ding, H., Enschede, S.H., Fairbrother, W.J., *et al.* (2013). ABT-199, a potent and selective BCL-2 inhibitor, achieves antitumor activity while sparing platelets. *Nat Med* 19, 202-208.

Starenki, D., and Park, J.I. (2015). Selective Mitochondrial Uptake of MKT-077 Can Suppress Medullary Thyroid Carcinoma Cell Survival In Vitro and In Vivo. *Endocrinol Metab (Seoul)* 30, 593-603.

Sutedja, T., Baas, P., Stewart, F., and van Zandwijk, N. (1992). A pilot study of photodynamic therapy in patients with inoperable non-small cell lung cancer. *Eur J Cancer* 28A, 1370-1373.

- Teicher, B.A., Holden, S.A., Jacobs, J.L., Abrams, M.J., and Jones, A.G. (1986). Intracellular distribution of a platinum-rhodamine 123 complex in cis-platinum sensitive and resistant human squamous carcinoma cell lines. *Biochem Pharmacol* 35, 3365-3369.
- Tikoo, A., Shakri, R., Connolly, L., Hirokawa, Y., Shishido, T., Bowers, B., Ye, L.H., Kohama, K., Simpson, R.J., and Maruta, H. (2000). Treatment of ras-induced cancers by the F-actin-bundling drug MKT-077. *Cancer J* 6, 162-168.
- Trachootham, D., Alexandre, J., and Huang, P. (2009). Targeting cancer cells by ROS-mediated mechanisms: a radical therapeutic approach? *Nat Rev Drug Discov* 8, 579-591.
- Umesh, K.J., Grover, A., Narayan, M., Hirani, A., and Sutariya, V. (2014). Preparation and Characterization of MKT-077 Nanoparticles for Treatment of Alzheimer's Disease and Other Tauopathies. *Pharmaceutical Nanotechnology* 2, 10.
- Vaidya, B., and Vyas, S.P. (2012). Transferrin coupled vesicular system for intracellular drug delivery for the treatment of cancer: development and characterization. *J Drug Target* 20, 372-380.
- Vegt, E., de Jong, M., Wetzels, J.F., Masereeuw, R., Melis, M., Oyen, W.J., Gotthardt, M., and Boerman, O.C. (2010). Renal toxicity of radiolabeled peptides and antibody fragments: mechanisms, impact on radionuclide therapy, and strategies for prevention. *J Nucl Med* 51, 1049-1058.
- Wadhwa, R., Sugihara, T., Yoshida, A., Nomura, H., Reddel, R.R., Simpson, R., Maruta, H., and Kaul, S.C. (2000). Selective toxicity of MKT-077 to cancer cells is mediated by its binding to the hsp70 family protein mot-2 and reactivation of p53 function. *Cancer Res* 60, 6818-6821.
- Weissig, V. (2015). DQAsomes as the prototype of mitochondria-targeted pharmaceutical nanocarriers: preparation, characterization, and use. *Methods Mol Biol* 1265, 1-11.
- Weissig, V., Lasch, J., Erdos, G., Meyer, H.W., Rowe, T.C., and Hughes, J. (1998). DQAsomes: a novel potential drug and gene delivery system made from Dequalinium. *Pharm Res* 15, 334-337.
- Williams, J.L., Stamp, J., Devonshire, R., and Fowler, G.J. (1989). Methylene blue and the photodynamic therapy of superficial bladder cancer. *J Photochem Photobiol B* 4, 229-232.
- Yang, H., Zhou, X., Liu, X., Yang, L., Chen, Q., Zhao, D., Zuo, J., and Liu, W. (2011). Mitochondrial dysfunction induced by knockdown of mortalin is rescued by Parkin. *Biochem Biophys Res Commun* 410, 114-120.

Zigman, S., and Gilman, P., Jr. (1980). Inhibition of cell division and growth by a redox series of cyanine dyes. *Science* 208, 188-191.

Zimmermann, A., Ritsch-Marte, M., and Kostron, H. (2001). mTHPC-mediated photodynamic diagnosis of malignant brain tumors. *Photochem Photobiol* 74, 611-616.

Zu, X.L., and Guppy, M. (2004). Cancer metabolism: facts, fantasy, and fiction. *Biochem Biophys Res Commun* 313, 459-465.